Aspects of transport in strongly correlated systems with gravity duals

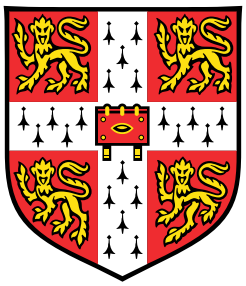

Aurelio Romero Bermúdez

Supervisor: Dr. Antonio Miguel García García

Theoretical Condensed Matter group, Department of Physics
University of Cambridge

This dissertation is submitted for the degree of
Doctor of Philosophy

Queens' College July 2016

To my grandfather, José, and his joyful pursuit of knowledge for the sake of it

Declaration

I hereby declare that except where specific reference is made to the work of others, the contents of this dissertation are original and have not been submitted in whole or in part for consideration for any other degree or qualification in this, or any other university. This dissertation is my own work and contains nothing which is the outcome of work done in collaboration with others, except as specified in the text and Acknowledgements. This dissertation contains fewer than 60,000 words including summary, tables, footnotes and appendices.

The core part of the thesis is based on research published in

- A. M. García-García and A. Romero-Bermúdez, *Conductivity and entanglement entropy of high dimensional holographic superconductors*, JHEP **09** (2015) 33, [arXiv:1502.03616].

- A. M. García-García and A. Romero-Bermúdez, *Drude weight and Mazur-Suzuki bounds in holography*, Phys. Rev. D **93** (2016) 066015, [arXiv:1512.04401].

- A. M. García-García, B. Loureiro and A. Romero-Bermúdez, *Transport in a gravity dual with a varying gravitational coupling constant*, Phys. Rev. D **94** (2016) 086007, [arXiv:1606.01142].

The research completed in the first year of the PhD lies outside the main topic of this thesis. More details may be found in

- A. Romero-Bermúdez and A. M. García-García, *Shape resonances and shell effects in thin-film multiband superconductors*, Phys. Rev. B **89** (2014) 024510, [arXiv:1311.0698].

- A. Romero-Bermúdez and A. M. García-García, *Size effects in superconducting thin films coupled to a substrate*, Phys. Rev. B **89** (2014) 064508, [arXiv:1311.4193].

Aurelio Romero Bermúdez

Acknowledgements

Foremost, I would like thank my supervisor and colleague Antonio. His guidance and constant patience have been very supporting throughout the way. He has been a fantastic mentor both in the academic and practical aspects.

I would also like to thank all my loving family, your guaranteed and reassuring support has allowed me to keep on going. Aurelio and Ángeles, your lessons made this possible. Paula you have been an inspiring example. Part of this thesis is owed to all of you.

Special thanks go to my partner, Duna, and her family. Thanks for always making me try to put things in perspective. Duna, thanks for believing it was possible and never giving up, certainly this thesis is also partly yours.

I am also grateful to the numerous and good friends that have made these past five years more fulfilling. Cristina, who took me to her Department five minutes after having arrived at Cambridge for the first time. I later understood this was a taster of the PhD lifestyle; since then your advice is highly valued. I am grateful for the cultural mingling, especially with the Latin American corner at Queens', in particular to Fernando, Marcos, Eduardo and Jorge, with whom I have shared many good times. I would like to thank Musabbir and Charles for interesting and, occasionally extremely random, conversations; I have learned a lot from these. Thanks to Charles and Audrey who gave me a hobby that has helped me during the PhD. I would like to thank Bruno, a friend and colleague, for interesting culinary and academic conversations.

Aurelio Romero Bermúdez

Summary

In this thesis we consider various applications the gauge/gravity duality to study transport in strongly coupled systems. The main content is organized in three parts.

In the first part we investigate the interrelation between dimensionality and strength of interactions. It is known that the dynamics of systems in Condensed Matter and General Relativity simplify for high dimensionality. Therefore, in this limit of large dimensionality, analytic results are usually possible. We study the dependence of the conductivity and the entanglement entropy on the space-time dimensionality in two different models of holographic superconductors: one dual to a quantum critical point with spontaneous symmetry breaking, and the other modeled by a charged scalar that condenses at a sufficiently low temperature in the presence of a Maxwell field. In the large dimensionality limit we obtain explicit analytical results for the conductivity at zero temperature and the entanglement entropy. Our results suggest that, as dimensionality increases, the condensate interactions become weaker.

In the second part we first investigate the Drude weight and the related Mazur-Suzuki (MS) bound in a broad variety of strongly coupled field theories with a gravity dual at nonzero temperature and chemical potential. We show that the MS bound, which in the context of Condensed Matter provides information on the integrability of the theory, is saturated in Einstein-Maxwell-dilaton (EMd) and R-charged backgrounds. We then explore EMd theories with $U(1)$ spontaneous symmetry breaking, and gravity duals of non-relativistic field theories, in which the MS bound is not saturated. Finally, we study the effect of a weak breaking of translational symmetry and we show that the MS bound sets a lower bound on the DC conductivity for a given scattering time.

In the last part, we study asymptotically anti de Sitter Brans-Dicke (BD) backgrounds as effective models of metals with a varying coupling constant. We show that, for translational invariant backgrounds, the zero-frequency conductivity (dc conductivity) deviates from the universal result of EMd models. Once translational symmetry is broken, the shear viscosity to entropy ratio is always lower than the Kovtun-Son-Starinets bound, in line with other gravity backgrounds with momentum relaxation. In the BD models studied, we observed insulating like features in the dc conductivity. However, the module and argument of the optical conductivity at intermediate frequencies are not consistent with cuprates experimental results, even assuming several channel of momentum relaxation.

We have also included the research carried out in the first year of the PhD as appendices. The topics studied in these appendices lie outside the main framework of this thesis and will not be further discussed.

Aurelio Romero Bermúdez

Contents

List of tables

List of figures

Nomenclature

Symbols

r	Holographic coordinate $r \in [r_0, \infty)$, unless otherwise stated
G_n	n-dimensional Newton's constant
$2\kappa^2$	$2\kappa^2 = 16\pi G_n$
d	Boundary theory space-time dimensionality
s	Entropy density
ρ	Charge density
ϵ	Energy density, unless otherwise stated
η	Shear viscosity, unless otherwise stated
e	Maxwell coupling constant
T_c	Critical temperature

Abbreviations

AdS	Anti de Sitter
BD	Brans-Dicke
CFT	Conformal field theory
EMd	Einstein-Maxwell-dilaton
EOM	Equation of motion
IR	Infrared
KSS	Kovtun-Son-Starinets
MS	Mazur-Suzuki
QCD	Quantum chromodynamics
QFT	Quantum field theory
QGP	Quark-gluon plasma
RN	Reissner-Nordström
ST	String Theory
SUGRA	Supergravity
SYM	Supersymmetric Yang-Mills
UV	Ultraviolet

1

Introduction and Overview

The study of interactions in many-body systems is arguably the common denominator of most areas in Physics. This problem also presents great difficulties when exact solutions are sought, even in classical systems. Indeed, for a large ensemble of particles, interactions (quantum or otherwise) broaden the system's phase space so significantly that the system cannot be handled without the use of approximations which may oversimplify the problem. Fortunately, in some cases a description that captures the essential features is possible by a clever identification of the low-energy excited levels. With this identification, typically, the many-body problem reduces to essentially a one-body problem and, possibly, a perturbative analysis. A typical example of this computational strategy in Condensed Matter is Landau's Fermi liquid theory [1–4].

Landau's strategy is to establish a one-to-one map between the excited states of a noninteracting system and a system in which interactions have been turned on adiabatically[1] [5–8]. For example, for electrons in three space-dimensional metals, the noninteracting model used to establish this map is the Sommerfeld Fermi gas [9]. In this description the ground state consists on a (noninteracting) gas of particles, the Fermi sea, distributed on states according to a step function with the discontinuity placed at the Fermi wavevector k_F; the excitations correspond to adding (removing) electrons with a well-defined energy and momentum above (below) k_F. Moreover, in the absence of interactions, these excitations leave all the particles of the Fermi sea unchanged.

However, if interactions are adiabatically turned on this picture no longer holds [5–7, 10–12].[2] The interactions will change the bare electrons step-function distribution, which is depleted (populated) below (above) k_F, i.e., holes and particles are created below and

[1] For simplicity we restrict to weak interactions where perturbation theory is still valid. However, as we will comment later, Landau's theory holds in many cases even if interactions are strong.

[2] We assume the ground state of the interacting system can be achieved by turning on interactions adiabatically, i.e., we exclude cases like superconducting ground states [7].

above k_F, respectively. Moreover, each of these particles and holes no longer moves freely but becomes 'dressed' by the rest of particles and holes. Provided interactions are not very strong they still behave very similarly to free electrons, albeit with some renormalized parameters like their mass [8, 5–7, 12]. These dressed particles are the quasi-particles (and quasi-holes) which, similarly to the noninteracting Fermi gas, correspond to the lower excitations of the ground state[3] and thus control the physical properties at energies close to the Fermi level. Moreover, close to the Fermi level the quasi-particles are weakly interacting and their distribution function obeys a Boltzmann-like kinetic equation [7, 6].

The key feature of this description is that, in a neighbourhood of the Fermi level, quasi-particles are not infinitely-lived, but have a finite 'lifetime' τ, which is parametrized by the self-energy: Σ. Therefore, the quasi-particles correspond to poles slightly away from the real line of the Green's functions [8, 5, 11, 13, 14]:

$$G(\omega,k)=\frac{1}{\omega-\epsilon_k-\Sigma(\omega,k)}\,,\quad \tau^{-1}=Z(k)\,\mathrm{Im}\,\Sigma(\omega(k),k)\,,\quad Z(k)=\frac{1}{1-\frac{\partial\Sigma(k,\omega)}{\partial\omega}} \tag{1.1}$$

The energy ω is measured with respect to the Fermi level, ϵ_k is the noninteracting particle dispersion relation, which together with $\mathrm{Re}\,\Sigma$, defines the quasi-particle dispersion relation, and Z is called the renormalization coefficient. $\mathrm{Im}\,\Sigma=0$ yields the one-particle spectral function consisting on Dirac's deltas with spectral weight Z, while for $\mathrm{Im}\,\Sigma\neq 0$ the spectral function has broad peaks with widths and spectral weights given by τ^{-1} and Z with some ambiguity [5, 14]. Therefore, around the Fermi level quasi-particles are well defined as long as the renormalization coefficient is nonzero and the peaks are narrow enough (compared to their separation) to be distinguishable.

Imposing $Z(\omega,k)$ to be nonzero together with eq. (1.1) set a regularity condition on Σ and its first derivative at $\omega=0$, $k=k_F$. In a Fermi liquid it turns out [2, 8, 5, 12, 11, 14, 15] that $\mathrm{Im}\,\Sigma(k\sim k_F,\omega)\propto\omega^2$ and $\mathrm{Re}\,\Sigma(k\sim k_F,\omega)\propto\omega$ to leading order. This result follows from scattering processes of quasi-particles between energy states. The Pauli principle restricts the scattering processes allowed: a quasi-particle $k\gtrsim k_F$ cannot scatter to occupied states $k<k_F$ and thus will have a very long lifetime, in particular right at $k=k_F$ the quasi-particle is infinitely lived. This small scattering phase space is essentially the reason why Landau's Fermi liquid works in some metals with strong interactions. The dominant scattering process close to the Fermi level is inelastic, which leads to a scattering rate $\Gamma\propto\omega^2+(\pi k_BT)^2$, where k_B is Boltzmann constant and T is temperature [15]. As a consequence, the quasi-particle lifetime $\tau^{-1}\propto\omega^2$ or $\tau^{-1}\propto T^2$ depending on which energy scale dominates.

[3] Additional excitations are possible: charge (or density for neutral fluids) and spin waves, however these can be treated as global modes or resonances of the particle-hole excitations [5]. For simplicity of the argument we do not consider these collective excitations. We note however that in $1+1$ dimensions excitations are in general forced to be collective [12]. If there were to exist a quasi-particle, it would immediately interact with its neighbours since being forced to move in one dimension leaves no escape from scattering on very short timescales [12].

The form of the self-energy discussed above leads to a nonzero $Z(k \sim k_F, \omega \sim 0)$ and thus, as long as τ^{-1} is much smaller than the separation between states, the quasi-particles around the Fermi level are well defined. Furthermore, the study of transport properties together with the dependence of the quasi-particle scattering time leads to one of the hallmarks of Fermi liquids, the quadratic dependence of resistivity in temperature[4] [8, 16, 15].

Landau's Fermi liquid is not only ubiquitous in most metals but also applies in other fermionic systems like the normal phase of liquid ^{3}He.[5] However, there are various ways in which the Fermi liquid description breaks down, for example if, at low temperature, the ground state described by the Fermi liquid is unstable and there is a transition to a state involving superconductivity or charge or spin modulation [14, 18]. Moreover, on general grounds it is expected a quasi-particle description might break down when interactions are cranked up and the perturbative treatment is not valid. Interactions shorten the quasi-particle lifetime so much that the peaks of the spectral density are hardly distinguishable. In this situation, it is reasonable to expect the degrees of freedom of a quantum system to rearrange and the intuition about the theory based on the weakly interacting quasi-particles, if any, is lost. A natural question to ask is whether quasi-particles can nevertheless be found in strongly coupled theories. While in certain systems this is the case [18–24], it is not always guaranteed. Typical examples that challenge quasi-particle descriptions are the deconfined phase of Quantum Chromodynamics (QCD) and the strange metals. Let us first discuss the deviation from the Fermi liquid phenomenology in strange metals.

With the discovery of high temperature superconductors, in particular Copper based superconductors, it was realized that their properties in the 'normal' state, i.e. outside the superconducting and pseudogap region, were anomalous [25–27], see [8] for a review of earlier experiments. For example, the resistivity increases linearly with temperature [25, 26], which is inconsistent with the quadratic dependence of Fermi liquids mentioned above. Therefore, these materials received the name of *strange metals* or *non-Fermi liquids*. Other universal properties of the strange metals are: the anomalous temperature dependence of the Hall angle [27, 28], the suppression of the Lorenz ratio [29] and the intermediate frequency scaling of the absolute value and phase of the conductivity: $|\sigma| \sim \omega^{-2/3}$, $\arg(\sigma) \sim \pi/3$ [30].[6] After the earlier experiments, it was soon realized these anomalous

[4] This is easily seen from the Drude formula for the resistivity $\rho_{\rm dc} \propto \tau^{-1}$ [14]. We note however that, experimentally it is difficult to observe this dependence due to additional scattering processes involving for example scattering by phonons and impurities which in the case of metals may be equally important [14, 7].

[5] Similar descriptions based on quasi-particles have also been used in early models of nuclei [17, 6]. There are many subtleties involved in a quasi-particle description of nuclei we have not discussed here. For the purpose of this thesis we do not need to enter in these subtleties and only wish to convey the wide spectrum of fields where quasi-particle descriptions are found.

[6] The list of experimental evidence cited is not by all means exhaustive. Moreover, we have focused on three dimensional materials, however, in lower dimensions there are also examples [31–33, 16] of interacting fermions which are not described by Landau's theory. The most studied example is the one-dimensional

behaviors were not intrinsic only to Copper based materials but it was a generic feature of materials with 'strong' electron-electron repulsive interaction [35].

Based on the experimental evidence regarding the linear scaling of the resistivity, a phenomenological approach termed 'Marginal Fermi Liquid' was proposed in [36]. This model postulates that such scaling is consistent with a scaling of the quasi-particle lifetime given by $\tau^{-1} \propto \max\{T, \omega\}$, as opposed to Landau's theory prediction $\tau^{-1} \propto \omega^2$. However, imposing this dependence implies that $\operatorname{Im}\Sigma \propto \omega$, $\operatorname{Re}\Sigma \propto \omega \log \omega$ for $\omega > T$ [8, 36] and so $\frac{\partial \operatorname{Re}\Sigma}{\partial \omega}$ diverges logarithmically around the Fermi level. This leads to a vanishing spectral weight at the Fermi level $Z(\omega = 0, k_F) = 0$ in eq. (1.1). Moreover, since $\operatorname{Im}\Sigma$ is odd, the symmetry between adding a quasi-particle or a quasi-hole is broken. Therefore, both perturbation theory and the quasi-particle description break down in these materials with strong interactions [36] and a new approach is needed.

We now review the case of QCD as our second example which exhibits the breakdown of a perturbative quasi-particle description.

In [37, 38] it was found that non-Abelian gauge theories are asymptotically free and QCD was suggested [39] as an example in which at high temperatures the coupling constant is perturbatively small. In particular, in this regime quarks and gluons are said to be in the deconfined phase while at low energy, the coupling becomes strong and quarks and gluons are confined. Based on this brief description, it is reasonable to expect perturbation theory to be appropriate as the system approaches the deconfined phase. However, after experiments allowed to probe this phase it was soon realized that a perturbative approach failed to describe the experimental results [40].

The earliest evidence suggesting the plasma of quarks and gluons (QGP) generated soon after heavy-ion collisions was not weakly coupled is related to the *elliptic flow* of the plasma.[7] More specifically, the elliptic flow obtained from the measurements was not reproduced by the results of the perturbative QCD cross sections combined with kinetic theory of quarks and gluons scattering processes [40]. Therefore, the separation of scales on which Boltzmann's equation is based does not apply in this case. Additionally, a measure of the viscosity of the QGP suggested it behaved almost like a perfect fluid, namely the ratio of the shear viscosity and the entropy density η/s was small $O(10^{-1})$. On the other hand, a perturbative calculation of the shear viscosity at large temperature in (Abelian or non-Abelian) gauge theories η/s yields [41]

$$\frac{\eta}{s} \propto \frac{1}{g^4 \ln\left(g^{-1}\right)} ,$$

(in space) Luttinger liquid [34, 12], which is the playground of Condensed Matter theorists in the same way as Conformal Field Theory is in High Energy Physics.

[7] For the purposes of this thesis it is not important to go into details about this observable. It is a measure the response of the system to initial anisotropy of the energy density or particles, as viewed along the collision beam-line.

where g is the gauge coupling. A similar result is obtained in simpler theories, like scalar field theories ($\frac{\lambda}{4!}\phi^4$) [42]: $\eta/s \sim 1/\lambda^2$. This suggests that perturbative calculations for weak coupling lead to $\eta/s \gg 1$, in stark contrast with the smallness of the experimental results for the QGP. Moreover, the elliptic flow data is well fitted using a hydrodynamical calculation as long as the viscosity to entropy density ratio is $O(10^{-1})$ [43].

These findings changed the understanding of the QGP; they suggest that the QGP is almost an ideal fluid as described by hydrodynamics. Since a hydrodynamical description is valid only for length scales much longer that the mean free path of the real system constituents, then the constituents of the QGP must have very short mean free path and thus must be strongly interacting.

Summarizing, there is strong evidence that suggests the mechanism underlying the strange metals and the QGP is characterized by strong interactions and the absence of quasi-particles. This restricts the theoretical tools available to study these systems. Therefore, the motivation to find new theoretical descriptions in both Abelian and non-Abelian theories has grown dramatically; we now introduce the AdS/CFT correspondence [44–46] and the reasons it has become a useful tool for this purpose.

A first glance into the AdS/CFT correspondence

Before we present the main idea of the correspondence it is important to review part of the background that led to its formulation. It is also convenient to note at this point that we will usually use the name 'AdS/CFT correspondence' to refer a formulation given in [44], soon after developed in [45, 46]. For reasons that will become evident below, we will refer to generalizations of this correspondence as gauge/gravity dualities, bulk/boundary dualities or simply, holography.

Let us first review examples of dualities in Physics and the reason dualities can be useful. Broadly speaking, a duality consists on a map between theories with different physical content (at the level of the Lagrangian) or in different range of parameters. Each theory however may be very similar from a mathematical point of view (for example their Hilbert spaces), which is why such map can be constructed. If this map exists, it is possible to restrict the behaviour of a theory based on knowledge of its *dual* theory. Some important examples are the Kramers-Wannier duality [47, 48] and the S-duality [49, 50]. The first relates low and high temperature limits of a two-dimensional square-lattice Ising model, while the second relates strong and weak coupling regimes of string theories.

The relation between strong and weak coupling imposed by the S-duality is very useful to gain insight about the non-perturbative behavior of a String Theory (ST) which is invariant under the S-duality transformation. A similar situation exists in the AdS/CFT correspondence, it conjectures the equivalence between a ST and a QFT, which in certain regime ('large-N') becomes a reliable map between a strongly coupled QFT and a weakly coupled classical theory of gravity in one higher dimension [51]. However,

there are important differences with respect to the previous dualities: first, the different dimensionality of the theories involved and second, the former dualities relate quantum theories while the latter, in the large-N limit, establishes a connection between a classical and a quantum theory. Let us now discuss the role of these two features, different dimensionality and large-N limit, in the AdS/CFT correspondence.

G. 't Hooft: holographic principle and large-N

Two important components which precede gauge/gravity dualities are the holographic principle and the large-N limit.

The holographic principle introduced by 't Hooft [52] states that in a gravitational theory the information inside a volume V may be stored or encoded in its boundary area ∂V, much like a holographic image. This statement allows to understand intuitively why the AdS/CFT correspondence manages to bypass the Weinberg-Witten [53] theorem, which implies that the degrees of freedom needed in gravity cannot propagate in a Lorentz covariant quantum field theory in $3+1$ dimensions. This means that a theory of gravity and a quantum field theory can not be equivalent or dual in $3+1$ dimensions. As we will see however, the gauge/gravity duality bypasses this theorem by relating gravitational and quantum theories with different dimensionalities.

The large-N limit corresponds to the limit of large representation of a gauge group i.e., N parametrizes the rank of a gauge group: $U(N)$, $SU(N)$, $O(N)$, etc. This limit has been extensively used in various contexts such as Ising and Heisenberg models [54–58] as well as Yang-Mills and σ models [59, 60], and the so-called large-N QCD [61–63].

Taking $N \to \infty$ corresponds to a classical limit, since for large N an operator O is sharply concentrated around its expectation value [64]

$$\left\langle (O - \langle O \rangle)^2 \right\rangle \simeq \mathcal{O}(N^{-2}) \,.$$

The large-N limit plays a central role in the AdS/CFT correspondence [51, 50]. Namely, the correspondence, in its original formulation [44], states that for $N \to \infty$ the Hilbert space of $\mathcal{N} = 4$ supersymmetric Yang-Mills theory (SYM) with gauge group $U(N)$ should match that of type IIB supergravity (SUGRA) in a particular product space: $\mathrm{AdS}_5 \times S^5$, where AdS_5 is five dimensional anti de Sitter space (AdS) and S^5 is the five-sphere.

While this connection might seem unexpected, it had long been suspected that there should exist a relation between string theories and confining gauge theories.[8] Indeed, in the context of QCD_2 at large-N, which is a $1+1$ dimensional toy model of QCD, numerous similarities with String Theories had been pointed out [61, 65–69].

[8] The intuitive idea behind this relation in the case of QCD is based on the picture of bound quark and anti-quark pairs in the confined phase of QCD. The dynamics of such system were found to be similar to that of a string with massive quarks at each end [50].

As we will explain in Chapter 2, SYM gauge theory emerges by studying the low energy limit of non-perturbative objects in String Theory called *D-branes*, which had been previously linked [70] to solutions in classical supergravity: p-branes. The role of the large-N limit in the correspondence is to have a tractable (classical) gravitational description. Moreover, for large N the effective coupling in the emergent SYM theory ('t Hooft coupling) restricts the theory to the strongly coupled regime [59]. Therefore, according to the AdS/CFT correspondence, it is possible to study the strongly coupled limit of SYM by looking at a classical theory of (super)gravity.

While this is an interesting result on its own, its connection to strong interactions and the absence of quasi-particles in the QGP and strange metals is far from clear. Let us now clarify why AdS/CFT correspondence can potentially cast some light on these systems.

Connecting the duality to strongly coupled systems

Let us start with the connection between the AdS/CFT correspondence and the QGP, which we introduced in the context of QCD. Even though we have mentioned it was believed there should be a connection between gauge theories, QCD and String Theories, at first sight there are important differences between QCD and $\mathcal{N} = 4$ SYM [71]. Some of the differences that should be clarified for the correspondence to be useful in QCD are: SYM is supersymmetric and scale invariant, while QCD does not have supersymmetry and has a fundamental scale given by the confining/deconfining transition temperature. Nonetheless, scale invariance and supersymmetry are broken upon introducing temperature in $\mathcal{N} = 4$ SYM.[9] Another caveat is that QCD has a confining phase while $\mathcal{N} = 4$ SYM does not, but this is not relevant for the study of the QGP. Moreover, in SYM there are no flavour degrees of freedom[10] and the number colours $N \to \infty$, while in QCD there are $N_f = 3$ flavours and $N = 3$ colors.

Despite these differences, it has been found that, when comparing observables which do not depend on the number of degrees of freedom of the theory, the deconfined phase of QCD is qualitatively similar to $\mathcal{N} = 4$ SYM at nonzero temperature. Indeed, soon after the realization that the QGP was strongly coupled, Policastro, Son and Starinets [75] computed, using the AdS/CFT correspondence, the shear viscosity in $\mathcal{N} = 4$ SYM at nonzero temperature in the limit of strong coupling (large-N). The result yields $\eta/s = 1/4\pi$, which is much closer to what was expected from the experimental evidence $O(10^{-1})$, than the perturbative calculations mentioned earlier. Therefore, it seems that both the deconfined phase of QCD and $\mathcal{N} = 4$ SYM are described by a strongly coupled plasma, and η/s obtained holographically is consistent with that of the QGP. For recent studies combining the AdS/CFT correspondence and hydrodynamical approaches to

[9] As we will see in Sec. 2.3.2 it is possible to introduce temperature in $\mathcal{N} = 4$ SYM through the gauge/gravity duality by considering black branes in the gravity theory.

[10] These can be added by considering additional D-branes in the gravitational description [72, 73] though usually the number of flavours $N_f \ll N$ [74].

the QGP see [76–79, 43]. Other applications of the AdS/CFT correspondence to QCD were initiated in [80] to study confinement/deconfinement phase transitions and further developments about holographic approaches to QCD followed in [81, 74, 82–85].

Regarding the relation between the correspondence and the strange metals, since we lack a complete quantum theory for these materials, most of the information available comes from experimental sources, as we mentioned before. However, trying to use the AdS/CFT correspondence does not seem very promising either, after all the connection of SYM theory and strange metals is far less clear than in the case of QCD. Therefore, in order to account for the phenomenology of strange metals and of other Condensed Matter systems using gauge/gravity dualities, a *bottom-up* approach is usually taken. This is a phenomenological approach which consists on proposing an action for a theory of gravity plus matter fields. With this scheme at hand, the authors of [86–89] have studied the fermionic spectral functions of theories dual to charged black holes plus bulk spinor fields. Anomalous scaling with energy has been found in the self-energy; in particular in [88, 89] the phenomenological dependence proposed in the Marginal Fermi Liquid ($\Sigma \propto \omega \log \omega + ic\omega$ for some constant c) was recovered.[11] The linear in temperature resistivity found in strange metals has also been reproduced in holographic settings by using quantum critical points with Lifshitz exponent [88, 91–93] and in models with additional anomalous exponents [94, 95]. Moreover, by introducing an oscillatory (in space) distribution of charge an encouraging result was reported in [96, 97]: an intermediate scaling of the conductivity similar to that found in strange metals: $|\sigma| \sim \omega^{-2/3}$, $\arg(\sigma) \sim \pi/3$. However, it was later reported in [98] there was no evidence of such scaling. More recently [99] evidence of such intermediate-frequency behavior was found in a more sophisticated holographic model involving the Dirac-Born-Infeld action [50, 99]. Nonetheless, to our knowledge, holographic settings displaying both the intermediate-frequency behavior mentioned before, and a linear temperature dependence of the resistivity, remain to be found.

Bottom-up approaches, as those used in the references mentioned above, are usually easier to construct and allow to reproduce features of more general field theories than those obtained in top-down constructions. We note however this approach has important drawbacks. First, the nature of the dual field theory (if it exists) is not known. Nonetheless, usually it is possible to obtain some information from symmetry arguments, while the observables in the dual theory are calculated following the field-operator map developed for the original correspondence [45, 46, 100]. Second, by introducing matter fields *ad hoc* it is possible that some fields or interaction terms are neglected or unphysical. Moreover, the stability of such effective theories is *a priori* unclear as the model is not supported by a well-behaved String Theory compactification.

Another possibility is to follow *top-down* approaches, which consist on compactifying a String Theory on different spaces and, in the same spirit of the original correspondence,

[11] Spectral functions with Fermi liquid behavior have also been observed in holographic models [90].

identifying the degrees of freedom of the dual theory.[12] Top-down holographic models have been used to describe the phenomenology of metallic properties, superconductivity and Fermi surfaces in Condensed Matter systems [101–107], though we will not use these constructions here.

In this thesis we will follow the former approach. Even though the information about the degrees of freedom obtained using effective gravity models is only qualitative, it is still very useful, especially in the absence of a quantum field theory to describe a given strongly coupled system. The effective holographic models with strange metallic behavior mentioned before are clear examples of this. We have seen that by studying spectral functions and transport properties it is possible to obtain information about the strongly correlated character of the underlying interactions and, in some cases, identify whether there exist quasi-particles in the dual theory. These models rely on effective constructions involving charged black branes, which display metallic behavior in the boundary theory [90, 87, 108–111].[13] After the initial studies of these 'holographic metals' the interest of applying gauge/gravity dualities to other Condensed Matter systems grew considerably. For instance, the models of [112–117] display spontaneous $U(1)$ symmetry breaking and thus set the basic gravitational setup for phenomenological approaches of superconductivity. Indeed, these models received considerable attention as they aimed to describe high-temperature superconductors through the gauge/gravity duality. Even though they are far from doing so, they display interesting features like a broad peak in the optical electrical conductivity [113, 114], which is a clear indication of strong interactions. In this thesis we elaborate on these models to address the question of how the strength of interactions depends on dimensionality. It is known [118] that for large number of dimensions black hole dynamics in General Relativity simplifies and fields outside the black holes propagate in basically flat space. This universal behavior of gravity should be reflected in boundary theories of holographic constructions.

Moreover, motivated by the study of quantum phase transitions and quantum critical points (QCP) in Condensed Matter [119, 120], there have also been efforts aimed to study the low temperature dynamics of strongly correlated electron systems near a QCP [89, 94, 121–129, 99]. This has allowed to establish a robust but mysterious connection between quantum critical properties of the dual field theory and the emergence of AdS_2 in the infrared bulk geometry at zero temperature. Of particular interest in this thesis is the Einstein-Maxwell-dilaton (EMd) model put forward in [94]. This model refines Einstein-Maxwell theory by including a relevant (in the infrared) scalar field in the dynamics of the theory. This results in a rich and useful phenomenology in a bottom-up holographic approach to strongly coupled systems. We exploit this phenomenology to study transport

[12] There exist other well established gauge/gravity dualities which involve different conformal theories instead of SYM. We will mention two examples in Chapter 2.

[13] There also exist also top-down constructions with similar metallic properties [101–103], however soon after these studies the bottom-up constructions became more popular.

properties in theories with and without translational symmetry and introduce bounds which were known in the context of Condensed Matter but had not been applied to holographic models.

Despite the gradual sophistication of the models mentioned above, most of them are still too simplistic to establish a connection with the phenomenology of systems like strange metals. One of the main limitations is translational invariance which implies momentum conservation in the boundary theory. In holographic theories, momentum dissipation in the boundary theory has been introduced by breaking diffeomorphism invariance in the spatial dimensions in various ways: through a random chemical potential [130–135], using massive gravity theories [136–138] and introducing scalar fields with a simple spatial dependence [125, 139–141, 127]. Based on these studies it was conjectured [142] there existed a lower bound on the zero-frequency electrical conductivity (dc conductivity) in $2+1$ dimensions which precludes the transition to an insulator in holographic models. Recently [143, 144] this bound has been found to be violated. This has reinvigorated the search of effective holographic theories with insulating and, possibly, strange metallic behavior. In the spirit of [143, 144] we have used EMd-inspired models with an additional non-minimal coupling to look at the limits of the universal conductivity found using EMd models, as well as to study strong momentum dissipation when the couplings break diffeomorphism invariance.

Moreover, motivated by both top-down and bottom-up approaches, there has been recently more interest in finding exotic gravitational solutions numerically in asymptotic AdS spaces [145–150]. These solutions allow to explore a richer phenomenology through gauge/gravity dualities, however, this approach is out of the scope of this thesis.

Before we conclude the Introduction we give a brief overview of the contents of the next chapters.

Overview

We start next chapter, with a brief explanation of what 'AdS/CFT' stands for and look at the formulation of the AdS/CFT correspondence. We then review the practical aspects of the correspondence, such as the mapping from the gravity fields to the dual operators, the method to compute response functions through gauge/gravity dualities and, as an example, we show how to compute the electric conductivity using the AdS Reissner-Nördstrom black brane. We conclude Chapter 2 by reviewing the setup we use in this thesis to describe momentum relaxation and its implications for transport properties.

In Chapters 3-5 we consider various applications of the gauge/gravity duality to probe the phenomenology of strongly coupled systems. We follow three different strategies to investigate the universality of holographic models: 1) high dimensionality, 2) limit of weak momentum relaxation and 3) models with varying gravitational coupling constant and strong breaking of translational symmetry. Let us elaborate more on these strategies.

In Chapter 3 we study the interrelation between dimensionality and strength of interactions. We investigate the dependence of the electrical conductivity on the space-time dimensionality d in two models: one dual to a quantum critical point with spontaneous $U(1)$ symmetry breaking, and the other modeled by a charged scalar that condenses at a sufficiently low temperature in the presence of a Maxwell field. We also study the holographic entanglement entropy [151]; the entanglement entropy is an important observable which allows to estimate the level of quantum entanglement and propagation of information in a quantum system.

In Chapter 4 we investigate the infinite part of the dc conductivity in various models with translational symmetry. The infinite part is controlled by a Dirac's delta at zero frequency and its coefficient is called the Drude weight. We investigate to what extent the Drude weight is universal and introduce the related Mazur-Suzuki bound in a broad variety of strongly coupled field theories at nonzero temperature and chemical potential. We also explore the Mazur-Suzuki (MS) bound in EMd theories [94] with $U(1)$ spontaneous symmetry breaking [127] and gravity duals of nonrelativistic field theories [152, 153]. Finally, we study the effect of weakly breaking translational symmetry and how the MS bound enters in the regular part of the dc conductivity once translational invariance is broken.

Having studied the limit of weak momentum relaxation, in Chapter 5 we go to the opposite limit and allow the translational symmetry to be strongly broken; we also consider various couplings of the Ricci scalar in order to obtain a richer phenomenology. More precisely, we study asymptotically AdS Brans-Dicke backgrounds, where gravity is coupled to a scalar in the radial dimension, as effective models of metals with a varying coupling constant. We study how the known universal dc conductivity (the regular part) found through EMd is modified. We conclude by breaking translational symmetry through the gravity couplings to study the effect of strong momentum relaxation on the conductivity and shear viscosity.

In appendices C and D we include the research developed in the first year of the PhD. This research lays outside the framework of the gauge/gravity duality and will not be discussed hereafter.

2

The AdS/CFT correspondence

In the previous chapter we have motivated the AdS/CFT correspondence [44–46] as a useful tool to study strongly coupled systems, such as the quark-gluon plasma and strange metals. We have also vaguely mentioned the gravity and quantum theories involved in the correspondence. In order to give a more precise statement of the correspondence we first review in Secs. 2.1 and 2.2 the necessary background regarding conformal symmetry, anti de Sitter space and String Theory. We finish sec. 2.2 with a more precise formulation of the AdS/CFT correspondence. We do not present with utmost rigor the sophisticated steps [51] involved in the derivation of the correspondence, but only grasp the relevant ideas. The aim of these two sections is to understand the original framework of the AdS/CFT correspondence.

The next step is to identify the key aspects needed to use the gauge/gravity dualities to study strongly coupled systems. For this purpose we cover in Sec. 2.3 the relation between the gravitational and the field theory degrees of freedom; this is commonly known as the 'field-operator map' [45, 46, 100]. In this section we also review how to compute the field theory partition function from the bulk gravitational action [45, 46] and how temperature is introduced in a field theory with a gravity dual [51]. Next, in Sec. 2.4 we review linear response theory in QFT [154, 155] and the difficulties associated with computing finite temperature correlators [156–162]. We also explain how Green's functions are calculated holographically [163, 164]. We finish this section with the calculation of the electrical conductivity in the simplest holographic setting for this purpose: the Reissner-Nordström black brane [165]. This example will serve as the starting point to calculate transport properties in the models used in this thesis.

We finish this chapter with comments on how to break diffeomorphism invariance in spatial coordinates which, as we mentioned in the Introduction, is important to construct realistic models with momentum dissipation [136, 139].

In addition to the references mentioned above, most of this chapter is based on excellent reviews and books on the gauge/gravity duality, QFT, String Theory and related topics [5, 71, 50, 166–174].

2.1 Conformal invariance and anti de Sitter space

Conformal invariance

The conformal transformations are maps which preserve the metric up to a multiplicative factor, or scale. These coordinate transformations change the metric by an overall factor $g_{\mu\nu} \to \Lambda g_{\mu\nu}$. In other words, a transformation from x^μ and $\tilde{x}^\mu$ satisfies,

$$g_{\alpha\beta}(\tilde{x})\frac{\partial\tilde{x}^\alpha}{\partial x^\mu}\frac{\partial\tilde{x}^\beta}{\partial x^\nu} = \Lambda(x)g_{\mu\nu}(x) \ , \tag{2.1}$$

where $\Lambda(x) > 0$ is the *conformal factor*. For the case of $g = \eta = \text{diag}\{-1, \dots, +1, \dots\}$ and $\Lambda = 1$ the conformal transformations reduce to the Lorentz transformations.

The conditions for a transformation to be conformal are more easily understood by looking at the infinitesimal transformation $\tilde{x}^\mu = x^\mu + \epsilon^\mu(x) + \mathcal{O}(\epsilon^2)$, $\epsilon \ll 1$. After the substitution of $\tilde{x}^\mu$ in eq. (2.1) and simple manipulations, it follows that the most general ϵ_μ is [50, 175]

$$\epsilon_\mu = a_\mu + b_{\mu\nu}x^\nu + c_{\mu\nu\rho}x^\nu x^\rho \ , \quad a_\mu, b_{\mu\nu}, c_{\mu\nu\rho} \ll 1 \ ,$$

where the term a_μ corresponds to a translation transformation while $b_{\mu\nu}$ econdes a dilatation in its symmetric part and a rotation in its antisymmetric part. The last term $c_{\mu\nu\rho}x^\nu x^\rho$ receives the name of *special conformal transformations*, which can be cast as an inversion and translation according to

$$\frac{\tilde{x}^\mu}{\tilde{x}_\alpha\tilde{x}^\alpha} = \frac{x^\mu}{x_\alpha x^\alpha} - b^\mu \ .$$

The globally defined and invertible conformal transformations form a group and its Lie algebra receives the name of conformal algebra. The relevant case in this thesis is conformal group of $\mathbb{R}^{p,q}$, $d - 1 = p + q \geq 3$, which is isomorphic to the indefinite special orthogonal group $SO(p + 1, q + 1)$.

A field theory which is invariant under the transformations eq. (2.1) is a conformal field theory. The change of a scalar field, $\phi(x^\mu)$, in a conformal field theory under a dilatation or scaling transformation $x^\mu \to \tilde{x}^\mu = \lambda x^\mu$ is of special interest to holography. This transformation defines the *conformal dimension* Δ of a scalar field: $\phi(\lambda x^\mu) = \lambda^{-\Delta}\phi(x^\mu)$.

Moreover, conformal invariance imposes restrictions on two-point functions of scalar fields of conformal dimensions Δ_1 and Δ_2 as follows

$$\langle\phi_{\Delta_1}(x_1)\phi_{\Delta_2}(x_2)\rangle \propto \frac{\delta_{\Delta_1\Delta_2}}{|x_1 - x_2|^{2\Delta_1}} \ , \tag{2.2}$$

as well as on the stress energy tensor, which should be conserved and traceless.

Anti de Sitter spacetime

Anti de Sitter space, AdS_d, may be represented by a hyperboloid in flat space in $d+1$ dimensions through the embedding [176, 51, 168, 166]

$$X_0^2 + X_d^2 - \sum_{i=1}^{d-1} X_i^2 = L^2 \ .$$

The embedding above is invariant under $SO(2, d-1)$ transformations. A convenient coordinate choice is the *global* coordinate system defined by

$$X_0 = L\cosh\rho\cos\tau \ , \quad X_d = L\cosh\rho\sin\tau \ , \quad X_i = Lr_i\sinh\rho \ , \quad \sum_{i=1}^{d-1} r_i^2 = 1 \ .$$

The quantities r_i parametrize a sphere S^{d-2} and $\rho \geq 0$ while, in principle, $\tau \in [0, 2\pi)]$ but it may be extended to the whole Real line. In order to include spatial infinity ρ is parametrized according to $\sinh\rho = \tan\theta$, $\theta \in [0, \pi/2)$ and the point $\theta = \pi/2$ is added. At this point, which represents the boundary of AdS_d, the metric is conformal to the metric of the compactified Minkowski space in $d-1$ dimensions $\mathbb{R}^{1,d-2}$.

For the practical purposes of this thesis we however work in the Poincaré patch coordinates, which, contrary to the global coordinates defined above, does not cover the whole AdS_d. In the Poincaré coordinates the metric is given by:

$$ds^2_{\mathrm{AdS}_d} = \frac{L^2}{z^2}(-\mathrm{d}t^2 + \mathrm{d}z^2 + \mathrm{d}x_i\mathrm{d}x_i) \ , \quad i = 1, \ldots, d-2 \ , \tag{2.3}$$

where $z > 0$ and the boundary is located at $z = 0$.

Moreover, the geometry described above, is a solution of the Einstein's equations with a negative cosmological constant. As we will see later, the correspondence relates a theory of gravity in a product space containing AdS_5 to a conformal field theory in four dimensions, which in the previous coordinate system are represented by t and x_i. Moreover, the coordinate z is usually referred to as the *holographic* coordinate in the *bulk*: $z > 0$.

2.2 Formulation of the duality

Comments on string theory

String theory (ST) may be broadly defined as a quantum theory of interacting relativistic one-dimensional objects rather than point particles as in QFT [50, 177, 71, 168].

The starting point of some string theories (*type II*) is postulating that the action which governs the closed string dynamics is a measure of the area of its world sheet [50, 177, 71].

The world sheet is the generalization of the particle world line for a one dimensional object (string); it describes the embedding of a string in a spacetime.

The quantization of such action leads to constraints on different features of the theory, most notably the dimensionality of the spacetime and the allowed string vibration modes, or spectrum. The theory relevant for the correspondence contains amongst the degrees freedom both bosons and fermions, related to each other by supersymmetry. Moreover, adding open strings leads to the definition of important objects called *D-branes* [70, 51, 50, 177]. Shortly, we will see that the study of these objects and their connection to, seemingly unrelated, solutions of string theories in certain limit (*p-branes*) [178, 50] led to the proposal of the AdS/CFT correspondence.

Two important parameters in string theory are the dimensionless string coupling constant g_s and the Regge slope α' (with dimensions of square length). Instead of α' it is also common to use either the string tension per unit of length $T = \frac{1}{2\pi\alpha'}$ or the string length $l_s^2 = \alpha'$. The parameters g_s and α' may be used to obtain two independent expansions of the theory. Expansion in small g_s gives the *classical* limit; it suppresses quantum effects by allowing loop diagrams in the perturbative treatment of interactions to be neglected [168]. Expansion in small α' (compared to the square of a characteristic length $\alpha'/L^2 \ll 1$ or energy scale $\alpha' E^2 \ll 1$) suppresses 'stringy' effects, i.e., for small α' strings are well approximated by point particles. The latter expansion corresponds to the *supergravity* (SUGRA) limit [50, 168].

Open/closed string perspectives

Open string perspective

Here we focus on objects called D-branes. As briefly mentioned before, these are defined by adding open strings to a string theory of closed strings, and imposing appropriate boundary conditions on the endpoints of the open strings [70, 51, 50, 177]. These boundary conditions are Neumann on $p+1$ dimensions (p spatial plus time), and on the rest of the dimensions, the boundary conditions are Dirichlet. Since we focus on objects defined from open strings, this description is commonly referred to as the open string description or perspective [51].

Perturbatively (in g_s) a stack of N $D3$-branes is well described by N hyperplanes in flat spacetime. Excitations of the branes are open strings with endpoints on the branes, while excitations of the empty space are the closed strings (propagating 'outside' the branes).

At low energy $E \ll \alpha'^{-1/2}$,[1] the dynamics of the closed strings, outside the branes, and of the open strings, with endpoints on the branes, decouple.[2] The closed strings

[1] More specifically, by low energy we mean that the energy and dimensionless parameters like N are fixed and α' tends to zero [51].

[2] On a technical level, for low energy the type IIB supergravity action separates the dynamics of massless closed strings, open strings and interaction terms [168, 50]. The dynamics of open strings and

dynamics consist on gravity and a scalar field, the dilaton. The open strings dynamics are expressed through various gauge and scalar fields, while the coupling to closed strings is mediated through terms containing the dilaton and gauge fields. At low energy, the terms interaction and closed string terms are subleading with respect to the open string terms [51, 168]. Such decoupling leads to two distinct theories, namely

- Type IIB supergravity in ten-dimensional flat spacetime governing the closed string dynamics.
- $\mathcal{N} = 4$ super-Yang-Mills (SYM) theory in $3+1$ dimensions, with gauge group $U(N)$ and coupling constant $g_{YM}^2 = 4\pi g_s$ governing the open string dynamics.

Moreover, one may choose the gauge group in the SYM theory as $SU(N)$ since the gauge the $U(1)$ subgroup decouples from the rest of the $SU(N) \subset U(N)$ [51].

In this description, apart from the low energy limit we have also taken the classical limit (or loop expansion). The effective coupling that controls such loop expansion is g_s, as mentioned in the previous subsection, but it is $g_s N$ due to the presence of N D-branes [51]. Therefore the above description is valid for

$$g_s N \sim g_{YM}^2 N \ll 1\,. \tag{2.4}$$

Closed string perspective

We now focus on black p-branes, which are solutions of the classical limit (small g_s) of supergravity (small string length) theories charged under a non-trivial $p+1$ antisymmetric tensor field $A_{\mu_1\ldots\mu_{p+1}}$ and with the associated $p+2$-form field strength: $F_{p+2} = dA$ [178, 50]. Since these solutions were found in the aforementioned limits of a theory of closed strings, hence the discussion presented in this section is usually referred to as the closed string perspective.

These solutions were obtained before D-branes were defined and were thought to be unrelated. However, it was later suggested [70] that D-branes, obtained by adding open strings to a theory of closed strings as defined in the previous section, are an alternate description of p-branes. Hence, the name of Dp-brane.

The geometry of a Dp-brane is that of a flat hypersurface with Poincaré invariance group $\mathbb{R}^{p+1} \times SO(1,p)$. The solution may be written for a general p [180], but we now take the particular case $p = 3$:

$$\mathrm{d}s^2 = H^{-\frac{1}{2}}(-\mathrm{d}t^2 + \mathrm{d}x_1^2 + \mathrm{d}x_2^2 + \mathrm{d}x_3^2) + H^{\frac{1}{2}}(\mathrm{d}r^2 + r^2\mathrm{d}\Omega_5^2)\ , \tag{2.5}$$

their interactions with closed strings may be obtained from the expansion of the Dirac-Born-Infeld (DBI) action around a flat metric [168, 50]. In fact, the resummation of all higher order corrections in α' results exactly into the DBI action [179].

where t and x_i are the coordinates on the hyperplane, y_i are the transverse coordinates and $r^2 = \sum_{i=1}^{6} y_i^2$. The function H is parametrized by L:

$$H = 1 + \frac{L^4}{r^4} , \quad L^4 = 4\pi g_s \alpha'^2 . \tag{2.6}$$

Of special interest in the correspondence is the solution of N coincident $D3$ branes,[3] in which case the constant L is [168]

$$L^4 = 4\pi N g_s \alpha'^2 . \tag{2.7}$$

It is now easy to see that for $r \gg L$, the geometry given in eq. (2.5) reduces to flat space in ten dimensions. On the other hand, for $r \ll L$, the geometry factorizes into a five-sphere and anti de Sitter space in five dimensions: $\mathrm{AdS}_5 \times S^5$. More explicitly, performing the change of variable $z = L^2/r$, and taking $r \ll L$, eq. (2.5) reduces to

$$\mathrm{d}s^2 = \mathrm{d}s^2_{\mathrm{AdS}_5} + L^2 \mathrm{d}\Omega_5^2 , \tag{2.8}$$

where $\mathrm{d}s^2_{\mathrm{AdS}_5}$ is given in eq. (2.3). In other words, there are two regions $r \gg L$ and $r \ll L$, where the theory is well approximated by:

- Type IIB supergravity in ten-dimensional flat spacetime for $r \gg L$.
- Type IIB supergravity in $\mathrm{AdS}_5 \times S^5$ for $r \ll L$.

Notice however that the solution given in eq. (2.5) is obtained within the classical ($g_s \ll 1$) and supergravity approximations. The latter means that the characteristic length scale of this solution L should be much larger that the string length $l_s = \sqrt{\alpha'}$. These conditions, combined with eq. (2.7) imply

$$N \gg g_s N \gg 1 . \tag{2.9}$$

Reconciling perspectives

As was mentioned in the beginning of the section on the closed string perspective, D-branes and p-branes are equivalent objects. Therefore, it is natural to suggest that both the open and closed string perspective, together with the theories described in each of them, should also be equivalent or *dual*. Indeed, both perspectives contain a theory of gravity in flat ten-dimensional space. The other two theories which are expected to be dual are, $\mathcal{N} = 4$ $U(N)$ SYM and a classical theory of gravity on $\mathrm{AdS}_5 \times S^5$. There is however a caveat, the descriptions given in the previous sections are valid in different

[3] As it will become clear when we look at the statement of the duality, it is important to note that the flux of the five form F_5 through S^5 is given exactly by the number of coincident D3-branes: N.

regimes [51]: eqs. (2.4) and (2.9). This is the reason why it is conjectured [44] that the classical supergravity theory on $AdS_5 \times S^5$ (of the closed string perspective) is the same as the $\mathcal{N} = 4$ SYM theory when the latter is strongly coupled and its perturbative approximation breaks down. In this gauge theory the coupling strength is governed by the 't Hooft coupling $\lambda = g_{YM}^2 N$, where $g_{YM}^2 = 4\pi g_s$. Therefore eq. (2.9) implies $\lambda \gg 1$, which is the strongly coupled limit of SYM [59].

This relation between a strongly coupled gauge theory and a classical theory of gravity is usually referred to as the weak form of the correspondence. If the restrictions on the parameters ($N \to \infty$ and $\lambda \gg 1$) are relaxed one obtains the *strong* and *strongest* forms of the duality [168] as indicated in Tab. 2.1.

	$\mathcal{N} = 4$ SYM	IIB ST on $AdS_5 \times S^5$
Strongest form	Any N, any λ	Quantum ST $g_s \neq 0$, $\frac{l_s}{L} \neq 0$
Strong form	Any $N \to \infty$, any λ	Classical ST $g_s \to 0$, $\frac{l_s}{L} \neq 0$
Weak form	$N \to \infty$, $\lambda \gg 1$	Classical SUGRA $g_s \to 0$, $\frac{l_s}{L} \to 0$

Table 2.1 Different forms of the AdS/CFT correspondence.

Summarizing, the AdS/CFT correspondence [44–46] conjectures the equivalence of

- $\mathcal{N} = 4$ super Yang-Mills theory in $3 + 1$ dimensional Minkowski space with gauge group $SU(N)$ and Yang-Mills coupling g_{YM}.
- Type IIB superstring theory with string length $l_s = \sqrt{\alpha'}$ and coupling constant g_s on $AdS_5 \times S^5$ and the flux of self-dual form F_5 is given by $N = \int_{S^5} F_5$,

where the AdS curvature radius is L and the couplings of each theory are related by

$$g_{YM}^2 = 4\pi g_s \ , \quad L^4 = 4\pi N g_s \alpha'^2 \ . \tag{2.10}$$

Apart from the duality summarized above, there exist other examples of dualities between gravity theories and quantum theories which have been established by using different branes configurations. Typical well established examples are [51, 44, 181, 50]

- Aharony-Bergman-Jafferis-Maldacena superconformal theory in $2 + 1$ dimensions and 11-dimensional SUGRA on $AdS_4 \times S^7/\mathbb{Z}_k$.
- $\mathcal{N}$=(4,4) SCFT in $1 + 1$ dimensions and type IIB SUGRA on $AdS_3 \times S^3 \times M^4$ where there are different choices for M^4.

With these relations between theories in different ranges of the parameters we conclude the introductory chapters of the AdS/CFT correspondence. We now turn to the more practical or applied side of the correspondence. Namely, we review how the fields in the boundary theory are identified with bulk gravitational fields. We also give the operational version of the statement of the correspondence: the Gubser-Klebanov-Polyakov-Witten formula, which specifies how to compute the dual field theory partition function. Moreover, since we are interested in transport at nonzero temperature and charge density we review how these two features arise naturally in holographic settings.

2.3 From gravity to field theory

In the previous section we have introduced the statement of the duality, which relates four-dimensional $\mathcal{N} = 4$ $U(N)$ SYM with IIB String Theory on $\mathrm{AdS}_5 \times S^5$. We have outlined the arguments to establish a connection between them in the limit of strong coupling on the gauge theory side and the limit of classical SUGRA on the ST theory side. While this classical theory of gravity is more tractable than the strongly coupled gauge theory, the correspondence becomes more functional and practical after a further simplification is done. This consists on reducing or simplifying the gravity theory in ten dimensions to a five-dimensional theory of gravity on AdS_5. This process is highly involved and we only outline the main idea below.

A generic field $\Phi(y, \Omega)$ of the ten-dimensional IIB SUGRA on $\mathrm{AdS}_5 \times S^5$ may be decomposed by separating variables on those on AdS_5: y, and on S^5: Ω [168, 71]. This is the same method used to solve Schrödinger's equation for the Hydrogen atom. More explicitly: $\Phi = \sum_l \phi_l^{(\mathrm{AdS}_5)}(y) Y_l^{(S^5)}(\Omega)$, where $\phi_l^{(\mathrm{AdS}_5)}$ and $Y_l^{(S^5)}$ are fields on AdS_5 and S^5, respectively, and the sum is over the spherical harmonics of S^5. With this scheme at hand, and after an laborious dimensional reduction of IIB SUGRA on S^5 [182–185], the ten-dimensional SUGRA action may be simplified to an action involving Einstein's gravity plus other fields in five dimensions. The five-dimensional Newton's constant is given in terms of the ten-dimensional Newton's constant

$$G_5 = \frac{G_{10}}{L^5 V_{S^5}} = \frac{L^3 \pi}{2N^2} \,, \tag{2.11}$$

where $V_{S^5} = \pi^3$ is the five-sphere volume and L the AdS_5 curvature radius. In the second equality we have used eq. (2.10) and that ten-dimensional Newton's constant is given in terms of the string theory parameters by $16\pi G_{10} = (2\pi)^7 g_s^2 l_s^8$.

After these technical details, it is clear that the correspondence stated in the previous section can be taken as an map between a five-dimensional gravity theory (*bulk* theory) and a four-dimensional gauge theory (*boundary* theory). This is an example of the holographic principle [52, 186] mentioned in the Introduction, suggesting the information

of the boundary theory may be obtained from the bulk theory. This justifies the use of the name holography.

2.3.1 Field-operator map and correlation functions

In order to study boundary fields, it is first necessary to establish a precise relation to the bulk fields. One of the earliest and simplest examples, and one we will use throughout this thesis, is the massive scalar field in AdS_{d+1} [45, 46, 100]. The solution of the Klein-Gordon equation for a scalar field $\phi(z,x)$ in AdS space eq. (2.3) asymptote to [100]

$$\phi(z,x) \underset{z\to 0}{\to} z^{d-\Delta}\left[\phi_0(x)+\mathcal{O}(z^2)\right]+z^{\Delta}\left[A(x)+\mathcal{O}(z^2)\right] \ , \tag{2.12}$$

where $\Delta = d/2+\sqrt{d^2/4+m^2L^2}$ and m^2 is the square-mass of the scalar field. While in flat space $m^2 \geq 0$, in AdS the lower bound is the Breitenlohner-Freedmand bound $m^2L^2 > -d^2/4$, without any instability for the negative values allowed.

The natural question is what the role of ϕ on the boundary theory is. The boundary theory can only be consistent with the bulk fields if the action S_{bdy} is modified as

$$S'_{\mathrm{bdy}}[\phi_0(x)] = S_{\mathrm{bdy}} - \int \mathrm{d}^d x \phi_0(x)\mathcal{O}[A(x)] \ , \tag{2.13}$$

where ϕ_0 is the same as in eq. (2.12)[4] and $\mathcal{O}$ is a local, gauge-invariant operator *dual* to the bulk field ϕ. Moreover, the boundary theory partition function $Z_{\mathrm{bdy}}[\phi_0(x)] = \int [DA]\exp\left(iS'_{\mathrm{bdy}}\right) = \exp(-W_{\mathrm{bdy}}[\phi_0(x)])$ where $W_{\mathrm{bdy}}[\phi_0]$ is a generating functional. The expectation value of $\mathcal{O}$ is [100] is

$$\langle\mathcal{O}(x)\rangle = -\frac{i}{Z_{\mathrm{bdy}}[0]}\frac{\delta Z_{\mathrm{bdy}}[\phi_0]}{\delta\phi_0}\bigg|_{\phi_0=0} = (2\Delta-d)A(x) \ . \tag{2.14}$$

A few comments are in order at this point. First, since the duality establishes the equivalence of the gravity and boundary theories, the Euclidean partition functions should be identified, subject to appropriate boundary conditions for the bulk fields. In other words

$$Z_{\mathrm{bdy}}[\phi_0(x)] = Z_{\mathrm{SUGRA}}[\phi(z,x)]\Big|_{\phi\to z^{\#}\phi_0(x)} \ , \tag{2.15}$$

or equivalently, the gauge theory generating functional $W_{\mathrm{bdy}} = -\log Z_{\mathrm{bdy}}$ is

$$W_{\mathrm{bdy}}[\phi_0] = S_{\mathrm{SUGRA}}[\phi(z,x)]\Big|_{\phi\to z^{\#}\phi_0(x)} \ , \tag{2.16}$$

[4] Usually $\phi_0(x)$ is referred to as the 'boundary value' of the bulk field $\phi(z,x)$. Due to the $z^{d-\Delta}$ factor in eq. (2.12), it is not strictly a boundary value but the leading falloff. However, as we will see below, the Gubser-Klebanov-Polyakov-Witten formula eq. (2.15) establishes a relation between the bulk and boundary actions in a way that ϕ_0 in eq. (2.12) should match the ϕ_0 of the boundary theory, hence the name 'boundary value'. We will use this abuse of notation to refer to ϕ_0 in this section.

where S_{SUGRA} and Z_{SUGRA} are the supergravity (Euclidean) action and partition function evaluated on-shell. The constraint $\phi \to z^{\#}\phi_0(x)$ schematically reminds us that one should impose appropriate boundary conditions on the bulk field, such that it matches $\phi_0(x)$ in the boundary theory. From eq. (2.13) it is clear $\phi_0(x)$ is interpreted as the source of the operator $\mathcal{O}$ in the boundary field theory.[5]

The equivalence between the partition functions eq. (2.15) is known as the Gubser-Klebanov-Polyakov-Witten (GKPW) formula [45, 46] and it establishes the starting point of all practical or computational purposes of the correspondence. Once the field theory partition function is calculated from the bulk theory on-shell action, it is possible to calculate correlation functions in the field theory (including one-point correlation functions, as in eq. (2.14)). The GKPW formula is only valid for large N and λ ('t Hooft coupling). Loop and stringy corrections to the saddle point approximation ($S_{ST} \simeq S_{\text{SUGRA}}$) of the full string theory action appear as inverse powers of N and λ. These corrections also appear in the field theory observables, typically at $O(\lambda^{-3/2}, N^{-2})$.

Another important, but rather technical, comment is related to the actual computation of the on-shell gravity action. Typically, and in fact including the example of the scalar field mentioned above, the on-shell action diverges once the integral in the holographic coordinate z is carried. These divergences are subtracted by adding boundary covariant *counterterms* [187] leading to a regularized action at the boundary. We will comment in more detail about holographic renormalization in Chapter 4 in the particular models used in this thesis.

Holographic correlation functions

We have seen that, provided appropriate boundary conditions are imposed and the on-shell action is renormalized, the GKPW rule allows to compute boundary expectation values from the bulk partition function. In principle the GKPW rule also allows to compute more general correlation functions [51, 173, 168]:[6]

$$\langle \mathcal{O}(x_1) \dots \mathcal{O}(x_n) \rangle = -\frac{\delta^n S^{(ren)}_{bulk}[\phi^{(i)}]}{\delta\phi_0^{(1)}(x_1) \dots \delta\phi_0^{(n)}(x_n)}\Big|_{\phi_0^{(i)}=0} , \tag{2.17}$$

where we remind ourselves the gravitational action that depends on bulk fields $\phi^{(i)}$ should be appropriately renormalized and the boundary conditions are consistent with sources of the boundary operators (through the boundary values $\phi_0^{(i)}$). Indeed, using eq. (2.17)

[5] Notice that introducing the last term of eq. (2.13) is more than a mathematical trick within perturbation theory to calculate expectation values. Its physical interpretation becomes particularly clear in the case the operator $\mathcal{O}$ is a gauge field and the perturbation ϕ_0 corresponds to a perturbation on some spatial component. This perturbation is simply an electric field along the spatial component and the response of the system to such perturbation allows to compute the electrical conductivity. We will exploit this particular type perturbation and the response of the boundary theory.

[6] Notice that in eq. (2.17) we have replaced the SUGRA action by some generic bulk gravitational action, in line with a phenomenological holographic approach.

the two-point holographic function of the scalar field introduced in Sec. 2.3.1 has been computed in [100]. This result is consistent with the known result of conformal field theory given in eq. (2.2).

In this section we have restricted to the example of a scalar field to identify the corresponding degrees of freedom in the boundary, however it is expected every degree of freedom in the boundary should have a bulk counterpart [51, 165, 172]. In other words, there should be a one-to-one map between bulk fields and local, gauge-invariant operators in the boundary theory. Moreover, both the bulk field and boundary operator should behave similarly under global symmetries.

Two examples relevant in this thesis are the $U(1)$ and translational invariance symmetries. The conserved current associated to these global symmetries allows to identify the bulk and boundary degrees of freedom. For example, in the case of the $U(1)$ symmetry, the operator $\mathcal{O}$ in eq. (2.13) is the conserved current J^μ of the $U(1)$ symmetry, while the source ϕ_0 is a gauge field in the boundary: a_μ which may be thought as the 'boundary value' of a bulk gauge field A_μ. Moreover, the conservation of the boundary current J^μ is a consequence of the invariance of the bulk action under gauge transformations [165, 172, 71, 168].

Similarly, in a translationally invariant boundary theory the energy-momentum tensor $T^{\mu\nu}$ is conserved. In this case the source is the boundary metric, which is nothing but the metric induced by the bulk metric. In this case, the bulk diffeomorphism invariance leads to the conservation of the boundary energy-momentum tensor [165, 172, 71, 168].

2.3.2 Role of black holes: nonzero temperature and charge

The correspondence we briefly presented in Sec. 2.2 involves zero temperature $\mathcal{N} = 4$ SYM theory. For nonzero temperature the time component is compactified on a circle while the $D3$-brane solution used in the closed string perspective, eq. (2.5), is promoted to a *black* brane solution [168]:

$$\mathrm{d}s^2 = H^{-\frac{1}{2}}(-f(r)\mathrm{d}t^2 + \mathrm{d}x_1^2 + \mathrm{d}x_2^2 + \mathrm{d}x_3^2) + H^{\frac{1}{2}}\left(\frac{\mathrm{d}r^2}{f(r)} + r^2\mathrm{d}\Omega_5^2\right) , \tag{2.18}$$

where $f(r) = 1 - (r_h/r)^4$ and $H(r)$ is given in eq. (2.6). With this geometry, the closed string perspective explained in Sec. 2.2 carries through in a similar way, with the exception that in the region $r \ll L$ the AdS part of the geometry given in eq. (2.8) should be replaced by

$$\mathrm{d}s^2 = \frac{r^2}{L^2}\left(-f(r)\mathrm{d}t^2 + \mathrm{d}x_1^2 + \mathrm{d}x_2^2 + \mathrm{d}x_3^2\right) + \frac{L^2}{r^2 f(r)}\mathrm{d}r^2 , \quad r \in [r_0, \infty) , \tag{2.19}$$

which is the five dimensional Schwarzschild AdS black brane.

The temperature of a black hole is defined through the thermodynamic laws of black holes and is proportional to surface gravity [176, 188]. However, it is also possible to use the Euclidean continuation $t \to it_E$ of eq. (2.19) and require regularity of the geometry, which periodically identifies the time coordinate. For consistency with the thermodynamic properties, its period should be the inverse of the temperature [189]. Moreover, since the correspondence relates the time components of the boundary and bulk theories, it is natural to identify their periods and thus, too, the temperature of the boundary theory and the black hole temperature. In the case of the Schwarzschild AdS black brane of eq. (2.19) the temperature is simply [166]

$$T = \frac{|\partial_r r^2 f|_{r=r_h}}{4\pi L^2} = \frac{r_h}{\pi L^2}\left(\frac{\hbar c}{k_B}\right) .$$

The term inside parenthesis involves Planck's constant, the speed of light and Boltzmann's constant. We wrote these constants explicitly to indicate the units, however, in the natural system this term is set to unity and we omit it in the rest of the thesis.

Similarly, by identifying other thermodynamic properties it follows that the entropy of the strongly coupled $\mathcal{N} = 4$ SYM, which was unknown, is given by the entropy of the $D3$-black brane [190]. From the the first law of black hole thermodynamics the Bekenstein-Hawking entropy of eq. (2.18), in the appropriate region ($r \ll L$), is given by the area of the horizon [190]

$$S_{\text{BH}} = \frac{A_h}{4G_{10}} = \frac{L^5 V_{S^5}}{4G_{10}} \int d^3x \sqrt{g_{x_1x_1} g_{x_2x_2} g_{x_3x_3}} = \frac{L^5 V_{S^5}}{4G_{10}} \frac{V_{\mathbb{R}^3} r_h^3}{L^3} = \frac{V_{\mathbb{R}^3}}{2}\pi^2 N^2 T^3 ,$$

where in the last equality we substituted the temperature and the ten-dimensional Newton's constant eq. (2.11). Therefore the entropy density in the dual theory (strongly coupled $\mathcal{N} = 4$ SYM) is $s = S_{BH}/V_{\mathbb{R}^3}$, which is 3/4 of the result obtained in the non-interacting regime of this theory [167]. This is one of the earliest examples that showed the potential of the correspondence to calculate observables in strongly coupled theories by using a classical theory of gravity.

We have seen how to introduce the notion of temperature and entropy. Using the GKPW formula eq. (2.15) it is straightforward to obtain the free energy. The (Euclidean) action which is minimized by the Schwarzschild AdS black brane is [168]

$$S_E = -\frac{1}{16\pi G_5}\int_{\mathcal{M}} d^5x\sqrt{g}\left(R + \frac{12}{L^2}\right) - \frac{1}{8\pi G_5}\int_{\partial\mathcal{M}} d^4x\sqrt{\gamma}\left(K - \frac{3}{L}\right) . \tag{2.20}$$

The last two terms, *counterterms*, are needed to avoid boundary divergences. The first of these is the Gibbons-Hawking-York term, which involves the trace of the extrinsic curvature: $K = \gamma^{\mu\nu}\nabla_\mu n_\nu$, with n^ν the outward pointing unit normal to the boundary and $\gamma^{\mu\nu}$ the induced metric on the boundary. The second counterterm removes divergences

in the on-shell action of asymptotically AdS spaces [191, 187]. As mentioned before, the evaluation of this renormalized action on the Schwarzschild AdS black brane (S_{os}^{ren}) together with the GKWP rule yields the free energy in the boundary theory

$$F = -T \ln e^{-S_{os}^{ren}} = -\frac{\pi^2 V_{\mathbb{R}^3}}{8} N^2 T^4 \,. \tag{2.21}$$

Moreover, the entropy obtained from $S = -\partial F/\partial T$ is consistent with the Bekenstein-Hawking entropy given before.

Apart from nonzero temperature, in this thesis we will be interested in charged systems. Based on the way temperature has been introduced we can straightforwardly anticipate how charge density may be added: using a charged object in the bulk, namely, a black hole/brane with nonzero charge.

As we have mentioned in the previous section, a boundary gauge field may naturally be included from a bulk gauge field. In order to support the bulk gauge field, the black hole must also be charged. The simplest way to achieve this is to add the Maxwell term to the Einstein Hilbert action of eq. (2.20) [165]

$$S_{\text{Maxwell}} = \frac{1}{16\pi G_5} \int_{\mathcal{M}} d^5x \frac{1}{4e^2} F_{\mu\nu} F^{\mu\nu} \,.$$

The basic setting involving a Schwarzschild AdS black brane is thus replaced by the AdS Reissner-Nordström black brane, which serves as the starting point for studying electric transport through holography.

Until this section we have restricted to one of the cases where the duality is fully specified and both theories, in the bulk and boundary, are clearly defined. Constructions such as those given at the end of Sec. 2.2, based on branes configurations and compactifications of supergravity theories, are usually referred to as *top-down* dualities. However, in general these cases may be highly complicated and are very especial due, for example, to the presence of supersymmetry. Another phenomenological approach, *bottom-up*, consists on postulating effective gravitational actions which, typically but not exclusively, contain Einstein gravity with a negative cosmological constant and additional matter. The features of the dual boundary theory, if it exists, may be inferred from the bulk theory following the mapping and identifications established in the well-studied case of the original correspondence.

One of the motivations for the bottom-up approach is that, if the underlying idea behind the gauge/gravity duality holds more generally in other quantum theories, one expects the features of the gravitational theory could be useful to describe real systems. As we anticipated in the Introduction, in this thesis we follow this approach. In the next Section we review the study of transport in QFT and the main difficulties encountered

to compute real-time Green's functions at nonzero temperature. We then explore the holographic techniques developed to study transport through gauge/gravity dualities.

2.4 Linear response in thermal QFT from black holes

We start by reviewing the field theory framework to describe, perturbatively, the response of a system to external forces [154, 155].

Consider weak external fields $\phi_i(t,x)$ coupled to operators $\mathcal{O}^i(t,x)$ so that, at $t=t_0$, a time-independent Hamiltonian H_0 is modified with a time dependent term $H^{ext}(t)$ ($H = H_0 + H^{ext}$) given by

$$H^{ext}(t) = -\int d^d\mathbf{x}\phi_i(t,\mathbf{x})\mathcal{O}^i(t,\mathbf{x}) \ . \tag{2.22}$$

Using the time translation operator in the interaction picture: $U_H(t,t_0) \simeq 1 - \frac{i}{\hbar}\int_{t_0}^{t} \mathrm{d}t' H^{ext}(t') + \ldots$, it is straightforward to show that the change in the expectation value of $\mathcal{O}^i$ can be obtained from equilibrium expectation values as

$$\begin{aligned}\delta\langle\mathcal{O}^i(t,\mathbf{x})\rangle = \langle\mathcal{O}^i(t,\mathbf{x})\rangle_H - \langle\mathcal{O}^i(t,\mathbf{x})\rangle_{H_0} \simeq -\frac{i}{\hbar}\int_{t_0}^{t}\mathrm{d}t'\langle[\mathcal{O}^i(t,\mathbf{x}),H^{ext}(t')]\rangle_{H_0} + \cdots = \\ = \frac{i}{\hbar}\int \mathrm{d}t' d^d\mathbf{x}'\langle[\mathcal{O}^i(t,\mathbf{x}),\mathcal{O}^j(t',\mathbf{x}')]\rangle_{H_0}\phi_j(t',\mathbf{x}') \ ,\end{aligned} \tag{2.23}$$

where in the last equality we used eq. (2.22). We have assumed time ordering $t > t'$ and neglected second order terms in the sources ϕ_j. In eq. (2.23) we identify the retarded Green's function between $\mathcal{O}^i$ and $\mathcal{O}^j$: $G_R^{ij}(t,\mathbf{x};t',\mathbf{x}') = -\frac{i}{\hbar}\theta(t-t')\langle[\mathcal{O}^i(t,\mathbf{x}),\mathcal{O}^j(t',\mathbf{x}')]\rangle_{H_0}$. Since H_0 is time-independent $G_R^{ij}(t,\mathbf{x};t',\mathbf{x}') = G_R^{ij}(t-t',\mathbf{x};\mathbf{x}')$ and if H_0 is also translationally invariant in space $G_R^{ij}(t,\mathbf{x};t',\mathbf{x}') = G_R^{ij}(t-t',\mathbf{x}-\mathbf{x}')$.

It is also customary to use the *response function* [154, 155]:

$$\chi''_{\mathcal{O}^i,\mathcal{O}^j}(t,\mathbf{x};t',\mathbf{x}') = \frac{i}{2\hbar}\langle[\mathcal{O}^i(t,\mathbf{x}),\mathcal{O}^j(t',\mathbf{x}')]\rangle_{H_0} \ , \tag{2.24}$$

or the *dynamic susceptibility*: $\chi_{\mathcal{O}^i,\mathcal{O}^j} = 2i\theta(t-t')\chi''_{\mathcal{O}^i,\mathcal{O}^j}$. Moreover, in Fourier space $k=(\omega,\mathbf{k})$ the linear response of the system is simply

$$\delta\langle\tilde{\mathcal{O}}^i(k)\rangle \simeq -\tilde{G}_R^{ij}(k)\tilde{\phi}_j(k) \, , \tag{2.25}$$

where $\tilde{G}_R^{ij}$ is the Fourier transform of the retarded Green's function. These definitions are crucial for the calculation of transport coefficients.

Let us now comment on the main difficulties in the standard approach to the calculation of Green's functions in QFT at nonzero temperature. These difficulties need also to be taken into account to introduce the holographic Green's functions.

Comments on the standard approach to finite temperature correlators

At finite temperature, real-time response may, in principle, be computed by Wick rotation of the Euclidean correlation functions. In this case the time ordering, which is not well defined due to complex times, is substituted by choosing a direction of integration along a straight contour (from t to $t - i\beta$) in the complex plane. This is the broad idea behind the so-called Matsubara formalism [5, 170].

However, there are some inconvenients with this method [161]. First, even at equilibrium the main difficulty is the analytic continuation back to real time. The main inconvenient for our purposes is that out of equilibrium this method does not apply. First of all it is not clear how to define the exponential form of the density matrix since there is no obvious definition of temperature. Second, by adiabatically switching on and off time-dependent interactions, the initial $|\phi(-\infty)\rangle$ and final $|\phi(\infty)\rangle$ states are not, in principle, equal. In other words, it is not guaranteed that the system returns to the initial equilibrium state (up to a phase factor). Therefore, it is not possible to calculate the partition function needed in the denominator of the correlators.

In order to avoid the problem that the final equilibrium state differs from the original one, one doubles the integration region by returning to the initial equilibrium state. In other words the integration is along a closed contour (t_0, ∞) and back. Time ordering is defined according to the 'forwards' (normal time ordering) and 'backwards' (anti-time ordering) branches. This method is known in the literature as Schwinger-Keldysh formalism [156–160, 192, 161, 162] and the closed contour as the Keldysh contour.[7]

The forward C_+ and backward C_- branches define a contour $C = C_+ \cup C_-$ and the Green's functions of bosonic fields $\phi(\mathbf{x}, t)$ are [192, 161]:

$$G(\mathbf{x}, \tau; \mathbf{x}', \tau') = \begin{cases} G^T(\mathbf{x}, t; \mathbf{x}', t') \equiv -i\langle T\phi(\mathbf{x}, t)\phi^*(\mathbf{x}', t')\rangle & \text{if } \tau, \tau' \in C_+ \\ G^{\tilde{T}}(\mathbf{x}, t; \mathbf{x}', t') \equiv -i\langle \tilde{T}\phi(\mathbf{x}, t)\phi^*(\mathbf{x}', t')\rangle & \text{if } \tau, \tau' \in C_- \\ G^<(\mathbf{x}, t; \mathbf{x}', t') \equiv -i\langle \phi^*(\mathbf{x}', t')\phi(\mathbf{x}, t)\rangle & \text{if } \tau \in C_+, \tau' \in C_- \\ G^>(\mathbf{x}, t; \mathbf{x}', t') \equiv -i\langle \phi(\mathbf{x}, t)\phi^*(\mathbf{x}', t')\rangle & \text{if } \tau \in C_-, \tau' \in C_+ \end{cases}$$

where τ, τ' are coordinates in C and T ($\tilde{T}$) is the time (anti-time) ordering operator used in the forwards C_+ (backwards C_-) branch. In $G^>$ and $G^<$ (Wightman functions) each

[7] The initial state can be considered to be immersed in a thermal bath. This leads to an extra contour piece or branch (Matsubrara branch), which is added at the end of the backward branch and runs along a purely imaginary direction [162].

field is inserted in different branches, e.g., in $G^<$, $\phi(\mathbf{x},t)$ is in C_+ and $\phi(\mathbf{x}',t')$ in C_-.[8] The retarded (R), advanced (A) and Keldysh (K) correlators are related to the previous by [192]:

$$\begin{aligned} G^R(\mathbf{x},t;\mathbf{x}',t') &\equiv -i\theta(t-t')\langle[\phi(\mathbf{x},t),\phi^*(\mathbf{x}',t')]\rangle &= G^T - G^<\,, \\ G^A(\mathbf{x},t;\mathbf{x}',t') &\equiv \;\; i\theta(t'-t)\langle[\phi(\mathbf{x},t),\phi^*(\mathbf{x}',t')]\rangle &= G^T - G^>\,, \\ G^K(\mathbf{x},t;\mathbf{x}',t') &\equiv -i\theta(t-t')\langle\{\phi(\mathbf{x},t),\phi^*(\mathbf{x}',t')\}\rangle &= G^> + G^<\,, \end{aligned}$$

where $[\cdot,\cdot]$ is the commutator and $\{\cdot,\cdot\}$ the anticommutator.

2.4.1 Real time holographic Green's functions

As we have commented in Sec. 2.3.2, in a field theory with a gravity dual temperature is introduced by considering a black hole in the bulk theory. Therefore, the natural question to ask is whether it is possible to compute real time Green's functions in the boundary theory using this setup.

The method to calculate boundary Green's functions in holographic theories has been justified by considering the Schwinger-Keldysh contour method mentioned before and its analog in the bulk theory [164]. However, before this was understood, a clear prescription, which passed several consistency checks, had been proposed in [163]. We review this proposal below.

The GKPW formula eq. (2.15) suggests that, formally, the correlators are simply obtained by functional differentiation of of the bulk gravitational action as given in eq. (2.17). There are however certain cases in which problems arise using this method [163].

The first problem is that imposing regularity at the horizon $r = r_0$ is not a consistent boundary condition since it does not allow (together with boundary conditions at $r \to \infty$) to fully fix the solution. On physical grounds it was argued [163] that the appropriate horizon boundary condition is to impose bulk waves to be 'ingoing' at the horizon.

Even after imposing this, more refined, boundary condition at the horizon, the result obtained from the functional derivative of the partition function is still incorrect. For the particular case of a scalar field it was shown [163] that this yields a real Green's function and therefore causality in the boundary theory would be violated. The proposal of [163] is summarized as follows.

Consider fluctuations of the a scalar field in the background of eq. (2.19) (in the variable $z = 1/r$) [163]

$$S = \frac{1}{16\pi G_5}\int d^4x \int_{z_B}^{z_0} dz\,\sqrt{-g}\left[g^{zz}(\partial_z\phi)^2 + g^{\mu\nu}\partial_\mu\phi\partial_\nu\phi + m^2\phi^2\right]\,.$$

[8] Other standard notation [192] for these correlators is $G^T = G_{11} = G_{++}$, $G^{\tilde{T}} = G_{22} = G_{--}$, $G^< = G_{12} = G_{+-}$, $G^> = G_{21} = G_{-+}$ where '1' and '+' refer to the forward branch C_+, while '2' and '−' to C_-.

The solution of the scalar is decomposed in Fourier modes $f_k(z)$ as

$$\phi(z,x) = \int \frac{d^4k}{(2\pi)^4}\, e^{ik\cdot x} f_k(z)\phi_0(k)\,,$$

where $\phi_0(k)$ is the determined from the boundary value of the bulk field $\phi(z,x)$ at $z_B \to 0$. The on-shell action is

$$S = \int \frac{d^4k}{(2\pi)^4}\, \phi_0(-k)\mathcal{F}(k,z)\phi_0(k)\Big|_{z_B}^{z_0}\,, \quad \mathcal{F}(k,z) = \frac{\sqrt{-g}}{16\pi G_5} g^{zz} f_{-k}(z)\partial_z f_k(z)\,, \tag{2.26}$$

and the proposal of [163] for the correct result of the retarded Green's function is

$$G^R_{\mathcal{O}\mathcal{O}}(k) = -2\mathcal{F}(k, z=0)\,, \tag{2.27}$$

where $\mathcal{O}$ is the dual operator of the scalar field ϕ.

To summarize, the first essential point is the ingoing boundary condition at the horizon, which is related to causality in the bulk. Second, the straightforward application of functional derivatives of the partition function yields the incorrect result and should be replaced with the prescription given above.

From the difficulties mentioned above, it is clear that the problem is related to the causality structure of the bulk theory and how to preserve causality in the boundary theory. In [164] the bulk causal structure was studied using Kruskal coordinates. In these coordinates it is easy to write the extended Penrose diagram of the AdS black brane of eq. (2.19) containing two copies or quadrants. In each of quadrant the time component runs (far from the horizon) in opposite directions [164, 193], this is precisely what allows to establish the parallelism with the forward and backward branches of the Keldysh contour. The prescription of eq. (2.27) is recovered after imposing which modes are ingoing and outgoing in each quadrant.

In Chapter 3 we will adapt the prescription of eqs. (2.26) and (2.27) to the case of a vector field instead of a scalar field. This will allow to obtain the retarded Green's function associated to the current-current correlation function necessary to compute the electrical conductivity. Let us now review the calculation of electrical conductivity in the simplest holographic setting with finite charge density.

2.4.2 Electrical conductivity from a charged black hole

In this section we use the AdS Reissner-Nordström (RN) black brane to compute the electrical conductivity in the dual theory [165]. This background is the classical solution to the Einstein-Hilbert-Maxwell action and is the simplest setting that allows to introduce charge density in the dual theory. Therefore, it is the starting point to investigate metallic properties through the gauge/gravity duality [166].

The background, in the $z = 1/r$ coordinate, is simply

$$\mathrm{d}s^2 = \frac{1}{L^2 z^2}\left(-f(z)\mathrm{d}t^2 + \frac{\mathrm{d}z^2 L^4}{f(z)} + \mathrm{d}x^2 + dy^2\right),$$
$$f = 1 - (1+Q^2)\left(\frac{z}{z_0}\right)^3 + Q^2\left(\frac{z}{z_0}\right)^4, \quad Q^2 = \mu^2 z_0^2 \gamma^{-2},$$

where $\gamma^{-2} = \frac{L^2}{4}\frac{2\kappa^2}{e^2}$ measures the ratio of the gravitational $\kappa^2 = 8\pi G_4$ and electromagnetic coupling constants e^2. The time component of the gauge field is

$$A_t = \mu(1 - z/z_0),$$

and Q is the charge of the black brane and is parametrized by μ. The constant μ is the boundary value of the gauge field, which, as we discussed in previous sections, sources the boundary gauge field. It also plays the role of the electrostatic potential difference between the horizon and the asymptotic AdS boundary [194]. Proceeding in a similar fashion as in Sec. 2.3.2, the free energy in the boundary theory is obtained from the bulk action evaluated at the Euclidean background[9]

$$\begin{aligned}\Omega =& -T\log e^{-S_E} = -T\int_{\mathbb{R}^2} d^2x \int_0^{1/T} \mathrm{d}t_E \left[\frac{2}{L^4}\frac{f}{z^3} + \frac{\sqrt{f}}{z^3 L^3}\left(\frac{4}{L} + \frac{-6f + zf'}{2\sqrt{f}L}\right)\right] \\ =& -\frac{V_{\mathbb{R}^2}}{2\kappa_4^2}\frac{1+Q^2}{z_0^3 L^4},\end{aligned}$$

where $\kappa_4^2 = 8\pi G_4$. We have made explicit the integral in the periodic time coordinate cancels the factor T in front of the logarithm. The first term in the integral corresponds to the bulk action integrated in the holographic coordinates. The terms in parenthesis are derived from the gravitational boundary counterterms $\sqrt{\gamma}(2K - 4/L)$ [195, 187, 165], which are analog to those introduced for the five-dimensional Schwarzschild AdS black brane in eq. (2.20). Taking the derivative with respect to the chemical potential gives the charge density, which is clearly proportional to the black brane charge Q as we had anticipated.

We now proceed to study the response function in the theory dual to this background. In order to do so we introduce perturbations in a spatial component of the bulk gauge field $\delta A_x(z,t) = a_x(z)e^{-i\omega t}$, which reproduces the external electric field in the boundary theory. More explicitly, in eq. (2.22) the external field or source ϕ_i is replaced by $a_x(z \to 0) = a_x^{(0)}$

[9] This corresponds to the Gibbs free energy: variation with respect to the bulk gauge field yields a boundary term of the form $\int_{\partial\mathcal{M}} d^3x\sqrt{\gamma}F^{\mu\nu}n_\mu\delta A_\mu$, where n_μ is the outward pointing unit normal, $\gamma_{\mu\nu}$ the boundary induced metric and the fields are evaluated at the boundary ($\delta A_t = \delta\mu$). Therefore, this boundary term vanishes for fixed chemical potential [94].

and the electric field is $E_x = i\omega a_x(z \to 0)e^{-i\omega t} = i\omega a_x^{(0)} e^{-i\omega t}$. The operator $\mathcal{O}^i$ that couples to the source is in this case the current J^x. Moreover, in the absence of the external field the expectation value of the current is zero $\langle J^x \rangle_{eq} = 0$, therefore the term $\delta\langle \mathcal{O}^i \rangle$ in eq. (2.23) reduces to the non-equilibrium value of the current $\langle J^x \rangle_{ne}$. With these considerations we rewrite eq. (2.23) in momentum space (see eq. (2.25)) as

$$\langle J^x \rangle_{ne} = G^R_{J^x J^x}(\omega) a_x^{(0)} = \frac{G^R_{J^x J^x}(\omega)}{i\omega} E_x \,,$$

from where it is clear that the conductivity is simply

$$\sigma_{xx}(\omega) = \frac{G^R_{J^x J^x}(\omega)}{i\omega} \,. \tag{2.28}$$

Based on the discussion of Sec. 2.4.1 the only thing left to be done is to follow the prescription to compute the holographic retarded Green's function of eq. (2.28) for which we need to solve the bulk equation of motion of the perturbation δA_x. Note however, that this perturbation also couples to perturbations in metric components δg_{xt} and δg_{xr}. At present the perturbation in the xr components of the metric can be set to zero.[10] The perturbation δg_{xt} may be eliminated from the equation of the perturbation $a_x(z)$, which reduces to

$$\big(f a_x'(z)\big)' + a_x \left(\frac{\omega^2 L^4}{f} - \frac{2\kappa_4^2 L^2}{e^2} z^2 A_t'(z)^2 \right) = 0 \,,$$

which is subject to the following boundary conditions:

$$a_x(z \to z_0) \simeq (z_0 - z)^{-\frac{i\omega}{4\pi T}} \left[a_h^{(0)} + a_h^{(1)}(z_0 - z) + \dots \right] \,, \tag{2.29}$$

$$a_x(z \to 0) \simeq a_x^{(0)} + a_x^{(1)} z + \dots \,, \tag{2.30}$$

where higher order terms $\mathcal{O}(z_0 - z)$ and $\mathcal{O}(z^2)$ are given in terms of the three unknowns $a_h^{(0)}$, $a_x^{(0)}$ and $a_x^{(1)}$. Either two of these unknowns may be fixed arbitrarily and the solution of the differential equation subject to these boundary condition fixes the unique value of the other two unknowns.

The horizon boundary condition of eq. (2.29) is of the type discussed in discussed in Sec. 2.4.1, namely ingoing at the horizon. Moreover, applying the generalization of the prescription of eqs. (2.26) and (2.27) for the gauge field perturbation yields

$$G^R_{J^x J^x}(\omega) = \frac{1}{e^2} \frac{a_x^{(1)}}{a_x^{(0)}} \,. \tag{2.31}$$

[10] This choice fixes the gauge and is known as *axial* gauge. In general, this does not fully fix the gauge as there is an residual gauge freedom associated to a constant shift of g_{xt} and (possibly) other perturbations. We will comment more on this gauge fixing in backgrounds without translational symmetry.

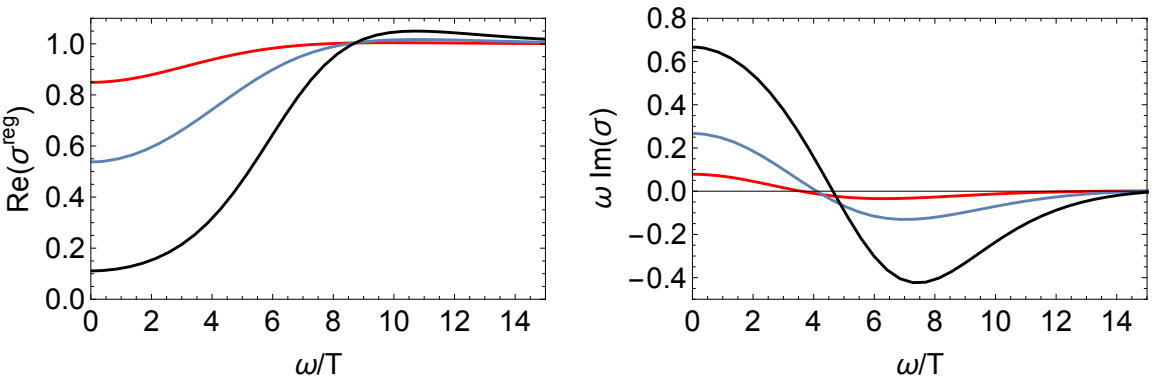

Fig. 2.1 Electrical conductivity eqs. (2.31) and (2.28) in $2+1$ dimensions calculated from the Reissner-Nordström black brane. Left: real part of the regular part of the conductivity. Right: imaginary part rescaled by the frequency. This shows there is a pole in the imaginary part at zero frequency. This is related to an infinite real conductivity at zero frequency. The plots correspond to fixed temperature and chemical potential. From top to bottom in the left plot μ/T increases. See [165] for more details.

We show in figure 2.1 the regular part of the real part of the conductivity as well as the imaginary part rescaled by the frequency. These plots correspond to fixed chemical potential (Grand Canonical ensemble) and fixed temperature.

We have obtained an expected feature, namely, the existence of a pole at zero frequency in the imaginary part of the conductivity, which indicates the real part should be infinite at zero frequency (though this is not directly seen in the left plot of Fig. 2.1). This feature can be understood easily; assuming the general expansion of the Green's function is

$$G^R_{J^xJ^x}(\omega) \approx -K/\pi + i\omega\sigma_{\rm Q} + \mathcal{O}(\omega^2)\,,$$

we see the limit $\omega \to 0^+$ in eq. (2.28) might be problematic. More explicitly, the real part of the conductivity for vanishing frequency is

$$\begin{aligned}\sigma_{\rm dc} =& {\rm Re}\lim_{\omega\to 0}\frac{G^R_{J^xJ^x}(\omega)}{i(\omega+i\epsilon)} = \sigma_{\rm Q} - {\rm Re}\frac{1}{i}\frac{K}{\omega+i\epsilon} = \\ =& \sigma_{\rm Q} - {\rm Re}\left[\mathcal{P}\left(\frac{1}{\omega}\right)(-i)K - \pi K\delta(\omega)\right] = \sigma_{\rm Q} + K\delta(\omega)\,.\end{aligned} \tag{2.32}$$

Indeed, the Kramers-Kronig relation between the real and imaginary parts of the conductivity connects the two distributions inside the brackets: if there is a simple pole in the imaginary part of the conductivity, there should be a delta in the real part. The coefficient of this delta is called the Drude weight and will be the object of study in Chapter 4.

Simple analytical results for σ_Q and K, involving only thermodynamic quantities, have been obtained in $2+1$ (boundary) dimensions in [109, 110]

$$\sigma_Q = \frac{1}{e^2}\left(\frac{sT}{\epsilon+P}\right)^2, \quad K = \frac{\rho^2}{\epsilon+P}, \tag{2.33}$$

where s, ϵ and ρ are the entropy, energy and charge densities, while T is the temperature and P the hydrodynamic pressure, which is proportional to the energy density. It has been shown [122, 128] that these expressions are actually valid in more general models: Einstein-Maxwell-dilaton models [94]. We will review the universality of the expression of the Drude weight in Chapter 4 and we will see that in R-charged backgrounds with multiple R-charges the result is very similar.

The physical origin of the infinite conductivity is the same as in the Drude model; in the presence of translational invariance, the response of the system to an external electrostatic field is to accelerate charge without 'scattering' (whatever the microscopic mechanism may be). In the next section we discuss how to explicitly break the continuous translational symmetry in the spatial coordinates. Numerous approaches to break translational symmetry in holography have been suggested [130, 136, 139–141, 126, 131–135]. However, in Sec. 2.5 we only review the possibility used in [136, 139] on which we base our study.

2.5 Holography without translational invariance

In a field theory momentum conservation is a consequence of imposing the conservation of certain components of the energy-momentum tensor $\partial_i T^{ij} = 0$ where the indices run over spatial dimensions. As we mentioned in Sec. 2.3.1, in theories with holographic duals, the energy-momentum tensor T^{ij} is related to the bulk metric $g_{\mu\nu}$. Moreover, the conservation of T^{ij} is a consequence of diffeomorphism invariance of $g_{\mu\nu}$. Therefore, to violate $\partial_i T^{ij} = 0$ one should break diffeomorphism invariance in the spatial coordinates. The simplest option for this purpose is to add a graviton mass term [136]; hence, these theories are broadly known as massive gravity.

In general, including a graviton mass term leads to numerous problems and instabilities which we are not going to cover in this thesis. A ghost-free model of massive gravity [196, 197] has been used in [136] to describe a boundary theory with finite charge density and without translational symmetry. In this model the bulk metric tensor $g_{\mu\nu}$ is coupled to a 'reference metric' $f_{\mu\nu}$ which gives the mass term to $g_{\mu\nu}$. The reference metric is flat and may be chosen to have only nonzero spatial components, i.e., for coordinates $x^\mu = (t, r, x, y)$, the reference metric is $f_{\mu\nu} = \mathrm{diag}(0, 0, 1, 1)$ [136].[11] It is more generally parametrized as $f_{\mu\nu} = \partial_\mu \phi^a \partial_\nu \phi^b \eta_{ab}$ where $\eta_{\mu\nu}$ is the Minkowski metric and $\phi^t = \phi^r = 0$,

[11] There are more sophisticated massive gravity models which treat the reference metric dynamically [198].

$\phi^a = \delta^a_i x^i$ for $i = 3, 4$. In this way, diffeomorphism invariance is broken only in the x and y dimensions.

Moreover, the fields which parameterize the components of the reference metric ϕ^a are usually called Stükelberg fields [199, 136]. The reason for this name comes from the use of the *Stükelberg trick* in the context of massive gravity. Broadly speaking, this trick consists on adding a new field, Stükelberg field, to a given theory which lacks gauge symmetry in such a way that the new action enjoys this symmetry [199]. Moreover, in the context of massive gravity, adding the Stükelberg fields allows the massless limit of the theory to be well defined [199].

As shown in [136], in order to compute the electric conductivity in the dual theory of this massive gravity model one proceeds the same way as we did in Sec. 2.4.2 for the RN background. Namely, one adds perturbations on a spatial component of the gauge field δA_x and on the xt component of the bulk metric δg_{xt}. However, in this massive gravity background, the Stükelberg field should also be perturbed: $\delta\phi^x$. Alternatively, if the Stükelberg field is left unperturbed, the xr component of the metric should be perturbed δg_{xr}. This is choice is a gauge choice.

In [200] a plethora of (static) of solutions similar to the massive gravity solution mentioned above were found. These solutions, which consist on black holes dressed with p-forms, were called axionic black holes and were first used in [139] to calculate the transport properties through holography. For concreteness we write the action used in [139] below.

$$S = \frac{1}{2\kappa^2}\int_{\mathcal{M}} d^{d+1}x\sqrt{-g}\left[R - 2\Lambda - \frac{1}{2}\sum_{I=2}^{d+1}\partial_\mu X^I \partial^\mu X^I - \frac{2\kappa^2}{4e^2}F^2\right] + S_{\rm ct}\,, \quad \Lambda = \frac{d(d-1)}{2L^2}\,. \tag{2.34}$$

The term $S_{\rm ct}$ contains the gravitational counterterms discussed in 2.3.2, but in arbitrary dimensions, plus counterterms involving the massless scalar fields $X^I = \alpha x^I$. Since the geometry that solves this model is known analytically [200, 139] the model of eq. (2.34) started to be extensively used by many other authors. As a consequence, the name *axions* has been popularized to refer to the scalar fields X^I of eq. (2.34). We note however that the use of this name in the context of holography might raise confusion.

In order to solve the apparent violation of the CP symmetry of strong interactions in QCD, Peccei and Quinn [201] proposed to add the term $\theta\epsilon_{\mu\nu\rho\sigma}F^{\mu\nu}_\alpha F^{\rho\sigma}_\alpha$, the '$\theta$-term', to the QCD Lagrangian. This term predicts the existence of a light spinless particle which receives the name of *axion* [169].

In $\mathcal{N} = 4$ SYM, the θ-term has been realized holographically by considering intersections of $D3$ and $D7$ branes [202, 203]. The solution of this $D3$-$D7$ brane system contains a field (axion field) which is dual to the θ parameter of the θ-term in the dual gauge theory. This

field is also linear in one of the spatial coordinates [202, 203] but is not related to the fields X^I of eq. (2.34).

On the other hand, in the context of String Theory, there are pseudoscalars X with shift symmetry: $X \to X + \text{const}$. These fields, called axions, result from dimensional reductions of antisymmetric fields e.g., RR p-forms of some String Theory [50, 204]. Perturbatively, these fields have no potential, like X^I in eq. (2.34), but in certain situations the kinetic term of axions sources the dilaton and the solution of eq. (2.34) should be modified [144].

Therefore, in order to avoid these subtleties and the confusion with terminology in related fields, a better name for the massless scalar fields X^I of eq. (2.34) in the context of effective holographic models would be Stükleberg fields. The reason for this terminology instead of axions is first that the mass term that breaks diffeomorphism invariance in the spatial dimensions is parametrized precisely by the fields X^I. Second, as we will see below, at the level of the perturbations introduced to study conductivity, the fields X^I play the role of the Stükleberg fields ϕ^a of massive gravity. In this thesis we will still choose the name axions for simplicity and due to its widespread use, but we remind ourselves these fields must not be confused with the axion fields related to the θ-term.

After this small digression we turn back to the role of momentum relaxation in the boundary theory of eq. (2.34). As in the case of massive gravity, in the model of eq. (2.34) one may choose to either perturb the Stükelberg field δX^x or δg_{xr}, namely, adding the perturbations $\{\delta A_x, \delta g_{xt}, \delta X^x\}$ or $\{\delta A_x, \delta g_{xt}, \delta g_{xr}\}$ [139]. In [139] the following harmonic perturbations were chosen

$$A_x = a_x(r)e^{-i\omega t}\,, \quad \delta g_{xt} = h_{xt}(r)e^{-i\omega t}\,, \quad \delta X^x = \chi(r)e^{-i\omega t}\,,$$

The corresponding equations of motion were decoupled by using gauge-invariant combinations of the fields and taking the zero frequency limit. Using this solution, the dc conductivity is simply [139]

$$\sigma_{\text{dc}} = r_0^{d-3}\left[1 + (d-2)^2\frac{\mu^2}{\alpha^2}\right]\,,$$

where r_0 is the horizon radius, μ is the boundary theory chemical potential and the parameter α, which controls the strength on momentum dissipation, was defined through the axion fields $X^I = \alpha x^I$.

This method had been previously used in a massive gravity setting [137] and later in more sophisticated dilatonic models without translational invariance [125, 127]. There is however a simpler and more general method initiated in [141], which consists on using the following perturbations

$$A_x = -Et + a_x(r)\,, \quad \delta g_{xt} = h_{xt}(r)\,, \quad \delta X^x = \chi(r)\,,$$

to solve the equations of motion at the horizon. The conductivity is obtained from the radially conserved Maxwell current at the horizon divided by the electric field E. We will review this method more carefully in Chapter 5.

After this discussion we conclude the review on the subjects of the gauge/gravity duality relevant for this thesis. We are ready to move on to the original research of the thesis, which is organized according three main strategies or approaches to strongly coupled systems: 1) high dimensionality, 2) limit of weak breaking of translational symmetry and 3) models with varying gravitational coupling constant and strong breaking of translational symmetry. We start with the first strategy.

3

Conductivity and entanglement entropy of high dimensional holographic superconductors[†]

We investigate the dependence of the conductivity and the entanglement entropy on the space-time dimensionality d in two holographic superconductors: one dual to a quantum critical point with spontaneous symmetry breaking, and the other modeled by a charged scalar that condenses at a sufficiently low temperature in the presence of a Maxwell field. In both cases the gravity background is asymptotically Anti de Sitter (AdS). In the large d limit we obtain explicit analytical results for the conductivity at zero temperature and the entanglement entropy by a $1/d$ expansion. We show that the entanglement entropy is always smaller in the broken phase. As dimensionality increases, the entanglement entropy decreases, the coherence peak in the conductivity becomes narrower and the ratio between the energy gap and the critical temperature decreases. These results suggest that the condensate interactions become weaker in high spatial dimensions.

[†]A version of this chapter may be found in [205], which has been published at *Journal of High Energy Physics* and is authored by Antonio M. García-García and A. R. B.

3.1 Introduction

It is a well known fact in condensed matter and statistical physics that the dynamics of many systems simplifies drastically in the limit of large space dimensions $d-1$ [206–214]. Analytical results are typically obtained for $d \to \infty$ [207, 206] and, in some cases, it is also possible to compute explicitly small corrections [212] due to a large but finite dimensionality by a $1/d$ expansion. A typical example is the Hubbard model in the strong coupling region where in the large d limit the problem maps onto a mean-field quantum impurity model that is solved self consistently. Meaningful results are only obtained [206] after the kinetic energy is properly rescaled so that the trivial non-interacting limit is avoided for $d \to \infty$. The application of these ideas to the Hubbard model was a key step for the later development of dynamical field theory [213]. Another problem in which large d expansion is relevant is that of a particle in a random potential. According to the selfconsistent theory of localization, [215] explicit analytical results for the critical disorder that induces a metal-insulator transition are only known for a Cayley tree geometry which corresponds to a lattice of infinite dimensionality. However, there is still qualitative agreement with the numerical results in a three dimensional lattice [216].

Similarly, many problems in percolation [214] and spin chains [211] have explicit analytical results in the limit of large spatial dimensions. In many of these cases just keeping the leading term in the $1/d$ expansion is enough to find good agreement with experimental or numerical results [208] in $d = 3$. In the context of quantum gravity, large d expansions have also been employed [217, 218] to simplify Feynman diagrams in a spirit similar to the large N approximation, broadly used in quantum chromodynamics, $N = 3$, and other gauge theories. However, renormalization of quantum theories of gravity is even more problematic as dimensionality increases so it is not clear whether it is a viable approximation scheme. The situation is different in classical theories of gravity which are finite for any dimensionality. The study of properties of black holes [219] and general relativity [118] in large dimensions has shown that there are intriguing features that only occur for a sufficiently large number of dimensions. More recently [220–222] this large d limit was studied in the context of AdS spaces and then applied, by AdS/CFT techniques, to the study of holographic superconductors [220].

One of the main conclusions of [220] is that it is possible to find an explicit analytical expression of the critical temperature in the limit of large dimensionality and negligible backreaction of the scalar on the metric and on the gauge field. Even for $d = 2 + 1$, this simple analytical prediction for the critical temperature is already a good approximation of the numerical results. Moreover, as dimensionality increases the condensation of the scalar occurs always close to the horizon as the gravitational effects of the black hole are only important in this region.

In this chapter we continue the study of holographic superconductors in the large d limit with a twofold motivation. Firstly, we aim to emphasize the usefulness of large

d expansions in holography by carrying out analytical calculations of the entanglement entropy and the conductivity that are only possible in this limit. Secondly, we seek to clarify the qualitative effect of dimensionality in holography. We have found that as d increases the coherence peak becomes narrower and the ratio between the energy to break the condensate and the critical temperature decreases. This is a strong suggestion that the effective coupling that controls the interactions of the condensate seems to be weaker as dimensionality increases.

The organization of the chapter is as follows: In Sec. 3.2 we introduced the two models that we employ to study a large d holographic superconductor, then in Sec. 3.3 we compute numerically the conductivity up to $d = 9$. Based on these results we compute in Sec. 3.4 the superconducting energy gap, roughly the maximum of the conductivity, and the order parameter $\langle \mathcal{O} \rangle$ as a function of d. We also discuss certain ambiguity in the relation between these two quantities. In Sec. 3.5 we study analytically at $T = 0$, the low and large frequency-dependence of the electrical conductivity. Similarly, in Sec. 3.6, we provide simple analytical expressions for the entanglement entropy between a rectangular strip and its complement in the boundary; we analyze both the case $T = 0$ and $T \sim T_c$.

3.2 Models

We study the dimensional dependence of holographic superconductivity [112, 114] in two models, one at $T = 0$ and other at $T > 0$.

3.2.1 d-dimensional holographic superconductivity at $T = 0$

For the $T = 0$ limit we choose the model introduced in Ref.[115], to describe a quantum critical point with spontaneous symmetry breaking,

$$S = \int d^{d+1}x\sqrt{-g}\left[R - \frac{1}{4}F^2 - |\partial_\mu\psi - iq^2A_\mu\psi|^2 - V(|\psi|)\right], \tag{3.1}$$

where

$$V(|\psi|) = 2\Lambda + m^2|\psi|^2 + \frac{u}{2}|\psi|^4, \tag{3.2}$$

$\Lambda = -d(d-1)/2L^2$ is the cosmological constant, $m^2 < 0$ is the scalar mass and $u > 0$. Symmetry breaking is directly related to the existence of a minimum of the potential at $|\psi| = \psi_{\text{IR}} = \sqrt{-m^2/u} \neq 0$.

Following [115] we consider the metric ansatz

$$ds^2 = e^{2A(r)}\left(-h(r)dt^2 + dx^i dx^i\right) + \frac{dr^2}{h(r)}, \tag{3.3}$$

$i = 1, \ldots, d-1$, such that in the infrared limit $A(r) = r/L_{\rm IR}$ and $h(r) = 1$ where $L_{\rm IR}$ is defined through $\frac{-d(d-1)}{L_{\rm IR}^2} \equiv V(|\psi_{\rm IR}|)$.

In order to recover the SO(d-1,1) Lorentz symmetry and SO(d,2) conformal symmetry deep in the IR the metric should approach

$$ds^2_{\rm IR} = e^{2r/L_{\rm IR}}\left(-dt^2 + dx^i dx^i\right) + dr^2 \tag{3.4}$$

where we have imposed

$$h(r) \to h_{\rm IR} = 1, \;\; A(r) \to \frac{r}{L_{\rm IR}}, \;\; \text{as } r \to -\infty. \tag{3.5}$$

Similarly, in the UV limit, the appropriate symmetries are restored provided,

$$h(r) \to h_{\rm UV}, \;\; A(r) \to A_{\rm UV}\frac{r}{L}, \;\; \text{as } r \to \infty, \tag{3.6}$$

with $h_{\rm UV}$ and $A_{\rm UV}$ constants related by the rr component of the Einstein equations:

$$(d-1)(A'h'h + dh^2A'^2) + hV(|\psi|) - h^2\psi'^2 - e^{-2A}q^2\psi^2\phi^2 + \frac{h}{2}e^{-2A}\phi'^2 = 0, \tag{3.7}$$

where ϕ is the t component of the gauge field. Evaluated at the UV boundary, the previous equation, yields

$$h_{\rm UV} = \frac{1}{A^2_{\rm UV}}. \tag{3.8}$$

Moreover, the null energy condition requires $h_{\rm UV} > h_{\rm IR} = 1$ [115] which means that $A_{\rm UV} < 1$. At the same time, $A(r)$ must increase monotonically in the whole range $-\infty < r < \infty$ and the slope in the UV-limit must be lower than in the IR-limit, i.e., $A_{\rm UV}/L < 1/L_{\rm IR}$, [223].

The resulting equations of motion are,

$$\begin{gathered}\psi'' + \psi'\left(\frac{h'}{h} + dA'\right) + \psi\frac{q^2\phi^2}{e^{2A}h^2} + \frac{V'(|\psi|)}{2h} = 0, \quad \phi'' + \phi'(d-2)A' - \phi\frac{2\psi^2q^2}{h} = 0, \\ h'' + dh'A' - \frac{2}{h}q^2\phi^2\psi^2e^{-2A} - \phi'^2e^{-2A} = 0, \quad A'' + \frac{1}{d-1}\psi'^2 + \frac{e^{-2A}q^2\phi^2\psi^2}{(d-1)h^2} = 0\end{gathered} \tag{3.9}$$

with boundary conditions in the IR-limit ($r \to -\infty$),

$$\phi \sim \phi_0 e^{\frac{r}{L_{\rm IR}}[\Delta_{\phi_{\rm IR}} - (d-2)]}, \quad \psi = \psi_{\rm IR} + a_\psi e^{\frac{r}{L_{IR}}(\Delta_{\psi_{\rm IR}} - d)}, \tag{3.10}$$

where $\Delta_{\phi_{\rm IR}}$ and $\Delta_{\psi_{\rm IR}}$ are the larger roots of: $\Delta_{\phi_{\rm IR}}[\Delta_{\phi_{\rm IR}} - (d-2)] = 2q^2\psi^2_{\rm IR}L^2_{\rm IR}$ and $\Delta_{\psi_{\rm IR}}(\Delta_{\psi_{\rm IR}} - d) = \frac{1}{2}V''(\psi_{\rm IR})L^2_{\rm IR} = -2m^2L^2_{\rm IR}$. Similarly in the UV limit ($r \to \infty$),

$$\phi = \mu - \rho e^{-\Delta_{\phi_{\rm UV}}\frac{r}{L}}, \quad \psi = \psi_{\rm UV}e^{-\frac{r}{L}A_{\rm UV}(d-\Delta_{\psi_{\rm UV}})}, \tag{3.11}$$

where, $\Delta_{\phi_{\rm UV}} = d-2$ and $\Delta_{\psi_{\rm UV}}$ is the smaller root of: $\Delta_{\psi_{\rm UV}}(\Delta_{\psi_{\rm UV}}-d) = m^2L^2/(h_{\rm UV}A^2_{\rm UV})$. The boundary conditions for h and A are given in eqs. (3.5) and (3.6). Moreover, we will take the parameters m^2 and u such that the operators dual to ψ and ϕ are irrelevant in the IR so that the IR AdS space is a fixed point of the RG flow. Repeating the argument presented in [224] it is straightforward to see this corresponds, in our notation, to:

$$\Delta_{\psi_{\rm IR}} > d, \quad \Delta_{\phi_{\rm IR}} > d-1. \tag{3.12}$$

3.2.2 d-dimensional holographic superconductivity at $T > 0$

For the study of holographic superconductors at finite temperature we employ the, by now, standard model introduced in [112, 114] by coupling anti-de Sitter gravity to a Maxwell field and a charged scalar and a quadratic (in $|\psi|$) potential. Here we state the action and equations of motion in d dimensions directly in order to settle down notation and refer to the reviews Refs. [172, 117] for more details. The action is given by,

$$S = \int d^{d+1}x\sqrt{-g}\left[R - \frac{1}{4}F^2 - |D_\mu\psi|^2 - V(|\psi|)\right], \quad V(|\psi|) = -2\Lambda + m^2|\psi|^2, \tag{3.13}$$

with $D_\mu = \partial_\mu - iq^2A_\mu$. In probe limit, corresponding to a negligible backreaction of the scalar and the Maxwell field on the geometry, is simply given by the planar-Schwarzchild AdS black hole,

$$ds^2 = -\frac{r^2}{L^2}h(r)dt^2 + \frac{L^2dr^2}{r^2h(r)} + r^2dx^idx^i, \quad i = 1,\ldots,d-1, \tag{3.14}$$

with $h(r) = 1 - r_0^d/r^d$. Assuming for the moment that the only component of the Maxwell field is $A_t = \phi(r)$ it is straightforward to obtain:

$$\psi'' + \psi'\left(\frac{h'}{h} + \frac{d+1}{r}\right) + \psi\frac{\phi^2}{r^4h^2} + \frac{V'(|\psi|)}{2r^2h} = 0, \quad \phi'' + \phi'\frac{d-1}{r} - \phi\frac{2\psi^2}{r^2h} = 0. \tag{3.15}$$

The boundary conditions are fixed from to the usual expansions:

$$\begin{aligned} \psi(r\to\infty) &= \frac{\alpha}{r^{\Delta_-}} + \frac{\beta}{r^{\Delta_+}} + \ldots, \quad \phi(r\to\infty) = \mu + \frac{\rho}{r^{d-2}} + \ldots \\ \psi(r\to r_0) &= \psi_0 + \psi_1\left(1-\frac{r_0}{r}\right)\ldots, \quad \phi(r\to r_0) = \phi_1\left(1-\frac{r_0}{r}\right) + \ldots, \end{aligned} \tag{3.16}$$

where $\Delta_\pm = \frac{1}{2}\left(d \pm \sqrt{d^2+4m^2L^2}\right)$ and ψ_1 is given in terms of the undetermined constants ψ_0, ϕ_1.

3.3 Electrical conductivity in the large d limit at $T > 0$

We start our analysis by computing the electrical conductivity, σ, at $T > 0$. For the sake of completeness we review the procedure to compute it for a general d. To this end one should add a perturbation to the vector potential $\delta A = A_x$ as well as one to the metric $\delta g = g_{tx}$. However, we will solve for σ numerically in the probe limit where,

$$ds^2 = \frac{1}{z^2}\left(f(z)dt^2 + \frac{1}{f(z)}dz^2 + dx_i^2\right), \quad f(z) = 1 - z^d, \quad i = 1, \ldots, d-1, \tag{3.17}$$

with $z = 1/r$, and choosing the horizon position $z_0 = 1$ and $L = 1$. As usual, the linear response of an operator, in our case the current $J^\mu(x)$, to an external source or field perturbation, A_x, is related, in momentum space, to the retarded Green's function, [172]:

$$\delta J^x(k) = \tilde{G}_R^{xx}(k)\delta\tilde{A}_x(k), \tag{3.18}$$

where $k = (\omega, \vec{k})$ is the d-momentum and $\tilde{G}_R^{xx}(k)$ is the Fourier transform of the retarded Green's function. Moreover, the charge current response to an electric field is $J^i(\omega) = \sigma^{ij}(\omega)E_j(\omega)$, with $E_x = -\partial_t A_x(t, z, x)$, $A_x(t, z, x) = e^{i\omega t}A_x(z, x)$, therefore, it follows that,

$$\sigma^{xx}(\omega) = \frac{\tilde{G}_R^{xx}(\omega, 0)}{i\omega}. \tag{3.19}$$

We now compute this Green's function following the procedure first outlined in Ref. [163]. First, we write the Fourier transform of the vector potential,

$$A_\mu(z, x) = \int \frac{d^d k}{(2\pi)^d} e^{ikx}\tilde{A}_\mu(z, k) \tag{3.20}$$

where $kx = -\omega t + \vec{k}\cdot\vec{x}$ and $\tilde{A}_\mu^{(0)}(k) = \tilde{A}_\mu(z = 0, k)$ is defined from the boundary value $A_\mu(z = 0, x)$. The Fourier transform of the gauge-field-part of the action leads to,

$$S_{gauge} = \int \frac{d^d k}{(2\pi)^d}\mathcal{F}(k, z)\Big|_{z=0}^{z=1} + \ldots, \quad \mathcal{F}(k, z) = -\frac{\sqrt{-g}g^{zz}g^{xx}}{2}\tilde{A}_x(z, -k)\partial_z\tilde{A}_x(z, k), \tag{3.21}$$

where the dots correspond to terms not containing A_x and its derivatives. The final expression for the conductivity is obtained by combining the proposal of Ref. [163] $\tilde{G}_R^{xx}(\omega, 0) = -2\frac{\delta^2}{\delta\tilde{A}_x^{(0)}(-k)\delta\tilde{A}_x^{(0)}(k)}\lim_{z\to 0}\mathcal{F}(k, z)$ together with eq. 3.19,

$$\mathrm{Re}[\sigma(\omega)] = \frac{1}{i\omega}\frac{\delta^2}{\delta\tilde{A}_x^{(0)}(-\omega)\delta\tilde{A}_x^{(0)}(\omega)}\lim_{z\to 0}\sqrt{-g}g^{zz}g^{xx}\tilde{A}_x(z, -k)\partial_z\tilde{A}_x(z, k)\Big|_{\vec{k}=0}. \tag{3.22}$$

In order to compute $\tilde{A}_x(z,k)$ we write the equation for $A_x(z,x)$ in the fixed background given in eq. (3.17). As was mentioned above, we assume a harmonic time dependence for A_x. The derivatives are taken with respect to the holographic coordinate, z:

$$A_x'' + \left(\frac{-d+3}{z} + \frac{f'}{f}\right) A_x' + \left(\frac{\omega^2}{f^2} - \frac{|\vec{k}|^2}{z^2 f} - \frac{2\psi^2}{z^2 f}\right) A_x = 0, \quad f = 1 - z^d. \tag{3.23}$$

Finally, we impose the usual boundary conditions, in-falling close to the horizon, $A_x \sim (f/z^2)^{-i\omega/d}(1 + \dots)$ and $A_x \sim A_x^{(0)} + A_x^{(1)} g_d(z,\omega)$ close to the boundary. The function $g_d(z,\omega)$ is easily obtained, for each d, by solving the asymptotic expansion of eq. (3.23), App. A.3. By combining eqs. (3.20) and (3.23) we obtain an analytically solvable differential equation for $\tilde{A}_x(z,k)$ at zero spatial momentum, which in the $z \to 0$ limit reduces to,

$$\tilde{A}_x''(z,\omega) + \tilde{A}_x'(z,\omega)\frac{3-d}{z} + \tilde{A}_x(z,\omega)\omega^2 = 0. \tag{3.24}$$

We choose the regular solution at $z = 0$. We note that at $\omega = 0$ the conductivity $\mathrm{Re}(\sigma)$ develops a delta function as a consequence of the translational invariance of the system.

For odd d we have now all the ingredients to compute the conductivity $\sigma(\omega)$ (3.22). However for even d, logarithmic divergences at non-zero ω appear [225]. In order to study the large-d limit of σ, it is enough to restrict our analysis to odd d. Therefore, in order to avoid the intricacies of adding the counterterms to the action to remove the divergences mentioned above, we take the prescription for $d = 4$ given in [225] and for $d = 3, 5, 7, 9$ we employ eq. (3.22).

3.3.1 Numerical calculation of the conductivity at low temperature for $d \leq 9$

In this section we compute numerically the electrical conductivity in the probe limit for $3, 4, 5, 7$ and 9 dimensions of the dual boundary theory and for two scalar masses $m^2 = 0,\ d+1$. We follow the procedure described in the previous section and solve the resulting differential equations by the shooting method. See Appendix A.3 for the specific expressions of the electrical conductivity in each dimension. The results depicted in Fig. 3.1 and Fig. 3.2 indicate that as dimensionality increases, the coherence peak becomes narrower and the position to the peak ω_g moves to lower frequencies. The physical interpretation of these features is clear. The condensate becomes less coupled as it costs less energy to break it (smaller ω_g) as d increases. Moreover, the effective bulk coupling also decreases as a narrower coherence peak is a signature of a longer life-time of the relevant excitations around ω_g. A tentative explanation of this behaviour in the gravity dual is that [118, 220] as the dimensionality increases the condensation of the scalar gradually occurs

closer to the horizon which corresponds to the less strongly interacting[1] limit of the dual field theory. A natural question to ask is whether the gravity dual has a well defined limit for $d \to \infty$. In order to answer this question in Fig. 3.3 we plot ω_g/T_c as a function of d. The ratio decreases monotonically as d increases and it is likely to converge to a finite value in the $d \to \infty$ limit still above the prediction ~ 3.528 of the Bardeen-Cooper-Schrieffer (BCS) theory of weakly coupled superconductors. It seems that this limiting value only depends weakly on the scalar conformal weight. More specifically we expect this result to hold provided that both the chemical potential, related to the kinetic energy, and the conformal weight, related to interaction energy, have the same scaling with d. It would be interesting to explore whether there exists a strict minimum bound for this quantity in the large d limit.

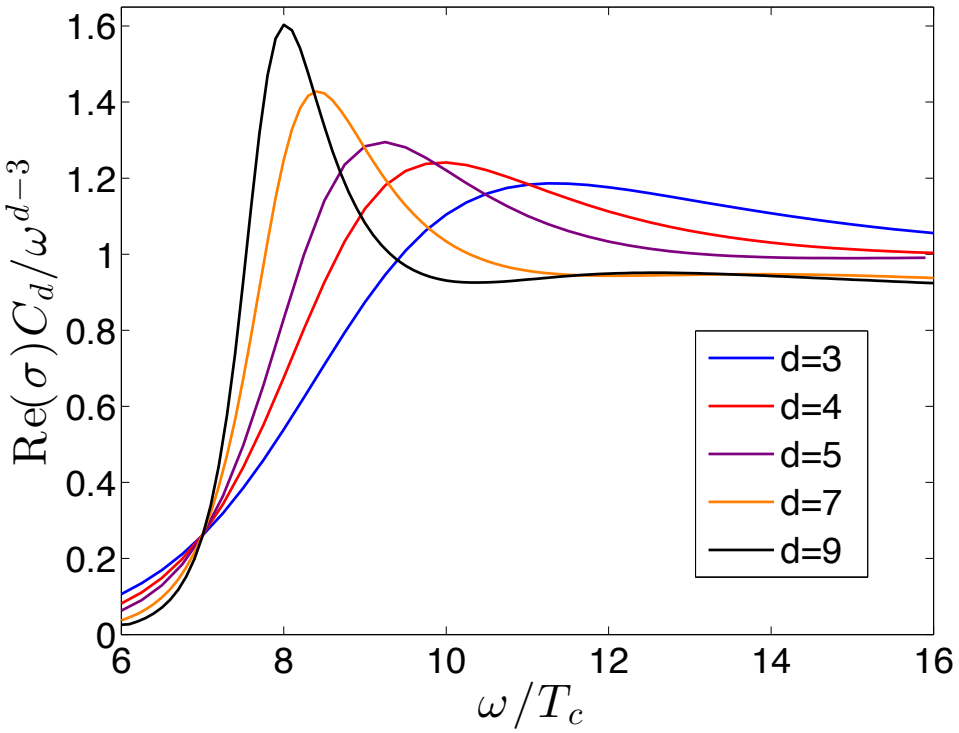

Fig. 3.1 Conductivity (3.22) in different dimensions for a massless scalar field at $T/T_c \sim 0.1$. As the dimensionality increases the coherence peak is narrower and moves to the region of lower frequencies.

Regarding Fig. 3.2 few comments are in order: a) we omit the case $d = 3$ for $m^2L^2 = d + 1$ in what follows since we have observed an anomalous behavior of the AC conductivity similar to that reported in Ref.[225], b) in Fig. 3.2, corresponding to $m^2L^2 = d + 1$, the 'crossing point' where all curves meet, $\omega/T_c \sim 7$, is slightly blurred due to the presence of extra poles, not shown, at lower frequency [225], c) although for $m^2L^2 = d + 1$ we found difficult to decrease the temperature below $T/T_c \sim 0.6$ it is clear, see Fig. 3.3, that the behavior for both masses is strikingly similar.

[1] Here we refer to the interaction responsible for the condensate.

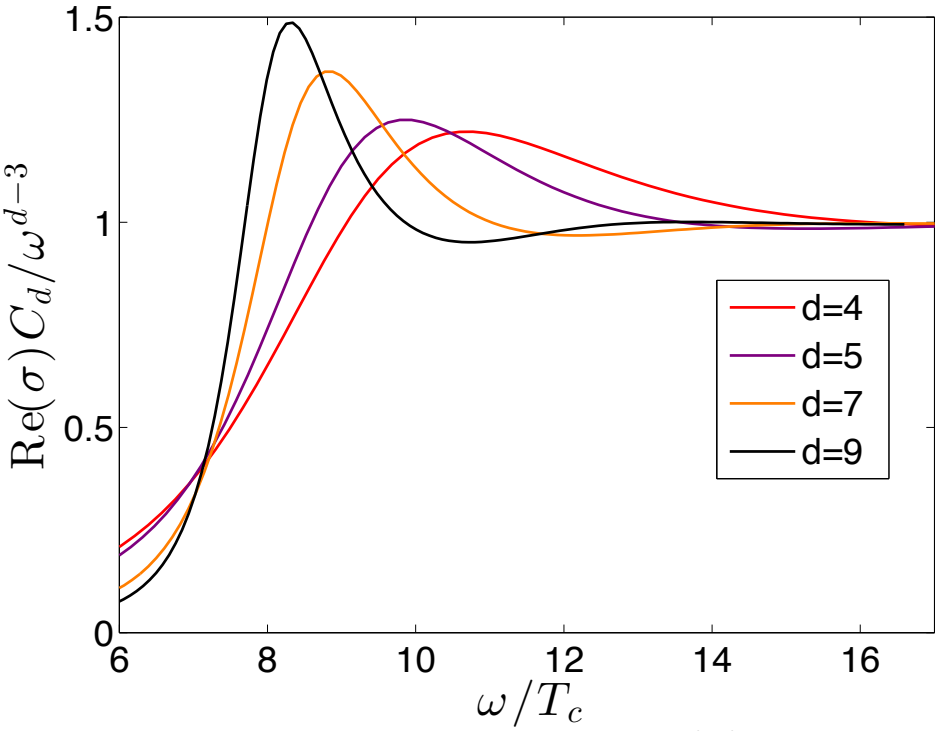

Fig. 3.2 Conductivity (3.22) in different dimensions for $m^2L^2 = d + 1$ at $T/T_c \sim 0.6$. Results are similar to those of Fig. 3.1 for $m = 0$

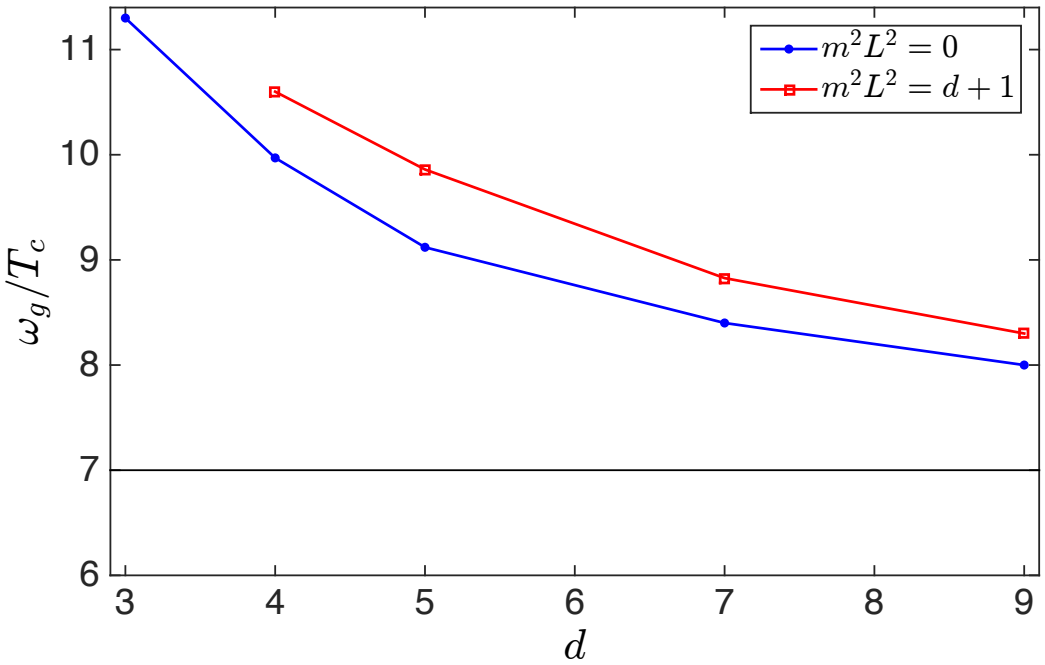

Fig. 3.3 Ratio between the peak of the conductivity ω_g and the critical temperature for $m^2L^2 = 0$ ($\Delta = d$) at $T \sim 0.1T_c$, and $m^2L^2 = d+1$ ($\Delta = d+1$) at $T \sim 0.6T_c$ as a function of the dimensionality. It always decreases as d increases and only depends weakly on the scalar mass m^2, see figures 3.1, 3.2. The horizontal black line indicates the approximate position of the crossing point in figures 3.1 and 3.2, which we also expect to correspond to the location of the peak of the conductivity for $d \to \infty$ limit. We note that even in the $d \to \infty$ limit the ratio is still substantially larger than the BCS prediction 3.528.

3.4 Relation between the order parameter $\langle\mathcal{O}\rangle$ and ω_g in the large d limit

In BCS superconductors the coherence peak in the conductivity is simply two times the value of the order parameter also referred to as the superconducting energy gap. Physically it means that since a Cooper pair is composed of two electrons it takes twice the energy gap to break a Cooper pair and place these two electrons in the first state available above the Fermi energy. For strongly coupled superconductors there is no clear relation between these two quantities as the coherence peak broadens substantially and in some materials the quasiparticle picture based on the Fermi liquid approximation breaks down. However, in the context of holographic superconductivity it is well known [116] that these two observables are still comparable, though the relation between them is not universal and different from the BCS prediction [226]. We now study to what extent this relation still holds in the large d limit. The order parameter $\langle\mathcal{O}\rangle$ is computed by following the usual steps. First we find the numerical solution of the equations of motion eq. (3.15) by the shooting method for a scalar field, $\psi(r)$, charged under the gauge field $A_t = \phi(r)$ in a non-dynamical Schwarzchild background, i.e., in the probe limit. We consider a fixed charge density and different scalar masses. The order parameter is simply $\langle\mathcal{O}\rangle^{\frac{1}{\Delta}} = [(2\Delta - d)\beta]^{\frac{1}{\Delta}}$, where Δ is the conformal dimension of the operator dual to ψ, d is the number of dimensions of the dual theory, and β is given in the boundary condition, eq. (3.16). In Table 3.1 we present results for ω_g and $\langle\mathcal{O}\rangle$ for different dimensions and masses. As dimensionality increases $\langle\mathcal{O}\rangle$ becomes much smaller than ω_g. Indeed, it seems that the ratio $\langle\mathcal{O}\rangle^{1/\Delta}/\omega_g \to 0$ as $d \to \infty$. Presently we do not have a solid explanation for this discrepancy. A finite value of the order parameter $\langle\mathcal{O}\rangle$ in holographic superconductivity is interpreted as a signature of spontaneously symmetry breaking rather than a energy gap in the spectrum. It might therefore be that these two quantities are not related and the similar value in low dimensions is a coincidence. Another more speculative explanation is that the standard recipe to compute $\langle\mathcal{O}\rangle$ misses some dimensionality prefactor. We went over the original derivation of the expression for the order parameter but we could not find any discrepancy with the expression used above. However we found that by rescaling, see Fig. 3.4, $\langle\mathcal{O}\rangle$ by $\Gamma(\Delta)$ the ratio seems to converge to a finite positive value in the $d \to \infty$ limit.[2] Whether this is just a coincidence or has a deeper physical meaning remains to be understood. Finally, we note the fact that the rescaling by $\Gamma(\Delta)$ depends on the scalar mass indicates that it is not related to the dimensional dependence of the coupling constant in the action which is usually set to the unity.

[2] Our numerical results suggest $[(2\Delta - d)\beta]^{\frac{1}{\Delta}} \to$ constant for $d \to \infty$. Thus, a factor depending only on d such as $\Gamma(d)$, instead of Δ, does not result in a finite $\langle\mathcal{O}\rangle^{1/\Delta}/T_c$ in the the limit $d \to \infty$.

	$\frac{\omega_g}{T_c}$	$\frac{\langle\mathcal{O}\rangle^{1/\Delta}}{T_c}$	$\frac{\langle\tilde{\mathcal{O}}\rangle^{1/\Delta}}{T_c}$	$\frac{\langle\mathcal{O}\rangle^{1/\Delta}}{\omega_g}$	$\frac{\langle\tilde{\mathcal{O}}\rangle^{1/\Delta}}{\omega_g}$
$d=3$	11.3	12.7	16.0	1.1	1.4
$d=4$	10.0	8.7	13.6	0.9	1.4
$d=5$	9.1	6.4	12.1	0.7	1.3
$d=7$	8.4	4.1	10.5	0.5	1.3
$d=9$	8.0	2.9	9.4	0.4	1.2

Table 3.1 Comparison of the position of the conductivity (3.22) coherence peak with the order parameter $\langle\mathcal{O}\rangle = (2\Delta - d)\beta$ and the alternate definition $\langle\tilde{\mathcal{O}}\rangle = (2\Delta - d)\Gamma(\Delta)\beta$, for $m^2L^2 = 0$ ($\Delta = d$). Convergence for large d is only observed after the order parameter is rescaled by $\Gamma(\Delta)$. We do not have a clear understanding of why the order parameter and ω_g have a different parametric dependence on the dimensionality.

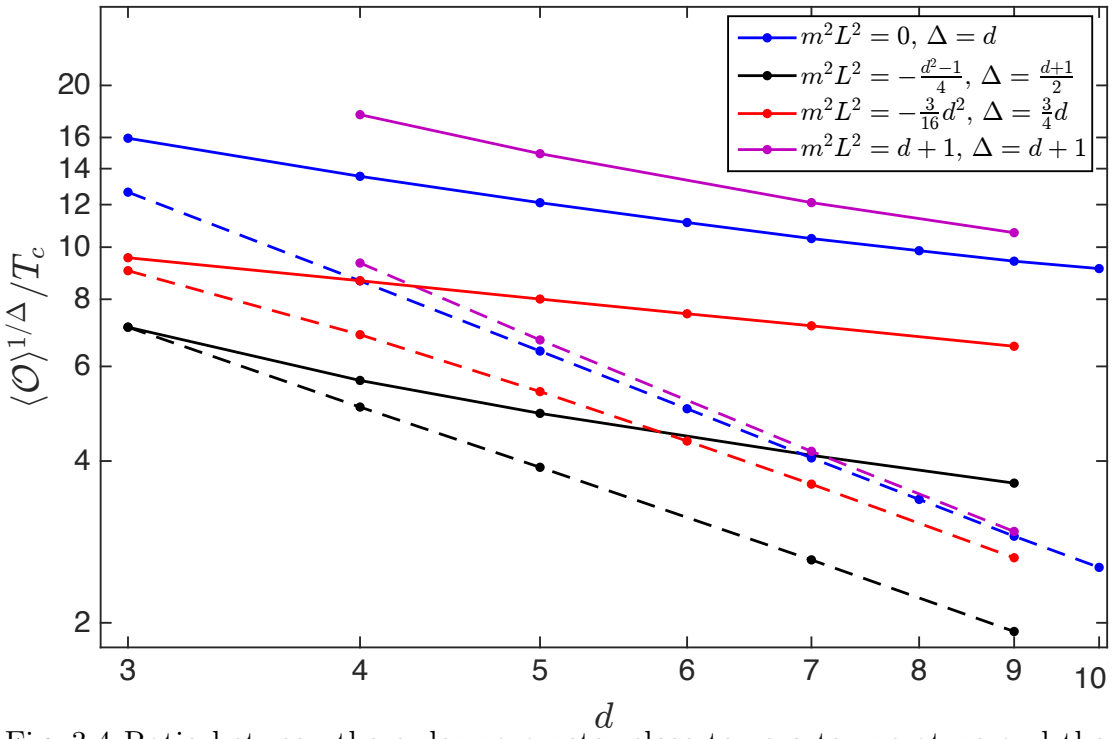

Fig. 3.4 Ratio between the order parameter close to zero temperature and the critical temperature for different dimensions and scalar masses. Dashed lines correspond to the usual definition: $\langle\mathcal{O}\rangle = (2\Delta - d)\beta$, continuous lines include a speculative factor $\Gamma(\Delta)$, $\langle\tilde{\mathcal{O}}\rangle = (2\Delta - d)\Gamma(\Delta)\beta$. Only in the latter case convergence of the ratio to a non-zero value in the $d \to \infty$ limit is likely.

3.5 Analytical calculation of the conductivity at $T = 0$ for different dimensions

We now switch to the background introduced previously in Sec. 3.2.1 to describe holographic superconductivity at $T = 0$. From now the main focus of this chapter will be to compute analylitically the conductivity and later the entanglement entropy in the large d limit in order to illustrate the interest of large $1/d$ expansion in holography.

In this section we compute the electrical conductivity at zero temperature. As was mentioned previously one must consider fluctuations of $A_x(t,r)$ and $g_{tx}(t,r)$, [114], which source an electric field E_x and carries momentum T_{tx}. These perturbations are usually assumed to have a harmonic time dependence, $A_x(r)e^{-i\omega t}$, $g_{tx}(r)e^{-i\omega t}$. Furthermore, the Einstein and Maxwell equations are expanded in $g_{tx}(r)$ keeping only linear terms in $A_x(r)$,

$$A_x''(r) + A_x'(r)\left[(d-2)A' + \frac{h'}{h}\right] + \frac{A_x(r)}{h}\left[\frac{\omega^2}{he^{2A}} - 2q^2\psi^2 - \phi'^2 e^{-2A}\right] = 0. \tag{3.25}$$

We then impose that near the UV boundary $A_x(r) = A_0 + A_1 e^{-(d-2)A(r)}$. In the infra-red limit we expect the perturbation A_x to become small. This is indeed the case for $d = 3$ but not for $d \geq 4$ [227] where it grows exponentially for $r \to -\infty$. This cast doubts about the stability of the background to small perturbations in large dimensions. Indeed, it has been observed that the addition of a gauge field increases the temperature of the dual field theory [228] even in the limit of an extremal black hole. However a full stability analysis is beyond the scope of the thesis as the main motivation here is to employ the large d limit as a computation tool to obtain analytical results. As in the $d = 4$ case studied in Ref. [229] we overlook the potential instability induced by the gauge field and proceed to solve analytically eq. 3.25 in the following three different limits.

3.5.1 Low frequencies

The small frequency dependence of σ is studied by solving eq. (3.25) in the IR limit. The scalar is now locked around its minimum, $\psi_{\rm IR}$. By using the asymptotic values of A and h in the IR limit eq. (3.25) simplifies to,

$$A_x''(r) + A_x'(r)\frac{d-2}{L_{\rm IR}} + A_x(r)\left(\frac{\omega^2}{e^{2r/L_{\rm IR}}} - 2q^2\psi_{\rm IR}^2\right) = 0, \tag{3.26}$$

where we have assumed that $e^{\frac{2r}{L_{\rm IR}}}\phi'(r) \to 0$ as $r \to -\infty$. The solution of the above equation can be written in terms of a Hankel function as:

$$A_x(r) = e^{-\frac{d-2}{2L_{\rm IR}}r} H_\alpha^{(1)}\left(\omega L_{\rm IR} e^{-\frac{r}{L_{\rm IR}}}\right), \quad \alpha = \Delta_{\phi_{\rm IR}} - \frac{d-2}{2} = \frac{1}{2}\sqrt{(d-2)^2 + 8q^2\psi_{\rm IR}^2 L_{\rm IR}^2}. \tag{3.27}$$

As was pointed out previously, [115, 116], the frequency dependence of the conductivity at zero temperature is extracted from the conservation of the flux ($\partial_r \mathcal{F} = 0$) with $\mathcal{F} = \frac{-he^{(d-2)A}}{2i} A_x^* \overleftrightarrow{\partial_r} A_x$,

$$\mathrm{Re}\,(\sigma) \propto \frac{\mathcal{F}}{\omega |A_0|^2} \tag{3.28}$$

Notice that, modulo a factor $i/2$, the flux $\mathcal{F}$ coincides with the definition of $\mathcal{F}(k,z)$ given in eq. (3.21), namely $\mathcal{F}(k,z) = -\frac{\sqrt{-g} g^{zz} g^{xx}}{2} \tilde{A}_x(z,-k)\partial_z \tilde{A}_x(z,k)$, where in this case the metric is given by eq. (3.3). In the latter the holographic coordinate is r, instead of $z = 1/r$, and we take the gauge field in position space instead of momentum space.

To obtain A_0 we need to match the solution given in eq. (3.27) to $Z(r)$, the solution of eq. (3.25) with $\omega = 0$, which is assumed to satisfy $Z(r) \to e^{-\frac{r}{L_{\rm IR}}\left(\frac{d-2}{2}-\alpha\right)}$ as $r \to -\infty$.

For ω small enough, such that $r^* \ll r_{\rm IR}$, where $r^* = L_{\rm IR} \log \omega L_{\rm IR}$ and $r_{\rm IR}$ is the scale at which the geometry is significantly deformed from eq. (3.4), the convergent part of the solution, eq. (3.27), is matched to $Z(r)$ in the region $r^* \ll r \ll r_{\rm IR}$:

$$A_x(r) \simeq C\ Z(r)(\omega L_{\rm IR})^{-\alpha}, \tag{3.29}$$

where C is a constant. Therefore, taking the limit of the previous expression when $r \to \infty$ results in

$$A_0 \propto \omega^{-\alpha}, \tag{3.30}$$

and, from eq. (3.28), the conductivity is,

$$\mathrm{Re}\,(\sigma) \propto \omega^{2\alpha-1}, \tag{3.31}$$

with $\alpha = \Delta_{\phi_{IR}} - \frac{d-2}{2} = \frac{1}{2}\sqrt{(d-2)^2 + 8q^2\psi_{\rm IR}^2 L_{\rm IR}^2}$. The exponent α that controls the strength of the low energy excitations increases with d. This is a strong suggestion that, in agreement to the results at finite temperature, high dimensionality suppress low energy excitations and therefore make the system less strongly interacting. The d dependence of the conductivity in low frequency limit was previously investigated in Ref.[227]. However the expression for the conductivity in [227] is not the same as eq. (3.31). We note that eq. (3.31) agrees with the results of Refs.[115, 229] for $d = 3, 4$ as well as with our numerical results up to $d = 9$. We observe that as d increases, the region where eq. (3.31) is a good approximation is restricted to smaller frequencies. Moreover, since for larger d the divergence in A_x is stronger, see eq. (3.27), the numerical results become less reliable, and harder to obtain, in this limit.

Finally we also note that, in Lifshitz backgrounds with hyperscaling violation, the DC conductivity for small frequencies shows a similar power law behavior [94, 230]. It would be interesting to carry out a $1/d$ expansion in these type of backgrounds in order to explore universal features in the large d limit.

3.5.2 Large frequencies

We now explore the large frequency limit of the conductivity corresponding to the region where the frequency ω is the largest energy scale in the problem, namely, it is much larger than the chemical potential or the condensate. Since the conductivity has units of energy to $d-3$ we expect that in this limit its real part $\propto \omega^{d-3}$. This can be confirmed explicitly by rewriting the prefactor in front of A_x in the third term of the left hand side of eq. (3.25) as:

$$\frac{1}{h}\left(\frac{\omega^2}{h}e^{-2A} - 2q^2\psi^2 - \phi'^2 e^{-2A}\right). \tag{3.32}$$

For $\omega L \to \infty$ and $r \to \infty$ such that $\omega L e^{-r/L} \sim \mathcal{O}(1)$, the last two terms are negligible with respect to the first,

$$2q^2\psi(r)^2 + e^{-2A(r)}\phi'(r)^2 \sim 2q^2\psi_{UV}^2 e^{-\frac{r}{L}A_{UV}(d-\Delta_{\psi_{UV}})} + \frac{\rho^2(d-2)^2}{L^2}e^{-2d\frac{r}{L}}, \tag{3.33}$$

by virtue of the boundary conditions given in eq. (3.11). These terms are negligible compared to the term $\propto \omega^2$, which by assumption is

$$\frac{\omega^2}{he^{2A}} \sim \mathcal{O}(1), \tag{3.34}$$

in the region of r considered. For even larger r, the previous term becomes arbitrarily small and no additional ω dependence is introduced. Thus, all the frequency dependence of A_x is obtained, in this region of frequency, by setting the scalar to zero and $h \simeq 1$ and $A \simeq r/L$. This leads to

$$A_x(r) = e^{-\frac{d-2}{2L}r}\left[H^{(1)}_{\frac{d-2}{2}}\left(\omega L e^{-\frac{r}{L}}\right) + C_2 H^{(2)}_{\frac{d-2}{2}}\left(\omega L e^{-\frac{r}{L}}\right)\right], \quad C_2 \in \mathbb{R}. \tag{3.35}$$

C_2 has to be determined from the solution in the bulk, however since we set $h \simeq 1$ and $A \simeq r/L$ in the whole domain of r, the solution in the IR is approximatively given by setting the solution above. Therefore, the ingoing boundary conditions imply $C_2 \sim 0$. Physically, for large enough ω the perturbation is insensitive to the flow between the two AdS spaces, and, in particular, to the presence of a nonzero scalar field in the degenerate horizon.

Close to the boundary, eq. (3.35) reads

$$A_x(r) \sim C\omega^{\frac{2-d}{2}} + \ldots, \tag{3.36}$$

where C is a constant and the dots stand for terms which depend on ω but decay exponentially with r. Therefore,

$$A_0 = \lim_{r\to\infty} A_x(r) \propto \omega^{\frac{2-d}{2}} \tag{3.37}$$

and, as before, using eq. (3.28) leads to,

$$\mathrm{Re}\,(\sigma) \simeq C_d^{-1}\omega^{d-3}\,, \quad C_d = \frac{\pi}{2}\left[\Gamma(2-d/2)\right]^{-2}2^{d-2}\,. \tag{3.38}$$

We note that this result is strictly valid for odd dimensions only. The case $d = 4$ has been discussed in [225] where, it was found $\sigma \simeq \omega[\pi/2 + i(\gamma + \log\frac{\omega}{2T_c})]$ for large frequencies.

3.6 Analytical calculation of the entanglement entropy in $d \gg 1$ dimensions

The entanglement entropy is a valuable source of information of strongly interacting systems including the classification of the different quantum phases, the estimation of the effective number of degrees of freedom of the theory, the rate of propagation of information after a perturbation or the location and characterization of phase transitions even in cases where there is no order parameter. In the context of holography it has also been intensively investigated after the landmark conjecture of Ref.[151] provided a relatively straightforward procedure to compute it. Several papers [231–235] have already discussed the entanglement entropy in holographic superconductors [232, 233], metal-superconductor transitions [234], metal-insulators transitions [231] or in a superconducting interface [235]. It has been found that the entanglement is a good observable to characterize these transitions. Its value is always smaller in the condensed phase and has a discontinuity or a kink (discontinuous derivative) that signals the transition point. It is also sensitive to a mass gap or to the proximity effect in an interface. These calculations in holographic superconductors are numerical as the calculation of the entanglement entropy requires to compute the backreaction of the scalar and gauge fields on the background. The main goal of this section is to show that explicit analytical results are possible in certain $T = 0$ backgrounds and also around the critical temperature but only in the limit of large spatial dimensions. This is a strong indication that $1/d$ expansions in holography broadens substantially the scope of the problems that can be addressed analytically.

3.6.1 Entanglement entropy at zero temperature

We now calculate analytically the entanglement entropy at zero temperature related to the background eqs. (3.1)-(3.6). According to the usual prescription [151] proposed by Takayanagi and Ryu, given a field theory in d dimensions, the entanglement entropy of a region of space $\tilde{A}$ and its complement is calculated from the gravity dual by finding the minimal $d-1$-dimensional surface $\gamma_{\tilde{A}}$ which extends into the bulk such that $\partial\gamma_{\tilde{A}} = \partial\tilde{A}$. In other words, the boundary of $\gamma_{\tilde{A}}$ at the AdS_{d+1} boundary is equal to the boundary of $\tilde{A}$.

To illustrate the calculation we choose $\tilde{A}$ to be a $d-1$ dimensional strip of width ℓ: $\tilde{A} = \{x \in \mathbb{R}^{d-1} : \ -\ell/2 < x^1 < \ell/2, \ -a/2 < x^i < a/2, \ i = 2, \ldots, d-2\}$, where a is the "length" of the strip. The entanglement entropy related to the metric eq. (3.3) is,

$$S_{\tilde{A}} = \frac{2a^{d-2}}{4G_N^{d+1}} \int_0^{\ell/2} dx e^{(d-1)A(r)} \sqrt{1 + \frac{e^{-2A(r)}}{h(r)} r'(x)^2}, \tag{3.39}$$

where, $x = x^1$, a^{d-2} results from integrating x^i with $i = 2, \ldots, d-2$ and G_N^{d+1} is the $d+1$-dimensional Newton's constant.

Sharp domain wall approximation

As was mentioned above, the background given in eq. (3.3) interpolates between two copies of AdS space in the IR and UV regions, eqs. (3.5) and (3.6). Since there is no analytical expression for $h(r)$ and $A(r)$ in the whole range of r we follow [236] and assume a sharp transition between the two AdS domains at a position denoted by r_{DW}. Numerical results show that there exists a $-\infty < r_m < 0$ such that $\psi'(r_m) = 0$. It is therefore natural to choose $r_{\text{DW}} = r_m$. Even though we will not be interested in the specific value of r_{DW} we will require $r_{\text{DW}} < 0$ in the following sections. Moreover, numerical results suggest $r_m \propto d^{-1}$.

More specifically the sharp domain wall approximation consists in taking $A(r)$ and $h(r)$ as the asymptotic values given in eq. (3.5) for $r < r_{DW}$. Similarly, for $r > r_{DW}$ we take those given in eq. (3.6).

As usual in the calculation of $S_{\tilde{A}}$ with $\tilde{A}$ a strip, eq. (3.39) does not depend on the integration variable x explicitly. Therefore, the Euler-Lagrange equations that minimize $S_{\tilde{A}}$ reduce to the Beltrami identity which states that, given a Lagrangian L, if $\partial L/\partial x = 0$, then $L - r'\partial L/\partial r'$ is a constant. In our case:

$$\frac{e^{(d-1)A(r)}}{\sqrt{1 + e^{-2A(r)} r'(x)^2/h(r)}} = \begin{cases} e^{(d-1)A_{\text{UV}} \frac{r_*}{L}}, & r > r_{DW} \\ e^{(d-1)\frac{r_*}{L_{\text{IR}}}}, & r < r_{DW} \end{cases}. \tag{3.40}$$

In the previous equation we took into account the different AdS radii, L and L_{IR} in each region, and r_* is the "turning" point of the surface $\gamma_{\tilde{A}}$ which occurs for $x = 0$. We will consider the general case $r_* < r_{DW}$, i.e. the minimal surface extends into the IR region. With the previous considerations eq. (3.40) is easily integrated,

$$\int_0^{\ell/2} dx = \frac{\ell}{2} = I_{\text{IR}} + I_{\text{UV}}, \tag{3.41}$$

where

$$I_{\rm IR} = \int_{r_*}^{r_{\rm DW}} \frac{dr}{e^{\frac{r}{L_{\rm IR}}}\sqrt{e^{2(d-1)\frac{r-r_*}{L_{\rm IR}}}-1}}, \quad I_{\rm UV} = \int_{r_{\rm DW}}^{r_{\rm UV}} \frac{dr}{\sqrt{h_{\rm UV}}e^{A_{\rm UV}\frac{r}{L}}\sqrt{e^{2(d-1)A_{\rm UV}\frac{r-r_*}{L}}-1}}, \tag{3.42}$$

$r_{\rm UV}$ being the UV cutoff. $I_{\rm IR}$ is calculated with the change of variables $t = e^{2(d-2)\frac{r-r_{\rm DW}}{L_{\rm IR}}}$,

$$I_{\rm IR} = -L_{\rm IR}e^{-\frac{r_*}{L_{\rm IR}}}\left[-\frac{\sqrt{\pi}}{d}\frac{\Gamma(\frac{3d-2}{2d-2})}{\Gamma(\frac{2d-1}{2d-2})} + \frac{e^{d\frac{r_*-r_{\rm DW}}{L_{\rm IR}}}}{d}\,{}_2F_1\left(\frac{1}{2},\frac{d}{2d-2},\frac{3d-2}{2d-2},e^{2(d-1)\frac{r_*-r_{\rm DW}}{L_{\rm IR}}}\right)\right], \tag{3.43}$$

while an analogous change of variables, $t = e^{2(d-2)A_{\rm UV}\frac{r-r_{\rm DW}}{L}}$ in $I_{\rm UV}$ yields

$$I_{\rm UV} = L\frac{e^{[(d-1)r_*-dr_{\rm DW}]\frac{A_{\rm UV}}{L}}}{d}\,{}_2F_1\left(\frac{1}{2},\frac{d}{2d-2},\frac{3d-2}{2d-2},e^{2(d-1)A_{\rm UV}\frac{r_*-r_{\rm DW}}{L}}\right), \tag{3.44}$$

where we used the relation between $h_{\rm UV}$ and $A_{\rm UV}$ given in eq. (3.8). Similarly, inserting eq. (3.40) into eq. (3.39), the entanglement entropy can be calculated by integrating in r in the two domains ($r < r_{\rm DW}$ and $r > r_{\rm DW}$):

$$S_{\tilde{A}} = \frac{2a^{d-2}}{4G_N^{d+1}}\left[S_{\rm IR} + S_{\rm UV}\right], \tag{3.45}$$

$$\begin{aligned} S_{\rm IR} &= \int_{r_*}^{r_{\rm DW}} \frac{e^{(d-2)\frac{r}{L_{\rm IR}}}dr}{\sqrt{1-e^{-2(d-1)\frac{r-r_*}{L_{\rm IR}}}}} = \frac{L_{\rm IR}e^{(d-2)\frac{r_*}{L_{\rm IR}}}}{2(d-1)}\int_0^1 du\frac{y^{1/2}}{u^{1/2}}\frac{1}{(1-yu)^{\frac{3d-4}{2d-2}}} = \\ &= \frac{L_{\rm IR}e^{(d-2)\frac{r_*}{L_{\rm IR}}}}{2(d-1)}2\sqrt{y}\,{}_2F_1\left(\frac{1}{2},\frac{3d-4}{2d-2},\frac{3}{2},y\right), \end{aligned} \tag{3.46}$$

where we made the change of variables: $u(r) = \frac{1}{y}\left(1-e^{-2(d-1)(r-r_*)/L_{\rm IR}}\right)$, $y = 1 - e^{-2(d-1)(r_{\rm DW}-r_*)/L_{\rm IR}}$. eq. (3.46) can be rewritten using the following Hypergeometric function identities,

$$\begin{aligned} {}_2F_1(a,b,c,z) =& \frac{\Gamma(1-a)\Gamma(1-b)(1-z)^{c-a-b}}{\Gamma(1-c)\Gamma(c-a-b+1)}\,{}_2F_1(c-a,c-b,c-a-b+1,1-z) + \\ &+ \frac{\Gamma(1-a)\Gamma(1-b)\Gamma(c)}{\Gamma(2-c)\Gamma(c-a)\Gamma(c-b)}z^{1-c}\,{}_2F_1(a-c+1,b-c+1,2-c,z), \end{aligned} \tag{3.47}$$

with $b = 0$, $c = \frac{3d-4}{2d-2}$, $a = c - 1/2$ and

$$c\,{}_2F_1(a-1,b,c,z) - c\,{}_2F_1(a.b-1,c,z) - (a-b)\,{}_2F_1(a,b,c+1,z) = 0, \tag{3.48}$$

with $a = 1/2,\ b = c = \frac{d}{2d-2}$, as follows

$$S_{\rm IR} = L_{\rm IR}\left[-\frac{\sqrt{\pi}e^{(d-2)\frac{r_*}{L_{\rm IR}}}}{d(d-2)}\frac{\Gamma(\frac{3d-2}{2d-2})}{\Gamma(\frac{2d-1}{2d-2})} + \frac{e^{(d-2)\frac{r_{\rm DW}}{L_{\rm IR}}}}{d-2}\sqrt{1-e^{-2(d-1)\frac{r_{\rm DW}-r_*}{L_{\rm IR}}}} + \right.$$
$$\left. + \frac{e^{-d\frac{r_{\rm DW}}{L_{\rm IR}}+2(d-1)\frac{r_*}{L_{\rm IR}}}}{d(d-2)}\,{}_2F_1\left(\frac{1}{2},\frac{d}{2d-2},\frac{3d-2}{2d-2},e^{2(d-1)\frac{r_*-r_{\rm DW}}{L_{\rm IR}}}\right)\right], \tag{3.49}$$

On the other hand, for $S_{\rm UV}$, one must take care of the usual divergence for $r \to \infty$. Defining the auxiliary variables $t = e^{-2(d-1)A_{\rm UV}\frac{r-r_{\rm DW}}{L}}$, the cutoff in the t variable $t_{\rm UV} = e^{-2(d-1)A_{\rm UV}\frac{r_{\rm UV}-r_{\rm DW}}{L}}$ and $y = e^{-2(d-1)A_{\rm UV}\frac{r_{\rm DW}-r_*}{L}}$ we integrate $S_{\rm UV}$:

$$\begin{aligned}
S_{\rm UV} &= \frac{1}{\sqrt{h_{\rm UV}}}\int_{r_{\rm DW}}^{r_{\rm UV}}\frac{e^{(d-2)A_{\rm UV}\frac{r}{L}}dr}{\sqrt{1-e^{-2A_{\rm UV}(d-1)\frac{r-r_*}{L}}}} = \frac{Le^{(d-2)A_{\rm UV}\frac{r_{\rm DW}}{L}}}{2(d-1)}\int_{t_{\rm UV}}^{1}\frac{dt}{t^{\frac{3d-4}{2d-2}}}\frac{1}{\sqrt{(1-yt)}} = \\
&= \frac{Le^{(d-2)A_{\rm UV}\frac{r_{\rm DW}}{L}}}{2(d-1)}\left[-2y^{\frac{d-2}{2(d-1)}}\sqrt{1-ty}\,{}_2F_1\left(\frac{1}{2},\frac{3d-4}{2d-2},\frac{3}{2},1-yt\right)\right]_{t=t_{\rm UV}}^{t=1} = \\
&= L\left[\frac{e^{(d-2)A_{\rm UV}\frac{r_{\rm UV}}{L}}}{d-2} - \frac{e^{(d-2)A_{\rm UV}\frac{r_{\rm DW}}{L}}}{d-2}\sqrt{1-e^{-2(d-1)A_{\rm UV}\frac{r_{\rm DW}-r_*}{L}}} + \right. \\
&\left. - \frac{e^{[-dr_{\rm DW}+2(d-1)r_*]\frac{A_{\rm UV}}{L}}}{d(d-2)}\,{}_2F_1\left(\frac{1}{2},\frac{d}{2d-2},\frac{3d-2}{2d-2},e^{2(d-1)A_{\rm UV}\frac{r_*-r_{\rm DW}}{L}}\right)\right].
\end{aligned} \tag{3.50}$$

In the last equality we used the relations given in eqs. (3.47) and (3.48) and left the cutoff $r_{\rm UV}$ explicit in the divergent term.

We stress eqs. (3.45), (3.49) and (3.50) are an approximation to the entanglement entropy between a strip of width ℓ and its complement in the d-dimensional boundary when the scalar field condensates. It is interesting to compare these results with the entanglement entropy between a strip of the same width ℓ and its complement in the situation in which the scalar is absent, [237]. To do so we should express $S_{\tilde{A}}$ in terms of ℓ, however, from eqs. (3.41), (3.43) and (3.44) it is clear that r_* cannot be expressed in terms of ℓ in a closed form and thus the comparison cannot be made easily. Instead, in the next section we make this comparison only in UV and IR limits of $S_{\tilde{A}}$. Additionally, we also study the large-d limit of $S_{\tilde{A}}$.

UV, IR and large-d limits

UV limit: we first consider $r_* > r_{\rm DW}$, i.e. the minimal surface $\gamma_{\tilde{A}}$ is embedded in the AdS copy that contains the boundary $r \to \infty$. In this situation $I_{\rm IR} = S_{\rm IR} = 0$ and

$r_{\rm DW} = r_*$ in eqs. (3.44) and (3.50):

$$\begin{aligned}\frac{\ell}{2} &= L e^{-A_{\rm UV}\frac{r_*}{L}}\frac{\sqrt{\pi}}{d}\frac{\Gamma(\frac{3d-2}{2d-2})}{\Gamma(\frac{2d-1}{2d-2})},\\ S_{\tilde{A}}^{\rm UV} &\sim \frac{2a^{d-2}L}{4G_N^{d+1}}\left\{\frac{e^{(d-2)A_{\rm UV}\frac{r_{\rm UV}}{L}}}{d-2} - \left(\frac{2}{\ell}\right)^{d-2}\frac{L^{d-2}\pi^{\frac{d-1}{2}}}{d-2}\left[\frac{\Gamma\left(\frac{d}{2d-2}\right)}{\Gamma\left(\frac{1}{2d-2}\right)}\right]^{d-1}\right\}.\end{aligned} \tag{3.51}$$

As was expected we recover the result for the infinite strip in an AdS space, found in [238]. It is observed the strip width tends to zero following $e^{-A_{\rm UV}\frac{r_*}{L}}$, while the "finite" part of the entanglement entropy diverges as $e^{(d-2)A_{\rm UV}\frac{r_*}{L}}$.

IR limit: In case $r_* \ll r_{\rm DW}$, i.e. the $\gamma_{\tilde{A}}$ extends deeply into the IR region. From eqs. (3.43), (3.44), (3.49) and (3.50)

$$\begin{aligned}\frac{\ell}{2} &= L_{\rm IR} e^{-\frac{r_*}{L_{\rm IR}}}\frac{\sqrt{\pi}}{d}\frac{\Gamma(\frac{3d-2}{2d-2})}{\Gamma(\frac{2d-1}{2d-2})},\\ S_{\tilde{A}}^{\rm IR} &\sim \frac{2a^{d-2}}{4G_N^{d+1}}\left\{L\frac{e^{(d-2)A_{\rm UV}\frac{r_{\rm UV}}{L}}}{d-2} - \left(\frac{2}{\ell}\right)^{d-2}\frac{L_{\rm IR}^{d-1}\pi^{\frac{d-1}{2}}}{d-2}\left[\frac{\Gamma\left(\frac{d}{2d-2}\right)}{\Gamma\left(\frac{1}{2d-2}\right)}\right]^{d-1} + \right.\\ &\left. + \frac{L_{\rm IR}e^{(d-2)\frac{r_{\rm DW}}{L_{\rm IR}}} - Le^{(d-2)A_{\rm UV}\frac{r_{\rm DW}}{L}}}{d-2}\right\}.\end{aligned} \tag{3.52}$$

In this limit, the strip width, ℓ, diverges and the finite part of the entanglement entropy saturates to a constant value given by the first term in the following expression:

$$\lim_{r_*\to-\infty} S_{\tilde{A}}^{\rm IR} = \frac{2a^{d-2}}{4G_N^{d+1}(d-2)}\left[L_{\rm IR}e^{(d-2)\frac{r_{\rm DW}}{L_{\rm IR}}} - Le^{(d-2)A_{\rm UV}\frac{r_{\rm DW}}{L}}\right] + \frac{2a^{d-2}}{4G_N^{d+1}}\frac{e^{(d-2)A_{\rm UV}\frac{r_{\rm UV}}{L}}}{d-2}. \tag{3.53}$$

At this point, it is easy to compare eq. (3.52) to the entanglement entropy between the strip $\tilde{A}$ (of same width ℓ) and its complement in the d-dimensional AdS boundary when $\psi = 0$. Were the scalar field be zero, there would be a single AdS space and $S_{\tilde{A}}$ would be given by the first two terms of eq. (3.52) while the last term would be zero for all d. In the presence of the condensate, the third term in the previous equation corresponds to the contribution of the flow from one AdS copy to the other. Indeed it is easy to see that this term is negative. From the definition of $L_{\rm IR}$: $-d(d-1)/L_{\rm IR}^2 \equiv V(|\psi_{\rm IR}|) = -d(d-1)/L^2 - m^4/(2u)$, it follows $L_{\rm IR} < L$. Since we require $r_{\rm DW} < 0$, the term in square brackets of eq. (3.53)

$$L_{\rm IR}e^{(d-2)\frac{r_{\rm DW}}{L_{\rm IR}}} - Le^{(d-2)A_{\rm UV}\frac{r_{\rm DW}}{L}} < e^{(d-2)A_{\rm UV}\frac{r_{\rm DW}}{L}}(L_{\rm IR} - L) < 0. \tag{3.54}$$

The conclusion is that the entanglement entropy between a strip of length ℓ and its complement is lower if the scalar is present. This means the theory has less degrees of freedom in this case. In the limit of a strip of infinite width ($\ell \to \infty$), the finite contribution of $S_{\tilde{A}}$ reaches the maximum value given by the first term in eq. (3.53). These results are expected as the entanglement entropy counts the degree of freedom of the theory. It is therefore natural that it is smaller in the condensed phase.

Let us turn to the study of the large-d limit of $S_{\tilde{A}}$. Before we do so, we must analyze the behavior of the strip length as $d \to \infty$. From eqs. (3.41), (3.43) and (3.44) it is clear that if r_* either remains constant or increases, as d increases, both $I_{\rm IR}$ and $I_{\rm UV}$ would tend to zero and $l \to 0$. In order to compare $S_{\tilde{A}}$ for different d we must keep ℓ constant. Therefore, $r_* \to -\infty$, as $d \to \infty$, which corresponds to the IR limit ($r_* \ll r_{\rm DW}$) studied above. Taking d large and ℓ constant in eq. (3.52) yields,

$$r_*(d \to \infty) \sim -L_{\rm IR} \log \frac{\ell d}{\pi L_{\rm IR}}, \tag{3.55}$$

and

$$\begin{aligned} S_{\tilde{A}}(d \to \infty) \sim \frac{1}{4G_N^{d+1}} \Bigg[& \frac{2a^{d-2} L e^{(d-2)A_{\rm UV}\frac{r_{\rm UV}}{L}}}{d-2} - \frac{\pi^{d-1} L_{\rm IR}^{d-1}}{(d-2)(d-1)^{d-1}} \left(\frac{a}{\ell}\right)^{d-2} + \\ & + 2a^{d-2} \frac{L_{\rm IR} e^{(d-2)\frac{r_{\rm DW}}{L_{\rm IR}}} - L e^{(d-2)A_{\rm UV}\frac{r_{\rm DW}}{L}}}{d-2} \Bigg]. \end{aligned} \tag{3.56}$$

The second term of the previous equation corresponds to the universal contribution for the infinite strip in an AdS space, [238] which is strongly suppressed in the $d \to \infty$ limit as it is proportional to d^{-d}. The third term has some interesting features. It is independent of ℓ as it is expected in gapped systems where the typical length, the numerator in this case, is closely related to the coherence length of the holographic superconductor. Its d-dependence, arising from the flow of one AdS space to another, is dictated by the d-dependence of $r_{\rm DW}$ and $A_{\rm UV}$. As mentioned before, numerical results for $d \leq 9$ suggest $\frac{r_{\rm DW}}{L_{\rm IR}} \propto d^{-1}$ and $r_{\rm DW} < 0$ which implies a behavior like d^{-1} for these contributions. In the limit of a vanishing scalar field, the third term vanishes for all d and the result of Ref.[238] is recovered.

Let us simplify eq. (3.56) for the particular set of parameters: $m^2L^2 = -3d^2/16$, $\psi_{\rm IR} = \sqrt{\frac{d-1}{d}}$, $u = -\frac{m^2L^2}{\psi_{\rm IR}^2}$, $L = 1$. These values, together with the definition of $L_{\rm IR}$: $\frac{-d(d-1)}{L_{\rm IR}^2} \equiv V(|\psi_{\rm IR}|)$, yield a constant, in d, $L_{\rm IR} = \sqrt{32/35}L$. Moreover, as discussed earlier,

$\frac{A_{\rm UV}}{L} < \frac{1}{L_{\rm IR}}$. These considerations allow a further simplification of eq. (3.56),

$$\begin{aligned} S_{\tilde{A}}(\ell, a, d \to \infty) &\lesssim \frac{a^{d-2}}{4G_N^{d+1}} \left[S_{div} - \frac{\pi^d L_{\rm IR}^{d-1}}{d^d} \frac{1}{\ell^{d-2}} + 2e^{\frac{\alpha}{L_{\rm IR}}} \frac{L_{\rm IR} - L}{d} \right] \\ &\sim \frac{a^{d-2}}{4G_N^{d+1}} \left[S_{div} - \frac{\pi^d}{d^d} \left(\frac{32}{35} \right)^{\frac{d-1}{2}} \frac{1}{\ell^{d-2}} + 2\Delta L e^{\alpha} \frac{1}{d} \right], \end{aligned} \tag{3.57}$$

where ℓ and a are the width and the characteristic length (infinite) of the transverse dimensions of the strip. The radius of curvature of the IR asymptotic AdS space, $L_{\rm IR}$, does not depend on d, α is the constant of proportionality in $r_{\rm DW} \simeq \frac{\alpha}{L_{\rm IR} d}$ which can only be obtained numerically and $\Delta L = L_{\rm IR} - L = \sqrt{32/35} - 1 < 0$. S_{div} is the (divergent) part containing the UV integration cutoff.

As we mentioned previously, were the condensate vanish, the last term in eq. (3.57) would be identically zero, since the asymptotic IR and UV AdS radii would be the same, $L_{\rm IR} = L$. Moreover, this term is negative, which means the finite part of the entanglement entropy is lower, and thus indicates less degrees of freedom in the presence of the condensate. Finally, as $d \to \infty$, this contribution is smaller, suggesting the difference between the entanglement entropy in the presence and absence of the condensate is smaller. The latter is an indication that, in agreement with the conductivity results, the condensate interactions become weaker as d increases.

3.6.2 Entanglement entropy close to the transition

In this section we compute analytically the entanglement between the semi-infinite strip, $\tilde{A}$, defined in the previous section and its complement at finite temperature. We employ the action eq. (3.13) but we have to go beyond the probe limit. We assume the following parametrization of the metric:

$$ds^2 = \frac{1}{L^2 z^2} \left(-f(z) e^{-\chi(z)} dt^2 + \frac{L^4}{f(z)} dz^2 + dx_i^2 \right), \tag{3.58}$$

where $i = 1, \ldots, d-1$, $z = 1/r$. Above the transition, the metric corresponds to the AdS planar Reissner-Nordström in $d+1$ dimensions. More precisely, $\chi(z) = 0$, the gauge field $A_t = \phi = \mu[1 - (z/z_0)^{d-2}]$ and $f(z) = f_{\rm RN} \equiv 1 - (1+Q^2)\left(\frac{z}{z_0}\right)^d + Q^2 \left(\frac{z}{z_0}\right)^{2d-2}$, where $Q^2 = \mu^2 z_0^2 \gamma^{-2}$, $\gamma^{-2} = \frac{d-2}{d-1}\frac{L^2}{2}$ and z_0 is the inverse of the outer horizon r_0.

Throughout this section we take d to be large so we can get explicit analytical results. We also consider strips of length ℓ for which the minimal surface $\gamma_{\tilde{A}}$, associated to the strip, does not extend too deeply into the bulk, such that the turning point, z_*, satisfies $(z_*/z_0)^d \ll 1$. This is in general a good approximation in the $d \to \infty$ limit, even for $z_* \lesssim z_0$. Moreover we restrict ourselves to the region $T \sim T_c$ and therefore, the dual order parameter $\langle \mathcal{O} \rangle$ is very small compared to the typical energy scale T_c. This regime

restricts the generality of the results for the entanglement entropy but allows to estimate analytically the correction in the presence of the scalar field close to the phase transition.

The entanglement between the strip and its complement is given by:

$$s_{\tilde{A}} \equiv S_{\tilde{A}} \frac{4G_N^{d+1}}{a^{d-2}L^{d-1}} = 2\int_0^{\ell/2} dx \frac{1}{z^{d-1}}\sqrt{1+\frac{z'(x)^2}{f(z)}} = 2z_*^{d-1}\int_{z_{\rm UV}}^{z_*} \frac{dz}{z^{d-1}} \frac{1}{\sqrt{f(z)\left(z_*^{2d-2}-z^{2d-2}\right)}}, \tag{3.59}$$

where we have rescaled $z \to z/L^2$ in order to compare with the results in Ref.[232]. We have also introduced the UV cutoff $z_{\rm UV} \to 0$ and, as before, we have used the fact that the integral does not depend on x. The turning point, z_*, of the surface $\gamma_{\tilde{A}}$ embedded into the bulk is given by $z_*^{d-1} = z^{d-1}\sqrt{1+z'(x)^2/f(z)}$. The strip width, ℓ is related to z_* as follows:

$$\frac{\ell}{2} = \int_0^{z_*} dz \frac{z^{d-1}}{\sqrt{f(z)\left(z_*^{2d-2}-z^{2d-2}\right)}}. \tag{3.60}$$

Even in the absence of the scalar field in eq. (3.1), i.e., the Reissner-Nordström background, the previous two integrals cannot be computed analytically for arbitrary d. However, an analytical calculation is possible in the large d limit.

First, we calculate the width of the strip from eq. (3.60), by setting $f(z) = f_{\rm RN}(z)$ and expanding $\sqrt{f_{\rm RN}(z)}$ in powers of z/z_0:[3]

$$\frac{\ell}{2} = \frac{z_*\sqrt{\pi}}{d}\frac{\Gamma\left(\frac{3d-2}{2d-2}\right)}{\Gamma\left(\frac{2d-1}{2d-2}\right)} + z_*\sum_{n=1}^{\infty}\sum_{l=0}^{n} C_{nl}\alpha^l(-\beta)^{n-l}\left(\frac{z_*}{z_0}\right)^{b_{nl}}, \tag{3.61}$$

where,

$$C_{nl} = \frac{(2n-1)!!}{2^n(n-l)!l!}\frac{\Gamma\left(\frac{2d+a_{nl}-1}{2d-1}\right)}{\Gamma\left(\frac{a_{nl}+d}{2d-2}\right)}\frac{\sqrt{\pi}}{a_{nl}+1}, \tag{3.62}$$

$\alpha = 1+Q^2$, $\beta = Q^2$ and $a_{nl} = 2dn + d(1-l) + 2(l-n) - 1$, $b_{nl} = (2d-2)(n-l) + dl$. In the large d limit, assuming ℓ fixed, it is enough to keep only the terms corresponding to $n = 1$ in the series above. The resulting expression of the strip length, ℓ, as a function of the turning point of the minimal surface, z_*, is,

$$\frac{\ell}{2} \simeq \frac{z_*}{d}\left[\frac{\pi}{2} + \frac{1+Q^2}{2d}\left(\frac{z_*}{z_0}\right)^d - \frac{Q^2\pi}{8d}\left(\frac{z_*}{z_0}\right)^{2d-2} + \dots\right]. \tag{3.63}$$

[3]For simplicity it is more convenient to expand in $\delta = -(1+Q^2)\left(\frac{z}{z_0}\right)^d + Q^2\left(\frac{z}{z_0}\right)^{2d-2}$.

Similarly, from eq. (3.59), with $f(z) = f_{\rm RN}(z)$,

$$s_{\tilde{A}} = \frac{2}{(d-2)z_{\rm UV}^{d-2}} - \frac{2\sqrt{\pi}}{(d-2)z_*^{d-2}} \frac{\Gamma\left(\frac{d}{2d-2}\right)}{\Gamma\left(\frac{1}{2d-2}\right)} + \frac{2}{z_*^{d-2}} \sum_{n=1}^{\infty} \sum_{l=0}^{n} C_{nl} \alpha^l (-\beta)^{n-l} \left(\frac{z_*}{z_0}\right)^{b_{nl}}, \quad (3.64)$$

where C_{nl} is given in eq. (3.62), $a_{nl} = (2d-2)(n-l)+d(l-1)+1$, $b_{nl} = (2d-2)(n-l)+dl$. For large d, taking the first two terms of the series,

$$\begin{aligned} s_{\tilde{A}} &\simeq \frac{2}{dz_{\rm UV}^{d-2}} - \frac{\pi}{d^2 z_*^{d-2}} + \frac{1+Q^2}{2z_*^{d-2}} \left(\frac{z_*}{z_0}\right)^d - \frac{\pi Q^2}{2z_*^{d-2}} \left(\frac{z_*}{z_0}\right)^{2d-2} + \dots \\ &\simeq \frac{2}{dz_{\rm UV}^{d-2}} - \frac{\pi^{d-1}}{d^d} \frac{1}{\ell^{d-2}} + \frac{1+Q^2}{2z_0^d} \frac{d^2}{\pi^2} \ell^2 - \frac{Q^2}{2\pi^{d-1} z_0^{2d-2}} d^d \ell^d + \dots, \end{aligned} \quad (3.65)$$

where, in the last equality we substituted $z_* \sim \frac{d\ell}{\pi}$, which is a good approximation as long as $z_* \ll z_0$ (small ℓ) and d fixed or, for a fixed $z_* \lesssim z_0$, and sufficiently large d. In the latter case, ℓ should also be small, which means that as d increases the minimal surface $\tilde{A}$ should reach the near-horizon region for smaller strip lengths. Q is related to the chemical potential and the position of the outer horizon, through μ and z_0, $Q^2 = \mu^2 z_0^2 \gamma^{-2}$, $\gamma^{-2} = \frac{d-2}{d-1}\frac{L^2}{2}$.

In the presence of the scalar field, ψ, analytical results are harder to obtain close to the phase transition $T \lesssim T_c$ since $f(z)$ is subject to the backreaction of ψ, and, in general, cannot be written in a closed form.

However, we show below that it is still possible to find an explicit analytical expression in the large-d limit.

In order to proceed we solve perturbatively the equations of motion close to the transition. To do so we expand the fields in the equations of motion (see the appendix A.1 for more details) in a power series in a quantity related to the VEV of the operator dual to the scalar field. More specifically, from the UV boundary condition of the scalar field, $\psi \sim \frac{\alpha}{r^{\Delta_-}} + \frac{\beta}{r^{\Delta_+}} + \dots$, given in eq. (3.16), we set $\alpha = 0$ and *define* $\epsilon \equiv \beta$. Close to the transition this expansion parameter is related to temperature in the usual way, $\epsilon^{\Delta_+} \propto \langle \mathcal{O} \rangle \propto (T - T_c)^{1/2}$, with Δ_+ being the conformal dimension.
The blackening function can be expanded as $f(z) \simeq f_{\rm RN} + \epsilon^2 (f_2^a(z) + \dots)$ with $f_2^a(z) = -\mu_0 \kappa z_0^2 \left[\left(\frac{z}{z_0}\right)^d - \left(\frac{z}{z_0}\right)^{2d-2}\right]$ and the dots indicate subleading terms, see appendix eq. (A.10), where μ_0 is the chemical potential at the phase transition and κ is an integration constant which is calculated from the perturbative analysis of the equations of motion, eq. (A.12). It is negative $\kappa < 0$ for $d \geq 3$.

The calculation of the entanglement entropy including the leading correction $\epsilon^2 f_2^a(z)$ is totally analogous to the one corresponding to the Reisnner-Nordström case given in detail

above. The main difference is that α and β in eqs. (3.61) and (3.64) are replaced by,

$$\tilde{\alpha} = 1 + \tilde{Q}^2 + \epsilon^2 \mu_0 \kappa \tilde{z}_0^2, \quad \tilde{\beta} = \tilde{Q}^2 + \epsilon^2 \mu_0 \kappa \tilde{z}_0^2. \tag{3.66}$$

Here, $\tilde{Q}^2 = \mu_0^2 \tilde{z}_0^2 \gamma^{-2} \neq Q^2$ and $\tilde{z}_0 \neq z_0$, in order to take into account the different horizon radius with respect to a pure Reissner-Nordström black hole at the same temperature.

Consequently, in the large-d limit, the relation between the strip width and the turning point of $\gamma_{\tilde{A}}$ in the hairy black hole background is,

$$\frac{\ell}{2} \simeq \frac{\tilde{z}_*}{d} \left[\frac{\pi}{2} + \frac{\tilde{\alpha}}{2d} \left(\frac{\tilde{z}_*}{\tilde{z}_0} \right)^d - \frac{\tilde{\beta}\pi}{8d} \left(\frac{\tilde{z}_*}{\tilde{z}_0} \right)^{2d-2} + \dots \right] \tag{3.67}$$

Similarly, $\tilde{s}_A$ is

$$\tilde{s}_A \simeq \frac{2}{d z_{\rm UV}^{d-2}} - \frac{\pi}{d^2 \tilde{z}_*^{d-2}} + \frac{1 + \tilde{Q}^2 + \mu_0 \kappa \epsilon^2 \tilde{z}_0^2}{2 \tilde{z}_*^{d-2}} \left(\frac{\tilde{z}_*}{\tilde{z}_0} \right)^d - \pi \frac{\tilde{Q}^2 + \mu_0 \kappa \epsilon^2 \tilde{z}_0^2}{2 \tilde{z}_*^{d-2}} \left(\frac{\tilde{z}_*}{\tilde{z}_0} \right)^{2d-2} + \dots, \tag{3.68}$$

where, $\kappa < 0$ is given in the appendix A.1. In order to compare the entanglement entropy between the strip and its complement in the condensed phase with the one in the symmetry unbroken phase one needs, in principle, to compute the charge, Q, and horizon position, z_0, of a Reisnner-Nordström black hole at the same temperature, eq. (3.69). However it is important to note that the contribution due to the condensate, contained in the ϵ^2 term, always leads to less entanglement in the condensed phase ($\mu_0 > 0$ and $\kappa < 0$).

To compute the Reissner-Nordström black hole parameters at the same temperature as the hairy black hole we fix the horizon in the superconducting phase, $\tilde{z}_0 = 1$, and solve the following equations in the horizon, z_0, and charge, Q:

$$\mu = \frac{Q}{z_0 \gamma}, \quad \frac{T}{\rho^{\frac{1}{d-1}}} = \frac{1}{4\pi} \frac{d - (d-2) Q^2}{(Q/\gamma)^{\frac{1}{d-1}}}, \tag{3.69}$$

where $T/\rho^{\frac{1}{d-1}}$ is a function of ϵ (proportional to $\langle \mathcal{O} \rangle^{1/\Delta}$), the metric components at the horizon and the chemical potential at the the transition, μ_0, eq. (A.13), and $\mu = \mu_0 + \epsilon^2(\kappa + \phi_2^b(0)) > \mu_0$, where κ and $\phi_2^b(0)$ are integration constants given in the App. A.1. From eq. (3.69) it follows that $\tilde{z}_0 > z_0$ and $\tilde{Q} < Q$, and solving eqs. (3.63) and (3.67) one obtains $\tilde{z}_* > z_*$. Consequently, comparing the finite contributions in eqs. (3.65) and (3.68), we conclude that below, but close, to the phase transition the number of degrees of freedom in the dual field theory is smaller than in the normal phase (no condensate, $\epsilon = 0$, $\mu = \mu_0$). This is again consistent with the theoretical expectation that the entanglement entropy is closely related to the effective number of degrees of freedom of the system at a given temperature.

For completeness, we express $\tilde{s}_{\tilde{A}}$ in terms of the strip length ℓ, the expansion parameter $\epsilon \propto \langle \mathcal{O} \rangle^{1/\Delta}$, μ_0 and κ. From eq. (3.67), $\tilde{z}_* \sim \frac{d\ell}{\pi} \left[1 + \mathcal{O}(d^{-2d})\right]$. Substituting $z_* = \frac{d\ell}{\pi}$ in eq. (3.68), the final expression of the entanglement entropy in terms of the strip length is given by,

$$\tilde{s}_{\tilde{A}} \simeq \frac{2}{d z_{\mathrm{UV}}^{d-2}} - \frac{\pi^{d-1}}{d^d} \frac{1}{\ell^{d-2}} + \frac{1 + \tilde{Q}^2 + \mu_0 \kappa\, \epsilon^2 \tilde{z}_0^2}{2 \tilde{z}_0^d} \frac{d^2}{\pi^2} \ell^2 - \frac{\tilde{Q}^2 + \mu_0 \kappa\, \epsilon^2 \tilde{z}_0^2}{2 \pi^{d-1} \tilde{z}_0^{2d-2}} d^d \ell^d + \dots . \tag{3.70}$$

Before we compare eq. (3.70) with numerical results we discuss the limits of applicability of the linear approximation $z_* \sim \tilde{z}_* \propto \ell$.

In figures 3.5, 3.6 we depict the dependence of the tip of the surface $\tilde{A}$ on ℓ resulting from solving eqs. (3.60) and (3.61). For small ℓ, the linear approximation agrees well with the exact result, eq. (3.60). As ℓ grows this agreement worsens substantially. Additionally, as d increases, the approximation $z_* = \tilde{z}_* = \ell \frac{d\ \Gamma\left(\frac{2d-1}{2d-2}\right)}{2\sqrt{\pi}\Gamma\left(\frac{3d-2}{2d-2}\right)}$ is valid for smaller values of ℓ but, at the same time, since the corrections $\mathcal{O}(d^{-2d})$ are smaller, it remains a good approximation closer and closer to the horizon for both the normal ($T < T_c$), Fig. 3.5, and the condensed phase close to the transition, Fig. 3.6. This is nothing else but a consequence of the simplification of general relativity in the large-d limit. For a black hole, as dimensionality increases, its region of influence shrinks to a neighbourhood of the horizon [118].

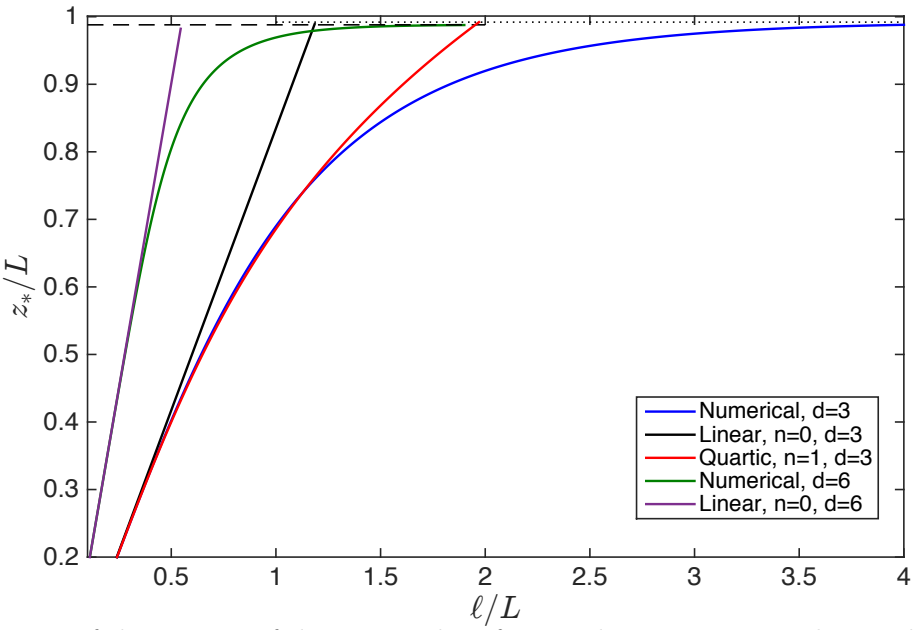

Fig. 3.5 Position of the tip, z_*, of the minimal surface in the Reissner-Nordström background for $d = 3$ and $d = 6$. For $d = 3$, $\mu = 2.02$, $Q^2 = \mu^2 z_0^2 \gamma^{-2}$, $\gamma^{-2} = \frac{d-2}{d-1}\frac{L^2}{2}$ and $z_0 = 0.992$ (dotted line), while for $d = 6$, $\mu = 0.38$ and $z_0 = 0.988$ (dashed line). The "numerical" results are obtained from the numerical integration of eq. (3.60) with $f(z) = f_{\rm RN}$. The linear approximation $z_* \propto \ell$ corresponds to $n = 0$ in eq. (3.61) and $\alpha = 1 + Q^2$, $\beta = Q^2$. The analytical solution of the fourth degree polynomial in z_* contains the leading correction, the first term of the series given in eq. (3.61). The linear approximation $z_* \propto \ell$ is clearly only valid for small ℓ and, for larger d, it becomes gradually better deep in the bulk. Including more corrections in higher powers of z_*/z_0 gives a better approximation but requires, in general, numerical methods.

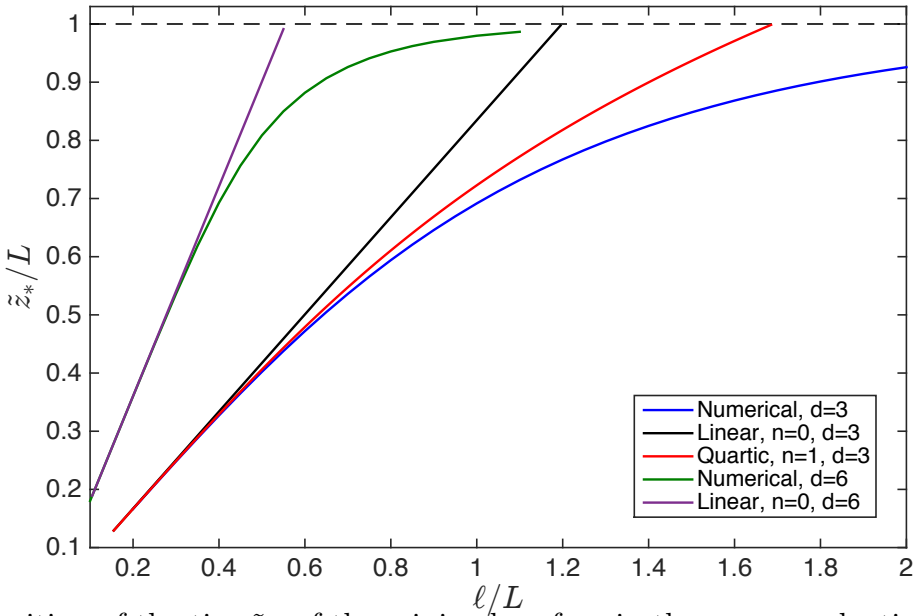

Fig. 3.6 Position of the tip, $\tilde{z}_*$, of the minimal surface in the superconducting phase for $d = 3$, $\mu = 2.00$ and $d = 6$, $\mu = 0.37$. In both cases the horizon is fixed at $z_0 = 1$ (dashed line) and $Q^2 = \mu_0^2 \tilde{z}_0^2 \gamma^{-2}$, $\gamma^{-2} = \frac{d-2}{d-1}\frac{L^2}{2}$. Similarly to Fig. 3.5 the numerical results are obtained from eq. (3.60) with $f(z) = f_{\rm RN} + \epsilon^2 f_2$ and f_2 given in eq. (A.10). The rest of the lines are obtained by truncating the series in eq. (3.61) at linear and quartic powers of z_* with α and β given in eq. (3.66). Similarly to the symmetry unbroken phase, Fig. 3.5, the linear approximation $\tilde{z}_* \propto \ell$ is better for larger d.

Another relevant feature of the entanglement entropy eq. (3.70), that requires clarification, is that it does not obey the volume law. It is well known that for a sufficiently large ℓ, the finite contribution of the entanglement entropy at finite temperature satisfies the volume-law, not the area, i.e., a linear-in-ℓ term is expected. The analytical prediction eq. (3.70) does not reproduce such behavior since we are neglecting terms $(z_*/z_0)^d \ll 1$ in eqs. (3.61), (3.64). This is fine for small ℓ or, for a fixed ℓ and T, and a sufficiently large d. However, for a large, but *fixed* d, the approximation breaks down for large ℓ since z_* eventually becomes sufficiently close to the horizon z_0 so that $(z_*/z_0)^d \approx 1$. As seen in figures 3.5, 3.6, in principle a remedy to this problem is to include more terms in the expansions given in eqs. (3.61), (3.64). The first correction, proportional to $(z_*/z_0)^{d+1}$, coming from the $n = 1$ term, still leads to an analytical, but cumbersome, expression for $z_*(\ell)$ in the case of $d = 3$. Indeed, as is shown in figures 3.5, 3.6, by including this term, the analytical expression agrees with the numerical results up to larger values of ℓ, however we do not yet observe the expected area law for and $\ell \to \infty$. Indeed, for any finite number of terms the approximation inevitably still breaks down at some finite ℓ, and, already for $d = 3$, the subleading correction, $\propto (z_*/z_0)^{2d-1}$, coming from the $n = 1$ term in eq. (3.61), leads to a fifth degree polynomial whose roots cannot in general be found numerically. Consequently we keep only the leading correction in the equations for z_* and $\tilde{z}_*$ so our results are fully analytical. As is shown in Fig. 3.7, by including this additional term only, the analytical expression for the finite part of the entanglement entropy agrees well with the numerical results in the range of ℓ shown. However, as was mentioned previously, we do not yet observe the expected area law for $\ell \to \infty$. If, on the other hand, we carry out an analogous expansion in the parameter $1 - (z_*/z_0)^d$, see appendix A.2, we obtain the expected linear dependence of the entanglement entropy $s \propto \ell$.

We also note that the finite subleading contribution, second term of eq. (3.70), that does not depend on the scalar, has already been reported in Ref. [237, 151]. The dependence on the scalar, proportional to $\kappa < 0$, is consistent with previous numerical results [232]. It is smaller in the symmetry broken phase and its temperature dependence is not analytical at T_c due to the different prefactors in the temperature dependence of the entanglement entropy in the broken and unbroken phase. We note the temperature enters both through $\tilde{z}_0$ and μ and it depends quadratically on the strip length ℓ, for small ℓ. These results illustrate the potential of $1/d$ expansions to obtain analytical results in problems where only numerical calculation were available.

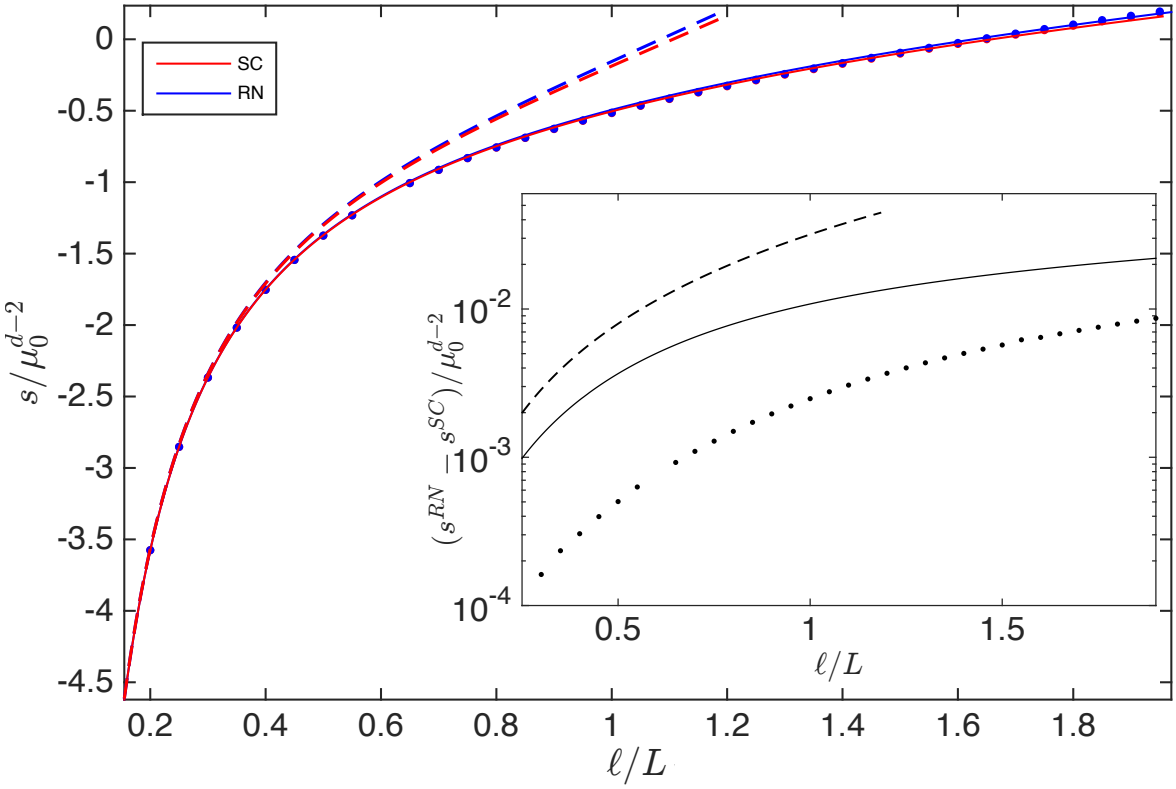

Fig. 3.7 Finite part of the entanglement entropy, s, of a rectangular strip, $\tilde{A}$, of width ℓ in 2 spatial dimensions ($d = 2+1$), where $s_{\tilde{A}} = s_{div} + s$ and s_{div} contains the UV-cutoff. The blue dots are obtained by numerical integration of eqs. (3.59) and (3.60) in the Reissner-Nordström background with $f(z) = f_{\rm RN}$, $z_0 = 0.992$, $\mu = 2.02$, $Q^2 = \mu^2 z_0^2 \gamma^{-2}$, $\gamma = \frac{d-2}{d-1}\frac{L^4}{2}$. Similarly, the red dots, hardly indistinguishable from the blue, correspond to the integration of these equations in the superconducting phase where $f(z) = f_{\rm RN} + \epsilon^2 f_2$ and $f_2 = f_2^a + f_2^b$ is given in eq. A.10. We set $m^2L^2 = 0$, $\tilde{z}_0 = 1$, $q = 4$ and $\epsilon = 0.2$ corresponding to $T/T_c \sim 0.995$. The expansion parameter $\epsilon = \langle \mathcal{O}/(2\Delta - d)\rangle^{1/\Delta}$ is defined in the same appendix. In the superconducting phase $f_{\rm RN}$ is given in terms of $\mu_0 = 2.00$, eq. (A.5), and f_2^a in terms of $\kappa = -0.78$, eq. (A.12). The solid lines are obtained from the analytical results for the superconducting and normal background from eqs. (3.61) and (3.64) by neglecting terms of $\mathcal{O}(z_*/z_0)^{2d-1}$ and $\mathcal{O}(z_*/z_0)^{2d-2}$, respectively. The dashed lines are obtained from the linear approximation, $z_* = \tilde{z}_* = \ell \frac{d\ \Gamma\left(\frac{2d-1}{2d-2}\right)}{2\sqrt{\pi}\Gamma\left(\frac{3d-2}{2d-2}\right)}$. As anticipated, the analytical estimation of the entanglement entropy, calculated in the large d limit, breaks down as ℓ increases. Nonetheless the qualitative behavior is very similar even for $d = 2+1$ dimensions in the UV-boundary. Inset: difference between the finite parts of the entanglement entropies in both phases as a function of the strip length. As before, the dots correspond to the numerical results while the dashed and continuous lines are our analytical results corresponding to the linear approximation and the subleading quartic correction, respectively. The lines are restricted to the region, in ℓ, where the estimations of the tip of the minimal surface in each background $\tilde{z}_*$, $z_* < z_0$, see figures 3.5, 3.6.

3.7 Conclusions

In this Chapter, we have studied the entanglement entropy and the conductivity in holographic superconductors at zero and nonzero temperature in the limit of large spatial dimensionality. The coherence peak of the optical conductivity, which measures the typical energy range at which condensate is lost, becomes narrower for larger dimensionality. Moreover, the ratio between the maximum of the peak ω_g and the critical temperature also decreases has a well defined (nonzero) $d \to \infty$ limit. This is a clear indication that the coupling of the scalar with the bulk is weaker in the large dimensionality limit. It would be interesting to explore whether there is a bound for these quantities in theories with gravity duals.

We have also computed the dependence on the dimensionality d on the entanglement entropy at zero and close to the critical temperature and for the conductivity at zero temperature. Our results confirm the expectation that the entanglement entropy is smaller in the symmetry broken phase with a difference that decreases with the spatial dimensionality. The results of the frequency scaling of the optical conductivity indicate the low energy excitations are suppressed in the $d \to \infty$ limit.

As we mentioned in the Introduction of this Chapter, it is known that the limit of large number of dimensions allows a drastic simplification of the dynamics of many different systems and thus a better understanding is possible. In particular, this is a fruitful strategy within gravity theories [118, 239, 221] and in holography [220, 222]. Indeed, the results of this Chapter support the indication that large d expansions are a helpful tool to obtain analytical results in holography. Moreover, given the universal behavior of General Relativity for large dimensionality, we expect the feature of weaker interactions for high dimensionality to be a general feature in holographic theories.

Finally, we would like to point out that since the appearance of the papers mentioned above, and ours [205], the large dimensionality limit has become more popular within the gauge/gravity duality community [240–249].

This concludes our first strategy to study strongly coupled systems with gravity duals. We now move on to the second strategy, which is to introduce mechanisms which induce weak momentum dissipation in the boundary theory. The motivation of the next Chapter is twofold. On the one hand, before breaking translational symmetry we aim to apply bounds, introduced in the context of Condensed Matter and Statistical Physics, to theories with gravity duals. On the other hand, we aim to clarify which are the degrees of freedom that control the dc conductivity for weak momentum dissipation and to establish a connection to the previously introduced bounds in translationally invariant theories.

4

Drude weight and Mazur-Suzuki bounds in holography[†]

We investigate the Drude weight and the related Mazur-Suzuki (MS) bound in a broad variety of strongly coupled field theories with a gravity dual at finite temperature and chemical potential. We revisit the derivation of the recently proposed universal expression for the Drude weight for Einstein-Maxwell-dilaton (EMd) theories and extend it to the case of theories with multiple massless gauge fields. We show that the MS bound, which in the context of condensed matter provides information on the integrability of the theory, is saturated in these holographic theories including R-charged backgrounds. We then explore the limits of this universality by studying EMd theories with $U(1)$ spontaneous symmetry breaking and gravity duals of non-relativistic field theories including an asymptotically Lifshitz EMd model with two massless gauge fields and the Einstein-Proca model. In all these cases, the Drude weight, computed analytically, deviates from the universal result and the MS bound is not saturated. In general it is not possible to deduce the low temperature dependence of the Drude weight by simple dimensional analysis. Finally we study the effect of a weak breaking of translational symmetry by coupling the EMd action, with and without $U(1)$ spontaneous symmetry breaking, to an axion field. We show the coherent part of the conductivity in this limit is simply the product of the MS bound and the relaxation time obtained from the leading quasinormal mode. For asymptotically AdS theories it seems that the MS bound sets a lower bound on the DC conductivity for a given relaxation time.

[†]A version of this chapter may be found in [250], which has been published at *Physical Review D* and is authored by Antonio M. García-García and A. R. B.

4.1 Introduction

Momentum is conserved in the absence of interactions, impurities and lattice defects. Transport is ballistic and the material is a perfect conductor with an electrical conductivity that diverges in the limit of vanishing frequencies. This is, in principle, a highly idealized situation as even for good metals there are different mechanisms of momentum relaxation, from impurities and electron-electron interactions to Umklapp scattering, that render the transport diffusive. It is therefore plausible to expect that quantum ballistic motion, especially at finite temperature and in the presence of a lattice, cannot occur in a strongly interacting system. However, this is far from being true [251–255]. Paradigmatic examples of one-dimensional systems with this property in a broad range of parameters are the spin 1/2-XXZ chain [256, 253] or the repulsive Hubbard model [252]. Ballistic transport is usually characterized by the strength of the delta function in the conductivity for vanishing frequencies, the so-called Drude weight K.

Explicit analytical expressions in some interacting one-dimensional systems [256] are available by expressing the Drude weight [257] as a function of the flux dependence of the spectrum, which is obtained by Bethe ansatz. Monte Carlo and DMRG techniques [254], together with a finite size scaling analysis, have also been heavily used to determine the conditions for a finite Drude weight to occur and its explicit temperature dependence. Despite these advances there are still conflicting results in the literature (see [255, 254] for the exact range of parameters in which transport is ballistic). This is not surprising as the extrapolation of the numerical results to the thermodynamic limit is especially challenging in the case of the direct current conductivity and analytical approaches contain reasonable but uncontrollable approximations.

However, the very existence of a finite Drude weight is in many cases guaranteed by the Mazur-Suzuki (MS) bounds [258, 259]. These bounds relate [251] the Drude weight to a weighted positive-definite sum of correlation functions between the electrical current and the conserved quantities of the system.

A sufficient condition for a finite Drude weight is thus the existence of some overlap between the current and a single conserved quantity. More recently, Mazur-Suzuki bounds have been generalized [260, 261] to quasilocal conservation laws and systems with open boundary conditions. The new derivation of the bounds [261] is heavily based on causality constraints as given by Lieb-Robinson bounds [262]. A finite bound is also deeply related to the nonergodicity of the operator in question, in this case the current though it can be generalized to any other bound observable. More explicitly in Refs. [263, 251] it was conjectured that a finite Drude weight implies nonergodicity of the dynamics and, consequently, some form of quantum integrability of the model. In the case that the Mazur-Suzuki bound is saturated, it was recently proposed [264] that the thermodynamic properties of the system are well described by the generalized Gibbs ensemble.

So far, severe technical limitations, both analytical and numerical, have prevented a systematic study of Mazur-Suzuki bounds and Drude weights in higher dimensional systems. An important exception are strongly coupled theories with a gravity dual [44, 165, 265], where Drude weights have been computed analytically in many situations [122, 266, 267, 102, 128, 127, 109, 110, 121, 268, 269, 107]. For instance, the Drude weight for Einstein-Maxwell theories with a single massless gauge field was discussed in Refs. [110, 109]. The Drude weight in some R-charged and SUGRA backgrounds was worked out in [269, 107, 127] and in [268] for probe D-branes in a Lifshitz spacetime. The calculation of the Drude weight in more general Einstein-Maxwell theories and the proposal of universality was first made in [122, 266] and then revisited in [128]. For holographic superconductors, the Drude weight was computed numerically in [114]. In the context of holographic theories, it is rather unclear whether a finite Drude weight at finite temperature is related to integrability. However, we note that there are recent claims [270, 271] that asymptotically AdS Einstein-Maxwell theories are classically integrable.

Here, we extend these studies to the calculation of MS bounds[1] and also Drude weights in a broader ensemble of holographic theories at finite temperature and chemical potential. More specifically, in the first part of the chapter we investigate Einstein-Maxwell-dilaton gravity theories with and without $U(1)$ symmetry breaking, R-charged backgrounds, multiple massless gauge fields and gravity theories with massive gauge fields and EMd theories with a non-AdS boundary for which the dual field theories are nonrelativistic. These are known [94] to be a fertile ground for phenomenological approaches to condensed matter systems. Indeed, we have found a rich phenomenology. For the models where the Drude weight K is given by the universal expression [272, 128], which depends only on thermodynamic quantities, the MS bound is saturated. The temperature dependence of K is not, in general, given by simple dimensional analysis. In the case of $U(1)$ scalar condensation the Drude weight is larger than the universal prediction and the MS bound is finite but not saturated. For the nonrelativistic field theories we have investigated, the MS bound involving only the momentum operator vanishes and the Drude weight is different from the universal prediction. In the second part of the chapter we study the dc conductivity once momentum conservation is weakly broken in EMd-axion models with and without $U(1)$ symmetry breaking. We show that the coherent part of the dc conductivity is controlled by the MS bound and the relaxation time, which is obtained independently by an explicit calculation of the leading quasinormal mode. At least for asymptotically AdS theories it seems that the MS bound sets a lower nontrivial bound on the dc conductivity for a given relaxation time.

The organization of the chapter is as follows: Next, we review previous holography literature on the Drude weight and revisit the analytical calculation of the universal Drude

[1]We only consider the MS bound involving the momentum operator only. As we will see in the derivation of the bound, taking into account all conserved quantities would lead to saturation.

weight [128, 122, 266]. In Sec. 4.3 we extend this result by proposing a universal Drude weight for theories for multiple massless gauge fields. In Sec. 4.4 we introduce Mazur-Suzuki bounds and detail how to compute them in some EMd holographic theories. The calculation of the Drude weight and the MS bounds in EMd theories with $U(1)$ symmetry breaking and with a nonrelativistic dual field theory, where universality does not apply, is carried out in Secs. 4.5 and 4.6. Finally, in Sec. 4.7 we study EMd-axion models, with and without $U(1)$ symmetry breaking, in the limit of weak breaking of translational invariance, where we show that the dc conductivity is controlled by the leading quasinormal mode and the MS bound for the Drude weight.

4.2 Universality of the Drude weight revisited

Although the holography literature has focused mostly on the calculation of the finite part of the dc conductivity, the infinite part, characterized by the Drude weight, has already received some attention [122, 266, 267, 102, 128, 127, 109, 110, 121, 268, 269, 107].

Interestingly, the Drude weight corresponding to a single massless gauge field in an Einstein-Maxwell-dilaton theory has been found to be universal and given only by thermodynamic quantities [122, 266, 128]. In these papers the focus was on the study of universal aspects of the finite, or regular, part of the dc conductivity, usually referred to as σ_Q, rather than the Drude weight, though the latter was also computed explicitly. We start our analysis by revisiting the derivation of this universal dc conductivity. We adapt it to the analytical calculation of the Drude weight as this is the starting point for the generalization of these results in the following sections. We follow closely the approach of [128], though with some modifications so that the calculation of the Drude weight is more direct and easier to generalize beyond universality. The slightly different method of Jain and co-workers [122, 266], proposed earlier, leads to exactly the same results.

The full dc conductivity is given by the current-current Green's function [273],

$$\sigma_{\rm dc} = -{\rm Re} \lim_{\omega\to 0, q\to 0} \frac{G^R_{J^xJ^x}(\omega,q) - G^R_{J^xJ^x}(0,q)}{i(\omega+i\epsilon)} \ , \tag{4.1}$$

which physically represents the linear response of the system to an external small field perturbation, a_x. We note that this form of the Kubo formula ensures, that the limit $\omega\to 0$, $\epsilon\to 0^+$ captures the full diamagnetic response [273]. More specifically, assuming $\lim_{q\to 0} G^R_{J^xJ^x}(\omega,q) - G^R_{J^xJ^x}(0,q) \approx K - i\omega\sigma_{\rm Q} + \mathcal{O}(\omega^2)$, eq. (4.1) leads, for $\epsilon\to 0^+$, to

$$\sigma_{\rm dc} = \sigma_{\rm Q} - {\rm Re}\frac{1}{i}\frac{K}{\omega+i\epsilon} = \sigma_{\rm Q} - {\rm Re}\left[\mathcal{P}\left(\frac{1}{\omega}\right)(-i)K - \pi K\delta(\omega)\right] = \sigma_{\rm Q} + \pi K\delta(\omega) \ . \tag{4.2}$$

A few comments are in order regarding the derivation of eq. (4.1). Kadanoff and Martin [274][2] studied the response of the system to an adiabatically turned on perturbation at $t \to -\infty$: $\phi_i(\mathbf{x})e^{\epsilon t}$, $\epsilon \to 0^+$ which is then turned off at $t = 0$:

$$H_{ext}(t) = \begin{cases} -\int \mathrm{d}^d x \mathcal{O}^i(\mathbf{x}, t)\phi_i(\mathbf{x})e^{\epsilon t}\,, & t < 0\,, \\ 0\,, & t > 0\,, \end{cases}$$

where $\mathcal{O}^i$ and ϕ_i are operators and sources. We now review the derivation of the response of an observable for $t > 0$ due to the above perturbation.

$$\begin{aligned} \delta\langle \mathcal{O}^i(t,\mathbf{x})\rangle &= -i\int_{-\infty}^{0} \mathrm{d}t'\theta(t-t')\langle[\mathcal{O}^i(t,\mathbf{x}), H_{ext}(t')]\rangle = \\ &= i\int_{-\infty}^{0} \mathrm{d}t' e^{\epsilon t'}\theta(t-t')\int \mathrm{d}\mathbf{x}'\langle[\mathcal{O}^i(t,\mathbf{x}), \mathcal{O}^j(t',\mathbf{x}')]\rangle\phi_j(\mathbf{x}') = \\ &= -\int_{-\infty}^{0} \mathrm{d}t'\int \mathrm{d}\mathbf{x}' e^{\epsilon t'} G_R^{ij}(t-t';\mathbf{x}-\mathbf{x}')\phi_j(\mathbf{x}')\,, \end{aligned}$$

where G_R^{ij} is the retarded Green's function $G_R^{ij}(\mathbf{x},t;\mathbf{x}',t') = G_R^{ij}(t-t';\mathbf{x}-\mathbf{x}') = -i\theta(t-t')\langle[\mathcal{O}^i(\mathbf{x},t), \mathcal{O}^j(\mathbf{x}',t')]\rangle$.[3] We now express G_R^{ij} in momentum space:

$$\delta\langle \mathcal{O}^i(t,\mathbf{x})\rangle = -\int_{-\infty}^{0} \mathrm{d}t'\int \mathrm{d}\mathbf{x}' e^{\epsilon t'}\int \frac{\mathrm{d}\mathbf{q}}{(2\pi)^d} G_R^{ij}(t-t',\mathbf{q})\phi_j(\mathbf{x}')e^{i\mathbf{q}\cdot(\mathbf{x}-\mathbf{x}')}\,.$$

Multiplying by $e^{-i\mathbf{k}\cdot\mathbf{x}}$ and integrating in $\mathbf{x}$ gives a $\delta(\mathbf{q}-\mathbf{k})$:

$$\begin{aligned} \delta\langle \mathcal{O}^i(t,\mathbf{k})\rangle &= -\int_{-\infty}^{0} \mathrm{d}t'\int \mathrm{d}\mathbf{x}' e^{\epsilon t'}\int \frac{\mathrm{d}\mathbf{q}}{(2\pi)^d} G_R^{ij}(t-t',\mathbf{q})\phi_j(\mathbf{x}')e^{-i\mathbf{q}\cdot\mathbf{x}'}\int \mathrm{d}\mathbf{x} e^{i(\mathbf{q}-\mathbf{k})\cdot\mathbf{x}} \\ &= -\int_{-\infty}^{0} \mathrm{d}t' e^{\epsilon t'} G_R^{ij}(t-t',\mathbf{k})\int \mathrm{d}\mathbf{x}'\phi_j(\mathbf{x}')e^{-i\mathbf{k}\cdot\mathbf{x}'} = -\int_{-\infty}^{0} \mathrm{d}t' e^{\epsilon t'} G_R^{ij}(t-t',\mathbf{k})\phi_j(\mathbf{k})\,. \end{aligned}$$

[2] See [273] for a brief review of previous relevant literature on this topic.

[3] The upper or lower position of the indices i, j in G_R^{ij} does not matter and we will use G_R^{ij} and G_{ij}^R to mean the same retarded Green's function.

Finally, multiplying by e^{izt} with the usual regularization of retarded Green's functions: $\mathrm{Im}\, z = \eta \to 0^+$ and integrating in $t \in [0, \infty)$ (for $t < 0$ G_R^{ij} vanishes) gives:

$$\begin{aligned}
\delta\langle \mathcal{O}^i(z,\mathbf{k})\rangle &= -\int_0^\infty \mathrm{d}t e^{izt} \int_{-\infty}^0 \mathrm{d}t' e^{\epsilon t'} \int \frac{\mathrm{d}\omega}{2\pi} G_R^{ij}(\omega,\mathbf{k})\phi_j(\mathbf{k}) e^{-i\omega(t-t')} = \\
&= -\int_0^\infty \mathrm{d}t e^{izt} \int \frac{\mathrm{d}\omega}{2\pi} e^{-i\omega t} G_R^{ij}(\omega,\mathbf{k})\phi_j(\mathbf{k}) \left.\frac{e^{\epsilon t' + i\omega t'}}{i\omega+\epsilon}\right|_{-\infty}^0 = \\
&= -\int_0^\infty \mathrm{d}t \int \frac{\mathrm{d}\omega}{2\pi} e^{izt - i\omega t} G_R^{ij}(\omega,\mathbf{k})\phi_j(\mathbf{k}) \frac{1}{i\omega+\epsilon} = \\
&= -\int \frac{\mathrm{d}\omega}{2\pi} G_R^{ij}(\omega,\mathbf{k})\phi_j(\mathbf{k}) \frac{1}{i\omega+\epsilon} \left.\frac{e^{izt - i\omega t}}{iz - i\omega}\right|_0^\infty = \\
&= -\int \frac{\mathrm{d}\omega}{2\pi} G_R^{ij}(\omega,\mathbf{k})\phi_j(\mathbf{k}) \frac{1}{i(\omega - i\epsilon)} \frac{-1}{i(z-\omega)} .
\end{aligned}$$

In the first line we integrate in t' and in the third line in t. Using the residue theorem, the integral results in two terms involving G_R^{ij} evaluated at the two poles: $\omega = i\epsilon \to 0$ and $\omega = z$:

$$\delta\langle \mathcal{O}^i(z,\mathbf{k})\rangle = \phi_j(\mathbf{k}) \frac{G_R^{ij}(z,\mathbf{k}) - G_R^{ij}(0,\mathbf{k})}{iz} . \tag{4.3}$$

Outside the framework of holography, there have been interesting discussions [275, 273] about the importance of the subtraction of the static terms like the $G_R^{ij}(0,\mathbf{k})$ in eq. (4.3). The subtraction of these terms is also understood as retaining the contact terms in the response function [275, 273].

The derivation of eq. (4.3) has been recently reviewed in [276] in the context of relativistic hydrodynamics and in [277] it was shown that this subtraction is crucial to obtain the correct heat conductivity.[4]

In [273] it is discussed the subtraction of a purely imaginary term from the $G^R_{J^x J^x}(\omega,\mathbf{k})$ to compute the electrical conductivity is crucial to obtain the correct result of the real part of the conductivity at zero frequency. As seen in eq. (4.2) the real part is infinite at zero frequency. If the subtraction is not performed, the real part of the conductivity is regular while its imaginary part contains a $1/\omega$ divergence leading to a violation of the Kramers-Kronig relation between the real and imaginary part of the conductivity. In Sec. 5.6 we will also discuss the contribution of the contact terms in the calculation of the shear viscosity.

[4] As we discuss below, in some cases the contact terms only add or remove poles at zero frequency, but they can also introduce finite corrections. This is the case in the heat conductivity, for which the imaginary part receives finite corrections at nonzero frequency [277].

In this chapter we compute the Green's function by the standard holographic techniques that involve the solution of the equations of motion (EOMs) corresponding to the perturbations to the metric g_{tx} and to a_x. By using the bulk EOMs it is possible to express the equation for the fluctuation a_x as a function of the bulk fields only. Using the solution of a_x together with the bulk fields close to the boundary, it is possible to write down the renormalized boundary action, which according to the usual holographic dictionary is related to the current. The current-current Green's function is finally obtained by functional differentiation of the action.

We now revisit [122, 266, 128] the calculation of the Drude weight in the case of an Einstein-Maxwell-dilaton model with a Lagrangian,

$$\mathcal{L} = R - \frac{Z(\phi)}{4} F_{\mu\nu} F^{\mu\nu} - \frac{1}{2} \partial_\mu \phi \partial^\mu \phi + V(\phi) \ , \tag{4.4}$$

which includes a nonminimal electromagnetic coupling Z that may depend on the dilaton. The potential V satisfies $V(\phi = 0) = -2\Lambda$, where Λ is the cosmological constant. For a detailed treatment of this model we refer to [94]. The conditions for the universal results of [122, 266, 128] are that the gauge field has no mass terms and the boundary is still AdS.

We assume that solutions of the EOMs only depend on the radial coordinate, $u = r_0/r$ (r_0 is the outer horizon) and $A_t(u) = A(u)$.

The equation of motion of the fluctuation $\delta A_x = a_x e^{-i\omega t}$ is given by

$$\frac{1}{\sqrt{-g_{tt} g_{uu}}} \left(\sqrt{\frac{-g_{tt}}{g_{uu}}} g_{xx}^{\frac{d-3}{2}} Z a_x' \right)' + \frac{Z \omega^2 g_{xx}^{\frac{d-3}{2}}}{-g_{tt}} a_x = \left(\frac{Z^2 g_{xx}^{\frac{d-3}{2}} A'^2}{-g_{tt} g_{uu}} \right) a_x \, . \tag{4.5}$$

We stress that this equation is only valid assuming that there is no vector potential mass terms in eq. (4.4). The ω^2 term is needed to have consistent boundary conditions, though it does not enter in the calculation of the dc conductivity. The Maxwell coupling is assumed to satisfy $Z \to 1 (Z_+)$ at $u = 0$ ($u = 1$), where Z_+ is determined by the value of the dilaton at the horizon. The component g_{tt} (g_{uu}) is assumed to have a single zero (pole) at the horizon and to be consistent with an asymptotically AdS geometry. In other words, we assume $g_{tt} \sim g_0(1-u)$, $g_{uu} = \tilde{g}_0 (1-u)^{-1}$, close to the horizon, where the constants g_0 and $\tilde{g}_0$ are temperature dependent. We also assume an AdS boundary $g_{xx} \propto u^{-2}$ where the constant of proportionality may be written in terms of the entropy density; $A(u)$ must vanish at the horizon, and close to the boundary $A(u) \simeq \mu - \rho / r_0^{d-2} u^{d-2} + \ldots$, with ρ the charge density and μ the chemical potential of the dual field theory.

The boundary condition at the horizon is

$$a_x = e^{-\frac{i\omega}{4\pi T} \log(1-u)} \left[a_1 + \mathcal{O}(1-u) \right] \ , \tag{4.6}$$

where the prefactor of the logarithm follows from the constants g_0 and $\tilde{g}_0$ in the ansatz of the metric. The sign in the exponential, together with the time dependence ($e^{-i\omega t}$), determines the ingoing character at the horizon. For small frequency, the general solution consistent with this boundary condition is

$$a_x = C_1 a_x^{(0)}(u) + C_2 i\omega a_x^{(1)}(u) \ , \tag{4.7}$$

where, at $u = 1$, $a_x^{(0)}$ is a regular everywhere and $a_x^{(1)}$ has a singularity at the horizon. Moreover, $C_2 = C_1 Z^+ a_x^0(u=1)^2 \left(\frac{s}{4\pi}\right)^{\frac{d-3}{d-1}}$ and C_1 is undetermined. It is fixed by imposing the second boundary condition at the asymptotic AdS boundary,

$$a_x(u \to 0) = a_x^{(0)}(u \to 0) = a_0 = 1 \ . \tag{4.8}$$

In order to use eq. (4.1) we need the current-current retarded Green's function, which, as we mentioned earlier, is obtained from the boundary action of the Lagrangian eq. (4.4). It is easy to see that the only term which contributes to the required Green's function is obtained by double differentiation of

$$\lim_{u\to 0} \sqrt{-g} g^{xx} g^{uu} Z a_x' a_x \ , \tag{4.9}$$

with respect to the boundary value of a_x. We have omitted the integral over space dimensions in the boundary. Moreover, as discussed before [eq. (4.2)], the Drude weight is given by the $\mathcal{O}(\omega^0)$ contribution of the Green's function. Therefore, in the previous equation we only need to use the solution, $a_x^{(0)}$, namely,

$$K = \lim_{u\to 0} \sqrt{-g} g^{xx} g^{uu} Z a_x^{(0)\prime} \ . \tag{4.10}$$

As we mentioned before, $a_x^{(0)}$ is regular in the whole domain. Therefore, we take $a_x^{(0)} = \sum_n a_n u^n$, $n \geq 0$ with $a_0 = 1$ (normalization of the electric field). We now expand eq. (4.5) with $\omega \to 0$ close to the boundary using the asymptotic form of A_t together with the ansatz for $a_x^{(0)}$ and $g_{\mu\nu}$. This imposes constraints on the coefficients of a_n, which leads to

$$a_x^{(0)} = 1 - \frac{\rho^2}{\frac{d}{d-1}\epsilon} u^{d-2} + \dots \ , \tag{4.11}$$

where we used the fact that the energy density enters through the expansion of $g_{tt} = g_n u^n$, $g_{d-2} = -(d-1)\epsilon$. From eqs. (4.11) and (4.10), it follows that the Drude weight agrees with the result derived in [122, 266, 128],

$$K_{\mathrm{U}} = \frac{\rho^2}{\epsilon + P} \ , \tag{4.12}$$

where $\epsilon + P = \frac{d}{d-1}\epsilon$.

In the next sections we explore in more detail the limitations and extensions of the universal result $K_{\rm U}$ in several gravity backgrounds, including one with a vector potential mass term.

For the moment we just comment on the effect of a mass term $W A_\mu A^\mu$ in the Lagrangian (4.4). As we comment in Sec. 4.5, in order to avoid divergences, W and its first derivative close to the boundary must tend to zero. Therefore, $W \propto u^n + \ldots$, for $u \to 0$, where the power and constant of proportionality depend on the boundary conditions of the dilaton. This mass term modifies eq. (4.5) as well as the constraints on the coefficients of the ansatz of $a_x^{(0)}$, a_n. The new constraints yield an extra term $\mathcal{O}(u^{d-2})$ in eq. (4.11). Therefore, in the presence of a massive vector potential, the Drude weight is in general different from the universal expression (4.12).

Finally, we turn briefly to the temperature dependence of the universal Drude weight eq. (4.12). In the canonical ensemble at least, it is expected that $K_{\rm U}$ will not scale with temperature in the low temperature limit since ρ is fixed and the denominator is temperature independent [128],[5] which is consistent with our numerical results (not shown).

In very specific cases, such as a dimensionless charge density or chemical potential,[6] the temperature scaling in the low temperature limit may be obtained from simple dimensional analysis. The dimensionality of the relevant thermodynamic quantities are, $[\rho] = \tilde{d} - \theta + \Phi$, $[\mu] = z - \Phi$, $[s] = \tilde{d} - \theta$, $[T] = z$, where $\tilde{d} = d - 1$ is the spatial dimension of the boundary, z is the dynamical critical exponent, $\theta \neq 0$ is a signature of hyperscaling violations, and Φ is another critical exponent that controls the scaling of the gauge field around the horizon. For dimensionless chemical potential, $\Phi = z$ and $K \sim T^{\frac{\tilde{d}-\theta+z}{z}}$ while for dimensionless charge density, $\Phi = \theta - \tilde{d}$ and $K \sim T^{-\frac{\tilde{d}-\theta+z}{z}}$. We stress this is the prediction of dimensional analysis, which will be correct provided the dimensions of the chemical potential and charge density are not given by any other scale but the temperature. In other cases an explicit numerical calculation is required.

4.3 Universality of the Drude weight in theories with multiple massless gauge fields

In this section we investigate the Drude weight in theories with several massless gauge fields. The finite part of the dc conductivity in the models we discuss, but not the Drude weight, was investigated in detail in [272, 122, 278]. We aim to clarify to what extent the universal results of the previous section can be extended to actions with multiple gauge fields. For that purpose we start with an action in $d+1$ bulk dimensions that is the

[5] We assume the chemical potential does not vanish at zero temperature, which yields $\epsilon + P \sim \mu\rho \neq 0$.
[6] Both are forbidden to be dimensionless simultaneously by the Gubser criterion [127].

natural generalization of eq. (4.4),

$$\mathcal{L} = R - \frac{1}{4}\sum_i Z_i F^i_{\mu\nu} F^{\mu\nu\, i} + \dots , \tag{4.13}$$

where ... stand for scalar fields or Chern-Simons terms. At this stage it is not necessary to specify them since the calculation of the Drude weight involves solving the equation of the fluctuations of A_x, for which it is not necessary to consider the fluctuations of the scalar fields. We only assume that these scalars do not condense in the boundary. The extra index (i) in the Maxwell tensor $F^i_{\mu\nu}$, with strength coupling Z_i that may depend of the scalar field, labels the ith $U(1)$ gauge field $A_{\mu i}$ of the theory. The equations of motion for the perturbations $\delta A_{xi} = A_{xi}(u)e^{-i\omega t+iqz}$ that control the conductivity are simply (see [272, 122] for details)

$$\frac{d}{du}\left(N_i \frac{d}{du} A_{xi}(u)\right) + \sum_{j=1}^{m} M_{ij} A_{xj}(u) + \mathcal{O}(\omega^2) = 0\,, \tag{4.14}$$

where the perturbation in the metric δg_{xt} decouples from the equations of A_{xi}. We have omitted the term $-\omega^2\ N_i\ g_{uu}g^{tt}A_{xi}(u)$ since it is not needed to study the Drude weight. The factors N_i and M_{ij} are (with no summation convention in i, j)

$$N_i = \sqrt{-g} Z_{ii} g^{xx} g^{uu}\,, \qquad M_{ij} = F^i_{ut}\sqrt{-g} Z_{ii} g^{xx} g^{uu} g^{tt} Z_{jj} F^j_{ut}\ . \tag{4.15}$$

As was shown in [272, 122], the regularized action at $u = u_c$ close to the boundary, necessary for the calculation of the conductivity, is simply

$$S_{u_c} = \frac{1}{16\pi G_{d+1}} \int \frac{\mathrm{d}^d q}{(2\pi)^d} \left(\sum_{i=1}^{m} N_i(u_c) \times \frac{d}{du} A_{xi}(u,\omega,q)\Big|_{u_c} A_{xi}(u_c,-\omega,-q) \right). \tag{4.16}$$

The general expression for the Drude weight K_{ij} is then obtained by functional differentiation of the boundary action,

$$\begin{aligned} K_{ij} &= -\lim_{u_c\to 0}\lim_{\omega,q\to 0} \mathrm{Re}\left(G^R_{J^i J^j}(\omega,q) - G^R_{J^i J^j}(\omega=0,q)\right), \\ G^R_{J^i J^j}(\omega,q) &= \frac{2}{16\pi G_{d+1}}\left[\sum_{k=1}^{m} N_k(u_c) \times \frac{\delta^2}{\delta A^{(0)}_{xi}\delta A^{(0)}_{xj}} A_{xk}{}'(u_c,\omega,q) A_{xk}(u_c,-\omega,-q)\right], \end{aligned} \tag{4.17}$$

where $A^{(0)}_{xi}$ is the value of A_{xi} at the boundary ($u_c = 0$). Even before any explicit calculation of the conductivity is done, the above expressions already suggest several interesting features of the Drude weight in the multicharge case. It is clear that it is a tensor, namely, a small electric field related to the i gauge field induces, in general, a

current not only of the i but also of the j charge. This is a consequence of the nonlinearity of the bulk equations.

Moreover, as in the case of a single gauge field, the Drude weight is still exclusively controlled by the regular (no singularity around the horizon) solution. Since for a single charge the regular solution is $A_x = a_0 + cu^{d-2}$, for simple cases where A_t is known explicitly, and eq. (4.14) is linear, we expect that the solution of eq. (4.14) is given by

$$A_{xi} = a_0^i + u^{d-2} f(a_0^j, \rho_j, T \ldots) \ , \tag{4.18}$$

where f depends, likely linearly, on a_0^i and the rest of the values of the gauge fields at the boundary and other parameters such as temperature or the charge densities. On physical grounds K_{ij} must be symmetric and in the limit of one charge must reproduce the universal result of the previous section. Moreover, the linearity of the equations suggests that off-diagonal terms should not depend on powers of the charge density larger than two. The simplest expression for the Drude weight that meets these requirements is,

$$K_{ij} \propto \frac{\rho_i \rho_j}{\epsilon + P} \ . \tag{4.19}$$

We now study in detail an example where the Drude weight is of the form given in eq. (4.19). This is a strong indication that this is the universal form of the Drude weight, eq. (4.12), for the case of multicharges associated with massless gauge fields assuming AdS geometry in the boundary and no scalar-condensation.

Instead of embarking on numerical simulations with several gauge fields, we focus on a class of systems, R-charged backgrounds, where explicit analytical ones are available even for multicharges. Moreover, the field theory duals of these models are well known as these backgrounds come directly from compactifications of string theory. More specifically, we study the five-dimensional R-charged black hole, also referred to as STU black holes [279, 280], whose field theory dual is an $\mathcal{N} = 2$ super Yang-Mills theory coming from the compactification of ten-dimensional IIB supergravity on S^5 (see [281] for other cases involving the reduction of $D = 11$ supergravity on S^7 and S^4). The action is given by

$$\begin{aligned} S = \frac{1}{16\pi G} \int \mathrm{d}^5 x \sqrt{-g} \Big(R + \frac{2}{l^2} \mathcal{V} + \frac{1}{2} G_{ij} F^i_{\mu\nu} F^{j\,\mu\nu} - G_{ij} \partial_\mu X^i \partial^\mu X^j + \\ \frac{1}{24\sqrt{-g}} \epsilon^{\mu\nu\rho\sigma\lambda} \epsilon_{ijk} F^i_{\mu\nu} F^{\rho\sigma j} A^k_\lambda \Big) \ , \end{aligned} \tag{4.20}$$

where l represents the scale associated with the cosmological constant. In addition to the metric, we have three scalar fields X^i, $i = 1, 2, 3$ while the scalar potential $\mathcal{V}$ and the

metric G_{ij} are given in terms of the scalar fields,

$$\mathcal{V} = 2\sum_{1}^{3}\frac{1}{X^i}, \quad G_{ij} = \frac{1}{2}\text{diag}\Big[(X^1)^{-2},(X^1)^{-2},(X^1)^{-2}\Big] \ . \tag{4.21}$$

$F^i_{\mu\nu}$, $i=1,2,3$, are the field strengths of A^i, the Abelian gauge fields.

As shown in [279], this effective action (4.20) admits asymptotically AdS black hole solutions with three $U(1)$ charges. These solutions can be written down using the outer horizon r_+, the variable $u = r_+^2/r^2$ and $T_0 = \frac{r_+}{\pi L^2}$ as

$$\mathrm{d}s^2 = -\mathcal{H}^{-2/3}(\pi L T_0)^2\frac{f(u)}{u}\mathrm{d}t^2 + \mathcal{H}^{1/3}\frac{L^2}{4f(u)u^2}\mathrm{d}u^2 + \mathcal{H}^{1/3}\frac{(\pi L T_0)^2}{u}(\mathrm{d}x^2+\mathrm{d}y^2+\mathrm{d}z^2) \ , \tag{4.22}$$

where

$$\begin{aligned} H_i =& (1+k_i u) \ , \quad i=1,2,3, \quad \mathcal{H} = H_1H_2H_3 \ , \\ f(u) =& \mathcal{H} - \Pi u^2, \quad \Pi = \prod_{i=1}^{3}(1+k_i) \ . \end{aligned} \tag{4.23}$$

The perturbed equations are given by

$$A''_{xj} + \left(\frac{f'}{f} - \frac{\mathcal{H}'}{\mathcal{H}} + 2\frac{H_j'}{H_j}\right)A'_{xj} + \frac{\tilde{\omega}^2\mathcal{H}}{uf^2}A_{xj} - u\frac{\Pi\sqrt{k_j}}{fH_j^2}\sum_{i=1}^{3}\sqrt{k_i}A_{xi} = 0 \ , \quad j=1,2,3 \ , \tag{4.24}$$

with $\tilde{\omega} = \frac{\omega}{2\pi T_0}$. Following [122, 278] we propose the following ansatz which satisfies the ingoing boundary condition,

$$A_{xi} = \frac{f^{-i\tilde{\omega}(T_0/2T)}}{1+k_i u}a_i(u) \ , \qquad i=1,2,3 \ . \tag{4.25}$$

Since we aim to compute the Drude weight it is only necessary to expand a_i up to leading order in $\tilde{\omega}$,

$$a_i(u) = \left[a_i^0(u) + i\tilde{\omega}a_i^1(u) + \mathcal{O}(\tilde{\omega}^2)\right] \ . \tag{4.26}$$

As before, the Drude weight tensor is extracted from a_i^0 only while for the real part of the conductivity a_i^1 is also needed. The equations of a_i^0 are simply

$$a_j^{0\prime\prime} + a_j^{0\prime}\left(\frac{f'}{f} - \frac{\mathcal{H}'}{\mathcal{H}}\right) + a_j^0\frac{H_j'}{H_j}\left(\frac{\mathcal{H}'}{\mathcal{H}} - \frac{f'}{f}\right) - u\frac{\Pi\sqrt{k_j}}{fH_j}\sum_{i=1}^{3}\frac{\sqrt{k_i}a_i^0}{H_i} = 0 \ , \quad j=1,2,3 \ . \tag{4.27}$$

A regular solution is easily found by substituting $a_i^0(u) = b_i + \tilde{b}_i u$ and solving the constraints resulting from the equations of motion, eq. (4.27). In this way $\tilde{b}_i$ is expressed as a function of the boundary values b_i by

$$\tilde{b}_j = \frac{b_j}{2}k_j - \sum_{i\neq j}\frac{b_i}{2}\sqrt{k_j k_i} \implies a_j^0(u) = b_j\left(1+\frac{k_j}{2}u\right) - \sum_{i\neq j} b_i \frac{\sqrt{k_j k_i}}{2}u \ . \tag{4.28}$$

We now have extracted all the information of the gauge fields required to compute the Drude weight. The part of the boundary action that contributes to the Drude weight, eq. (4.16), is

$$\begin{aligned} \mathrm{S}_{\text{boundary}} &= \lim_{u\to 0}\frac{-r_+^2}{16\pi G L}\int dt d\vec{x}\left[a_1^{0\prime}a_1^0 + a_2^{0\prime}a_2^0 + \dots\right] \\ &= \frac{r_+^2}{16\pi G L}\int dt d\vec{x}\sum_{j=1}^{3} - \left(b_j\frac{k_j}{2} - \sum_{i\neq j} b_i, \frac{\sqrt{k_j k_i}}{2}\right) b_j + \dots \ , \end{aligned} \tag{4.29}$$

which leads to

$$K = \frac{1}{16\pi G L}(-1)^{i+j}\sqrt{k_i k_j}\, r_+^2 \ . \tag{4.30}$$

In order to check the universality of this result it is illuminating to express the charges in terms of thermodynamic quantities, [102]. The relevant thermodynamic quantities are given by

$$\epsilon = \frac{3\pi^2 T_0^4 N^2 \Pi}{8} \ , \quad P = \frac{\epsilon}{3} \ , \quad \rho_i = \frac{\pi^2 T_0^3 N^2 2\sqrt{k_i}\sqrt{\Pi}}{8} \ , \tag{4.31}$$

where $2GN^2 = \pi L^3$ and Π is given in eq. (4.23). With these definitions the Drude weight can be expressed in terms of thermodynamic quantities,

$$K_{ij} = (-1)^{i+j}\frac{\rho_i \rho_j}{\epsilon + P} \ . \tag{4.32}$$

Note that the off-diagonal terms are negative. The same occurs for the finite part of the dc conductivity [278]. We do not yet have a clear physical interpretation of this feature. Obviously these prefactors cannot be universal as they can be modified by a linear recombination of the currents. Only the eigenvalues of K_{ij} are basis invariant. Because of this and the linearity of the equations leading to K_{ij}, we expect that, up to basis-dependent prefactors, the above form of the Drude weight is likely universal for theories with several massless gauge fields.

4.4 Mazur-Suzuki bounds and holographic correlation functions

In this section we introduce the so-called Mazur-Suzuki (MS) bounds [258, 259, 251], inequalities among correlation functions that describe transport in interacting many-body problems. We then discuss how these correlation functions are expressed in terms of holographic retarded Green's functions and relate them to the Drude weight studied in previous sections. We shall see, by working out some examples in Einstein-Maxwell and R-charged backgrounds, that the correlation functions are not given entirely by the zero-momentum retarded Green's functions obtained with the standard recipe in holography.

The main result of the section is that, in the models we study, the MS bound is saturated only if the Drude weight is given by the universal result (4.12).

As we mentioned previously a finite Drude weight is a signature of ballistic nondissipative transport. Indeed, Kohn [257] proposed to characterize nondisordered metals and insulators based on whether the Drude weight was finite or not respectively. This nondissipative transport must be caused by the nondecay of certain correlation functions, in this case the electrical current-current correlation. It is well known that the existence of conservation laws can protect the decay of certain correlation functions. This was precisely the starting point of the Mazur, and later Suzuki, analysis that we briefly review next.

We review the analysis presented in [259]. Let us consider all the conserved quantities Q_i' of the system, namely, $[H, Q_i'] = 0$, $[Q_i', Q_j'] = 0$. By some rearrangements, it is possible to choose them to be orthogonal to each other $\langle Q_i Q_j \rangle = Q_i^2 \delta_{ij}$. Without loss of generality we assume the constant of motion are Hermitian. The time averaged correlation of operators $A(0) = A$ and $B(t)$ may be expanded using a complete set of eigenstates:[7]

$$\lim_{t'\to\infty} \frac{1}{t'} \int_0^{t'} \mathrm{d}t \langle AB(t)\rangle = \lim_{t'\to\infty} \frac{1}{t'} \frac{1}{\mathcal{Z}} \int_0^{t'} \mathrm{d}t \sum_k e^{-\beta E_k} \langle k|AB(t)|k\rangle =$$

$$= \lim_{t'\to\infty} \frac{1}{t'} \frac{1}{\mathcal{Z}} \int_0^{t'} \mathrm{d}t \sum_k e^{-\beta E_k} \langle k|A \sum_{l,m} e^{i(E_l - E_m)t} |l\rangle\langle l|B|m\rangle\langle m|k\rangle =$$

$$= \lim_{t'\to\infty} \frac{1}{t'} \frac{1}{\mathcal{Z}} \int_0^{t'} \mathrm{d}t \sum_{k,l} e^{-\beta E_k} e^{i(E_l - E_k)t} \langle k|A|l\rangle\langle l|B|k\rangle =$$

$$= \frac{1}{\mathcal{Z}} \sum_{\substack{k,l \\ E_k = E_l}} e^{-\beta E_k} \langle k|A|l\rangle\langle l|B|k\rangle \equiv \langle A; B\rangle \,.$$

[7] Similarly to the operator A, to simplify notation we use $B(t=0) = B$.

In the second line we have substituted $B(t)$ in the Heisenberg representation. In the third line we have used the orthogonality of the complete set of states and we integrate in time to get the restriction $E_k = E_l$ of the last line.[8] The sum in the last line defines $\langle A; B\rangle$. To further simplify we decompose the operators A and B as

$$A = a_i Q_i + A' \,, \quad B = b_i Q_i + B' \,, \tag{4.33}$$

where sum over i is implied and A' and B' are orthogonal to Q_i and so,

$$a_i = \frac{\langle AQ_i\rangle}{\langle Q_i^2\rangle} \,, \; b_i = \frac{\langle BQ_i\rangle}{\langle Q_i^2\rangle} \,.$$

Moreover, we will use that $\langle k|Q_i|m\rangle = 0$ whenever $E_k \neq E_m$ which follows trivially by computing $\langle k|[H, Q_i]|m\rangle = 0$ and taking one term of the commutator to the other side of the equality. Moreover, the of orthogonality of A' with Q_i implies that $\langle k|A'|l\rangle = 0$ for $E_k = E_l$. Substituting the decomposition of eq. 4.33 into $\langle A; B\rangle$ leads to

$$\langle A; B\rangle = \langle a_i Q_i; b_j Q_j\rangle + \langle a_i Q_i; B'\rangle + \langle A'; b_j Q_j\rangle + \langle A'; B'\rangle \,.$$

Only the first term is nonzero because the sums in the definition of $\langle \,\cdot\,;\,\cdot\,\rangle$ are constrained to $E_k = E_l$ and $\langle k|A'|l\rangle = \langle l|B'|k\rangle = 0$ for $E_k = E_l$ as we mentioned above. The first term is simply

$$\begin{aligned}
\langle a_i Q_i; b_j Q_j\rangle &= \sum_{ij} a_i b_j \frac{1}{\mathcal{Z}} \sum_{\substack{k,l \\ E_k = E_l}} e^{-\beta E_k} \langle k|Q_i|l\rangle\langle l|Q_j|k\rangle = \\
&= \sum_{ij} a_i b_j \frac{1}{\mathcal{Z}} \sum_{k,l} e^{-\beta E_k} \langle k|Q_i|l\rangle\langle l|Q_j|k\rangle = \\
&= \sum_{ij} a_i b_j \frac{1}{\mathcal{Z}} \sum_{k} e^{-\beta E_k} \langle k|Q_i Q_j|k\rangle = \sum_i a_i b_i \langle Q_i^2\rangle \,.
\end{aligned}$$

In the second line we have unrestricted the sum to all k, l because $\langle k|Q_i|l\rangle = 0$ whenever $E_k \neq E_l$ and in the last line we used orthogonality of Q_i. Combining all these results leads to

$$\lim_{t'\to\infty} \frac{1}{t'} \int_0^{t'} \mathrm{d}t \langle AB(t)\rangle = \sum_i a_i b_i \langle Q_i^2\rangle = \sum_i \frac{\langle AQ_i\rangle\langle BQ_i\rangle}{\langle Q_i^2\rangle} \,,$$

[8] The integral in time is

$$\lim_{t'\to\infty} \frac{1}{t'} \int_0^{t'} \mathrm{d}t e^{i(E_l - E_k)t} = \begin{cases} \lim\limits_{t'\to\infty} \dfrac{e^{i(E_l-E_k)t'} - 1}{i(E_l - E_k)t'} = 0 \,, & E_k \neq E_l \\ 1 \,, & E_k = E_l \end{cases} .$$

where the sum is over all the conserved charges, though only those with non-trivial overlap with the operators A and B will contribute. In our case we take $A = B = J^x = J$, the electric current operator, which can be expressed in terms of these conserved quantities, and so the Drude weight is decomposed as:

$$K = \frac{\beta}{V} \lim_{t' \to \infty} \frac{1}{t'} \int_0^{t'} \mathrm{d}t \langle J(t) J(0) \rangle = \lim_{N \to \infty} \frac{\beta}{V} \sum_i^N \frac{\langle J Q_i \rangle^2}{\langle Q_i Q_i \rangle} \ , \tag{4.34}$$

where β is the inverse of the temperature and V the volume. The correlation functions on the right-hand side are for long times. Since each term on the right-hand side is positive,

$$K \geq K_{\mathrm{MS}} \equiv \frac{\beta}{V} \sum_i^k \frac{\langle J Q_i \rangle^2}{\langle Q_i Q_i \rangle}, \ k < \infty \ . \tag{4.35}$$

K_{MS} is the Mazur bound for the Drude weight, K, first obtained in Refs. [251, 256]. Its generalization to other operators is straightforward.

We stress that the inequality is usually more useful than the equality since, by picking up a single conserved quantity, it allows us to find out, at least in some cases, whether the Drude weight is finite or not. For instance, in strongly interacting one-dimensional systems an explicit calculation of the Drude weight is typically very demanding, while the calculation of the right-hand side, for example for the energy current, which sometimes is a conserved quantity, is much easier as it involves only static correlation functions. In the following sections we compute the MS bound in the following gravity duals: the Einstein-Maxwell theory with and without a scalar that induces $U(1)$ symmetry breaking and an R-charged background where explicit solutions for the background metric are available. For this purpose we first have to express the bound in terms of susceptibilities, namely, retarded Green's functions which is the natural language in holography. This is indeed the way that Suzuki [259] proceeded to extend the classical Mazur bounds to quantum mechanical systems.

In order to discuss the exact relation of the Green's functions and the correlation functions needed in the MS bound, let us consider a single conserved quantity $Q_1 = Q$ and the conserved current J in eqs. (4.34) and (4.35). As we mentioned before the correlation functions in these equations are for long times,

$$\langle JQ \rangle \equiv \lim_{t \to \infty} \langle J(t) Q(0) \rangle \ , \langle QQ \rangle \equiv \lim_{t \to \infty} \langle Q(t) Q(0) \rangle \ . \tag{4.36}$$

Before relating these correlation functions to Green's functions we introduce some standard notation in linear response theory [154, 155]. Consider the variation of an observable, $\delta \langle A_i(\mathbf{r}, t) \rangle$ due to external perturbations $\delta \langle a_i^{ext}(\mathbf{r}, t) \rangle$, where i is a spatial index. The *Kubo*

correlation function is defined as

$$C_{ij}(\mathbf{r},\mathbf{r}',t-t') = \frac{1}{\beta}\int_0^\beta d\lambda \langle e^{\lambda H}\delta A_i(\mathbf{r},t)e^{-\lambda H}\delta A_j(\mathbf{r}',t')\rangle \ , \tag{4.37}$$

where H is the unperturbed Hamiltonian. The Laplace transform in time of the Kubo correlation function satisfies [154, 155]

$$C_{ij}(\mathbf{r},\mathbf{r}';z) = -\frac{1}{\beta z}\left[\chi_{ij}(\mathbf{r},\mathbf{r}',z) - \chi_{ij}(\mathbf{r},\mathbf{r}',i0)\right] \ , \tag{4.38}$$

where z is the transformed variable of t and χ_{ij} is known in the literature as the admittance, matrix response function as well as the Green's function.

It is therefore natural to express the long time correlation functions in eq. (4.36) in terms of the zero frequency limit of the retarded Green's functions as

$$\begin{aligned}\langle JQ\rangle &= \frac{1}{\beta}\lim_{\omega\to 0,q\to 0}\left[G_{JQ}(\omega,q) - G_{JQ}(0,q)\right] \ , \\ \langle QQ\rangle &= \frac{1}{\beta}\lim_{\omega\to 0,q\to 0}\left[G_{QQ}(\omega,q) - G_{QQ}(0,q)\right] \ .\end{aligned} \tag{4.39}$$

With these definitions we now have all the information to compute the MS bound associated with transport properties in translationally invariant theories with gravity duals. In particular, we focus on the electrical conductivity.

4.4.1 Mazur-Suzuki bounds in Einstein-Maxwell theory

We start our analysis with the Einstein-Maxwell theory,

$$\begin{aligned}S = &-\frac{1}{2\kappa^2}\int_{\mathcal{M}} d^{d+1}x\sqrt{-g}\left(R + \frac{d(d-1)}{L^2} + \frac{1}{4e^2}F_{\mu\nu}F^{\mu\nu}\right) - \\ &\frac{1}{2\kappa^2}\int_{\partial\mathcal{M}} d^dx\sqrt{-\tilde{\gamma}}\left(-2K + 2\frac{d-1}{L}\right) \ ,\end{aligned} \tag{4.40}$$

where $\tilde{\gamma}$ is the boundary metric induced by g and K is the trace of the extrinsic curvature. The last integral includes the counterterms needed to have a well-defined energy tensor in the boundary. These counterterms include powers of the induced Ricci scalar on the boundary, but since $\mathcal{M}$ is asymptotically flat they do not contribute. The solution of the EOMs is the AdS planar Reissner-Nordström (RN) background in $d+1$ dimensions,

$$\begin{aligned}\mathrm{d}s^2 &= \frac{1}{L^2z^2}\left(-f(z)dt^2 + \frac{L^4}{f(z)}dz^2 + dx_i^2\right), \\ f(z) &= 1 - (1+Q^2)\left(\frac{z}{z_0}\right)^d + Q^2\left(\frac{z}{z_0}\right)^{2d-2} \ ,\end{aligned} \tag{4.41}$$

where $i = 1, \ldots, d-1$, $z = 1/r$. The only nonzero component of the gauge field is $A_t = \phi = \mu\left[1 - (z/z_0)^{d-2}\right]$, $Q^2 = \mu^2 z_0^2 \gamma^{-2}$, $\gamma^{-2} = \frac{d-2}{d-1}\frac{L^4}{2}$; z_0 is the inverse of the outer horizon and we set

$$\frac{2\kappa^2}{e^2} = 1 \,. \tag{4.42}$$

In order to calculate the electrical conductivity in the linear response approximation we add a time-dependent weak perturbation in the gauge field and the metric, $A_x(z)e^{-i\omega t}$, $g_{tx}(z)e^{-i\omega t}$. The equations of motion of A_x and g_{xt} are

$$\begin{aligned} &\partial_z(f z^{3-d} A_x) + A_x\left(\frac{\omega^2 z^{3-d}}{f} - \phi'^2 z^{5-d}\right) = 0\,, \\ &g'_{xt} + \frac{2}{z} g_{xt} + A_x \phi' = 0\,. \end{aligned} \tag{4.43}$$

Close to the boundary they satisfy

$$\begin{aligned} &A_x \sim A_x^{(0)} + A_x^{(1)}\left(\frac{z}{z_0}\right)^{d-2}\,, \\ &g_{xt} \sim \frac{g_{xt}^{(0)}}{z^2} + g_{xt}^{(1)} z^{d-2}, \quad g_{xt}^{(1)} = \mu\frac{d-2}{d}\frac{A_x^{(0)}}{z_0^{d-2}}\,, \end{aligned} \tag{4.44}$$

where the prime denotes differentiation with respect to z and $g_{xt}^{(0)}$ and $A_x^{(0)}$ source the operators dual to A_x and g_{xt}.

Calculation of the MS bounds

Assuming that the conserved quantity is momentum, the MS bound depends on boundary momentum-momentum and current-momentum correlators. The evaluation of the on-shell action eq. (4.40) on the boundary results in the following terms relevant for the calculation of the corresponding Green's functions,

$$\begin{aligned} S = \frac{V_{d-1}}{2\kappa^2 2\pi}\Bigg[&\frac{(d-1)(1+Q^2)}{2z_0^d} g_{xt}^{(0)}(-\omega) g_{xt}^{(0)}(\omega) + \\ &\frac{\mu(d-2)}{2z_0^{d-2}}\left(A_x^{(0)}(\omega) g_{xt}^{(0)}(-\omega) + A_x^{(0)}(-\omega) g_{xt}^{(0)}(\omega)\right)\Bigg] + \ldots \end{aligned} \tag{4.45}$$

where V_{d-1} is the boundary spatial volume. Therefore the retarded Green's functions at zero spatial momentum are,

$$\begin{aligned} G_{J_x\Pi_x}(\omega) &= \frac{e(d-2)\mu}{2\kappa^2 z_0^{d-2}}\frac{V_{d-1}}{2\pi}\,, \\ G_{\Pi_x\Pi_x}(\omega) &= \frac{(d-1)(1+Q^2)}{2\kappa^2 z_0^d}\frac{V_{d-1}}{2\pi}\,. \end{aligned} \tag{4.46}$$

This agrees with the results for $d = 3, 4$, available in [114] for holographic superconductors in the normal state, and in [282] for a Reissner-Nordström background after setting all the perturbations in the metric to zero, except h_{zt}, which corresponds in our notation to g_{xt}. We note however that the result in eq. (4.46) is not enough, in general, to obtain the correlation functions that enter in the MS bounds [see eq. (4.39)].

The MS bound relates the Drude weight K with correlation functions between the current and conserved charges [see eq. (4.35)]. For the case of the electrical conductivity σ, we use the following notation in eq. (4.35): $V = V_{d-1}$ is the spatial volume on the boundary, $\beta = 1/k_B T$, $J = J_x$ is the current associated with σ, Q_j are the conserved charges which overlap with J_x and k stands for a certain number of conserved charges. If all possible conserved charges are considered the bound is saturated. In our system momentum is conserved so it is natural to set $k = 1$ and $Q_1 = \Pi_x$, which in a relativistic field theory corresponds to the spatial components of the diagonal of the energy momentum tensor. With this identification the numerator of (4.35) is given in terms of $\langle J_x \Pi_x \rangle$, which according to eq. (4.39) is obtained from $G_{J_x \Pi_x}(\omega, q)$. However, due to the dependence of $G_{J_x \Pi_x}(\omega, q)$ on the frequency [282], $G_{J_x \Pi}(0, q) = 0$ and thus we may use the zero-momentum Green's function $G_{\Pi_x J_x}$ given in eq. (4.46),

$$\langle J_x \Pi_x \rangle = \frac{1}{\beta} \lim_{\omega \to 0} G_{J_x \Pi_x} = \frac{1}{\beta} \frac{e(d-2)\mu}{2\kappa^2 z_0^{d-2}} \frac{V_{d-1}}{2\pi} \ . \tag{4.47}$$

However, this is not the case for the denominator $\langle \Pi_x \Pi_x \rangle$, for which $G_{\Pi_x \Pi_x}(\omega = 0, q) \neq 0$, as seen in [282] for $d = 4$. For arbitrary $d \geq 3$ we cannot use the zero-momentum $G_{\Pi_x \Pi_x}$ given in eq. (4.46). Nonetheless, $\langle \Pi_x \Pi_x \rangle$ is the momentum static susceptibility, which may be written in terms of hydrodynamical quantities, $\chi_0 = \langle \epsilon + P \rangle$, ϵ and P being the energy density and pressure [172]. An identical result is obtained by using Ward identities [283]. Therefore the momentum-momentum correlation function needed in the MS bound is in this case,

$$\langle \Pi_x \Pi_x \rangle = \chi_0 = \langle \epsilon + P \rangle \ . \tag{4.48}$$

Finally, eqs. (4.35), (4.47) and (4.48) yield

$$K(T) \geq K_{\text{MS}} = \frac{\beta}{V_{d-1}} \frac{\langle J_x \Pi_x \rangle^2}{\langle \Pi_x \Pi_x \rangle} = \frac{(d-2)^2 \mu^2}{d(1+Q^2)} \frac{z_0^{4-d}}{2\kappa^2} \ . \tag{4.49}$$

The horizon z_0 depends on temperature through the standard relation for a RN black hole. For the Einstein-Maxwell theory given by eqs. (4.40) and (4.41), we used $\rho = \frac{(d-2)\mu z_0^{-d+2}}{e^2}$, $\epsilon = (d-1)P$, [276] and $\epsilon = z_0^{-d}(d-1)(1+Q^2)$, $Q = \mu z_0/\gamma$, defined above.

This result is to be compared with the explicit calculation of the Drude weight $K(T)$ that yields the universal result [110, 272, 128]

$$K = K_{\rm U} = \frac{\rho^2}{\epsilon + P} \ , \tag{4.50}$$

where ρ, ϵ and P are the charge and energy densities and the pressure, respectively. Substituting ρ, P and ϵ in eq. (4.50), and setting $e = 1$, it is clear that in this background the MS bound is saturated $K = K_{\rm MS}$.

We note that in the condensed matter literature it is conjectured [263, 251, 264] that a finite Drude weight is a signature of integrability. In principle, this result is applicable to the field theory dual of the gravity action we investigate. In classical gravity [270] integrability of various gravity backgrounds has recently been studied. More specficially, a relation was proposed between integrability and saturation of the null energy conditions, which precludes integrability in most nonrelativistic backgrounds. Integrability in four-dimensional Einstein-Maxwell theory with a cosmological constant has recently been studied [271]. Clearly, further research is needed to understand to what extent a finite Drude weight might be a signature of integrability of a classical gravity theory and its dual field theory. For the moment we only comment that in the large N limit there are drastic simplifications, even in QCD, in the dynamics of quantum field theories. Therefore, we cannot rule out that integrability plays a role in the occurrence of a finite Drude weight.

4.4.2 Mazur-Suzuki bounds in an R-charged black hole

We now study another example where explicit analytical results for the background metric are known. We work with the 2- and 1-R-charged black holes in five-dimensional $N = 2$ $U(1)^3$ gauged supergravity [269], which are particular cases of the more general model studied in Ref. [284]. They are obtained by setting two of the three $U(1)$ charges to be equal, $Q_1 = Q_2 = Q \neq Q_3$. The 2-R-charged black hole corresponds to $Q_3 = 0$, while setting $Q_1 = Q_2 = Q = 0$ is referred to as the 1-R-charged black hole [269].

In the 1-R-charged black hole, the conductivity

$$\sigma = \frac{r_H^2}{L^3} \frac{2A_x^{(1)}}{i\omega A_x^{(0)}} - i\frac{\omega}{2} \tag{4.51}$$

has been calculated perturbatively in [269]:

$$\sigma \sim i\frac{Q^2}{2\kappa^2 \omega L} + \frac{L(Q^2 + 2r_H^2)^2}{8r_H \kappa^2 \sqrt{Q^2 + r_H^2}} + \mathcal{O}(\omega) \ . \tag{4.52}$$

The temperature and chemical potential, expressed in terms of the charge Q and horizon r_H of the black hole are

$$T = \frac{Q^2 + 2r_H^2}{2\pi L^2\sqrt{Q^2 + r_H^2}}\,, \qquad \Omega = \frac{r_H Q}{L^2\sqrt{Q^2 + r_H^2}}\,. \tag{4.53}$$

We note that eq. (4.52) matches the universal result, eq. (4.12). The Green's functions needed to calculate the MS bound have been given in [102], and in the notation of [269] they are[9]

$$\begin{aligned} G_{\Pi_x,\Pi_x}(\omega,q) &= -\frac{2q^2 r_H^2(Q^2+r_H^2)}{\kappa^2 L^3(L^2q^2 - 4\omega i\sqrt{Q^2+r_H^2})}V_3, \\ G_{\Pi_x J_x}(\omega,q) &= \frac{4r_H\sqrt{Q^2+r_H^2}\sqrt{Q^2(Q^2+r_H^2)}\omega}{L^3\kappa^2(iL^2q^2 + 4\sqrt{Q^2+r_H^2}\omega)}V_3, \end{aligned} \tag{4.54}$$

where q is the spatial momentum of the perturbations $A_x(r)e^{i\omega t+iqx}$ and V_3 is the spatial volume in the boundary. With these considerations, from eq. (4.39)

$$\begin{aligned} \langle \Pi_x J_x\rangle &= \frac{1}{\beta}\lim_{\omega\to 0,q\to 0}\left[G_{\Pi_x J_x}(\omega,q) - G_{\Pi_x J_x}(0,q)\right]\,, \\ \langle \Pi_x \Pi_x\rangle &= \frac{1}{\beta}\lim_{\omega\to 0,q\to 0}\left[G_{\Pi_x \Pi_x}(\omega,q) - G_{\Pi_x \Pi_x}(0,q)\right]. \end{aligned} \tag{4.55}$$

Finally, the MS bound is obtained from eqs. (4.35) with a single conserved quantity $Q_1 = \Pi_x$ and eqs. (4.54) and (4.55),

$$K \geq \frac{Q^2}{2\kappa^2 L}\,. \tag{4.56}$$

Comparing the MS bound with the exact result, given by the ω^{-1} term in eq. (4.52), we see the bound is again saturated and the Drude weight is still the universal one, eq. (4.12).

Similarly, the zero frequency conductivity for the 2-R-charged black hole has been calculated exactly [269] and is also given by the universal result.

Based on these examples, it seems that if a theory with a gravity dual is well described by hydrodynamics, like those dual to asymptotically AdS EMd theories, the Drude weight is given by the universal result (4.50) and the MS bound is saturated.

[9] There is a difference definition for the vector potential in [102], which should be multiplied by $\sqrt{2}$ in the notation of [269].

4.4.3 Mazur-Suzuki bounds in $U(1)$ spontaneously broken symmetry backgrounds

We found previously that the MS bound is saturated in asymptotically AdS EMd backgrounds where the Drude weight $K = K_{\rm U} = \frac{\rho^2}{\epsilon+P}$. Here we compute the MS bound in Einstein-Maxwell-scalar theory [114], which displays a spontaneous $U(1)$ symmetry breaking due to scalar condensation. In this background, it has been shown, [114, 172], that the Drude weight receives an extra contribution related to the superfluid density.

In order to compute the Green's functions that enter the MS bound, it is necessary to obtain the properly renormalized boundary action. We just state the main result and refer to [114] for details,

$$\begin{aligned} S = \frac{V_{d-1}}{2\kappa^2 2\pi}\Bigg[& \frac{(d-2)A_x^{(0)}A_x^{(1)}}{2L^2} - g_{xt}^{(0)}(-\omega)g_{xt}^{(0)}(\omega)\left(\frac{\epsilon}{2} + c\psi^{(0)}\psi^{(1)}\right) \\ & - \frac{\rho(d-2)}{2}\left(A_x^{(0)}(\omega)g_{xt}^{(0)}(-\omega) + A_x^{(0)}(-\omega)g_{xt}^{(0)}(\omega)\right)\Bigg] + \dots \end{aligned} \tag{4.57}$$

where ϵ is the energy density and $\psi^{(0)}, \psi^{(1)}$ are the coefficients of the scalar expansion close to the boundary $\psi \sim \psi^{(0)} z + \psi^{(1)} z^2$ and $A_x \sim A_x^{(0)} + A_x^{(1)} z^{d-2}$ for odd d.[10] The constant c depends on the choice of boundary conditions for the scalar. We note that the only difference with respect to the noncondensed case is the last term. Interestingly, for a $U(1)$ symmetry breaking to be spontaneous, either $\psi^{(0)}$ or $\psi^{(1)}$ must vanish (depending on the quantization). This implies that the last term in the boundary action in eq. (4.57) does not contribute to the Green's functions G_{Π_x,Π_x} and G_{J_x,Π_x}. As a consequence the MS bound coincides with the one with no $U(1)$ symmetry breaking and

$$K_{\rm MS} = \frac{\beta}{V_{d-1}}\frac{\langle J_x \Pi_x\rangle^2}{\langle \Pi_x \Pi_x\rangle} = \frac{\rho^2}{\epsilon + P}\ . \tag{4.58}$$

However, the bound is not saturated because of the additional superfluid contribution so $K > K_{\rm MS} = K_{\rm U}$.

It would be interesting to compute the MS bound in theories with double trace deformations where it possible to have spontaneous symmetry breaking with both $\psi^{(0)}$ and $\psi^{(1)}$ nonzero. In Sec. 4.6 we investigate in more detail the extra contribution to the Drude weight on a more general background, an Einstein-Maxwell-dilaton background with a gauge mass term.

In the following sections we study the Drude weight and the MS bound in nonrelativistic backgrounds: the Einstein-Proca and an asymptotically Lifshitz EMd model with two gauge fields. As before, the calculation requires a properly renormalized boundary action and a careful evaluation of the correlation functions. We shall see that G_{J_x,Π_x} vanishes in

[10] For even d additional boundary terms appear, see for example appendix A.3.

all cases so $K_{\rm MS} = 0$ and the bound is trivial $K > 0$. Moreover, the Drude weight is not given by the universal result. This suggests that the bound is only saturated if the Drude weight is given by the universal expression.

4.5 Deviations from universality I: nonrelativistic boundary field theory

One of the conditions for the universal result of the zero-frequency conductivity is that the metric approaches AdS_d in the boundary. This a necessary condition for the dual field theory to be relativistically invariant. However, in recent years the potential for condensed matter applications, which are typically described by nonrelativistic theories, has stimulated the interest in asymptotic non-AdS gravity backgrounds. There are different actions that lead to these types of background [285, 286, 195]. Here, we compute the Drude weight for the case of an EMd action with two gauge fields [152] and for an Einstein-Proca action, which involves a massive gauge field [286]. A way to break relativistic invariance in the boundary is by imposing that after a change of scale λ, the time and space coordinates scale differently, $t \to \lambda^z t$, $x^i \to \lambda x^i$, where $z \geq 1$ is the dynamical critical exponent. The simplest metric with this symmetry is,

$$ds^2 = -\frac{r^{2z}}{L^{2z}}dt^2 + \frac{L^2}{r^2}dr^2 + \frac{r^2}{L^2}\sum_{i=1}^{d} dx_i^2 \ . \tag{4.59}$$

4.5.1 Asymptotically Lifshitz EMd model

We start with the case of an Einstein-Maxwell-dilaton action with two (massless) vector fields:

$$S = \frac{1}{16\pi G_4}\int \mathrm{d}^4x\sqrt{-g}\left(R - 2\Lambda - \frac{1}{2}\partial_\mu\phi\partial^\nu\phi \ - \frac{e^{\lambda_1\phi}}{4}F^2 - \frac{e^{\lambda_2\phi}}{4}G^2\right), \tag{4.60}$$

where $F = dA$, $G = dB$ and $\Lambda = -\frac{(z+2)(z+1)}{2L^2}$. The solution is given by [152]

$$\mathrm{d}s^2 = -\frac{r_h^{2z}}{L^{2z}}f(r)\mathrm{d}t^2 + \frac{L^2}{r^2 f(r)}\mathrm{d}r^2 + \frac{r^2}{L^2}(\mathrm{d}x^2 + \mathrm{d}y^2) \ , \tag{4.61}$$

with $z \geq 1$ and

$$\begin{aligned}
\phi &= \log\left[\phi_0 r^{\sqrt{4(z-1)}}\right], \ \lambda_1 = -\frac{2}{\sqrt{z-1}}, \ \lambda_2 = -\frac{2}{\lambda_1}\,, \\
f &= 1 - \left(1 + \frac{\rho_2^2}{\phi_0^{\sqrt{z-1}} 4z}\right)\left(\frac{r_h}{r}\right)^{z+1} + \frac{\rho_2^2 L^{2z}}{\phi_0^{\sqrt{z-1}} 4z}\frac{1}{r^{z+1}}\,, \\
A_t &= \frac{\sqrt{2(z-1)(z+2)}}{L^z(z+1)}\left(r^{2+z} - r_h^{2+z}\right), \\
B_t &= \frac{\rho_2 \phi_0^{-\sqrt{z-1}}}{z}\left(r_h^{-z} - r^{-z}\right).
\end{aligned} \tag{4.62}$$

Though the action given in eq. (4.60) is of the type discussed in Sec. 4.3, the asymptotic geometry, eq. (4.61) with $z > 1$, is not AdS. Therefore, we treat this background separately. For $z \to 1$ the gauge field A_μ decouples and the background in eq. (4.61) reduces to the AdS-RN background. As we have studied in Sec. 4.4.1 the AdS-RN background leads to the universal result of the Drude weight and saturates the MS bound [see eq. (4.50)]. In the rest of the section we take $z = 2$, in which case both A_μ and B_μ are present and the boundary is not AdS.

As seen in eq. (4.62), the time component of the gauge field A_μ diverges in the boundary. Therefore, it does not play the role of a usual gauge field with a finite time-component boundary value, which is interpreted as a chemical potential in the dual theory. Nonetheless, A_t, together with the scalar field ϕ, allows us to satisfy the non-AdS boundary conditions. In other words, A_μ and ϕ *support* the asymptotically Lifshitz brane geometry, but A_μ does not contribute to the thermodynamic properties of the boundary theory [152].[11] On the other hand B_μ allows the black brane to be charged and the charge density in the dual theory is given by

$$q_2 = \frac{L^{z-1}}{16\pi G_4}\rho_2, \tag{4.63}$$

while the boundary value of B_t may be read from eq. (4.62). The entropy density and temperature are as follows:

$$s = \frac{r_h^2}{4G_4}, \quad T = \frac{r_h^z}{4\pi L^{z+1}}\left[z + 2 - \frac{\rho_2^2 L^{2z}}{\phi_0^{\sqrt{z-1}} 4 r_h^{2z+2}}\right]. \tag{4.64}$$

[11] More concretely we refer to the fact that A_μ has no free parameter that enters in the thermodynamic properties. This does not mean A_μ does not affect the thermodynamics as, indeed, it is crucial to obtain the asymptotically Lifshitz background. This is more easily seen in related holographic actions [287–290] involving only A_μ, i.e., removing B_μ. In this case the boundary properties such as the charge density are determined by A_μ. Moreover, the time component of the gauge field may be sourced by the addition of external potentials, in particular Newtonian potential [287].

The boundary theory of eq. (4.60) is renormalized by adding the following counterterms [291]:

$$\begin{aligned} S_{ct} &= \frac{1}{16\pi G_4}\int d^3x\sqrt{-\gamma}\left(2K-\frac{4}{L}+c_A\sqrt{-e^{\lambda_1\phi}\gamma^{ij}A_iA_j}\right), \\ c_A &= -\sqrt{2(z-1)(2+z)}\ , \end{aligned} \tag{4.65}$$

where γ_{ij} is the induced metric in the boundary, γ its determinant and $K=\gamma^{\mu\nu}\nabla_\mu n_\nu$, n_μ is normal to the boundary and points outward. See [291] for a more general model with a hyperscaling violation exponent. It is easy to check that the renormalized boundary action given by eqs. (4.60) and (4.65) gives the correct result for the Gibbs thermodynamical potential. The following term

$$S_{\text{canonical}} = \frac{1}{16\pi G_4}\int \mathrm{d}^3x\sqrt{-\gamma}e^{\lambda_2\phi}n_\mu G^{\mu\nu}B_\nu, \tag{4.66}$$

should be added to obtain the Helmholtz free energy from the action.

In order to study the zero frequency conductivity we perturb a spatial component of the gauge field B_μ, under which the brane is charged. We leave A_μ unperturbed, as previously done in [292–294]. Since A_μ only supports the geometry and does not contribute to the charge of the black brane, it is natural to expect the conductivity in the dual theory to be determined entirely by B_μ,

$$\delta g_{xt} = \tilde{g}_{xt}e^{-i\omega t},\quad \delta B_x = \tilde{B}_x e^{-i\omega t}, \tag{4.67}$$

which satisfy

$$\begin{aligned} &\tilde{B}_x'' + \tilde{B}_x'\left(\frac{f'}{f}+\frac{z+1+r\lambda_2\phi'}{r}\right) - \tilde{B}_x\left(\frac{e^{\lambda_2\phi}L^{2z}B_t'^2}{fr^{2z}}+\omega^2\frac{L^{2z+2}}{f^2r^{2z+2}}\right)=0\ , \\ &\tilde{g}_{xt}' - \frac{2}{r}\tilde{g}_{xt} + e^{\lambda_2\phi}\tilde{B}_xB_t' = 0\ . \end{aligned} \tag{4.68}$$

We impose ingoing boundary conditions at the horizon,

$$\tilde{B}_x \simeq f(r)^{-i\frac{\omega}{4\pi T}}\left(b_x^{(0)}(r)+\omega b_x^{(1)}(r)+\dots\right), \tag{4.69}$$

and solve for $\tilde{g}_{xt}$ and $\tilde{B}_x$ perturbatively in frequency. To obtain the Drude weight we only need to find $b_x^{(0)}(r)$. We have not been able to get an analytical solution for $b_x^{(0)}$. However, it is easy to solve eq. (4.68) numerically. As is observed in Fig. 4.1, the Drude weight is finite but it is not given by the universal result $\frac{q_2^2}{\epsilon+P}$. Moreover, by computing the boundary action explicitly, it follows that the electric current dual to $\tilde{B}_x$ does not couple to the momentum. Therefore the MS bound computed considering only the momentum as

the conserved quantity is not of relevance since it vanishes. It would be interesting to find what are the conserved quantities relevant for the Drude weight in this model.

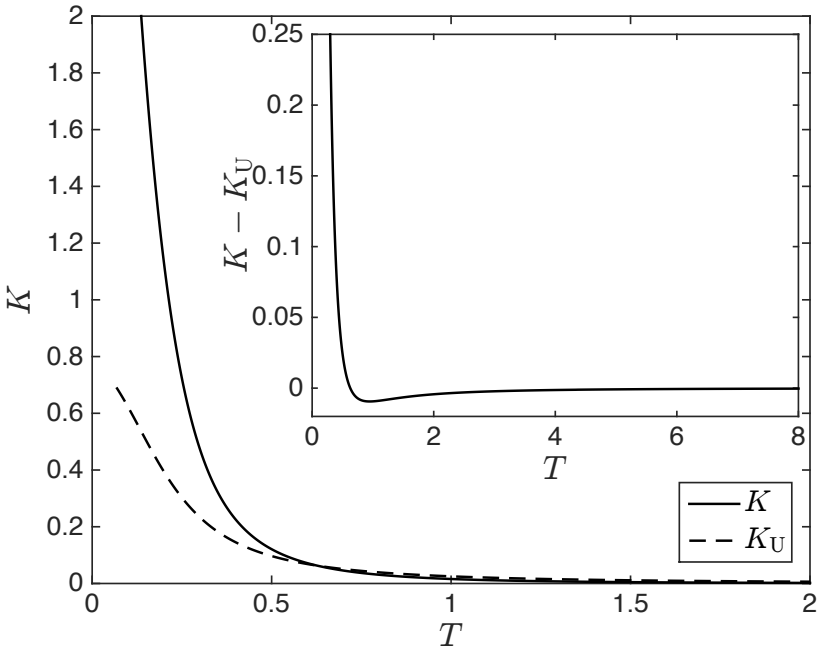

Fig. 4.1 Drude weight in the asymptotically Lifshitz model, eq. (4.60) with $z = 2$. We have fixed the charge density $q_2 = 1$, $\phi_0 = 1$ in units of $L = 1$. The dashed line is the universal result, $K_{\rm U} = \frac{q_2^2}{\epsilon+P}$, eq. (4.12), with the charge density q_2 given in eq. (4.63). The inset figure shows that the Drude weight is always different from the universal prediction $K_{\rm U}$. Interestingly, the difference is nonmonotonic. For low temperatures $K > K_{\rm U}$, while in the high temperature limit $K > K_{\rm U}$, since $K_{\rm U} \sim T^{-2}$ and $K \sim T^{-3}$. Moreover, the MS bound vanishes, $K_{\rm MS} = 0$, so there is no saturation, $K > K_{\rm MS} = 0$.

4.5.2 Asymptotically Lifshitz Einstein-Proca model

It has recently been shown [286] that the metric given in eq. (4.59) is also the solution of an Einstein-Proca action, which includes a massive gauge field and gravity with a negative cosmological constant. The renormalization of this theory has been extensively studied [295–298]. In [299, 300], an additional bulk scalar has also been included in the action. Finally, a comprehensive formalism to study the dual theory to

$$S = \frac{1}{2\kappa^2}\int \mathrm{d}^{d+1}x\sqrt{-g}\Big[R - \alpha(\partial\phi)^2 - Z(\phi)F^2 - W(\phi')A^2 - V(\phi)\Big] \tag{4.70}$$

has been introduced in [288–290], the holographic renormalization has also been discussed in [301]. An asymptotically Lifshitz background at finite temperature is obtained if there are two gauge fields $F = dA$, $F_1 = dB$ with only one being massive. More explicitly the action in this case is

$$S = \frac{1}{16\pi G_{d+2}}\int d^{d+2}x\sqrt{-g}(R - 2\Lambda - \frac{1}{4}F^2 - \frac{1}{2}m^2A^2 - \frac{1}{4}F_1^2)\ , \tag{4.71}$$

where the dynamical critical exponent is fixed to $z = 2d$. It is also possible to analytically solve the perturbations needed to compute the electrical conductivity at zero frequency. However, the proper renormalization of the action eq. (4.71) has not been settled. Therefore, the Drude weight or the MS bound of the dual theory cannot yet be computed rigorously.

For that reason we study the simpler model introduced in Refs. [153, 302] consisting of bulk gravity coupled to a single massive vector field.

Since we are interested in finite temperature solutions we focus on the action studied in [302],

$$S = \frac{1}{16\pi G_{d+2}} \int d^{d+1}x\sqrt{-g}\left(R - 2\Lambda - \frac{1}{4}F^2 - \frac{1}{2}m^2A^2\right), \tag{4.72}$$

with $d = 3$, $\Lambda = \frac{-d(d-1)}{2L^2}$, $m^2 = d - 1 + (d-2)\eta^2$, where $\eta \ll 1$ is used as an expansion parameter related to a small deformation of an AdS black brane,

$$\begin{aligned} \mathrm{d}s^2 &= -c(r)b(r)^2dt^2 + \frac{dr^2}{c(r)} + r^2(dx^2 + dy^2), \\ c &= c_0(r) + \eta^2\mu^2c_1(r), \quad c_0 = r^2\left(1 - \frac{r_0^3}{r^3}\right), \\ b &= 1 + \eta^2\mu^2b_1(r)\ . \end{aligned} \tag{4.73}$$

It is easy to see that the expansion in η of the metric given in eq. (4.59) with $z = 1 + \eta^2$ may be expressed in the form of eq. (4.73). The dynamical exponent is therefore $z = 1+\eta^2$ and $\eta = 0$ corresponds to the AdS-Schwarszchild black brane. The functions c_1 and b_1 have been given in [302]. Moreover [302],

$$\begin{aligned} A_t(u) &= \mu\eta a_t(u)\ , \quad u = \frac{r_0}{r}\ , \\ a_t &= r_0\frac{1-u^3}{u}\Gamma\left(\frac{4}{3}\right)\Gamma\left(\frac{5}{3}\right)\ {}_2F_1\left(\frac{1}{3}, \frac{2}{3}, 2, 1-u^2\right)\ , \end{aligned} \tag{4.74}$$

where the constants in $a(u)$ are chosen so that $A_t(r) \sim \mu\eta r$ close to the boundary.

As before, in order to study conductivity, we add perturbations on the metric and gauge field,

$$\delta g_{xt} = \eta^2 g_1 e^{-i\omega t}, \quad \delta A_x = \eta a_x e^{-i\omega t}. \tag{4.75}$$

We note that perturbations in the metric that couple to the perturbation in the gauge field enter at order η^2. The equation of the perturbation δA_x at all orders in η is

$$A_x'' - A_x'\left(\frac{g_{rr}}{2g_{rr}} - \frac{g_{xx}}{2g_{xx}}\right) - A_x\left(\frac{\omega^2 g_{rr}}{g_{tt}} + m^2 g_{rr} - \frac{A_t'^2}{g_{tt}}\right) = 0\ , \tag{4.76}$$

where by A_x we mean the full perturbation δA_x. Expanding the previous equation in η we obtain to leading order the following equation for δA_x,

$$a_x''(r) + a_x'(r)\frac{c_0'(r)}{c_0(r)} + a_x(r)\left(\frac{\omega^2}{c_0(r)^2} - \frac{2}{c_0(r)}\right) = 0 \ . \tag{4.77}$$

Clearly, the last term in eq. (4.76) is of $\mathcal{O}(\eta^3)$ and does not enter in eq. (4.77). To obtain the Drude weight we need to solve this equation perturbatively in frequency,

$$a_x \simeq \left(1 - \frac{r_0^3}{r^3}\right)^{-i\frac{\omega}{3r_0}} \left(a_x^{(0)}(r) + \omega a_x^{(1)}(r) + \dots\right) , \tag{4.78}$$

and to impose on $a_x^{(0)}$ regularity at the horizon. The multiplicative term in eq. (4.78) ensures a_x is purely ingoing at the horizon. The solution of $a_x^{(0)}$ is

$$a_x^{(0)} = r_0^2 C \ {}_2F_1\left(-\frac{1}{3}, \frac{2}{3}, \frac{1}{3}, \frac{r^3}{r_0^3}, \right) + r^2\tilde{C} \ {}_2F_1\left(\frac{1}{3}, \frac{4}{3}, \frac{5}{3}, \frac{r^3}{r_0^3}, \right) . \tag{4.79}$$

Imposing regularity at the horizon gives

$$\tilde{C} = -C\frac{\Gamma\left(\frac{1}{3}\right)^2\Gamma\left(\frac{4}{3}\right)}{\Gamma\left(\frac{-1}{3}\right)\Gamma\left(\frac{2}{3}\right)\Gamma\left(\frac{5}{3}\right)} \ . \tag{4.80}$$

We normalize $a_x^{(0)}$ by setting

$$C = \frac{a_0}{r_0^2}\frac{2^{2/3}\sqrt{\pi}\Gamma\left(\frac{2}{3}\right)}{\Gamma\left(\frac{1}{6}\right)} \ , \tag{4.81}$$

so that close to the boundary $a_x^{(0)} \sim \frac{a_0}{u} - \frac{a_0}{3}u^2\log u + a_1 u^2$. Moreover it has been shown in [153] that the counterterms,

$$S_{ct} = \frac{1}{16\pi G}\int d^dx\sqrt{\gamma}\left(2K - \frac{2(d-1)}{L} + \frac{1}{2}A_\mu A^\mu\right) , \tag{4.82}$$

renormalize the boundary action up to order η^2. Using the solution, eqs. (4.79)-(4.81), we obtain a finite Drude weight at order η^2,

$$K = \frac{\alpha}{16\pi G}\frac{\eta^2}{36r_0} \ , \tag{4.83}$$

with $\alpha = 37 - \log 729$.

In order to compare this result with the prediction of the universal Drude weight, eq. (4.50), we use the charge density, which may be obtained from the one-point function $\langle J_t\rangle \propto \mu\eta$ [302]. This leads to $K_{\rm U} \propto \mu^2\eta^2$. Therefore, the prediction of the universal Drude weight is different from the direct calculation of the Drude weight which is independent of μ at $\mathcal{O}(\eta^2)$, eq. (4.83).

Moreover, the MS bound vanishes $K_{\rm MS} = 0$ at this order in η since the terms coupling δg_{xt} and δA_x occur at $\mathcal{O}(\eta^3)$. In summary, non-AdS boundaries lead to a vanishing $K_{\rm MS}$[12] and a Drude weight different from the universal one.

4.6 Deviations from universality II: $U(1)$ symmetry breaking

We study another model in which the Drude weight is not given by the universal prediction and the MS bound is not saturated because of spontaneous symmetry breaking of the dilaton. We consider the following EMd theory which has been explored in detail in [94, 123, 127]:

$$S_{\rm EMd} = \frac{1}{2\kappa^2}\int d^{p+1}x\sqrt{-g}\left[R - \frac{1}{2}(\partial\phi)^2 + V(\phi) - \frac{Z(\phi)}{4}F^2\right] \ . \tag{4.84}$$

The AdS radius is set to $L = 1$ and

$$Z(\phi) = \cosh(\gamma\phi) \ , \ V(\phi) = -2\Lambda - \frac{2m^2}{\delta^2}\sinh^2(\delta\phi) \ , \tag{4.85}$$

where $\gamma,\ \delta > 0$. The UV completion of $V(\phi)$ is chosen such that no logarithmic divergences appear close to the UV, [127]. The UV completion of $Z(\phi)$ is fixed by requiring $Z'(\phi = 0) = 0$, which ensures the existence of a second order phase transition at finite temperature driven by the condensation of the dilaton. Moreover m^2 controls the scaling dimension of the operator dual to the dilaton in the usual way: $\Delta = \frac{1}{2}(p - \sqrt{p^2 + 4m^2})$. Following [127] we take the metric ansatz,

$$\begin{aligned} ds^2 &= -D(r)dt^2 + B(r)dr^2 + Cd\vec{x}^2, \\ D &= \frac{g(r)}{r^2 h(r)}, \quad B = \frac{1}{r^2 g(r)}, \quad C = \frac{1}{r^2} \ , \end{aligned} \tag{4.86}$$

where the UV is at $r = 0$ and the horizon at $r_H = 1$, $h(r_H) = 0$. The geometry is asymptotically AdS, so close to the boundary,

$$\begin{aligned} \phi &\sim \phi_a r^{\Delta} + \phi_b r^{p-\Delta} + \dots \ , \\ g &\sim 1 + \cdots + g_p r^p + \dots \ , \\ h &\sim 1 + \cdots + h_p r^p + \dots \ , \\ A_t &= \mu + \rho r^{p-2} + \dots \ . \end{aligned} \tag{4.87}$$

[12] When considering momentum as the only conserved charge in the sum over conserved charges of eq. (4.34).

We impose $\phi_b = 0$, and choose $m^2 = -2/L^2$, $\Delta = 1$ and $p = 3$. We add the usual perturbations δA_x and δg_{xt}. In $p = 3$ dimensions, the electrical conductivity is

$$\sigma = \sqrt{-g}\frac{Z(\phi)}{BC}\bigg|_{r\to 0}\frac{A_x^{(1)}}{i\omega A_x^{(0)}} = \frac{A_x^{(1)}}{i\omega A_x^{(0)}}\,, \tag{4.88}$$

where $A_x \sim A_x^{(0)} + A_x^{(1)} r + \ldots$.

As mentioned in Sec. 4.2, it has recently been shown [122, 266, 303] that in the EMd theory given by eq. (4.84), the regular part of the dc conductivity and the Drude weight may be expressed in terms of thermodynamic quantities and the electromagnetic coupling constant

$$\sigma_{dc}^{reg} = \left(\frac{sT}{\epsilon + P}\right)^2 Z_H C_H^{\frac{p-3}{2}}\,, \quad K = K_{\rm U} = \frac{\rho^2}{\epsilon + P}\,, \tag{4.89}$$

where s is the entropy density, T temperature, P pressure and ϵ energy density. The subindex H indicates that the corresponding term is evaluated at the horizon and C is the metric function in the general metric ansatz given in the first line of eq. (4.86). Similarly to the Einstein-Maxwell theory, eq. (4.40), the Drude weight above is given by the same expression and it saturates the MS bound.

The situation is different in the presence of a gauge field mass term in the EMd action,

$$S_W = -\int d^{p+1}x\sqrt{-g}\frac{W(\phi)}{2}A_\mu A^\mu\,, \tag{4.90}$$

and

$$W(\phi) = W_0\left[-1 + \cosh^2(\eta\phi/2)\right]. \tag{4.91}$$

We have chosen $W(\phi)$ such that $W(\phi = 0) = 0$ and $W'(\phi = 0) = 0$ to avoid divergencies in the UV. In the following we consider the action $S_{\rm EMd} + S_W$ given by (4.84) and (4.91).

More specifically, we investigate fractionalized *IR-charged* solutions [230, 127], with a constant scalar in the IR and extremality for vanishing temperature. In the context of AdS/CFT, a fractionalized state arises when the dual field theory charge density is not determined only by the charged bulk fields but also by a horizon charged flux [304, 305]. Recently, it has been claimed [306, 307] that the gravity dual of a fractionalized Fermi liquid is a background with an $AdS_2 \times \mathbb{R}^n$ horizon that has a finite entropy event at zero temperature. A fractionalized state occurs for a nonvanishing electric flux in the IR [230], which in our case is

$$\lim_{r\to r_h}\frac{1}{4\pi}\int_{\mathbb{R}^2} Z(\phi)\star F = \lim_{r\to r_h} -\frac{V_{\mathbb{R}^2}}{4\pi}Z(\phi)\frac{CA_t'}{\sqrt{BD}} \neq 0. \tag{4.92}$$

The action $S_{\rm EMd} + S_W$ still has translational symmetry, so we expect a finite Drude weight. Indeed, the numerical results, depicted in Fig. 4.2, show the Drude weight, for $T < T_c$, where dilaton condensation occurs, which is larger than the universal prediction.

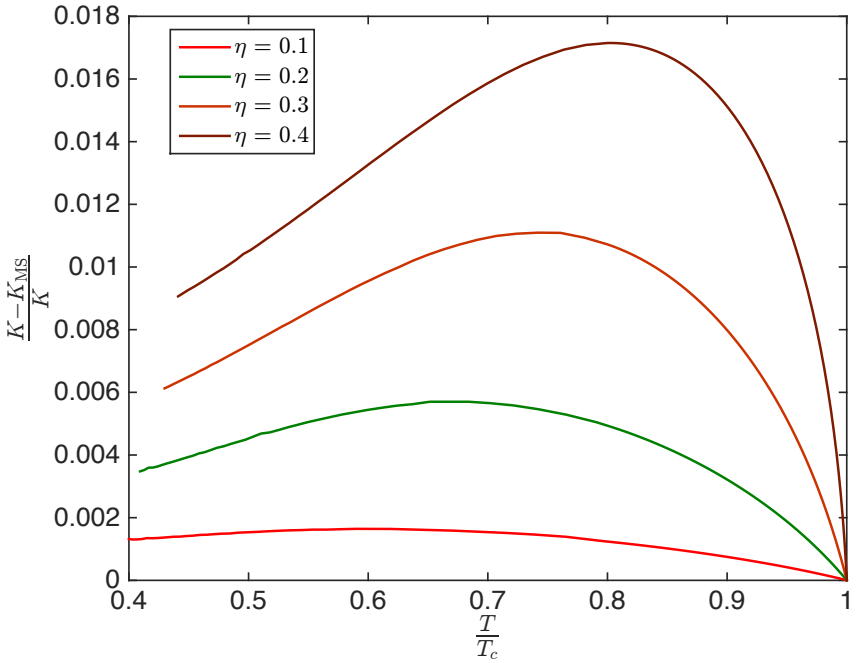

Fig. 4.2 Difference between the Drude weight and the MS bound in the theory given by $S_{\rm EMd} + S_W$, eqs. (4.84) and (4.90). At the critical temperature the Drude weight is given entirely by the universal expression. This is expected since the dilaton vanishes and the background is the Reissner-Nordström black hole, for which the Drude weight is given by the universal result, $K = K_{\rm MS} = \frac{\rho^2}{\epsilon+P}$. For $T < T_c$ the dilaton condenses and the physics is similar to that of holographic superconductors where the dilaton is interpreted as the modulus of a charged scalar. The Drude weight is always above the MS bound since the spontaneous breaking of the $U(1)$ symmetry produces an extra contribution proportional to the superfluid density which persists even in the presence of momentum dissipation. The parameters used are $W_0 = 1$, $\gamma\delta = 1$, $\delta = 1/2$. The parameter η is given in horizon units.

The MS bound, still given by eq. (4.35), is not saturated, as we expect an additional contribution from the superfluid density that does not depend on thermodynamic quantities. Similarly to holographic superconductors [114], this extra contribution is associated with the $U(1)$ spontaneous symmetry breaking, where the dilaton may be taken as the modulus of a complex scalar. With respect to the transport properties, the main difference[13] with respect to holographic superconductor narrows down to the different coupling between the gauge field and the dilaton. While in our model it is given by (4.91), for holographic superconductors it is quadratic in the scalar field with a coupling strength proportional to its charge.

Moreover, at least close to the transition temperature, we expect the Drude weight to be determined by two additive contributions: the universal one, given by $\frac{\rho^2}{\epsilon+P}$, and another one proportional to the superfluid density $n_s \propto \langle O_1 \rangle^2$ where $\langle O_1 \rangle$ is the expectation value of the operator dual to the dilaton. We also expect that the transition is controlled by

[13]The potential of the scalar field is not quadratic for the EMd model and the gauge field coupling is not constant.

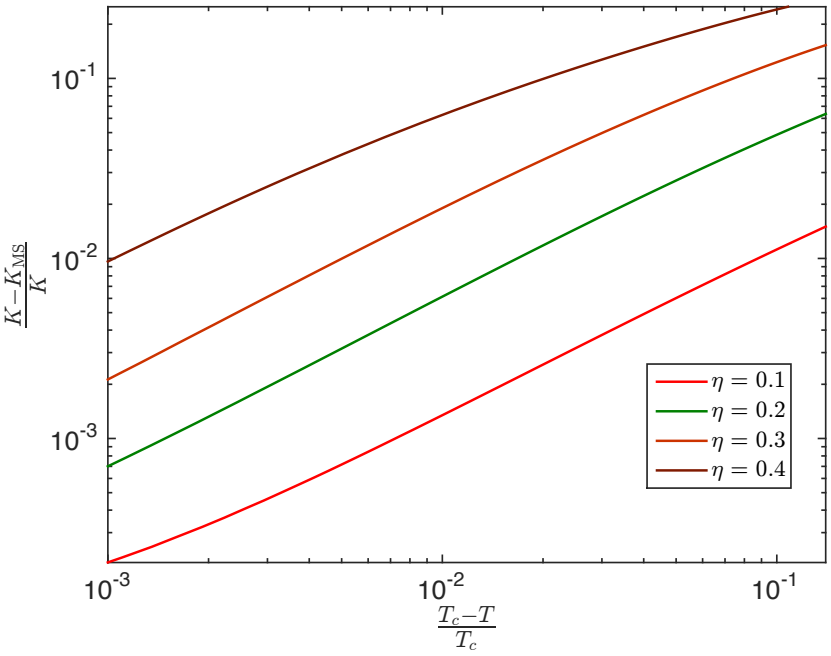

Fig. 4.3 Difference between the Drude weight and the MS bound in the theory given by $S_{\rm EMd} + S_W$ [see eqs. (4.84) and (4.90)]. Close to the critical temperature the mass term coupling $W(\phi) \sim \eta^2\phi^2 + \ldots$, in which case the model is similar to that of standard holographic superconductors. Therefore, the extra contribution to the Drude is expected to be proportional to $\langle O_1\rangle^2 \sim \frac{T-T_c}{T_c}$. Consequently, for some range of temperatures, the slopes of the lines shown in logarithmic scale are similar. For larger values of $\eta\phi$ (either far from T_c or for larger η) the mass coupling receives higher order corrections, which affect the extra contribution to the Drude weight. Thus, for a fixed η, deviations from a linear behavior are observed by increasing $\frac{T-T_c}{T_c}$ (increasing the expectation value of the dilaton). Similarly, for larger η, the linear behavior occurs closer and closer to T_c. The parameters used are the same as in Fig. 4.2.

mean-field critical exponents, $\langle O_1\rangle \propto (T-T_c)^{1/2}$. The results of Fig. 4.3 confirm these predictions: close to T_c the extra contribution to the Drude weight is linear in $\frac{T-T_c}{T_c}$. We use the logarithmic scale since the region of temperatures where the linear scaling is observed is small.

4.7 Momentum dissipation, relaxation time and bounds on conductivity

In this section we study the dc conductivity in systems where translational invariance is weakly broken. If the breaking is sufficiently weak, so that the relaxation time τ is sufficiently long, we still expect the Drude weight K (or more precisely the part of it related to conservation of momentum) of the translationally invariant theory to control the dc conductivity,

$$\mathrm{Re}(\sigma_{\rm dc}) \approx K\tau \ . \tag{4.93}$$

We confirm the validity of (4.93) by computing explicitly the scattering time τ which is nothing but the *dominant* pole of the relevant Green's function that controls the decay of momentum. The poles of the Green's functions are obtained from the quasinormal modes of the corresponding metric and field perturbations [308]. The *dominant* pole of the Green's functions corresponds to the pole with the smallest absolute value of the imaginary part describing the slowest decaying mode of the system. This is the only one which is relevant in the limit of weak momentum dissipation.

We employ the following Einstein-Maxwell-axion action [200, 139] to model momentum dissipation,

$$S_0 = \int_M \sqrt{-g}\left[R - 2\Lambda - \frac{1}{2}\sum_I^{d-1}(\partial\psi^I)^2 - \frac{1}{4}F^2\right] d^{d+1}x \ , \tag{4.94}$$

where for convenience we have omitted the counterterms needed to regularize the action in the boundary. The background solution is (with the AdS radius $L = 1$):

$$\begin{aligned}
&ds^2 = -f dt^2 + \frac{dr^2}{f} + r^2 dx_{d-2}^2 \,, \\
&f = r^2 - \frac{\alpha^2}{2(d-2)} - \left[r_0^2 - \frac{\alpha^2}{2(d-2)} + \frac{\mu^2(d-2)}{2(d-1)}\right]\left(\frac{r_0}{r}\right)^{d-2} + \frac{\mu^2(d-2)}{2(d-1)}\left(\frac{r_0}{r}\right)^{2d-4} \,, \\
&A_\mu = \mu\left[1 - (r_0/r)^2\right] \mathrm{d}t \,, \ \psi^I = \alpha x^I \,, I = 2, \ldots, d-2 \,.
\end{aligned}$$

In order to proceed we turn to a perturbation of the gauge field, $\delta A_x = e^{-i\omega t} a_x(r)$. For the axion model this perturbation couples to a metric and a scalar perturbation $\delta g_{xt} = e^{-i\omega t} r^2 H_{tx}(r)$, $\delta\psi = e^{-i\omega t}\alpha^{-1}\chi(r)$ [139], where $r \in (r_0, \infty)$ is the holographic radial coordinate and α is the parameter related to the breaking of translational symmetry. The equations for these perturbations at zero spatial momentum are given in Ref. [139] for arbitrary bulk dimensions $d+1$:

$$a_x'' + \left[\frac{f'}{f} + \frac{(d-3)}{r}\right] a_x' + \frac{\omega^2}{f^2} a_x + \frac{\mu(d-2)}{f}\frac{r_0^{d-2}}{r^{d-3}} H_{tx}' = 0 \ , \tag{4.95}$$

$$\chi'' + \left[\frac{f'}{f} + \frac{(d-1)}{r}\right] \chi' + \frac{\omega^2}{f^2}\chi - \frac{i\omega\alpha^2}{f^2} H_{tx} = 0 \ , \tag{4.96}$$

$$\frac{i\omega r^2}{f} H_{tx}' + \frac{i\omega\mu(d-2)}{f}\frac{r_0^{d-2}}{r^{d-1}} a_x - \chi' = 0 \ . \tag{4.97}$$

In general, the dominant quasinormal mode, and therefore τ can only be computed numerically. However, in the limit $\alpha \ll T$ an analytical expression for τ, associated with the transverse fluctuations above, was found for $d = 3$ [303],

$$\tau^{-1} \simeq \eta\frac{\alpha^2}{\epsilon + P} = \frac{\alpha^2}{3r_0\left[1 + \frac{\mu^2}{4r_0^2}\right]} \ . \tag{4.98}$$

We note that this expression is identical to that obtained in the context of massive gravity [139, 137] with the replacement $\alpha^2 \to 2m^2$, where m is the mass of the graviton. By following the approach of [303] we have generalized this expression to $d > 3$,

$$\tau^{-1} \simeq \eta \frac{\alpha^2}{\epsilon + P} = \frac{\alpha^2}{r_0 d \left[1 + \frac{(d-2)\mu^2}{2(d-1)r_0^2}\right]} \,. \tag{4.99}$$

This expression is valid only for weak breaking of translational symmetry, namely, up to $\mathcal{O}(\alpha^4/T^4)$ corrections. An obvious correction $\mathcal{O}(\alpha^4)$ is obtained by substituting the energy density and pressure corresponding to the system with $\alpha \neq 0$; however, as shown in [303], this is not the only one. We are not interested in such corrections and refer to [303] for details.

We also evaluate τ numerically following the method proposed in [308], which we summarize now. The method uses *independent* sets of boundary conditions BC_i, $(i = 1, \ldots, N)$ in the IR to find N different solutions. In our case $N = 3$ corresponding to the three fields a_x, H_{tx} and χ of eqs. (4.95)-(4.97). For arbitrary frequency (this is the unknown which we want to obtain), one constructs the following matrix:

$$\begin{pmatrix} i\alpha & \chi^{(1)}|_{r\to\infty} & \chi^{(2)}|_{r\to\infty} \\ 0 & a_x^{(1)}|_{r\to\infty} & a_x^{(2)}|_{r\to\infty} \\ 1 & H_{tx}^{(1)}|_{r\to\infty} & H_{tx}^{(2)}|_{r\to\infty} \end{pmatrix} \tag{4.100}$$

Each column contains the boundary value of the fields obtained from a given set of IR boundary conditions BC_k ($k = 1, 2, 3$ refers to the column). Each row has the boundary value of a field for each of the three boundary conditions. In our case, the boundary conditions at the horizon are

$$\begin{aligned} a_x(r \to r_0) &\sim (r - r_0)^{-i\omega/f'(r_0)} \left(a_x^H + a_x^1(r - r_0) + \ldots\right) \,, \\ \chi(r \to r_0) &\sim (r - r_0)^{-i\omega/f'(r_0)} \left(\chi^H + \chi^1(r - r_0) + \ldots\right) \,, \\ H_{tx}(r \to r_0) &\sim (r - r_0)^{-i\omega/f'(r_0)-1} \left(H_{tx}^H + H_{tx}^1(r - r_0) + \ldots\right) \,, \end{aligned}$$

where H_{tx}^H is fixed in terms of a_x^H and χ^H.[14] This constraint on the coefficients is due to a residual gauge symmetry [308–310]. Hence, the boundary conditions BC_k consist on specifying a_x^H and χ^H and only two sets of independent boundary conditions can be chosen. The second column of the matrix of eq. (4.100) is obtained using one set of boundary conditions: $\text{BC}_2 = \{a_x^H = 1, \chi^H = 0\}$ while the third column corresponds to $\text{BC}_3 = \{a_x^H = 0, \chi^H = 1\}$. The first column corresponds to the non-physical gauge solution

[14] There is a constraint between H_{tx}^H, χ^H and a_x^H and one could have also chosen either to express a_x^H in terms of H_{tx}^H and χ^H or χ^H in terms of H_{tx}^H and a_x^H, this choice is not important.

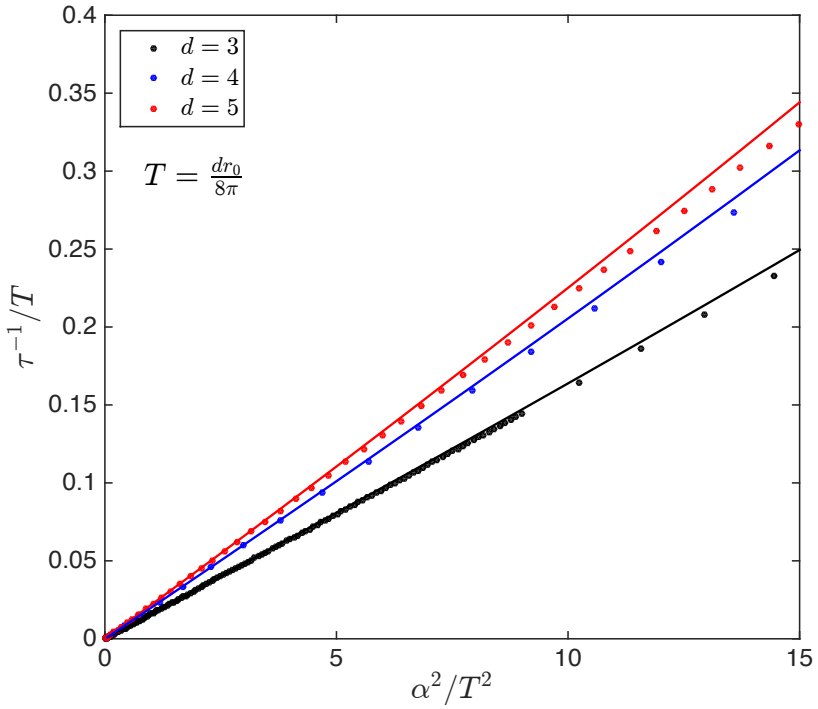

Fig. 4.4 Relaxation time in the Einstein-Maxwell-axion model, eq. (4.94), at fixed temperature in different numbers of dimensions. The dots are numerical results while the lines are obtained from the analytical expression proposed in eq. (4.99), valid to second order in α. As anticipated in [311], the analytical expression deviates from the numerical results progressively as the contribution of additional quasinormal modes to the total scattering rate increases continuously for larger α/T.

[308], $a_x = 0$, $H_{tx} = \text{const.}$, $\chi = \text{const}'$., where these constants are related by the equations of motion.[15]

The leading quasinormal mode ω_0 is the frequency with the smallest imaginary part (in absolute value) for which the determinant of the matrix given in eq. (4.100) vanishes. The relaxation time is then $\tau = -1/\,\text{Im}(\omega_0)$.

The numerical results, depicted in Fig. 4.4, are very close to the analytical prediction (4.99) even beyond its limit of applicability, $\alpha \ll T$. Interestingly, the dependence of τ on dimensionality is rather weak. In the high temperature limit, assuming $\mu/T \ll 1$, $\tau \propto T$ for all d's. We find it difficult to physically interpret this linear dependence on temperature. The temperature dependence of the relaxation time is very sensitive to the source of scattering (phonons, impurities, electrons), the range of temperatures and whether the material is an insulator, metal or semiconductor. Sometimes, it increases with temperature, as for charge impurities in semiconductors. In many other cases, it decrease with temperature as for phonon scattering at high temperature. However, we

[15] In the absence of residual gauge symmetry, the number of independent boundary conditions is equal to the number of fields (there is no extra constraint in the horizon) and this complication of adding the gauge solution is avoided [308].

are not aware of any simple situation in which is linear. It would be interesting to find a holographic model in which the relaxation time has a richer temperature dependence.

We have now all the information to compute the dc conductivity. For sufficiently small α/T, from eqs. (4.99) and (4.49) with $z_0 = 1/r_0$, $\sigma_{dc} \approx K\tau \approx \mu^2(d-2)^2 r_0^{d-3}/\alpha^2$. Not surprisingly, except for the incoherent contribution which is small in this limit, this is the analytical result already obtained in [139].

Since K is constrained by the MS bound, the conductivity, for a fixed large τ, has also a lower bound $\sigma_{\rm dc} \geq K_{\rm MS}\tau$. However, the bound is trivial here because the MS bound is saturated in this model. We see a different behavior in the next section when we study Einstein-Maxwell-dilaton actions.

4.7.1 Momentum relaxation and relaxation time τ in Einstein-Maxwell-dilaton backgrounds

We now repeat this analysis in a more general EMd theory $S_{\rm EMd} + S_{\rm axion}$, where $S_{\rm EMd}$ is given in eq. (4.84) and

$$S_{\rm axion} = -\frac{1}{2\kappa^2}\int d^{p+1}x\sqrt{-g}\frac{Y(\phi)}{2}\sum_{i=1}^{p-1}(\partial\psi_i)^2\,, \tag{4.101}$$

$$Y(\phi) = -1 + 2\cosh^2(\lambda\phi), \quad \psi_i = \alpha x_i, \quad i = 1,\ldots,p-1\,. \tag{4.102}$$

In this theory the conductivity at zero frequency is finite. It is obtained analytically by finding the massless mode of the system of equations for the perturbations of the gauge field, metric and axions, δa_x, δg_{xt} and $\delta\psi_x$. This allows us to decouple the system of equations and compute σ_{dc} analytically. This approach was first introduced in [138] for a model of massive gravity and later applied to $S_{\rm EMd} + S_{\rm axion}$ in, [125, 127]. We simply cite the final result,

$$\mathrm{Re}(\sigma_{\rm dc}) = Z_H C_H^{\frac{p-3}{2}} + \frac{\rho^2}{\alpha^2 C_H^{\frac{p-1}{2}} Y_H}\,, \tag{4.103}$$

where ρ is the charge density, α is defined in eq. (4.102) and, again, the subindex H means the corresponding quantity is evaluated at the horizon. As in the previous section we now compare this result for $p = 3$ with

$$\mathrm{Re}(\sigma_{\rm dc}) = Z_H + K_{\rm MS}\tau\,, \tag{4.104}$$

which, as we will see, is easier to interpret physically. $K_{\rm MS}$, the MS bound, is calculated from eq. (4.35) with a single conserved quantity associated with momentum conservation in the theory with axions turned off, $S_{\rm EMd}$, at the same temperature and charge density. It coincides with the universal value $K_{\rm MS} = K_{\rm U}$, eq. (4.12). The relaxation time τ is again computed from the dominant quasinormal model of the theory $S_{\rm EMd} + S_{\rm axion}$ as

explained in the previous sections. More specifically, we add perturbations of the gauge field, metric and axion in the theory given by $S_{\rm EMd}+S_{\rm axion}$ and solve for the dominant quasinormal mode using the equations analogous to those given in eqs. (4.95)-(4.97) for the Einstein-Maxwell theory. We follow the same method explained in Sec. 4.7 to compute the dominant quasinormal mode. The results, depicted in Fig. 4.5, clearly show that, again, in this case eq. (4.104) provides an excellent description of the dc-conductivity eq. (4.103), in the $S_{\rm EMd}+S_{\rm axion}$ model.

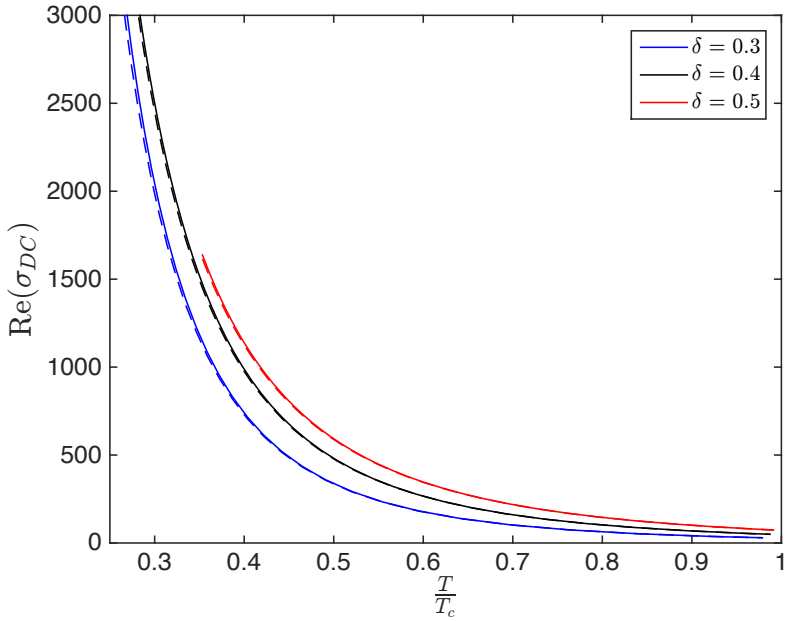

Fig. 4.5 The real part of the dc conductivity the theory $S_{\rm EMd}+S_{\rm axion}$. The continuous lines correspond to the numerical result. The dashed lines are obtained from eq. (4.104). Here, we have chosen $\gamma\delta=1$, $\lambda=1/2$, $\alpha/r_0=0.1$. Clearly, for weak breaking of translational invariance ($\alpha\ll T$), the conductivity has a contribution controlled by the MS bound of the translationally invariant theory ($S_{\rm EMd}$). As for the Einstein-Maxwell theory, the MS bound is saturated by the universal result, $K_{\rm MS}=\frac{\rho^2}{\epsilon+P}$.

As in the previous case the MS bound is saturated, and therefore the associated bound of the conductivity $\mathrm{Re}(\sigma_{\rm dc})\geq Z_H C_H^{\frac{p-3}{2}}+K_{\rm MS}\tau$ is not of special relevance. In light of these results, it is not difficult to understand that, once the axions are switched on and translational invariance is weakly broken, the Drude weight of the translational invariant theory still controls the coherent part of the dc conductivity. Similar results hold for theories $S_{\rm EMd}+S_{\rm axion}$ with $Z'(\phi=0)\neq 0$, which corresponds to a black hole with dilaton condensation for all temperatures.

4.7.2 Drude weight and momentum relaxation in theories with $U(1)$ symmetry breaking

In this section, we study the dc conductivity in the following theory with spontaneous $U(1)$ symmetry breaking and weak momentum dissipation,

$$S = S_{\text{EMd}} + S_W + S_{\text{axion}} \ , \tag{4.105}$$

together with eqs. (4.84) (4.90) and (4.101) and the couplings given in eqs. (4.85), (4.91) and (4.102).

As discussed in Secs. (4.2) and (4.6) we have seen that in the absence of axions, $S_{\text{EMd}} + S_W$, the Drude weight receives an extra contribution from the superfluid mode and $K > K_{\text{MS}}$. In Fig. 4.6 we show that in the presence of axions, which break translational symmetry, the dc-conductivity of the dual theory to the gravity action eq. (4.105) is controlled by the MS bound, K_{MS}, instead of by the Drude weight K of the theory in the absence of axions, $S_{\text{EMd}} + S_W$. In other words,

$$\text{Re}\,(\sigma_{\text{dc}}^{\text{reg}}) = Z_H + K_{\text{MS}}\tau \ , \tag{4.106}$$

where again $K_{\text{MS}} = K_{\text{U}}$ and the relaxation time τ is computed from the dominant quasinormal model of the theory eq. (4.105).

The results depicted in Fig. 4.6 show that, similarly to the EMd model+axion studied in Sec. 4.7.1, eq. (4.106) indeed describes the dc-conductivity. In the theory given by eq. (4.105), despite the fact that momentum is not conserved, the Drude weight is not zero because the superfluid density is finite for sufficiently low temperatures. Therefore, only the part of the Drude weight that disappears once the axions are switched on contributes to the dc conductivity. The bound on the dc conductivity associated with the MS bound is more relevant in this case as only a part of the Drude weight, the MS bound, contributes to the conductivity.

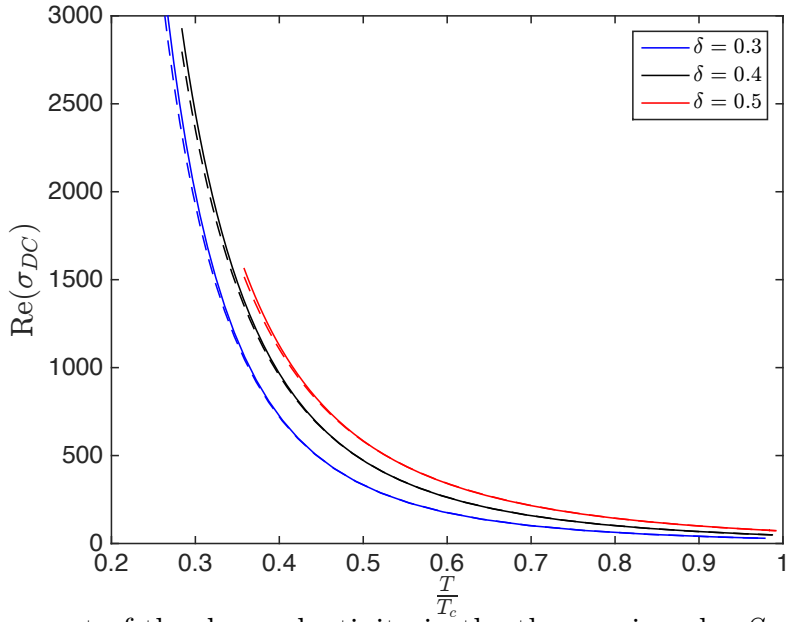

Fig. 4.6 Regular part of the dc conductivity in the theory given by $S_{\rm EMd} + S_W + S_{\rm axion}$ [see eqs. (4.84), (4.90) and (4.101)]. The continuous lines are numerical results while the dashed lines correspond to eq. (4.106). Clearly, the regular part of dc conductivity is controlled by the MS bound of the theory $S_{\rm EMd} + S_W$, while the superfluid mode still contributes to a finite Drude weight even when translational symmetry is broken. The parameters used are $\gamma\delta = 1$, $\delta = 1/2$, $W_0 = 1$, $\eta/r_0 = 0.3$, $\lambda = 1/2$, $\alpha/r_0 = 0.1$.

4.8 Conclusions

We have studied the Drude weight and the associated MS bound in a broad range of holographic theories. We have extended the universality of the Drude weight to the case of several massless gauge fields. We have shown that the MS bound is saturated only if the Drude weight is given by the universal expression first obtained in [272, 128]. For nonrelativistic theories the Drude weight is nonzero but different from the universal one, and the MS bound vanishes. In theories with spontaneous $U(1)$ symmetry breaking the Drude weight is larger than the universal prediction and the MS bound is nonzero but not saturated. Finally, in the limit of weak breaking of momentum conservation, we have shown that the coherent part of the dc conductivity in EMd-axion theories is controlled by the leading quasinormal mode and the MS bound which suggests a lower bound, depending on the relaxation time, for the conductivity as well.

Since the Mazur-Suzuki bounds allow to decompose large time auto-correlation functions of a current J in terms of conserved charges which overlap with J, we expect these bounds to be useful to identify the dominant degrees of freedom in other observables apart from the electrical conductivity. Moreover, as suggested in the context of Condensed Matter, the MS bounds may be useful to study integrability.

This concludes our second strategy to study strongly coupled systems with gravity duals. We now move on to the final strategy, which is to introduce mechanisms which induce strong momentum dissipation in the boundary theory. We aim to describe insulating features of strongly coupled systems. We base our study on a theory of gravity different from Einstein's theory as well as on previous suggestions regarding strong momentum dissipation in holographic settings.

5

Transport in a gravity dual with a varying gravitational coupling constant[†]

We study asymptotically AdS Brans-Dicke (BD) backgrounds, where the Ricci tensor R is coupled to a scalar in the radial dimension, as effective models of metals with a varying coupling constant. We show that, for translational invariant backgrounds, the regular part of the dc conductivity deviates from the universal result of Einstein-Maxwell-dilaton (EMd) models by a multiplicative factor. This factor is expected due to the conformal transformation relating BD and EMd models. However, the shear viscosity to entropy ratio saturates the Kovtun-Son-Starinet (KSS) bound. In four bulk dimensions we study momentum relaxation induced by gravitational and electromagnetic axion-dependent couplings. For sufficiently strong momentum dissipation induced by the former, a recently proposed bound on the dc conductivity is violated for any finite electromagnetic axion coupling. Interestingly, in more than four bulk dimensions, the dc conductivity for strong momentum relaxation decreases with temperature in the low temperature limit. In line with other gravity backgrounds with momentum relaxation, the shear viscosity to entropy ratio is always lower than the KSS bound. The numerical computation of the optical conductivity also reveals insulating features: it grows linearly with the frequency in the limit of low temperature, low frequency and large momentum relaxation. We have also shown that the module and argument of the optical conductivity for intermediate frequencies are not consistent with cuprates experimental results, even assuming several channel of momentum relaxation.

[†]A version of this chapter may be found in [312], which has been published at *Physical Review D* and is authored by Antonio M. García-García, Bruno Loureiro and A. R. B.
Contributions done solely by other authors have been removed. Contributions of a collaborative work have been rewritten or extended.

5.1 Introduction

Einstein general relativity assumes that gravity is mediated by a tensor two particle. Despite its immense conceptual and phenomenological success, generalizations [313] of general relativity, where gravity is also mediated by a scalar or a vector, have been intensively studied mostly for its potential interest in cosmology but also simply as toy models of new ideas in gravity. One of the most influential, though not the earliest [313], is the so called Brans-Dicke gravity [314] that aimed to reconcile Mach's principle with general relativity. Gravity is also mediated by a scalar coupled linearly to the Ricci tensor. The action also has a kinetic term for the scalar so BD has two coupling constants. Physically this scalar can be understood as a gravitation constant G that varies in time and space. General relativity is usually preferred as it predicts the same physics with less free parameters. Interestingly, after a conformal transformation, BD gravity maps into Einstein gravity with a dilaton field (EMd). As a result of this mapping, explicit analytical solutions of the BD gravity equations of motion are known not only for Einstein gravity but also for asymptotically dS and AdS spaces even if the theory also contains massless photons modelled by the Maxwell tensor. For a certain region of parameters it is also possible [315] to map onto BD more general $f(R)$ models where the action is not linear in the Ricci tensor R.

In light of this rich phenomenology, we study BD backgrounds with AdS asymptotic as effective duals of strongly coupled metals. Previous holographic studies [316, 317] involving BD backgrounds were restricted to thermodynamic properties only. By contrast here we focus on transport observables such as the optical, dc conductivity and shear viscosity in asymptotically AdS Brans-Dicke backgrounds. Our motivation is to explore the impact of the BD scalar running in the radial dimension, that acts as an effective gravitational constant, on the transport properties of holographic metals [94, 127]. More specifically we address whether the universality of the shear viscosity [75] and the dc conductivity [266, 122, 128, 250], reported in translational invariant Einstein-Maxwell-dilaton [94, 127] backgrounds with massless photons and no dilaton coupling to the Maxwell tensor also holds in the BD background. We have found that the universal shear viscosity ratio also holds in the BD background. Moreover, we explicitly check that, as expected, the regular part of the dc conductivity σ_Q obtained from a BD background is consistent with the conformal transformation of σ_Q obtained from EMd backgrounds [122, 266, 128].

We also investigate momentum relaxation by *gravitational axions*, namely, axions coupled to the Ricci tensor, a simplified form of BD backgrounds where the scalar has no dynamics. Axions [139] together with massive gravitons, or simply a random chemical potential [130–135], break translational invariance which modifies substantially the conductivity and other transport properties. For weak momentum relaxation the conductivity is to a good extent described by Drude physics. For low temperature or frequency the conductivity is large, the so called Drude peak, and decreases monotonously.

It was observed, in all models studied, that no matter the strength of the momentum relaxation the conductivity of Einstein-Maxwell holographic metals was always above a certain bound which precludes a metal-insulator transition. In part based on this numerical evidence, it was conjectured [142] the existence of a lower bound in the conductivity of more complicated holographic models models. However, in two recent papers [143, 144] violations of this bound have been reported in models where the axion is coupled to the Maxwell tensor, effectively screening charge. Here we show that gravitational axions, that do not screen charge, also lead to violations of the bound in the limit of strong, although still parametrically small with respect to the rank of the gauge group, axion gravitational coupling. For three space dimensions the dc conductivity decreases with T for low temperatures even without any other source of momentum relaxation.

We also study the optical conductivity in BD backgrounds. The optical conductivity in EMd models with translational invariance in the limit of small frequencies and temperatures is controlled by the infrared (IR) geometry that for Reissner-Nordstrom background is AdS_2 leading to $\sigma \sim \omega^2$. The effect of momentum relaxation in the optical conductivity of EMd theories was investigated in [127] but it is not yet fully understood whether, for low-frequencies and strong momentum relaxation, the conductivity scales as a power-law faster than linear as in Mott insulators and many-body localised states [318].

By contrast, in a model in which momentum relaxation occurs by a oscillatory chemical potential, it was claimed [319] the modulus of the optical conductivity for intermediate frequencies decays as a power-law with an exponent equal to that observed in most cuprates. Here we find that, even assuming several channels of momentum dissipation, we cannot reproduce the modules and argument observed in cuprates. However, we have found that, for strong momentum dissipation and close to zero temperature, the optical conductivity increases linearly, not quadratically with the frequency, for both gravitational and electromagnetic axions. Finally, we have computed the ratio of the shear viscosity and the entropy density in BD holography with momentum relaxation. We have observed that, unlike the translational invariant case, the ratio is temperature dependent. It decreases as the strength of momentum relaxation increases and it is always below the KSS bound. It can be made arbitrarily small for a finite amount of momentum relaxation.

The organization of this chapter is as follows: in Sec. 5.2 we repeat the analogous calculation of in Sec. 4.2 to compute in this case the dc conductivity and show that the shear viscosity to entropy ratio in translational invariant BD backgrounds is given by the KSS bound. In Sec. 5.3 we study the dc conductivity in BD like backgrounds with momentum relaxation induced by coupling the axion and the Ricci tensor in two boundary space dimensions. In Sec. 5.4 we address momentum relaxation by gravitational axions in higher space dimensions. In Sec. 5.5 we study the optical conductivity in BD backgrounds. We also compute the module and argument of the complex conductivity

in order to compare with results in cuprates. Finally, in Sec. 5.6 we compute the shear viscosity to entropy density ratio including different sources of momentum relaxation.

Next we introduce the BD action, the equations of motion and its analytical solution.

5.2 dc Conductivity in translationally invariant BD holography

We start our analysis by introducing the BD action and the equations of motion (EOM). We then compute the conductivity for a general background ansatz and show it is expressed in terms of thermodynamic quantities and the value of the scalar at the horizon. This is different from EMd models with no coupling between the dilaton and the Maxwell field where it only depends on thermodynamic quantities.

We then find that a calculation in the Einstein frame, resulting from a conformal transformation, leads to the same result. Finally, we discuss other modified gravity models that fall within the BD universality class.

5.2.1 Brans-Dicke Action and equations of motion

The Brans-Dicke-Maxwell action in a $d+1$-dimensional manifold and in units where $2\kappa^2 = 16\pi G_N = 1$ is given by

$$S = \int_{\mathcal{M}} \mathrm{d}^{d+1}x\sqrt{-g}\left[\phi R - \frac{\xi}{\phi}(\nabla\phi)^2 - V(\phi) - \frac{Y(\phi)}{4}F^2\right] . \tag{5.1}$$

We have included a non-trivial coupling $Y(\phi)$ between the Brans-Dicke scalar ϕ and the Maxwell term, as well as a (for now arbitrary) scalar potential $V(\phi)$. In this model gravity is not only mediated by the massless symmetric rank two tensor g but also by the real scalar field which has its own dynamics and a kinetic term parametrized by $\xi \geq 0$[1]. Intuitively the non-minimal coupling ϕR can be interpreted as the running of Newton's constant "$G(x) \equiv G_N/\phi(x)$" [315].

Variation of this action gives the following EOMs:

$$\begin{aligned}\phi G_{ab} = {}& \frac{\xi}{\phi}\left(\nabla_a\phi\nabla_b\phi - \frac{1}{2}(\nabla\phi)^2\ g_{ab}\right) - \frac{1}{2}V(\phi) - \frac{Y(\phi)}{2}\left(F_{ac}F^c_{\ b} + \frac{1}{4}F^2\ g_{ab}\right)\\ &+ \nabla_a\nabla_b\phi - \Box\phi\ g_{ab}\,, \end{aligned}\tag{5.2}$$

$$\partial_a\left(\sqrt{-g}Y(\phi)F^{ab}\right) = 0\,, \tag{5.3}$$

$$\Box\phi = \frac{1}{2(d-1)\xi + 2d}\left[(d-1)\phi V'(\phi) - (d+1)V(\phi) - \frac{(d-3)}{4}F^2 - \frac{Y'(\phi)}{4}\phi F^2\right] . \tag{5.4}$$

[1]The standard notation in the literature for the Brans-Dicke coupling is ω. We refrain from this notation to avoid confusion with the frequency ω in the optical conductivity $\sigma(\omega)$.

Note the 'extra terms' in the second line of eq. (5.2): $(\nabla_a\nabla_b\phi - \Box\phi\, g_{ab})$ which are absent in Einstein gravity; in appendix B.1 we derive the EOMs using the variational principle.

An important observation is that for $Y = 1$ and $d = 3$ the Maxwell term in the scalar equation vanishes. This is a consequence of the fact that in $d = 3$ the electromagnetic energy-momentum tensor is conformal and therefore traceless, and do not source the Ricci scalar. This invariance will play later a crucial role in our analysis.

5.2.2 dc Conductivity for a General Ansatz

The calculation of the Drude weight of Sec. 4.2 also allows to obtain the regulat part of the dc conductivity. As mentioned in Chapter 4 this calculation had been presented before in [122, 266, 128]. Since we have revisited only the calculation of the Drude weight, in this section we show the key steps to compute the regular part of the dc conductivity in a BD background. At this point it is useful to summarize the calculation done in Sec. 4.2. Namely, using two radially conserved quantities it is possible to find a particular solution to the second order differential equation of the gauge field perturbation $\delta A_x = a_x(r,t)$ at zero frequency. Moreover, imposing appropriate boundary conditions and using the Wronskian method allows to solve for the second independent solution a_x. Finally, the regular part of the dc conductivity follows from the value of a_x at the horizon. We now sketch this computation more precisely.

Background and conserved charges

Here we obtain the radially conserved quantities using the equations of motion of the background. Consider the following static and spherically symmetric ansatz for the field equations,

$$\mathrm{d}s^2 = -A(r)\mathrm{d}t^2 + B(r)\mathrm{d}r^2 + C(r)\delta_{ij}\mathrm{d}x^i\mathrm{d}x^j, \tag{5.5}$$

$$A = a_t(r)\mathrm{d}t, \tag{5.6}$$

$$\phi = \phi(r). \tag{5.7}$$

We assume this chart is globally defined and describes an asymptotically AdS_{d+1} black hole. We require that $A(r) = B(r)^{-1} = C(r) = r^2$ as $r \to \infty$ (asymptotic boundary) and that $A(r) \sim B(r)^{-1} \sim 4\pi T(r - r_0)$ for $r_0 > 0$. Moreover, we impose $Y(\infty) = 1$, $\phi(\infty) \neq 0$[2] and $V(\phi) \sim 2\Lambda\phi$ close to the boundary and, at the horizon $r = r_0$ we impose regularity on ϕ, Y and V together with $a_t(r_0) = 0$.

[2]Without loss of generality we set $\lim_{r\to\infty}\phi(r) \equiv 1$.

The first radially conserved charge is the charge density, that can be obtained by looking at the (t) component of Maxwell's equations,

$$\partial_a\left(\sqrt{-g}Y(\phi)F^{at}\right)=\partial_r\left(\sqrt{-g}Y(\phi)g^{rr}g^{tt}a_t'\right)=0\implies\rho=\frac{YC^{\frac{d-1}{2}}}{\sqrt{AB}}a_t'\,, \tag{5.8}$$

The second conserved quantity is related to the geometry. Using the (tt) and the (xx) components of the Brans-Dicke equations and assuming $\partial_t\phi=\partial_x\phi=0$ it follows directly [312]

$$\phi\left(R^t{}_t-R^x{}_x\right)=-\frac{Y}{2}F_{rt}F^{rt}+\nabla^t\nabla_t\phi-\nabla^x\nabla_x\phi\,. \tag{5.9}$$

Using useful identities for $R^t{}_t$ and $R^x{}_x$ [266], and simplifying the covariant derivative terms of the previous equation as follows

$$\begin{aligned}&\sqrt{-g}(R^t{}_t-R^x{}_x)=-\frac{1}{2}\partial_r\left[\frac{1}{\sqrt{AB}}C^{\frac{d+1}{2}}\left(\frac{A}{C}\right)'\right]\,,\\&\nabla^t\nabla_t\phi-\nabla^x\nabla_x\phi=g^{tt}\nabla_t\nabla_t\phi-g^{xx}\nabla_x\nabla_x\phi=\frac{1}{2B}\left(\frac{A'}{A}-\frac{C'}{C}\right)\phi'=\frac{C}{2BA}\left(\frac{A}{C}\right)'\phi'\,,\end{aligned}$$

allows to rewrite eq. (5.9) as a total derivative

$$\partial_r\left(\frac{\phi}{\sqrt{AB}}C^{\frac{d+1}{2}}\left(\frac{A}{C}\right)'-\rho a_t\right)=0\,. \tag{5.10}$$

We have also used the first radially conserved quantity of eq. (5.8).

In previous works, the conserved charge of eq. (5.10) has been related to thermodynamical quantities [122, 266, 128]. Indeed, by integrating it, evaluating it at the horizon and using the boundary condition $a_t(r_0)=0$ it reduces to

$$\frac{\phi}{\sqrt{AB}}C^{\frac{d+1}{2}}\left(\frac{A}{C}\right)'\Big|_{r=r_0}=\frac{\phi(r_0)}{\sqrt{AB}}C(r_0)^{\frac{d-1}{2}}A'(r_0)=sT\,,$$

where we use the fact that the entropy in BD theory satisfies

$$S=\frac{1}{4}\int_{r=r_0}\mathrm{d}^dx\;\phi\sqrt{-g}$$

instead of the standard area law. This is another simple manifestation that the strength of gravity in BD backgrounds is not constant, as in Einstein gravity, but governed by the scalar "G/ϕ"[3] [315].

[3]Note that in standard units the area law is $S=\frac{1}{4G}\int_{r=r_0}\mathrm{d}^dx\sqrt{-g}$

Fluctuations

In order to compute conductivities, we need to study fluctuations around the background solutions. It is sufficient to consider the following set of consistent fluctuations

$$\mathrm{d}s^2 \to \mathrm{d}s^2 + 2h_{tx}(t,r)\mathrm{d}t\mathrm{d}x \ , \qquad\qquad A \to A + a_x(t,r)\mathrm{d}x \ .$$

The calculation of the dc conductivity and Drude weight in EMd backgrounds [122, 266, 128], which we revisited in Sec. 4.2 for the Drude weight, follows through similarly in the BD background. Therefore, here we only point out the key steps while the full details can be found in [312]. The EOM for a_x, obtained by linearizing the (x) component of Maxwell's equations, is

$$\frac{\phi\, C^{\frac{d+1}{2}}}{\sqrt{AB}}\partial_r\left(\sqrt{\frac{A}{B}}C^{\frac{d-3}{2}}Y\partial_r a_x\right) - \sqrt{\frac{B}{A}}C^{\frac{d-3}{2}}Y\partial_t^2 a_x - \rho^2 a_x = 0 \ .$$

Since we are interested in the dc conductivity we can set $\partial_t a_x = 0$. Furthermore, using the conserved charge (5.10) the equation above is rewritten as

$$\partial_r\left(\frac{C^{d-1}Y\phi}{B}\left(\frac{A}{C}\right)'\partial_r a_x - \frac{A}{C}\rho^2 a_x\right) = 0\,, \tag{5.11}$$

which can be integrated to obtain a solution: $a_x^{(0)}(r)$. Before we write it explicitly, we must fix boundary conditions for eq. (5.11). As explained in Sec. 4.2, the correct boundary conditions on the gauge field perturbation are ingoing at the horizon, see eq. (4.6), while we impose $a_x(r\to\infty)\to 1$ as the second boundary. These boundary conditions fix the general solution of a_x, given in eqs. (4.7) and (4.8), which we repeat for clarity,

$$a_x = a_x^{(0)} + C_2 i\omega a_x^{(1)}(r)\,, \quad a_x^{(0)}(r) = \frac{a_t(r)\rho + sT}{\epsilon + P}\,. \tag{5.12}$$

We see the general solution above is a linear combination of $a_x^{(0)}$ and a solution obtained by the Wronskian method $a_x^{(1)}$; for the derivation it is only necessary to know $a_x^{(1)}(r\to\infty)\sim 1/r^{d-2}$, for the explicit expression see [128]. Moreover, the ingoing boundary conditions fix the coefficient of the linear combination $C_2 = Y(r_0)\left(a_x^{(0)}(r_0)\right)^2 C(r_0)^{\frac{d-3}{2}}$, see Sec. 4.2. Finally, the regular part of the dc conductivity follows directly

$$\begin{aligned}\sigma =& \operatorname{Re}\lim_{\omega\to 0}-\frac{1}{i\omega}\lim_{r\to\infty}Y(r)\sqrt{-g}g^{xx}g^{rr}a_x' a_x = C(r_0)^{\frac{d-3}{2}}\left(a_x^{(0)}(r_0)\right)^2 = \\ =& Y(r_0)C(r_0)^{\frac{d-3}{2}}\left(\frac{sT}{\epsilon+P}\right)^2 .\end{aligned}$$

Where in the last equality we obtained $a_x^{(0)}(r_0)$ from eq. (5.12). This result is the same as the one obtained in EMd models [122, 266, 128]. It is interesting to observe that in these works $T_t^t = T_x^x$ is given as a necessary condition for the universality of the dc conductivity. Here this condition is violated, but we can still write the equation for the fluctuation as a total derivative. Even though the result looks as in EMd models, taking into account the modified area law for the entropy density,

$$\sigma = \frac{Y(r_0)}{\phi(r_0)^{\frac{d-3}{d-1}}} \left(\frac{s}{4\pi}\right)^{\frac{d-3}{d-1}} \left(\frac{sT}{\epsilon + P}\right)^2 , \tag{5.13}$$

which depends explicitly on the BD field ϕ. For $d > 3$, we thus expect the scalar field to renormalize the universal result of the regular part of the dc conductivity.[4]

One can interpret this behaviour in a heuristic way. First note that Newton's constant G is related to the string coupling constant $g_s \sim G$. If we naively interpret the BD coupling "G/ϕ" as a dynamical Newton's constant, the flow of ϕ can be interpret as a flow from weaker ($\phi \gg 1$) to stronger ($\phi \ll 1$) coupling. More specifically, for the background of [317] $\phi \in [0, \phi(r_0)]$ with $0 < \phi(r_0) \leq 1$. Therefore the running of ϕ from the boundary to the horizon corresponds in the dual field theory to a flow from weaker to stronger coupling. For the purpose of the conductivity, this running has the effect of increasing σ by a factor $\phi(r_0)^{-\frac{d-3}{d-1}}$. Although tempting, one needs to be cautious with this heuristic interpretation. In the saddle point approximation, exact only in $N \to \infty$ limit, we always have $g_s \ll 1$ and $\lambda = 4\pi g_s N \gg 1$. Thus this interpretation should not be taken seriously in the limit of fixed large N and $\phi(r_0) \to 0$, where the saddle point is clearly not valid.[5]

Conformal transformations and Universality

The explicit result for the conductivity (5.13) is also expected from a well known trick broadly used in the Brans-Dicke literature that we now discuss (see for example [320] and references within).

Consider the following conformal mapping of the metric g,

$$\bar{g} = \phi^{\frac{2}{d-1}} g \ .$$

Taking into account the transformation of the volume element and the Ricci scalar, the action reads

$$\bar{S} = \int_{\mathcal{M}} \mathrm{d}^{d+1}x\sqrt{-g} \left[\bar{R} - \frac{4}{d-1}(\bar{\nabla}\bar{\phi})^2 - \bar{V}(\bar{\phi}) - \frac{\bar{Y}(\bar{\phi})}{4}\bar{F}^2\right] , \tag{5.14}$$

[4] The Drude weight on the other hand agrees with the universal result $K = \frac{\rho^2}{\epsilon+P}$. Based on the results of Chapter 4 it is likely the Mazur-Suzuki bound is also saturated in this model, though we have not checked this explicitly.

[5] For this reason we employ the term 'weaker' instead of 'weak'.

where

$$\bar{\phi} = \frac{d-3}{4\alpha}\log\phi\,, \qquad \bar{V}(\bar{\phi}) = \phi^{-\frac{d+1}{d-1}}V(\phi)\,, \qquad \bar{Y}(\bar{\phi}) = Y(\bar{\phi})e^{-\frac{4\alpha\bar{\phi}}{d-1}}\,, \tag{5.15}$$
$$\alpha = \frac{d-3}{2\sqrt{(d-1)\xi+d}}\,,$$

and all barred $\bar{.}$ quantities are computed with respect to the metric $\bar{g}$. Note that for $d=3$ the Maxwell coupling is not affected by the conformal mapping, which is a consequence of electromagnetism being conformal in $d=3$. It is also useful to note that $\bar{\phi}$ is well defined for $d=3$ since α has a factor $d-3$ as well.

The action of eq. (5.14) is nothing but the familiar Einstein-Maxwell-dilaton action used in Chapter 5. Since solutions of EMd theories are well known [321, 317, 94, 127], this map provides a useful way of constructing solutions to BD gravity. Moreover, the universal result of the regular part of the dc conductivity in EMd theories (in the notation of eq. (5.14)) is [122, 266, 128]

$$\bar{\sigma} = \bar{Y}(r_0)\left(\frac{\bar{s}}{4\pi}\right)^{\frac{d-3}{d-1}}\left(\frac{\bar{s}\bar{T}}{\bar{\epsilon}+\bar{P}}\right)^2.$$

It is not hard to check that the thermodynamic quantities $(\bar{s},\bar{T},\bar{\epsilon},\bar{P})$ are invariant under the conformal mapping [6]. The only part of the dc conductivity that is not invariant is the non-universal charge coupling $\bar{Y}$, which according to eq. (5.15) transforms as $\bar{Y}(\bar{\phi}) = \phi^{-\frac{d-3}{d-1}}Y(\phi)$, and thus we recover the explicit result of eq. (5.13).

This raises the interesting question of whether there are other theories of modified gravity that can be cast as an EMd theory in the Einstein frame, and if so, which those theories are. Indeed, this question has been much discussed in the gravity literature [322–324]. Moreover, it is known [325] that a combination of a conformal transformation and a Legendre transform can be used in more general theories of gravity like $f(R)$, Palatini gravity or $f(\phi)$ couplings to the Ricci, to considerably simplify calculations. In particular, it is easy to see [312] how the the regular part of the dc conductivity in a BD background, given in eq. (5.13), is modified in $f(R)$ theory; the result is simple: the term $\phi(r_0)$ in eq. (5.13) is replaced by $f'(R(r_0))$ [312].

A full discussion of the questions regarding the equivalence of such theories of gravity is beyond the scope of this thesis, see [325] for more details. Here we limit our discussion to the fact that theories that can be mapped to EMd will result in similar phenomenology from the point of view of holography. Indeed, in order to use holography to probe strongly coupled theories, it is important to compute the energy-momentum tensor in the Einstein frame.

[6] This is essentially a consequence of the regularity of ϕ at the horizon.

Of course, using conformal and Legendre transformations does not simplify the problem in general; for example, it is tempting to use this construction in theories of gravity such as Gauss-Bonnet, which in holography effectively correspond to leading $1/N$ corrections in the dual field theory. However, Gauss-Bonnet contain terms such as $R_{ab}R^{ab}$ which introduce further non-linearity and thus makes difficult the Legendre transformation [324]. Therefore Gauss-Bonnet gravity does not fall under BD universality.

A natural question to ask is what happens with other transport coefficients. For example, both the shear viscosity and the entropy contain the same power of G, and therefore η/s does not depend on G. As a consequence, we expect $\eta/s = 1/4\pi$ in BD holography to saturate the KSS bound. This is just a particular example of a general result that any theory related to standard gravity via a conformal transformation indeed saturates the KSS bound [326, 327]. However, quantities such as the entanglement entropy should be sensitive to ϕ in the expected way ($G \to G\phi^{-1}$). Indeed, this was explicitly calculated in the context of $f(R)$ theories, and agrees with our discussion since $\phi = f'(R)$ [328–330].

Let us now focus on Brans-Dicke-inspired models which include momentum dissipation in the dual theory and study its transport properties.

5.3 Momentum relaxation and dc conductivity in BD holography

We now study the effect of momentum relaxation in the transport properties of the field theory dual of BD gravity. We consider the linear coupling to the Ricci scalar to be a function of the gradient of axion fields that explicitely break diffeomorphism invariance in the boundary spacelike coordinates:

$$S = \int \mathrm{d}^{d+1}x\sqrt{-g}\left[Z(TrX)R - 2\Lambda - V(TrX) - \frac{Y(TrX)}{4}F^2\right] , \tag{5.16}$$

where $TrX = \frac{1}{d-1}\sum_I \nabla_\mu X^I \nabla^\mu X^I$ and $X^I = \alpha x^I$. We use the metric ansatz of eq. (5.5) with $A = g$, $B = 1/g$ and $C = r^2 c$:

$$\mathrm{d}s^2 = -g(r)\mathrm{d}t^2 + \frac{\mathrm{d}r^2}{g(r)} + r^2 c(r)\delta_{ij}dx^i dx^j , \quad i = 1, \ldots, d-1 , \quad r \in [r_0, \infty) . \tag{5.17}$$

Assuming that $g \to r^2$ and $c \to 1$ for large r and g has a (double) single zero at (zero) finite temperature, that defines the horizon, we follow the procedure devised by Donos and Gauntlett [141] to compute the dc conductivity from the solution of the EOM's at the horizon.

We add a perturbation in A_x linear in time, while the axion and metric perturbations are independent of time,

$$A \to A+(a_x(r)-Et)\mathrm{d}x, \quad X^x \to X^x+\chi(r), \quad \mathrm{d}s^2 \to \mathrm{d}s^2+2r^2h_{tx}(r)\mathrm{d}t\mathrm{d}x+2r^2h_{rx}(r)\mathrm{d}r\mathrm{d}x \ .$$

Maxwell's equation for a_x is:

$$\partial_r \left[Y\sqrt{-g}g^{rr}(g^{tx}F_{rt}+g^{xx}F_{rx})\right] = 0 \ , \tag{5.18}$$

which leads to the radially conserved quantity:

$$J = -Yr^{d-3}c^{\frac{d-3}{2}}ga_x' - h_{tx}\frac{\rho}{c} \ . \tag{5.19}$$

This conserved quantity is evaluated at the horizon where h_{tx} and a_x are obtained as we discuss below.

The perturbation on the gauge field close to the horizon is obtained from eq. (5.19) by choosing J such that a_x is ingoing in the horizon:

$$a_x' \sim -\frac{E}{g} \implies a_x \sim -Ev \ , \tag{5.20}$$

where v is the ingoing Eddington-Finkelstein coordinate $v = t + r_*$, given in terms of the tortoise coordinate $dr_* = \frac{dr}{g}$.

Eq. (5.20) gives the first term inside the parenthesis of eq. (5.19). To obtain the second term, we combine the (xt) and (xx) Einstein's equations. Since we will evaluate them at the horizon, we will only write down explicitly the non-zero terms after taking the limit $r \to r_0$.

For clarity we write down Einstein's equations only for $d = 3$:

$$\begin{aligned}
ZG_{ab} &= \frac{1}{2}T_{ab} + \frac{1}{2}\mathcal{Z}_{ab} \ , \\
T_{ab} &= Y\left(F_a^cF_{bc} - \frac{1}{4}g_{ab}F^2\right) - (2\Lambda+V)g_{ab} + \sum_I \nabla_a X^I \nabla_b X^I \left(-\dot{V} - \frac{\dot{Y}}{4}F^2 + \dot{Z}R\right) \ , \\
\mathcal{Z}_{ab} &= 2(\nabla_a\nabla_b - g_{ab}\nabla_c\nabla^c)Z \ ,
\end{aligned} \tag{5.21}$$

where the dot derivative stands for derivative with respect to $TrX = \frac{1}{2}g^{ab}\sum_I \partial_a X^I \partial_b X^I$ and R is the Ricci scalar.[7]

[7]The full dynamical stability of the model eq. (13) is beyond the scope of this thesis. Third order time derivatives occur beyond the linear analysis and have the potential to further restrict the parameters for which the model is stable.

The (tx) Einstein's equation is,

$$\mathcal{O}(h'_{tx}, h''_{tx}) + \frac{r^2}{2} Z h_{tx} r^2 \left[g'' + g' \left(\frac{2}{c} + \frac{c'}{c} \right) + \dots \right] =$$
$$\frac{r^2}{4} h_{tx} \left(-4\Lambda - 2V + Y a_t'^2 \right) + \frac{1}{2} g Y a_t a'_x + \frac{1}{2} r^2 g \dot{Z} Tr X' h'_{tx} - \frac{r h_{tx}}{2c} \left[2rcg' \dot{Z} Tr X' + \dots \right] , \tag{5.22}$$

where the dots and the terms $\mathcal{O}(h'_{tx}, h''_{tx})$ are zero at the horizon, the prime derivative is with respect to r and $TrX' = \partial_r TrX$. The first two terms on the right-hand side come from T_{ab} and the last term from $\mathcal{Z}_{ab}$. In order to simplify eq. (5.22) we eliminate $c''(r)$ from the (tt) Einstein's equation and substitute it into the (xx) Einstein's equation. The result is given in eq. (5.23) by specifying G_{xx}, T_{xx} and $\mathcal{Z}_{xx}$ separately,

$$\begin{aligned}
Z G_{xx} &= \frac{r^2 c}{2} Z g'' + \frac{r^2 Z}{4} \left(\frac{c'}{c} + \frac{2}{r} \right) g' + \frac{r^4 Z}{8} \frac{4\Lambda + 2V + Y a_t'^2}{k^2 \dot{Z} - r^2 c Z} + \dots , \\
\mathcal{Z}_{xx} &= \frac{\alpha^2 \dot{Z} g'}{2} \left(\frac{c'}{c} + \frac{2}{r} \right) + \frac{\alpha^2 r^2 c \dot{Z}}{4} \frac{4\Lambda + 2V + Y a_t'^2}{\alpha^2 \dot{Z} - r^2 c Z} + \dots , \\
\frac{1}{2} T_{xx} &= \frac{\alpha^2 \dot{Z}}{2} g'' + \frac{\alpha^2 \dot{Z}}{2} \left(\frac{c'}{c} + \frac{2}{r} \right) g' + \frac{r^2 Z}{4} \frac{r^2 c (4\Lambda + 2V - Y a_t'^2) + \alpha^2 (-2\dot{V} + \dot{Y} a_t'^2)}{\alpha^2 \dot{Z} - r^2 c Z} \\
&\quad + \frac{\dot{Z}}{4} \frac{2\alpha^2 \dot{V} + (2\alpha^2 r^2 c Y - \alpha^4 \dot{Y}) a_t'^2}{\alpha^2 \dot{Z} - r^2 c Z} + \dots ,
\end{aligned} \tag{5.23}$$

where the dots vanish at the horizon. Combining eqs. (5.23) and (5.22) allows to eliminate h_{tx}. Its value at the horizon $r = r_0$, is used to calculate the dc-conductivity from $\mathrm{Re}(\sigma_{\mathrm{dc}}) = J/E$. Before we do so, we define the expansions of the metric functions g and c close to the horizon as:

$$g \sim g_1 \left(1 - \frac{r_0}{r} \right) + \dots , \; c \sim c_0 + c_1 \left(1 - \frac{r_0}{r} \right) + \dots . \tag{5.24}$$

Restoring arbitrary bulk dimensionality $d+1$, the temperature is

$$T = \frac{1}{4\pi} \frac{c_0 r_0}{2c_0 + c_1} \frac{4\Lambda + 2V(r_0) + Y(r_0) a'_t(r_0)^2}{\frac{2\alpha^2 \dot{Z}(r_0)}{r_0^2 c_0} - (d-1) Z(r_0)} , \tag{5.25}$$

where we have used $TrX = \frac{\alpha^2}{r^2 c}$ to simplify the denominator. The dc-conductivity, obtained from eqs. (5.19), (5.20) and the value of h_{tx} at the horizon, calculated as indicated previously, are given by the following compact expression,

$$\mathrm{Re}(\sigma_{\mathrm{dc}}) = Y_0 r_0^{d-3} c_0^{\frac{d-3}{2}} + \frac{\rho^2}{m_{eff}^2} , m_{eff}^2 = 2 c_0^{\frac{d-1}{2}} r_0^{d-1} \left(T\mathcal{A} + Z_0^2 \mathcal{B} + \dot{Z}_0 \mathcal{C} \right) \tag{5.26}$$

where T is the temperature eq. (5.25) and $\mathcal{A}$, $\mathcal{B}$ and $\mathcal{C}$ are given in eq. (5.27). The term $a_t' = \frac{\rho}{Y(r)r^{d-1}c(r)^{\frac{d-1}{2}}}$ is also evaluated at the horizon. The subscripts $'0'$ in eqs. (5.26) and (5.27) indicate the variable is evaluated at the horizon.

Eq. (5.26) suggests that even at zero temperature the conductivity receives a correction given by the $\dot{Z}_0^2\mathcal{C}$ term. We note that although this is a fully analytical expression for the conductivity the metric at the horizon may only be computed numerically.

$$\begin{aligned}
\mathcal{A} &= \frac{4\pi(2c_0+c_1)}{r_0^3c_0^3}\frac{\frac{(d-1)(d-2)}{4}r_0^4c_0^2Z_0^2-(d-2)\alpha^2r_0^2c_0Z_0\dot{Z}_0+2\alpha^4\dot{Z}_0^2}{(d-1)Z_0-\frac{2\alpha^2\dot{Z}_0}{r_0^2c_0}}\,,\\
\mathcal{B} &= \frac{(d-1)c_0}{4\left[(d-1)Z_0-\frac{2\alpha^2\dot{Z}_0}{r_0^2c_0}\right]^2}\left[(d-2)r_0^2c_0\big(4\Lambda+2V_0+Y_0a_t'^2\big)+2\alpha^2\big(2\dot{V}_0-\dot{Y}_0a_t'^2\big)\right]\,,\\
\mathcal{C} &= \frac{\alpha^2}{r_0^2c_0^2\left[(d-1)Z_0-\frac{2\alpha^2\dot{Z}_0}{r_0^2c_0}\right]^2}\Big\{\alpha^2\dot{Z}_0\big(4\Lambda+2V_0-Y_0a_t'^2\big)-\\
&\qquad Z_0\Big[\frac{d-1}{2}r_0^2c_0\big(12\Lambda+6V_0+Y_0a_t'^2\big)+\alpha^2\big(2\dot{V}_0-\dot{Y}_0a_t'^2\big)\Big]\Big\}\,.
\end{aligned} \tag{5.27}$$

5.3.1 'Insulating' behavior induced by charge screening

Our result for the dc conductivity generalizes those obtained previously from the AdS RN+axions background ($Z=1$, $Y=1$ $V=TrX$) [139], and from the backgrounds studied in [143, 144] with $Z=1$, $Y=e^{-\kappa TrX}$ $V=TrX$, $\kappa>0$. In these models the Ricci scalar is not coupled directly to the axion. However, the axion-dependent coupling Y has a crucial role in the dc conductivity. For a fixed charge density ρ and axion parameter α it has been observed an *insulating* behavior [143, 144]. More specifically, for sufficiently large κ and α, and for low temperature, the dc conductivity increases with temperature as expected in an insulator. We note however that the physical reason for this behavior is not a smaller scattering time but the simple fact that Y screens the charge at low temperature and consequently reduces the conductivity which is proportional to the charge.

While the overall temperature dependence is similar to that expected in an insulator, it should be noted that it is not related to a shorter scattering time. The scattering time, controlled by the parameter α, in this model has the same temperature dependence than in RN+axions background for which no insulating behaviour was observed. In order to claim a true insulating behavior, it would be necessary to tune the temperature dependence of the scattering time while keeping charge screening effects negligible in the low temperature limit. In the following sections we identify a region of parameters in BD holography where we have found insulating behavior with these features.

5.3.2 The dc conductivity in BD axion backgrounds

In this section we explore the effect of the BD-type coupling Z on the background and on the dc conductivity in $d = 3$ boundary dimensions. More specifically, we break translational invariance by using an axion-dependent BD coupling $Z(TrX)$. First we consider the simpler case $V = TrX = \frac{1}{d-1}\sum_I \nabla_\mu X^I \nabla^\mu X^I = 0$ in eq. (5.16) and later study a more general BD-like model where $V = TrX \neq 0$ is also present. Initially we restrict our analysis to two space dimension. The dependence on dimensionality of our results is discussed in the last part of the section.

We note physically $Z(TrX)$ is an axion-dependent gravitational coupling constant that runs from the boundary to the horizon. For that reason we will refer to these axions coupled to the Ricci tensor as gravitational axions. The qualitative effect of this running in the holographic dimension, from weak to strong coupling, is less obvious than for $Y \neq 1$ or in the translational invariant case.

Momentum relaxation with $Z \neq 1$, $Y = 1$ and $V = 0$

We start our analysis with the simpler case of no axion potential and trivial coupling to the Maxwell tensor,

$$\begin{aligned} &Z = e^{\lambda TrX} \ , \quad \dot{Z} = \lambda Z \ , \quad TrX = \frac{\alpha^2}{r^2 c} \ , \\ &V = 0 \ , \qquad \dot{V} = 0 \ , \\ &Y = 1 \ , \qquad \dot{Y} = 0 \ , \end{aligned} \tag{5.28}$$

Although, *a priori*, λ and α are independent parameters, it is easy to see from eq. (5.28) that these parameters appear only in Z as a single parameter $\lambda_{eff} = \lambda\alpha^2$. Translational symmetry is broken for both $\lambda_{eff} > 0$ and $\lambda_{eff} < 0$. In the first case $c(r_0) < 1$ while in the second $c(r_0) > 1$. However, for $\lambda < 0$ the squared 'effective mass' m^2_{eff} in eq. (5.26) is negative. Therefore, λ_{eff} should be constrained to positive values.[8]

At high temperature, the background tends to AdS RN+axions [139] ($Z = 1$, $Y = 1$, $V = TrX$): it has a similar blackening factor and $c \to 1$ for all r. The effect of the coupling Z in the background is more evident at low temperatures where $c(r)$ has a stronger dependence on the radial dimension.

Regarding the dc conductivity, this model has qualitatively similar properties to that of the RN+axions. For example, for the allowed range of parameters, the dc conductivity increases as the temperature decreases and $\mathrm{Re}(\sigma_{\mathrm{dc}}) > Y_0 = 1$. Moreover, it is known [139] that for RN+axions in four bulk dimensions, this condition is $\mathrm{Re}(\sigma_{\mathrm{dc}}) > r_0^{d-3}$. In the model eq. (5.28) the condition is $\mathrm{Re}(\sigma_{\mathrm{dc}}) > (r_0^2 c_0)^{\frac{d-3}{2}}$, where $c(r_0) = c_0$.

[8] As we will demonstrate later in a similar background we have observed that $\lambda < 0$ also leads to the violation of the null energy condition. Therefore, we restrict to positive λ_{eff}.

It would be interesting to compare the dc conductivity for a fixed scattering time in the model of eq. (5.28) with the well-studied AdS RN+axions model. However, it is clear that both models display similar features since the respective actions are related by a conformal transformation. As was explained in detail in Sec. 5.2.2 for the translational invariant case, under a conformal transformation, the action of eq. (5.16) can be transformed into an action with $Z = 1$. The change of the Ricci scalar under this transformation involves additional terms which depend on TrX and contain the usual kinetic term proportional to $\sum_I \nabla_\mu X^I \nabla^\mu X^I$, $X^I = \alpha x^I$.
Moreover, as mentioned in Sec. (5.2.2), in $d = 3$ dimensions electromagnetism is conformal, therefore, the conformal transformation does not change the coupling of the F^2 term in the action, see eq. (5.15). This is consistent with the fact that for the choice of couplings given in eq. (5.28), the zero temperature dc conductivity is larger than one, as in the RN+axions model [139]. In higher dimensions, however, it is expected the model specified by eq. (5.28) will yield $\mathrm{Re}(\sigma_{\mathrm{dc}}) < 1$ in some range of parameters. Indeed we will see that this is the case in Sec. 5.4.

In the next section we study a more general model with a finite potential (V) and non-trivial BD (Z) and Maxwell (Y) couplings in four bulk dimensions.

Momentum relaxation with $Z \neq 1$, $Y \neq 1$ and $V \neq 0$

Before showing the results for the dc conductivity, it is illuminating to comment the general features of the gravitational background given in eq. (5.17) for the following choice of couplings,

$$\begin{aligned} Z &= e^{\lambda TrX} \ , & \dot{Z} &= \lambda Z \ , \\ V &= TrX = \frac{\alpha^2}{r^2 c(r)} \ , & \dot{V} &= 1 \ , \\ Y &= e^{-\kappa TrX} \ , & \dot{Y} &= -\kappa Y \ , \end{aligned} \tag{5.29}$$

where $\alpha, \kappa > 0$ and λ is real. The extremal charge density is:

$$\rho_e = r_0^2 c_0 \sqrt{Y(-2\Lambda - V)} \ . \tag{5.30}$$

It is clear that ρ_e decreases as Y decreases, which for the choice of eq. (5.29) corresponds to increasing α and κ. Similarly, for smaller $c(r_0) = c_0$ the extremal charge density is smaller.

We now comment on the allowed range of the BD coupling parameter λ according to the properties of the background. Similarly to Sec. 5.3.2, $\lambda > 0$ ($Z > 1$) is allowed, in which case the g/r^2 and $c(r)$ increase monotonically towards the boundary. Contrary to the model of Sec. 5.3.2, $\lambda = 0$ is also allowed due to the presence V, which breaks

translational invariance. In this case the BD coupling is trivial $Z = 1$ and has been studied previously [143, 144].

Moreover, we also find backgrounds satisfying all boundary conditions for $\lambda < 0$ ($Z < 1$). However, in this case g/r^2 does not increase monotonically towards the boundary; there exists a point inside the bulk where the derivative of g/r^2 vanishes. This suggests the odd feature that the background displays a repulsive behavior between this point and the boundary, which may violate energy null condition.[9] In [331] the energy conditions in theories of gravity different from Einstein's gravity have been re-derived from Raychaudhury's equation and imposing gravity to be attractive. For the action given in eq. (5.16) the null energy condition reduces to[10]

$$\frac{1}{Z}(T_{ab} + \mathcal{Z}_{ab})n^a n^b \geq 0 \ , \tag{5.31}$$

for all null vectors n^a and where T_{ab} and $\mathcal{Z}_{ab}$ are defined in eq. (5.21). We have found that for $\lambda < 0$ the background violates the null energy condition eq. (5.31). This is easily seen by expressing the background eq. (5.17) in the variable $u = r_0/r$ and plugging the following null vector: $N^t = 1/\sqrt{g}$, $N^r = \sqrt{g}$, $N^i = 0$ in eq. (5.31), which reduces to

$$(T_{ab} + \mathcal{Z}_{ab})N^a N^b \propto \ddot{Z}TrX'^2 + \dot{Z}TrX'' \propto c'(u)^2 - 2c(u)c''(u) \geq 0 \ . \tag{5.32}$$

For $\lambda \geq 0$, $c''(u) \leq 0$ and the null energy condition for this null vector is satisfied, however we have observed that for any $\lambda < 0$ this condition is violated.

Regarding the metric function $c(r)$, as the temperature increases, it becomes almost independent of the holographic coordinate $c(r) \approx c(r_0) = c_0 \to 1$. The blackening function is also modified in such a way that the geometry approaches that of AdS RN+axions. In the allowed region: $\lambda \geq 0$, the horizon value of c satisfies $c_0 \leq 1$ and c_0 decreases for larger λ. We have already observed this behavior in the model of Sec. 5.3.2 ($Y = 1$ and $V = 0$). On the other hand, in the forbidden region $\lambda < 0$, $c(r_0) = c_0 > 1$ and c_0 increases for smaller λ. We note that, at low temperatures the spatial metric functions $g_{ii} = r^2 c(r)$ could, in principle, be better understood in terms of Lifshitz and hyperscaling violation anomalous exponents, similarly to EMd theories [127]. While we do not rule out the behavior of g_{ii} close to the horizon may actually be cast using various anomalous exponents, we have not been able to re-express the metric at low temperatures using a single anomalous exponent.

Finally, in this model, contrary to that of Sec. 5.3.2, λ and α are independent parameters. In the presence of $V = TrX = \frac{\alpha^2}{r_0^2 c_0}$, the parameter α appears independently of the parameter λ in the action and the equations of motion. Therefore, it is expected

[9] We thank Roberto Emparan for discussion and suggestions on this matter.

[10] The presence of an extra term $\mathcal{Z}_{ab}$ is simply a consequence that we did not compute the energy momentum tensor in the Einstein frame.

that these two cannot be relabelled into a single parameter. For more explicit results regarding the background for different choices of the parameters, see the appendix B.2.

The dc-conductivity

We depict in figures 5.1 and 5.2 the dc conductivity eq. (5.26), in two space dimensions as a function of temperature for a wide range of the BD parameter λ and the charge screening parameter κ. The effect of λ and κ is very similar: both control the strength of momentum dissipation.

In Fig. 5.1 we observe that the increase of either the charge screening or the effective gravitational coupling ($Z > 1$) yields a lower dc conductivity especially for low temperatures and sufficiently large values of $\lambda > 0, \kappa$. We note that that in this range of parameters the conductivity is below the bound only because of charge screening.

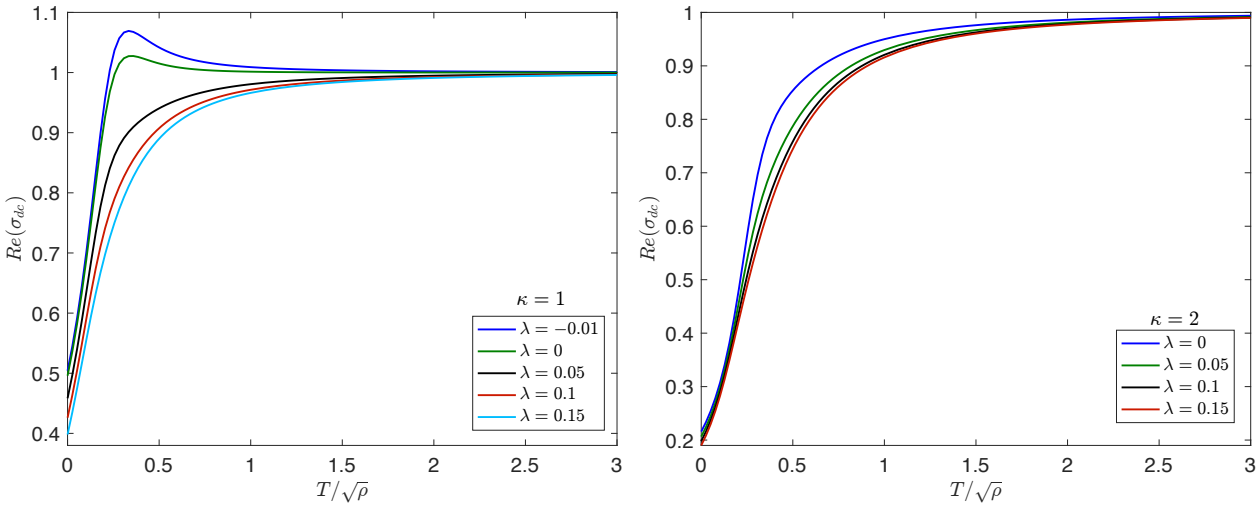

Fig. 5.1 Temperature dependence of the dc conductivity eq. (5.26) for fixed axion parameter $\alpha = 1$ and charge density $\rho = 1$. The charge screening parameter κ and the BD-coupling parameter λ are indicated in the plots. The effect of increasing λ for fixed κ is similar to increase κ for fixed λ. The case $\lambda < 0$ suggests that the effect of a weaker gravitational coupling $Z < 1$ on the dc conductivity is to weaken momentum dissipation. However, we stress this limit violates the null energy condition eq. (5.32) and should be excluded.

However, in figure 5.2 we observe that, even though the BD parameter does not appear explicitly in the Maxwell coupling Y, its effect is to *renormalize* the charge screening parameter κ through the change in the geometry. More explicitly, through the value of the metric function $c(r)$ at the horizon: c_0. This is possible even for small κ. As mentioned before, increasing λ leads to a smaller c_0 and BD coupling which manifests as stronger momentum dissipation. This is a quite interesting and unexpected feature of the model. For instance, the bound in the conductivity of [142] is violated, even for very weak charge screening $\kappa = 0.1$ provided that momentum dissipation by gravitational axions is strong enough $\lambda \geq 0.3$. Insulating features are observed that are not caused by charge screening but by the effective running of the gravitational coupling.

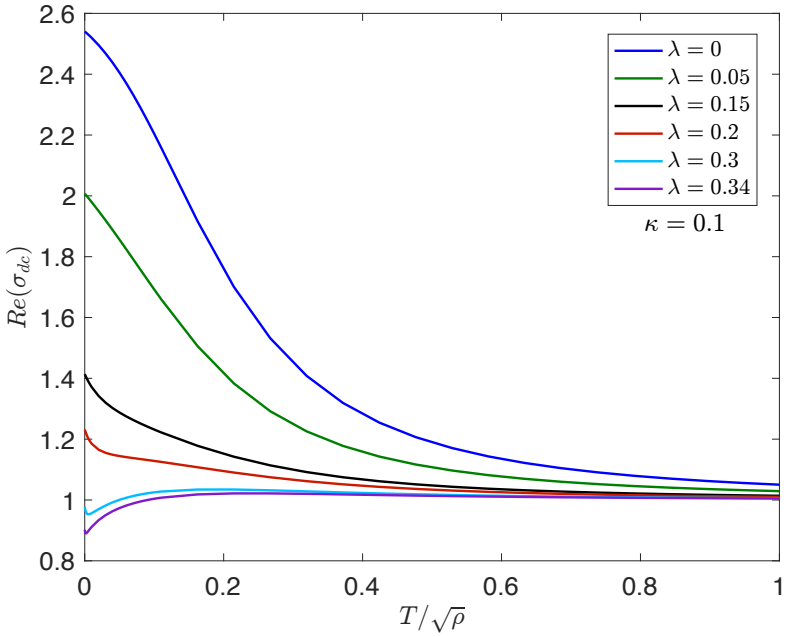

Fig. 5.2 Temperature dependence of the dc conductivity eq. (5.26) for fixed axion parameter $\alpha = 1$ and charge density $\rho = 1$. The charge screening parameter κ and the BD-coupling parameter λ are indicated in the plot. The effect of the BD parameter is similar to the charge screening parameter. Increasing λ yields a smaller $r_0^2 c_0$; as a consequence the first term in eq. (5.26): $Y_0 = \exp\left[-\kappa\alpha^2/(r_0^2 c_0)\right]$ decreases. The bound of [142] is violated for large λ even for weak charge screening.

Notice that in the left plot of figure 5.1 we have included a case in the forbidden range of the BD parameter: $\lambda < 0$, which corresponds to a BD coupling satisfying $Z < 1$ and $\dot{Z} = \partial_{TrX} Z < 0$. We have included this value only to tentatively suggest that the effect of a weaker gravitational interaction could be to effectively reduce the strength of momentum dissipation. Moreover, we have observed that the effective mass in eq. (5.26) becomes negative for some $\lambda_m < 0$, which depends on the rest of the parameters. A negative effective mass has been linked to instabilities of the theory [143]. However, we emphasize that, even for our choice of the BD coupling Z there is a region $\lambda_m < \lambda < 0$ in which the effective mass is positive but the null energy condition eq.(5.32) is violated.

5.4 BD holography in higher dimensions

So far we have restricted our analysis to $d + 1 = 4$ bulk dimensions. Here we briefly discuss the most salient features of higher dimensional backgrounds. The motivation to study $d > 3$ is to observe the explicit effect of the running of the gravitational constant associated to the extra factor $g_{xx}^{\frac{d-3}{2}} = r_0^{d-3} c_0^{\frac{d-3}{2}}$ in the first term of the conductivity eq. (5.26),

$$\mathrm{Re}(\sigma_{\mathrm{dc}}) = Y_0 r_0^{d-3} c_0^{\frac{d-3}{2}} + \dots \ . \tag{5.33}$$

The presence of this term is not exclusive to the BD model. Indeed, in EMd models where translational invariance is broken by axion fields, the same factor is present, [125]. We note however that, at least in EMd theories where the axions and the dilaton are coupled *minimally* through a dilaton-dependent coupling constant, [125, 127, 250], the metric function c is trivial, $c = 1$,[11]. Therefore, in EMd-axion theories , $c_0 = 1$.

We now discuss the two models of Secs. 5.3.2 and 5.3.2 for $d = 4, 5$ boundary spacetime dimensions. In Fig. 5.3 we plot the metric function $c(r)$ used in the ansatz eq. (5.17), in the model of eq. (5.29). In the absence of $V(TrX)$, eq. (5.28), the background has similar features.

The results, depicted in Fig. 5.3, indicate that increasing dimensionality decreases the curvature of the metric function c. This is more easily seen at low temperature (top row), where $c_0 = c(r = r_0)$ increases for $\lambda > 0$ and decreases for $\lambda < 0$. Though not shown in the figure, a similar effect is also observed in the blackening function. This is a manifestation of the large-dimensionality limit, [239, 205] where the shape of g and c is such that the gravitational effects are stronger closer to the horizon but weaker far from it.

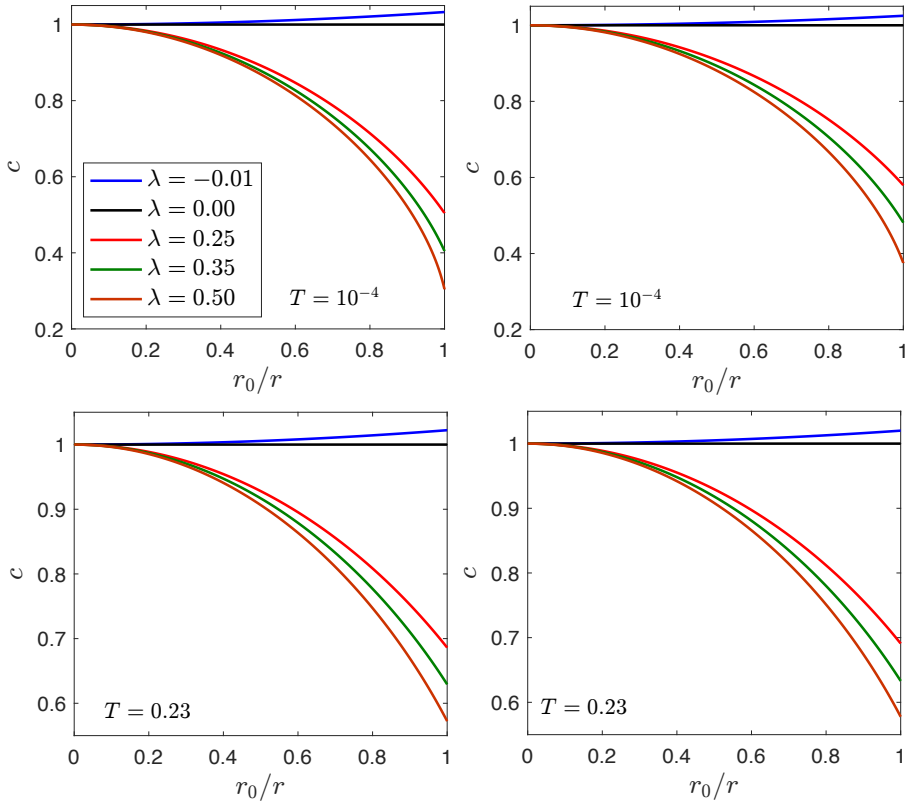

Fig. 5.3 Metric function c , eq. (5.17), in $d + 1 = 5$ (left column) and $d + 1 = 6$ (right column) bulk dimensions for the model given in eq. (5.29). The temperature is indicated in the plots and the charge density is $\rho = 1$. The charge screening parameter $\kappa = 1$ and the axion parameter $\alpha = 1$. The BD-coupling parameter λ is indicated in the legend, which refers to all figures. While the boundary conditions for $\lambda < 0$ are satisfied, this case leads to violation of the null energy condition.

[11] An additional difference in the background is that in the metric ansatz given in eq. (5.17), $g_{tt} = -1/g_{rr}$, which is not the case in a EMd plus axion theory, [127, 250].

Dimensionality effects on the dc conductivity eq. (5.33) are directly related to the dependence of c_0 and r_0 on the dimension. The quantities with tilde are in $\tilde{d}$ dimensions and those without tilde in d dimensions. If $\tilde{d} > d$, we observe that:

- For $\lambda > 0$ and low (high) temperature: $\tilde{c}_0 > (<) c_0$ and $\tilde{r}_0 < (>) r_0$.
- For $\lambda < 0$ (forbidden by the null energy condition) and low (high) temperature: $\tilde{c}_0 < (>) c_0$ and $\tilde{r}_0 > (<) r_0$.

For the temperature range studied, $\tilde{r}_0^2 \tilde{c}_0 < r_0^2 c_0$. Moreover, for low temperature $r_0^2 c_0 < 1$ but for large temperature $r_0^2 c_0 > 1$. Therefore, for low temperature one expects the suppression of the dc conductivity to be smaller for larger dimensionality.

We show in Fig. 5.4 that the term $g_{xx}^{\frac{d-3}{2}}$ in eq. (5.33) leads to a suppression of $\mathrm{Re}(\sigma_{\mathrm{dc}})$ at low temperature in three space (boundary) dimensions ($d = 4$). In order to isolate the effect of the background we couple the Maxwell field minimally by setting $Y = 1$, namely, the couplings used are those given in eq. (5.34).

$$
\begin{aligned}
Z &= e^{\lambda Tr X} \ , & \dot{Z} &= \lambda Z \ , \\
V &= Tr X = \frac{\alpha^2}{r^2 c(r)} \ , & \dot{V} &= 1 \ , \\
Y &= 1 \ , & \dot{Y} &= 0 \ .
\end{aligned}
\tag{5.34}
$$

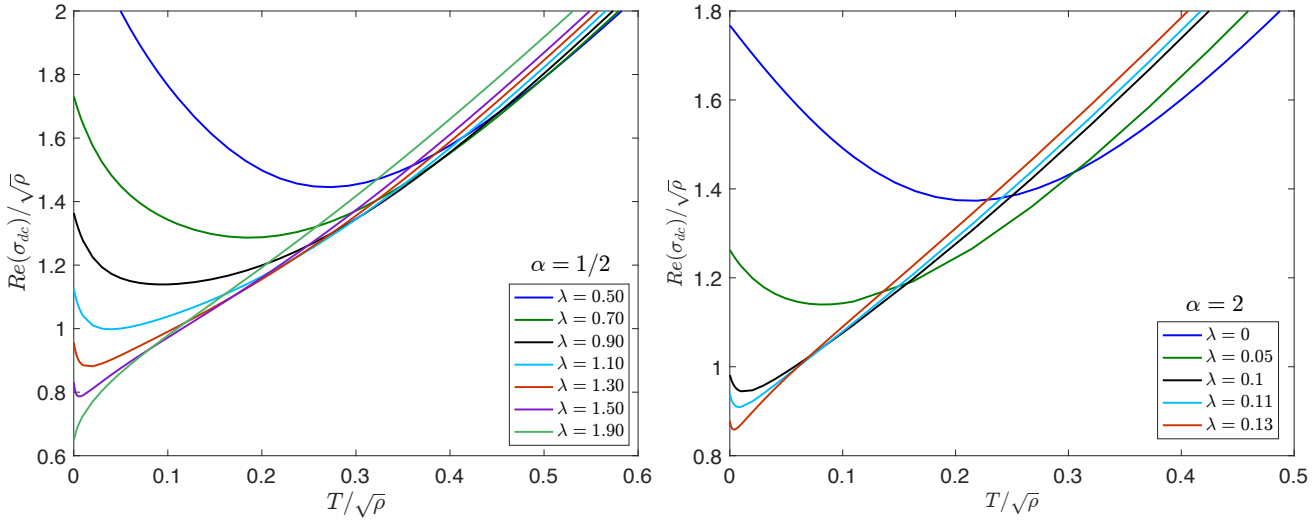

Fig. 5.4 Zero frequency conductivity eq. (5.26) in $d + 1 = 5$ bulk dimensions in a model with a minimally coupled Maxwell field, eq. (5.34). When the BD coupling λ is larger than some positive value the dc conductivity at zero temperature is below 1. This effect is due to the background rather than to an axion-dependent Maxwell coupling as in Fig. 5.1. The charge density is fixed $\rho = 1$.

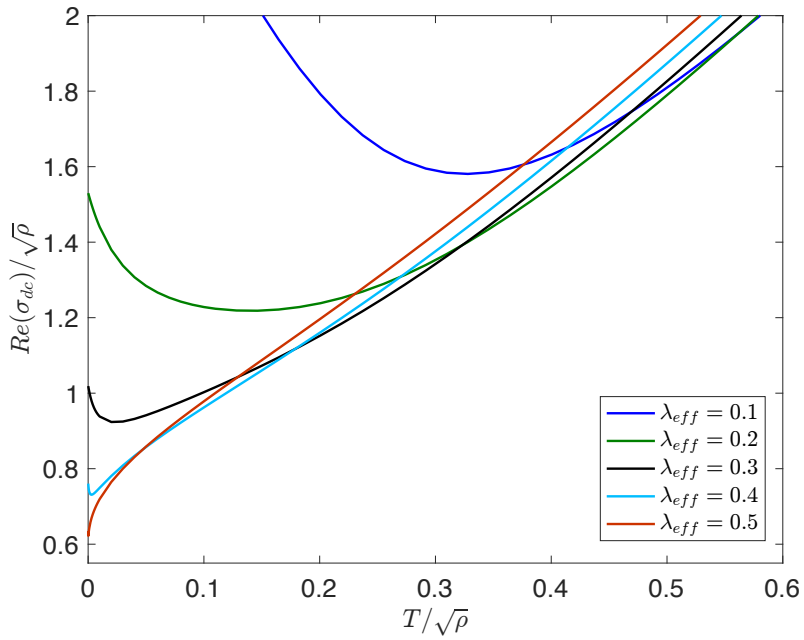

Fig. 5.5 Zero frequency conductivity eq. (5.26) in $d+1=5$ bulk dimensions in a model with a minimally coupled Maxwell field and $V(TrX)=0$, eq. (5.28). Similar behavior as in figure 5.4 is observed despite the absence of the usual kinetic term in the action ($V=0$). Again, the effective change in the gravitational interaction, through the BD coupling ZR, parametrised by $\lambda_{\text{eff}} = \alpha^2\lambda$, allows to decrease the dc conductivity despite the absence of charge screening $Y=1$. The charge density is fixed $\rho=1$.

A similar effect, depicted in Fig. (5.5), is observed even in the absence of $V(TrX)$ in the action (5.16), namely, we choose the couplings of eq. (5.28). As was explained in Sec. 5.3.2, in the absence of V, there is a single parameter that controls momentum dissipation $\lambda_{eff} = \lambda\alpha^2 > 0$. In summary, our results suggest that for higher dimensions gravitational effects, including those of the gravitational axions are suppressed except close to the horizon. As a consequence, the conductivity is closer to the RN limit for high temperature. However close to zero temperature, where gravitational effects are still important, the dc conductivity is heavily suppressed for strong momentum relaxation induced by the gravitational axion only. Therefore, also in this case, the background produces insulating like features without the need of any external source of charge screening. It would be interesting to explore whether this type of background is a genuine precursor of an insulator in the dual field theory.

5.5 Optical conductivity in BD holography with momentum relaxation

We continue our analysis of transport properties of BD holography by investigating the optical conductivity. We focus first in the low frequency scaling of the real part of the conductivity. In the low frequency limit we have found insulating like features

for strong momentum relaxation. In the second part of the section we show that BD holography, even if combined with other sources of momentum relaxation, does not reproduce the intermediate-frequency scaling of the absolute value and argument of the optical conductivity observed in cuprates.

5.5.1 Low-frequency behavior of the conductivity

In the context of massive gravity the equation for the perturbation leading to the optical conductivity at extremality has been solved analytically for low frequencies by using the method of matched asymptotic expansions [137]. In [139] it was shown that, in the previous model, the dc conductivity is equivalent to that obtained in the RN+axions model, upon a convenient identification of the parameters. Using the method of matched asymptotic expansions we have observed (not shown) that, as in massive gravity, the low-frequency behavior of the optical conductivity of the extremal RN+axions model is also linear in frequency with an always negative slope, which is consistent with Drude physics.

Although we have not been able to obtain analytical results of the low-frequency scaling for arbitrary couplings Z and Y, we observe numerically, see figure 5.6, the same linear scaling of the conductivity for small frequencies. Interestingly, provided that momentum relaxationis strong enough, the slope of this linear growth is positive, namely, the conductivity increases with the frequency. This is not exclusive of BD holography, it

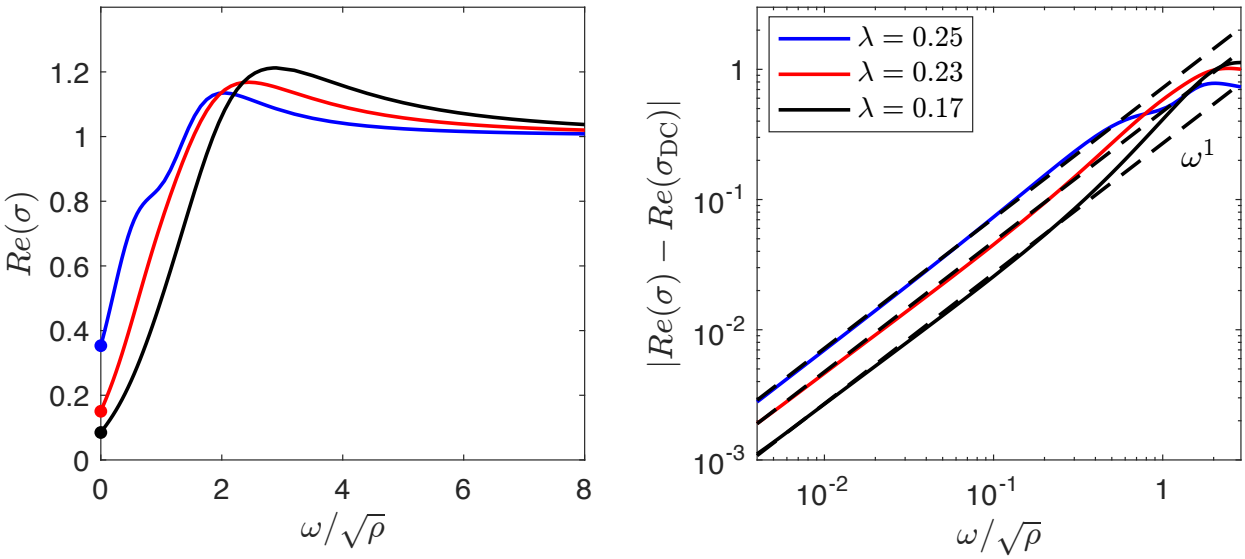

Fig. 5.6 Zero temperature [extremal background of eqs. (5.16), (5.29)] optical conductivity for strong breaking of translational symmetry. The charge screening parameter is $\kappa = 1$ and the axion parameter is $\alpha = 1$ (blue lines), $\alpha = 1.5$ (red lines) and $\alpha = 2$ (black continuous lines). The BD-coupling parameter λ, given in the legend, is fixed close to the maximum value allowed by the background boundary conditions. The extremal charge density is $\rho = 1$. The dashed black lines correspond to the linear scaling $\beta\omega$, where β is fixed from the lowest frequency point of the numerical data.

is also observed for $\lambda = 0$ in the limit of strong momentum relaxation induced by the axion coupled to the Maxwell field. This is an interesting insulator-like feature which we are not aware to have been reported in holographic systems which do not include charge screening.

At nonzero temperature, the numerical results of Fig. 5.7 show that the subleading term depends quadratically on the frequency. We conclude therefore that for the general class of models with action eq. (5.16), and for low frequency, the optical conductivity is

$$Re(\sigma) - \mathrm{Re}(\sigma_{\mathrm{dc}}) = a\omega + b\omega^2 + \dots \tag{5.35}$$

where $b \to 0$ for $T \to 0$ and, for $T \gg 0$, both constants tend to zero, but a does it faster than b. In other words, at large temperature we have observed a subleading contribution dominated by ω^2 while in the limit of zero temperature is proportional to ω^1. As was men-

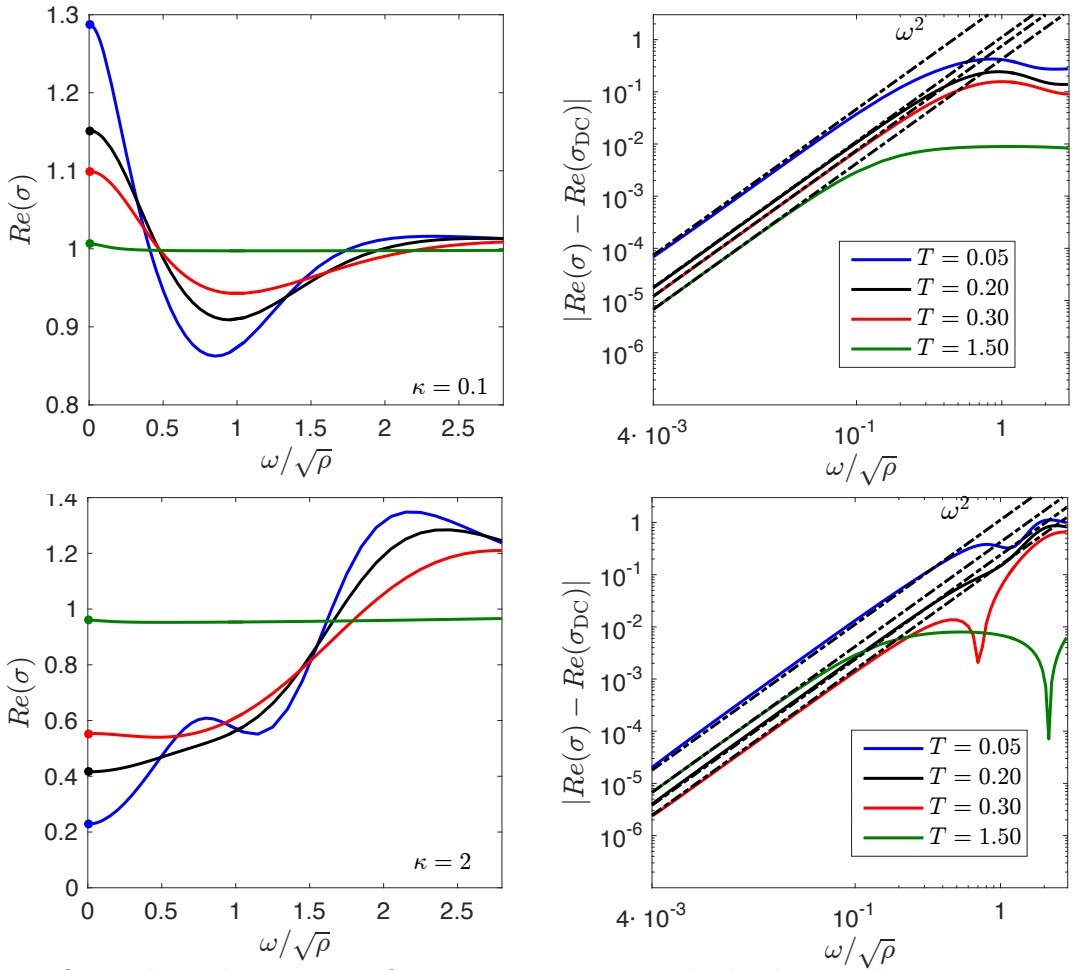

Fig. 5.7 Optical conductivity at finite temperature in the background given in eqs. (5.16) and (5.29). Each line corresponds to a fixed temperature, indicated in the legend of the right-hand side plots. The dashed-dotted black lines correspond to the quadratic scaling and are fixed in the same way as in Fig. 5.6. As temperature decreases (blue lines) a slight disagreement is observed. We expect for near extremal solutions the frequency scaling is given by eq. (5.35). The charge density $\rho = 1$, $\alpha = 1$, $\lambda = 0.15$ and κ is indicated in the left-hand side plots.

tioned above, for $Z = 1$ and a minimally a coupled Maxwell field ($Y = 1$), the constants a and b are always negative, describing the broadening of the Drude peak. For $Y \neq 1$ and both $Z \neq 1$ and $Z = 1$, a is negative when $\mathrm{Re}(\sigma_{\mathrm{dc}}) > 1$ and positive when $\mathrm{Re}(\sigma_{\mathrm{dc}}) < 1$, namely, the latter shares features of an insulator-like state.

For $Y \neq 1$ and both at zero (not shown) and nonzero temperature (bottom left plot in Fig. 5.7), we have observed a range of parameters for which the optical conductivity has a local maximum for relatively small frequencies. In figure 5.7 we observe that in the high temperature limit the local peak is smeared. A similar feature in the dc conductivity [143] has been recently related to a precursor of an insulator. Similarly to the phenomenology observed in the temperature dependence of the dc conductivity, we believe that, in the range of parameters of figure 5.7, this intermediate peak is a consequence of charge screening induced by a non-trivial axion-dependent Maxwell coupling and therefore it is not a precursor of insulating behavior.

We have observed that a stronger gravitational interaction (larger BD coupling Z) has a similar impact on the intermediate peak as increasing momentum dissipation. As was mentioned in Sec. 5.3.2, in $d = 3$ boundary dimensions this is a nontrivial effect: a conformal transformation of the action eq. 5.16 with $d > 3$ renormalizes the Maxwell coupling in an analogous way to the conformal transformation of the BD model, see eq. (5.15). However, for $d = 3$ the Maxwell coupling is invariant under such transformation and one could expect therefore the Maxwell coupling to be unchanged by a change in the BD coupling. Nonetheless, from a holographic point of view, it is known that the observables in the boundary theory are roughly determined by the gravitational background (plus boundary values of bulk fields). Therefore, at intermediate energy scales, and despite the fact the Maxwell coupling is invariant under a conformal transformation for $d = 3$, one should expect the features of the BD background at intermediate length-scales to determine the optical conductivity.

5.5.2 Argument and modulus of the optical conductivity in BD gravity with momentum relaxation

A well known property of the optical conductivity in most cuprates is that for intermediate frequencies the module of the conductivity scales as $\omega^{-2/3}$. It has been recently claimed [319] that a holographic setup where momentum relaxation is introduced by a modulating chemical potential share similar properties. However, we note that this holographic setup does not reproduce another property of the optical conductivity in cuprates: the argument of the conductivity is constant in the same range of frequencies. In this section we study whether field theory duals of gravity models with different channels of momentum dissipation can reproduce these features of the optical conductivity in cuprates.

Results for different values of the parameters are depicted in Fig. 5.8.

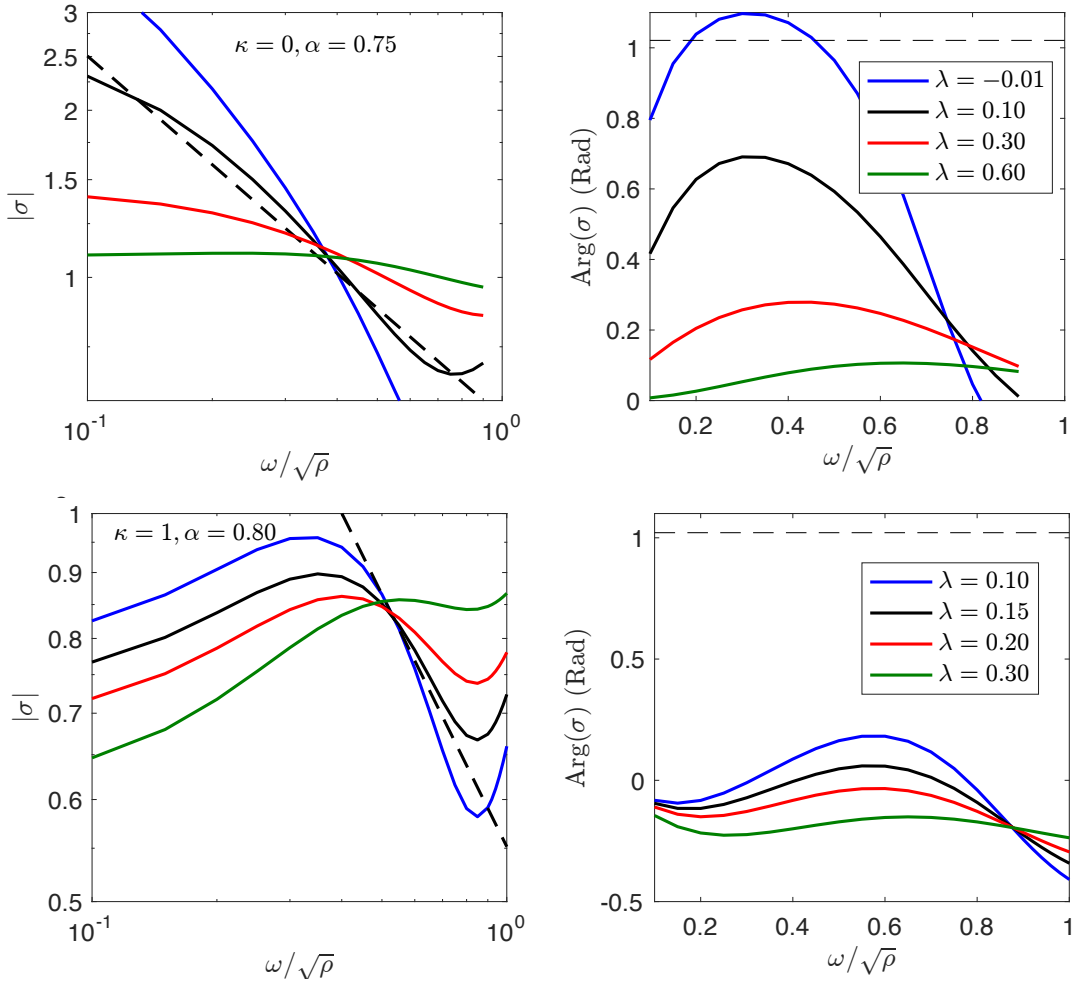

Fig. 5.8 Absolute value and argument of the optical conductivity for different values of the parameters. The temperature and charge density are $T = 0.05$ and $\rho = 1$. The BD model with the couplings of eq. (5.29) does not describe the experimental behaviour for intermediate frequencies observed for cuprates. The dashed lines are the exponent ξ, $|\sigma| = \omega^a$, $a = 1.35 - 2 = -0.65$, and $\arg(\sigma) = \frac{\pi}{2}(2 - 1.35) = 1.01$ Rad, according to experiments.

Either the constant argument or the desired 2/3 power-law decay can be observed for some values of the parameters. However, it is clear from our results that even by fine tuning all the available parameters we could not reproduce both features for a single set of parameters.[12]

[12]These two features, $|\sigma \sim \omega^{-2/3}$, $\arg(\sigma) = \pi/3$, have been reproduced in models involving the DBI action [99].

5.6 Shear viscosity to entropy density ratio in BD with momentum relaxation

In this section we study the ratio η/s between the shear viscosity η and the density of entropy s for BD holography with momentum relaxation. As shown in Ref.[275], the zero frequency limit of

$$\eta(\omega) = \lim_{\mathbf{k}\to 0} \frac{1}{\omega} \operatorname{Im} G^R_{T^{xy},T^{xt}}(\omega, \mathbf{k}) \,, \tag{5.36}$$

where T^{xy} is the xy component of the stress-energy tensor, gives the correct answer of the regular real part of the shear viscosity. However, the imaginary part is not given correctly by taking $\operatorname{Re} G_R^{xy,xt}(\omega, \mathbf{k})$ in the previous equation. For similar reasons to those discussed in Sec. 4.2, one needs to subtract a zero-frequency correlator which, in this case, contributes only to the imaginary part of η [275, 273]. This term measures the response in the stress-energy tensor to a static strain. In this case, as opposed to the case of the electrical conductivity discussed in Sec. 4.2, retaining the contact term leads to a cancellation of a pole at zero frequency [275, 273] which would otherwise be present.[13]

A second comment related to the interpretation of eq. (5.36) is that, the shear viscosity defined from the coefficient of the shear tensor in a hydrodynamical theory without translational symmetry differs from the standard result obtained the from $\operatorname{Im} G^R_{T^{xy},T^{xt}}$, eq. (5.36) [332]. In other words, due to the presence of momentum dissipation, the quantity obtained from eq. (5.36) cannot strictly be interpreted as a hydrodynamic shear viscosity. Nonetheless, the observable of eq. (5.36) is still interesting as it can be related to the entropy production rate [333]. For simplicity, we will still refer to it as shear viscosity.

In order to compute the viscosity in the model of eq. (5.16) we use the membrane paradigm in a similar way as it has been used in Sec. 5.2.2 for the calculation of the regular part of the dc conductivity. While we restrict ourselves to numerical results we expect that, as shown in [333], it should be possible to derive quasi-analytical approximations at low and large temperatures.[14]

[13] Additional poles at zero frequency could still exist; this is typically the case in non-interacting systems such as the Fermi gas in zero magnetic field [273].

[14] An analytical calculation in terms of the background expansion close to the boundary is possible, however, the background needs to be computed numerically.

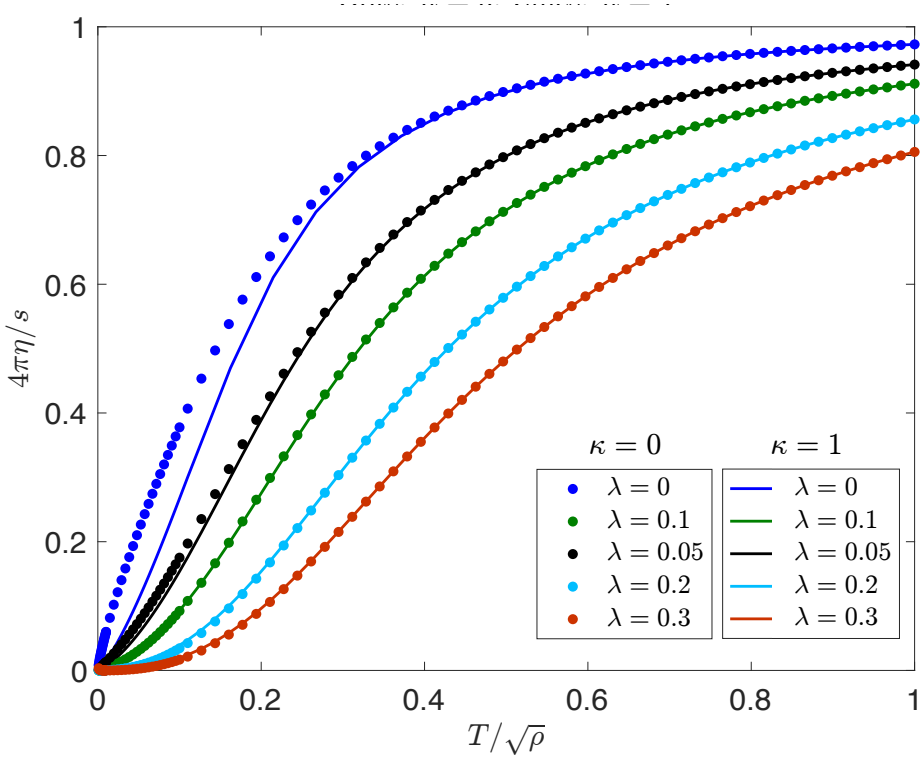

Fig. 5.9 Shear viscosity to entropy density ratio (η/s) for the couplings of eq. (5.29) in the model defined in eqs. (5.16) and eq. (5.29). The axion parameter $\alpha = 1$ and the charge density $\rho = 1$.

Previously it has been reported that in the presence of momentum relaxation [334, 335, 332, 333, 336] or anisotropy [337–339][15] the ratio is temperature dependent and in most cases below the KSS bound. We find similar results in the case of BD holography. For our analysis we use the couplings of eq. (5.29) with $V = TrX$ (Fig. 5.9) and $V = 0$ (figure 5.10) which include, as a particular case, some of the previously studied cases of AdS RN+axions [333, 336]. In the full range of parameters we have explored, the ratio decreases with temperature and is always below the KSS bound. It also decreases as the strength of momentum relaxation increases, by any of the channels explored. It seems that it can be made arbitrarily close to zero even for a finite momentum relaxation. We do not have a clear understanding of the physical reasons behind this behaviour however we note that similar results have been observed [341] in the context of the quark-gluon plasma with quenched impurities in the limit in which the phenomenon of Anderson localization becomes important.

[15] We note that in these models the effective mass of the graviton is nonzero. As shown in [340] this is a necessary condition to observe violation of the KSS bound. However, in theories without translational invariance and massless graviton [340] the KSS bound remains valid. Our model falls in the first class of theories.

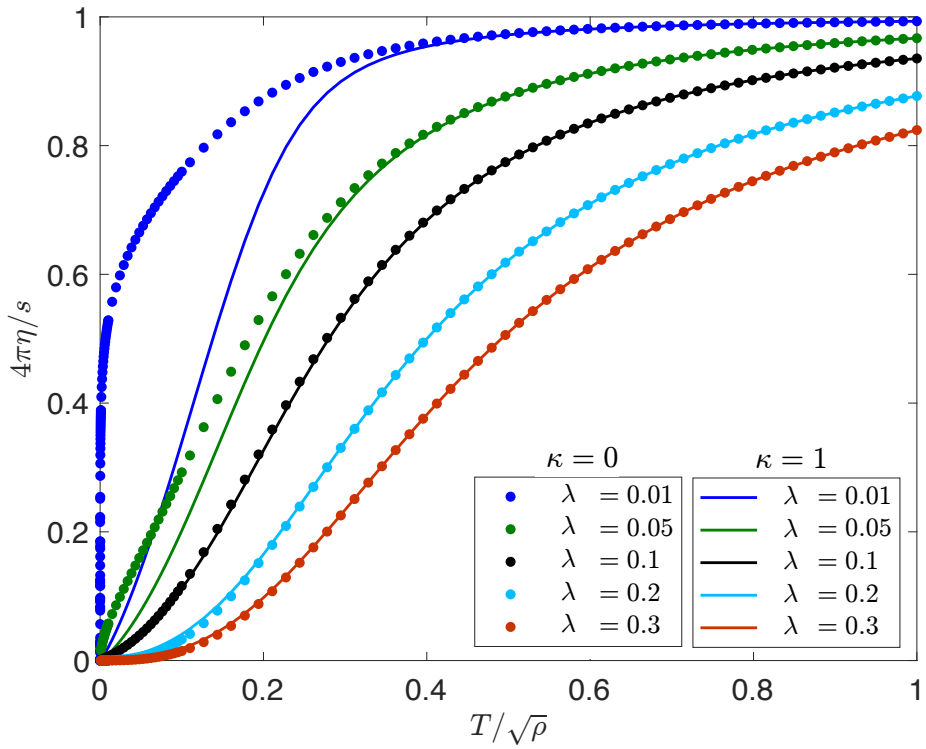

Fig. 5.10 Shear viscosity to entropy density ratio (η/s) for the couplings of eq. (5.29) in the model defined in eqs. (5.16) and eq. (5.29) but taking $V = 0$ and $\dot{V} = 0$. The axion parameter $\alpha = 1$ and the charge density $\rho = 1$. As discussed in Sec. 5.3.2, for $\kappa = 0 \implies Y = 1$ (dots) the theory has a single parameter that controls momentum dissipation, namely $\lambda_{eff} = \lambda\alpha^2$.

5.7 Conclusions

In this Chapter we have investigated the transport properties of strongly coupled field theories whose gravity-dual is a Brans-Dicke action where gravity is mediated by both a tensor, the graviton, and a scalar that depends on the radial dimension. In the translational invariant limit we have computed analytically several transport properties. The finite part of the dc conductivity, expressed in terms of thermodynamic quantities, is different from the universal prediction for EMd backgrounds [122] however the shear viscosity ratio is still given by the KSS bound. Unsurprisingly, this result agrees with that obtained by using the conformal transformation relating BD and EMd models. The difference with EMd models is that the entropy does not hold an area law as it also depends on the value of the scalar at the horizon.

Momentum relaxation is induced by a gravitational axion, namely, the linear coupling of the Ricci tensor and the axion. Following the procedure pioneered by Donos and Gauntlett [141] we compute analytically the dc conductivity as a function of the metric at the horizon which is evaluated numerically. In $d+1 = 4$ bulk dimensions momentum relaxation by BD axions is qualitatively similar to the results obtained by other mechanism of momentum

relaxation [139, 144, 143] in the limit of strong charge screening. Interestingly for strongly coupled gravitational axions, that induce strong momentum relaxation, the conductivity bound [142] is violated for any finite charge screening induced by the electromagnetic axion [143, 144]. In this limit insulating like features cannot be ascribed to charge screening. In higher spatial dimensions the dc conductivity for sufficiently strong momentum relaxation decreases in the low temperature limit. This suggests that analogous conductivity bound is violated even if there is no coupling between the axion and the Maxwell field. We have also computed numerically the optical conductivity in BD backgrounds with momentum relaxation. For sufficiently strong breaking of translational invariance, the conductivity grows linearly with the frequency in the limit of small frequencies and very low temperatures. This is a common feature in systems close to an insulating phase. We have also evaluated numerically the modulus and the argument of the optical conductivity for different momentum relaxation channels in order to find out whether the phenomenology of this model is similar to that of the cuprates for intermediate frequencies. Our results are not very encouraging. For any value of the parameters we could not reproduce the experimental results for both quantities simultaneously. Finally, we have shown that the shear viscosity to entropy ratio decreases with temperature and the KSS bound is violated by any strength of the momentum relaxation. As a side comment, we would like to add that the energy momentum tensor of a theory with a gravitational dual should be computed from the holographic background in the Einstein frame. Throughout the paper we did not work in this frame and to avoid mistakes we had to use unfamiliar expressions like the null energy condition of eq. (5.31).

The potential interest of BD backgrounds in holography is well beyond the problems discussed in this chapter. For instance, the entanglement entropy depends explicitly on the gravity coupling constant and it is also very sensitive to the strength of bulk interactions. Therefore we expect that the holographic entanglement entropy in inhomogeneous BD backgrounds may reveal interesting features not found in previous holographic duals. These features would not only be present to leading order (area of minimal surface) but also in the quantum correction originated by the entanglement between the bulk and the minimal surface [342]. Another topic of potential interest is that of holographic superconductivity. It is well known that the ratio between the order parameter at zero temperature and the critical temperature, or the width of the coherence peak are useful indicators of the strength of the interactions binding the condensate. For the former, values much larger than the Bardeen-Cooper-Schrieffer prediction, suggesting strong interactions, are expected. It would be interesting to investigate whether it is possible to tune this ratio in BD backgrounds. That would be a smoking gun that the scalar in BD backgrounds effectively controls the interactions in the bulk. Finally, we note that the introduction of randomness in the scalar is qualitatively different from other forms of disorder used in holography. It amounts to a random strength of the gravitational interaction. Mobile

charge introduced through the gauge field will feel these random interactions not very differently from the way in which electrons felt quench impurities. This is in stark contrast with the effect of a random chemical potential, quite popular in holography, where the mobile carriers are by construction randomly but homogeneously distributed through the sample. Coherence phenomena like Mott-Anderson localization could not be observed in this setting.

6

Conclusions and Outlook

In this thesis we have considered various applications of the gauge/gravity duality to probe the phenomenology of strongly coupled systems with gravity duals. In the Introduction we have used the QGP and various Condensed Matter systems to motivate the use of gauge/gravity dualities. We have also covered the progress made in the latter case by using bottom-up approaches. However, we learned that, since usually the dual field theory is unknown, the information that can be extracted with this approach is often qualitative. It is therefore essential to understand the role of interactions in the boundary theory and to identify the relevant degrees of freedom that control physical observables. With these goals in mind, we first opted for a strategy aimed at simplifying holographic models and having analytical control, namely we used the large dimensionality limit. Later on, in order to identify the dominant degrees of freedom in transport properties we have implemented bounds in holographic correlation functions of translationally invariant systems. We also saw how these bounds apply in the limit that this symmetry is weakly broken. Moreover, at this point it became clear that the holographic models studied had an important limitation that restricted their applicability: momentum does not relax strongly enough. This is important if holography is to describe insulating Condensed Matter systems with strong interactions. Therefore, we studied models with non-minimal couplings that break diffeomorphism invariance and gave a physical interpretation (in the boundary theory) of the origin of the insulating features observed.

Let us now summarise in more detail the key findings of this thesis.

In Chapter 3 we have studied the conductivity and the entanglement entropy between a strip and its complement, in models with gravity duals which display spontaneous $U(1)$ symmetry breaking, at zero and nonzero temperature and in different number of space-time dimensions d.

The first result we have reported concerns the coherence peak in the conductivity, which is a broad peak at nonzero frequency that indicates the typical energy at which the superconducting 'order' or interactions are annihilated or suppressed. This peak in was first observed in holographic superconductors in [113, 114]. What we have found is that, relative to the critical temperature T_c, the coherence peak becomes narrower for larger dimensionality and furthermore, the ratio between the superconducting gap (as measured by the conductivity) ω_g and T_c decreases as dimensionality increases. Moreover numerical results suggest this ratio saturates to $\omega_g/T_c \sim 7$ in the $d \to \infty$ limit.
We have also studied the low frequency scaling of the conductivity at zero temperature and observed a power-law (in frequency) similar to that found in [115]. We have observed the power increases with dimensionality or equivalently that the optical conductivity becomes flatter at low frequency. This leads to the conclusion that the low-energy collective excitations of the system are heavily suppressed for large d.

Finally, we have studied the dependence of the entanglement entropy between a strip and its complement on d, both at zero temperature and close to T_c. At nonzero temperature the entanglement entropy is not a good measurement of entanglement, however, we compare the entanglement entropy in the broken and unbroken ($U(1)$) symmetry phases at the same temperature. In this way an estimation of the effective number of degrees of freedom, based on the entanglement entropy, is less adventurous. Our results confirm previous expectations [232] that the entanglement entropy is smaller in the symmetry broken phase which suggests that this observable is useful to identify phase transitions. We have further shown the difference of the entanglement entropy between the broken and unbroken phases decreases with increasing dimensionality.

Both results on transport and entanglement entropy lead to conclude that the strength of interactions decreases as dimensionality increases. An infinitely high and narrow coherence peak in the conductivity indicates the quasi-particle paradigm and a mean-field treatment should be valid at $d \to \infty$; in this limit the superconducting gap would be well-defined by ω_g (provided ω_g/T_c saturates to a nonzero value). It would be interesting to explore in more detail whether there is a lower bound for ω_g/T_c and for the width of the coherence peak in theories with gravity duals.

Moreover, since the dynamics of gravitational theories simplify for high dimensionality, we expect the result that interactions become weaker for larger dimensionality to be a general feature in theories with holographic duals.

We have observed a puzzling feature regarding the relation of the expectation value of the scalar in the dual theory $\langle \mathcal{O} \rangle$. Namely, the dependence on dimensionality of $\langle \mathcal{O} \rangle^{1/\Delta}$ and ω_g (with respect to T_c) is different.[1] $\langle \mathcal{O} \rangle^{1/\Delta}$ is usually interpreted as the energy gap in the dual theory, therefore it should contain the same information as ω_g, which as we mentioned above has a crisp interpretation as the energy scale at which excitations due

[1] Δ is the conformal dimension of the dual operator $\mathcal{O}$.

to an external electric field appear. Therefore, either $\langle \mathcal{O} \rangle$, which signals the spontaneous symmetry breaking, is not actually related to the energy gap or a non-trivial rescaling with dimensionality is needed; we have not found a good justification for the latter.

As we have mentioned above, the large dimensionality limit has offered a better intuition about strongly coupled theories with gravity duals when the number of dimensions increases. However, apart from the analytical approximations obtained, we have not gained much intuition of theories at low dimensionality. For instance, it is desirable to identify the dominant degrees of freedom involved in transport at strong coupling in two and three space dimensions.

In principle the ballistic transport typical of translationally invariant systems is not expected to dominate in the presence of strong interactions. However, in Chapter 4 we have given examples of strongly interacting systems in which transport is ballistic in certain range of parameters. Therefore, the study of the MS bounds in holographic models could cast some light on properties of strongly coupled systems. We have applied the MS bounds to the Drude weight in a wide variety of strongly coupled field theories with a gravity dual at nonzero temperature and chemical potential. We have observed that in EMd and R-charged backgrounds the MS bound on the Drude weight is saturated. On the contrary, in backgrounds with $U(1)$ spontaneous symmetry breaking, and gravity duals of non-relativistic field theories (asymptotically Lifshitz backgrounds), this bound is not saturated. Therefore, there seems to be a wide universality class of theories (EMd theories) in which the MS bound on the Drude weight is saturated. The universal result of the Drude weight in this theory is given in terms of the charge density, energy density and pressure: $K = \frac{\rho^2}{\epsilon + P}$. Moreover, we have extended the universality of this result to theories with multiple R-charges, in which, again, the MS bound is saturated.

In the second half of Chapter 4 we have weakly broken translational invariance. The motivation of this part is not direct; after all this situation had been explored extensively in the literature of holographic models [111, 137, 138, 277, 95, 139, 303, 127]. Nonetheless, upon the introduction of a perturbation that weakly breaks this symmetry, there is a lowest-decaying mode associated to the weakly-broken symmetry; it is reasonable to expect this mode to control certain observables which were dominated by the conserved charge associated to the unbroken symmetry. Indeed, we have observed that the MS bound (as opposed to the Drude weight itself) of a translational invariant theory controls the coherent part of the dc conductivity, once translational symmetry is broken. This suggests that for weak momentum relaxation and a given scattering time, the dc conductivity is bound by below by the MS bound of the translationally invariant theory at the same temperature and charge density.

There are interesting points related to the MS bounds which have been suggested in Condensed Matter but not yet explored in the context of holographic theories. First, the MS bounds provide information on the integrability of the theory or equivalently, on the

non-ergodic character of its observables. Second, the saturation of the MS bounds has been linked to the Thermodynamics of a system being described by the generalized Gibbs ensemble.

Having studied the limit of weak breaking of translational symmetry and motivated by the possibility to study models with insulating features [143, 144], the natural objective was to study strong momentum relaxation. To do so, in Chapter 5 we have first used asymptotically AdS Brans-Dicke backgrounds with translational invariance as effective models of metals with a varying coupling constant. The motivation to use these backgrounds is that, with respect to Einstein's gravity, the gravitational strength is mediated by additional degrees of freedom associated to the Brans-Dicke scalar. Note however, that BD models are easily mapped to EMd theories, and thus it is not clear, *a priory*, that new phenomenology is possible. Nonetheless, in the translationally invariant dual to BD gravity, we have found the regular part of the dc conductivity is given by the EMd result but renormalised by the Brans-Dicke field in more than $2+1$-dimensions. On the other hand, the Drude weight agrees with the EMd result.

We have then studied BD-inspired backgrounds without translational symmetry. We have introduced axions, or more appropriately Stükelberg fields, in the coupling of the Ricci scalar as well as in the Maxwell coupling. We have investigated the dc and optical electrical conductivity in $2+1$ and $3+1$ dimensions as well as the shear viscosity in $2+1$ dimensions for various choices of the axion-dependent couplings.

Axion-dependent Maxwell couplings have been recently proposed [143, 144] as models displaying insulating transport properties, like an growing conductivity for low frequency and temperature. We argue that these settings correspond to charge-screening in the dual theory. On the other hand, we have shown that models with axion-dependent gravitational couplings, suggested as well in [144], also display insulating features without charge-screening. Furthermore, we have observed that for our choice of couplings, these models are not consistent with the universal phenomenology of the conductivity at intermediate frequency found in a wide variety of strange metals.

The potential interest of BD backgrounds is still considerable. For instance the calculation of the MS bounds in BD backgrounds remains to be done. More interestingly, we expect new features will appear in the entanglement properties of theories dual to inhomogeneous BD backgrounds. Moreover, random Brans-Dicke fields would be a new way to introduce disorder in holographic settings as this corresponds to random strength of gravitational interactions, which has not yet been explored.

The work described in this thesis contributes to identifying universal behavior of strongly coupled systems through gauge/gravity dualities. This is a highly active research area aiming to addressed an ample spectrum of unsolved problems. Below we mention some which are particularly interesting.

We have covered most of the relevant works aiming to describe strange metals. To date, we lack of a holographic model (or any other type of model) that describes the phenomenology of these enigmatic materials. There is an emerging and growing interest to borrow knowledge and techniques from Quantum Information, which in combination with gauge/gravity dualities in the context of Condensed Matter might cast some light on properties of quantum entanglement and perhaps allow strange metals to be less of a mystery.

Important phenomena which we have only briefly mentioned in this thesis is the effect of disorder and Many Body Localization. Though there have been recent efforts to address this problem using gauge/gravity dualities [130–134, 343–348] these constructions, which mostly involve a random chemical potential, have not been able to fully realize localized states in the boundary theory. Perhaps, it would be a more successful approach not impose a random distribution of charge by construction, but rather let this be the outcome of randomness in other sources of the holographic model.

Very recently Kitaev has raised [349] awareness of a toy model [350], introduced by Sachdev and Ye in a Condensed Matter context, in the holography community [351, 352]. This is a $0+1$-dimensional model of interacting fermions with random interactions which is solvable in the limit of strong coupling. As suggested by Kitaev the study of this model is relevant in holography since it might be related to the mysterious AdS_2 geometry found in many holographic settings and which is relevant for the study of quantum phase transitions and quantum criticality.

A

Entanglement and conductivity for large-d

A.1 Entanglement entropy at $T \sim T_c$

The equations of motion, expressed in the coordinate $z = 1/r$, are:

$$\begin{aligned}
&\psi'' - \left(\frac{\chi'}{2} + \frac{d-1}{z} - \frac{f'}{f}\right)\psi' - \left(\frac{m^2L^2}{z^2 f} - \frac{q^2 e^{\chi}\phi^2 L^4}{f^2}\right)\psi = 0,\\
&\phi'' + \left(\frac{\chi'}{2} - \frac{d-3}{z}\right)\phi' - \frac{2q^2L^2\psi^2}{z^2 f}\phi = 0,\\
&\chi' = \frac{2z}{d-1}\left(\psi'^2 + \frac{e^{\chi}q^2\phi^2\psi^2L^4}{f^2}\right),\\
&f' - \frac{d}{z}f + \frac{d}{z} = \frac{1}{(d-1)z}\left[m^2L^2\psi^2 + \frac{z^4 e^{\chi}\phi'^2L^4}{2} + z^2 f\left(\psi'^2 + \frac{q^2e^{\chi}\phi^2\psi^2L^4}{f^2}\right)\right].
\end{aligned} \tag{A.1}$$

Close to the transition, the fields can be expanded in powers of $\epsilon \equiv \beta$, [353, 354], where $\psi(z \to 0) \sim \beta(\frac{z}{z_0})^{\Delta}$, and $\Delta \equiv \Delta_+$ is the larger conformal dimension. More concretely,

$$\psi \simeq \epsilon\psi_1 + \epsilon^3\psi_3 + \ldots, \quad \phi \simeq \phi_0 + \epsilon^2\phi_2 + \ldots, \quad f \simeq f_0 + \epsilon^2 f_2 + \ldots, \quad \chi \simeq \epsilon^2\chi_2 + \ldots, \tag{A.2}$$

For the purpose of the entanglement entropy calculation given in section 3.6.2 we calculate analytically the first non-trivial terms of this field-expansion in the region where $\left(\frac{z}{z_0}\right)^d \ll 1$, which, for larger d allows z to approach z_0 with a better level of approximation than for small d. However, here we compute all the terms in the perturbative expansion up to $\mathcal{O}(\epsilon^2)$. From the equations of ϕ and f given in eq. (A.1), it is easy to see that the first

zeroth order terms of these fields are:

$$\phi_0 = \mu_0 \left[1 - \left(\frac{z}{z_0}\right)^{d-2}\right], \quad f_0(z) = 1 - (1+Q^2)\left(\frac{z}{z_0}\right)^d + Q^2\left(\frac{z}{z_0}\right)^{2d-2}, \tag{A.3}$$

where $Q^2 = \mu_0^2 z_0^2 \gamma^2$ and μ_0 is the chemical potential at which the scalar field condenses. $\chi = 0$ and $f = f_0$ corresponds to the Reissner-Nordström black hole with planar topology. The equation for the first term in the expansion of ψ, eq. (A.2), is well known:

$$0 = \psi_1'' - \left(\frac{d-1}{z} - \frac{f_0'}{f_0}\right)\psi_1' + \psi_1\left(\frac{q^2L^4\phi_0^2}{f_0^2} - \frac{m^2L^2}{z^2 f_0}\right), \tag{A.4}$$

giving the expected $(z/z0)^\Delta + \dots$ behavior close to the boundary. ψ_1 can be obtained by rewriting eq. (A.4) as a Sturm-Liouvillle eigenvalue problem, [355, 356], and using as ansatz $\psi_1 = z^\Delta F_0(z)$, $F_0 = 1 - \alpha z^{d-1}$, α is given by the value, α_c that minimizes the following expression,

$$M^2(\alpha) = \frac{\int_0^1 dz\ z^{2\Delta-d+1}(1-z^d)\left[F_0'^2 - \left(\frac{-m^2L^2}{1-z^d} + \Delta(\Delta-d) - \frac{\Delta d z^d}{1-z^d}\right)\frac{F_0^2}{z^2}\right]}{\int_0^1 dz\ z^{2\Delta-d+1}F_0^2 q^2 \frac{(1-z^{d-2})^2}{1-z^d}}, \tag{A.5}$$

and $\mu_0^2 = M^2(\alpha_c)$. The equation for χ_2 is:

$$\chi_2' = \frac{2z\psi_1'^2}{d-1} + \frac{2q^2 z L^4 \phi_0^2 \psi_1^2}{(d-1)f_0^2} \equiv F_\chi(z), \tag{A.6}$$

and thus $\chi_2(z) = \int_0^z dz'\ F_\chi(z')$. Similarly, from the equation for ϕ_2:

$$\phi_2'' - \frac{d-3}{z}\phi_2' = \frac{2q^2\phi_0\psi_1^2}{z^2 f_0} - \frac{1}{2}\phi_0'\chi_2' \equiv F_\phi(z), \tag{A.7}$$

and the leading behavior of ϕ_2 is given by the homogeneous solution. Close to the horizon, ϕ_2 is expected to receive corrections from the last two terms in eq. (A.7). However, we impose such corrections, controlled by ϕ_0 and ψ_1', to satisfy the boundary condition $\phi_2(z_0) = 0$ independently of the homogeneous solution. Therefore,

$$\begin{gathered}\phi_2(z) = \phi_2^a(z) + \phi_2^b(z), \\ \phi_2^a(z) \equiv \kappa\left[1 - \left(\frac{z}{z_0}\right)^{d-2}\right],\ \phi_2^b(z) \equiv \int_z^{z_0} du\ u^{d-3}\int_u^{z_0} dv\ \frac{F_\phi(v)}{v^{d-3}}.\end{gathered} \tag{A.8}$$

Finally, the equation for f_2 is given by:

$$f_2' - \frac{d}{z}f_2 - \frac{z^3L^4\phi_0'\phi_2^{a\prime}}{d-1} = \frac{1}{z(d-1)}\left(z^4L^4\phi_0'\phi_2^{b\prime} + z^2 f_0\psi_1'^2 + m^2L^2\psi_1^2\frac{q^2L^4z^2\phi_0^2\psi_1^2}{f_0}\right) \equiv F_f(z). \tag{A.9}$$

The previous equation can be integrated straightforwardly,

$$\begin{gathered} f_2(z) = f_2^a(z) + f_2^b(z), \\ f_2^a(z) \equiv -\frac{\mu_0 \kappa z_0^2 L^4}{(d-1)(d-2)} \left[\left(\frac{z}{z_0}\right)^d - \left(\frac{z}{z_0}\right)^{2d-2} \right], \quad f_2^b(z) \equiv -z^d \int_z^{z_0} du \, \frac{F_f(u)}{u^d} \end{gathered} \tag{A.10}$$

In the large-d limit, f_2^a dominates over f_2^b. The only parameter to be determined is κ, which follows from the equation of ψ_3:

$$\begin{gathered} \psi_3'' - \left(\frac{d-1}{z} - \frac{f_0'}{f_0}\right)\psi_3' + \left(\frac{q^2 L^4 \phi_0^2}{f_0^2} - \frac{m^2 L^2}{z^2 f_0}\right)\psi_3 = -\mathcal{T}\psi_0, \\ \mathcal{T}\psi_0 \equiv \left(\frac{f_2'}{f_0} - \frac{\chi_2'}{2} - f_2 \frac{f_0'}{f_0^2}\right)\psi_0' + \left[\frac{m^2 L^2}{z^2 f_0} f_2 - \frac{2q^2 L^4}{f_0^3}(f_2 \phi_0 - f_0 \phi_2) + \frac{q^2 \phi_0^2 \chi_2 L^4}{f_0^2}\right]\psi_0. \end{gathered} \tag{A.11}$$

From the previous equation and using eq. (A.4), it follows immediately, $0 = \int_0^{z_0} dz \, \frac{f_0 \psi_0 \mathcal{T}\psi_0}{z^{d-1}}$, which imposes a condition on κ:

$$\kappa = \frac{\int_0^{z_0} dz \, \frac{\psi_0' \psi_0}{z^{d-1}} \left(-f_2^{b\prime} + \frac{\chi_2' f_0}{2} + \frac{f_2^b f_0'}{f_0}\right) + \frac{\psi_0^2}{z^{d-1}} \left[\frac{-m^2 L^2 f_2^b}{z^2 f_0} + \frac{2q^2 L^4}{f_0}\left(\frac{f_2^b \phi_0^2}{f_0} - \phi_0 \phi_2^b\right) - \frac{q^2 \phi_0^2 \chi_2 L^4}{f_0}\right]}{\int_0^{z_0} dz \, \frac{\psi_0' \psi_0}{z^{d-1}} \left(f_2^{a\prime} - f_2^a \frac{f_0'}{f_0}\right) + \frac{\psi_0^2}{z^{d-1}} \left[\frac{m^2 L^2 f_2^a}{z^2 f_0} - \frac{2q^2 L^4}{f_0}\left(f_2^a \frac{\phi_0^2}{f_0} - \phi_0 \phi_2^a\right)\right]}. \tag{A.12}$$

Finally, from eq. (A.8), for some $\epsilon > 0$, the chemical potential is given by $\mu \sim \mu_0 + \epsilon^2(\kappa + \phi_2^b(0)) + \mathcal{O}(\epsilon^4)$, $\rho = \mu_0 + \epsilon^2 \kappa$ and the temperature $T < T_c$:

$$\begin{gathered} \frac{T}{\rho^{\frac{1}{d-1}}} = -\frac{f'(z_0) e^{-\chi(z_0)/2}}{4\pi \left(\mu_0 + \epsilon^2 \kappa\right)^{\frac{1}{d-1}}} \sim \\ \sim \frac{-f_0'(z_0)}{4\pi \mu_0^{\frac{1}{d-1}}} \left[1 + \epsilon^2 \left(\frac{f_2'(z_0)}{f_0'(z_0)} - \frac{\chi_2(z_0)}{2} - \frac{\kappa}{(d-1)\mu_0 f_0'(z_0)}\right)\right], \end{gathered} \tag{A.13}$$

where, $f_0'(z_0) = -d + \mu_0^2 \frac{(d-2)^2}{2d-2}$. For $\epsilon = 0$, the previous equation gives an estimation for the critical temperature. This expression is more complicated that the one given in Ref.[220], in which the backreaction of the scalar on the geometry is neglected. Notice however, that, we were not after an alternate result for T_c, in fact, in this section we have not used the large-d limit since we explicitly look for all the terms that modify the geometry close to the phase transition. In order to analytically evaluate the leading correction on the entanglement entropy of a strip with its complement, section 3.6.2, we take the leading correction on the blackening function, $f_2^a(z)$, given in eq. (A.10).

A.2 Large ℓ limit of the entanglement entropy at finite temperature and fixed d

In the RN background, from eq. (3.60),

$$\frac{\ell}{2} = \int_0^{z_*} dz \frac{z^{d-1}}{\sqrt{f(z)\left(z_*^{2d-2} - z^{2d-2}\right)}}. \tag{A.14}$$

Let us split the region of integration into two: $[0, z_*] = [0, z_a] \cup (z_a, z_*]$, for some $0 < z_a < z_*$ and let us rename the integral in the first interval as $\ell_1/2$. In the second interval we change variables to $z = z_0 - \epsilon$ and expand the integrand for $\epsilon/z_0 \ll 1$.

$$\begin{aligned} \frac{\ell}{2} &\sim \frac{\ell_1}{2} - \int_{z_0}^{z_0 - z_*} d\epsilon \frac{z_0^{d-1/2}}{\sqrt{(d-2)Q^2 - d}\sqrt{z_0^{2d-2} - z_*^{2d-2}}\sqrt{\epsilon}} + \cdots \sim \\ &\sim \ell_1 + \frac{z_0^{d-1/2}}{2\sqrt{(d-2)Q^2 - d}} \left[-\left(\frac{z_0 - z_*}{z_0^{2d-2} - z_*^{2d-2}}\right)^{1/2} + \frac{z_0 - z_a}{\sqrt{z_0^{2d-2} - z_*^{2d-2}}} \right] + \dots . \end{aligned} \tag{A.15}$$

In spite of the explicit dependence of the third term on z_*, in the limit $z_* \to z_0$ we can take it as a divergent contribution, ℓ_{div}, while the middle term remains finite, thus:

$$-\left(\frac{z_0 - z_*}{z_0^{2d-2} - z_*^{2d-2}}\right)^{1/2} \sim (\ell - \ell_1) \frac{\sqrt{(d-2)Q^2 - d}}{z_0^{d-1/2}} - \ell_{div}. \tag{A.16}$$

Similarly, splitting the integral of the entanglement entropy, eq. (3.59), into the same regions the integrations carries analogously,

$$s_{\tilde{A}} \sim s_1 - \frac{\sqrt{z_0}}{\sqrt{(d-2)Q^2 - d}} \left(\frac{z_0 - z_*}{z_0^{2d-2} - z_*^{2d-2}}\right)^{1/2} + \frac{\sqrt{z_0}}{\sqrt{(d-2)Q^2 - d}} \left(\frac{z_0 - z_a}{z_0^{2d-2} - z_*^{2d-2}}\right)^{1/2}, \tag{A.17}$$

where s_1 contains the UV-cutoff and the last term is also divergent in the limit $z_* \to z_0$. The middle term can be substituted using eq. (A.16) which leaves a term proportional to ℓ. In the limit $z_* \to z_0$, $\ell \to \infty$ however, the term in eq. (A.16) is regularized by ℓ_{div}, yielding a finite term.

A.3 Electrical conductivity at $T > 0$

The boundary conditions near $z \to 0$ are:

$$\tilde{A}_x(z,\omega) = \begin{cases} A_x^{(0)} + A_x^{(1)} z, & d = 3 \\ A_x^{(0)} + A_x^{(1)} z^2 + \frac{A_x^{(0)}\omega^2}{2} z^2 \log\frac{\Lambda}{z}, & d = 4 \\ A_x^{(0)} + A_x^{(1)} \sqrt{\frac{2}{\pi\omega}} \left[-z\cos(z\omega) + \frac{1}{\omega}\sin(z\omega) \right], & d = 5 \\ A_x^{(0)} + A_x^{(1)} \sqrt{\frac{2}{\pi\omega}} \left[-\frac{3z}{\omega}\cos(z\omega) - z^2\sin(z\omega) + \frac{3}{\omega^2}\sin(z\omega) \right], & d = 7 \\ A_x^{(0)} + A_x^{(1)} \sqrt{\frac{2}{\pi\omega}} \left[\left(z^3 - \frac{15z}{\omega^2}\right)\cos(z\omega) + \left(\frac{15}{\omega^3} - \frac{6z^2}{\omega}\right)\sin(z\omega) \right], & d = 9 \end{cases} \tag{A.18}$$

Λ is a cutoff which affects only the imaginary part of σ. We take $\Lambda = 1$. From the above expressions and the eq. (3.22), the conductivity is:

$$\sigma = \begin{cases} \frac{A_x^{(1)}}{i\omega A_x^{(0)}}, & d = 3 \\ \frac{2A_x^{(1)}}{i\omega A_x^{(0)}} + \frac{i\omega}{2}, & d = 4 \\ \frac{A_x^{(1)}}{iA_x^{(0)}} \sqrt{\frac{2\omega}{\pi}}, & d = 5 \\ \frac{3A_x^{(1)}}{iA_x^{(0)}} \omega^{3/2} \sqrt{\frac{2}{\pi}}, & d = 7 \\ \frac{15A_x^{(1)}}{iA_x^{(0)}} \omega^{5/2} \sqrt{\frac{2}{\pi}}, & d = 9 \end{cases} \tag{A.19}$$

B

Brans-Dicke holography

B.1 Equations of motion in Brans-Dicke gravity

In this appendix we review the derivation of the equations of motion of the Brans-Dicke and related actions used in Chapter 5. The purpose of this appendix is not to present new content, this is well-known in the literature [314, 324], but to complement Chapter 5. In particular, we are interested in understanding the origin of the 'extra terms' at the end of eq. (5.2) which are absent in the equations of motion of Einstein gravity. We anticipate at this point these terms originate from the variation of the Ricci tensor. In the case of Einstein gravity this variation yields only a boundary term but for an arbitrary function of the Ricci scalar, extra bulk terms appear. Indeed, this is the case of the non-minimal couplings of the Ricci scalar used in Chapter 5.

We start by rewriting the BD action given in eq. (5.1) as

$$S = \int_{\mathcal{M}} \mathrm{d}^{d+1}\sqrt{-g}\left[\phi R + \mathcal{L}_M\right] , \tag{B.1}$$

where $\mathcal{L}_M$ contain the rest of the matter terms. We concentrate on the term δR_{ab} in the variation $\delta\sqrt{-g}\phi R$ with respect to the metric:

$$\delta\sqrt{-g}\phi R = \phi\sqrt{-g}\delta g^{ab}G_{ab} + \phi g^{ab}\delta R_{ab} , \tag{B.2}$$

where the first term, which contains the Einstein tensor, contributes in the standard way as in Einstein's gravity while the last term will yield bulk and boundary terms. To see

this we use the Palatini identity:

$$\delta R_{ab} = \nabla_c \delta\Gamma^c_{ba} - \nabla_b \delta\Gamma^c_{ac}\,, \tag{B.3}$$

$$\delta\Gamma^c_{ba} = \frac{1}{2}\delta g^{cd}\left(g_{da,b} + g_{db,a} - g_{ba,d}\right) + \frac{1}{2} g^{cd}\left(\delta g_{da,b} + \delta g_{db,a} - \delta g_{ba,d}\right)\,. \tag{B.4}$$

The calculation follows more easily in normal coordinates with the origin at some point p such that the first three terms on the right-hand side of eq. (B.4) vanish ($\Gamma^d_{ba}(p) = 0$). Therefore, substituting the nonzero terms of eq. (B.4) into eq. (B.3) allows to simplify the last term of eq. (B.2) reduces to

$$\phi g^{ab}\delta R_{ab} = \phi\partial_c\left(\partial_d \delta g^{cd} - g^{cd}\partial_d \delta g^a_a\right)\,.$$

Moreover, since the variation of the Christoffel symbol is a tensor, the covariance principle allows to rewrite the previous equation in a covariant form

$$\phi g^{ab}\delta R_{ab} = \phi\left(\nabla_c\nabla_d \delta g^{cd} - \nabla_c\nabla^c \delta g^a{}_a\right)\,. \tag{B.5}$$

Substituting eq. (B.5) into the variation $\delta_g S$ gives

$$\delta_g S = \int_{\mathcal{M}} \mathrm{d}^{d+1}x\, G_{ab}\phi\delta g^{ab} + \phi(\nabla_c\nabla_d\delta g^{cd} - g_{ab}\nabla_c\nabla^c\delta g^{ab}) + \delta_g\sqrt{-g}\mathcal{L}_M\delta g^{ab}\,,$$

and integrating the terms in parenthesis by parts leads to

$$\delta_g S = \int_{\mathcal{M}} \mathrm{d}^{d+1}x\,\left(G_{ab}\phi + \delta_g\sqrt{-g}\mathcal{L}_M - \nabla_a\nabla_b\phi + g_{ab}\nabla_c\nabla^c\phi\right)\delta g^{ab} + \sqrt{-g}\nabla_c V^c\,, \tag{B.6}$$

where $V^c = \nabla_d(\phi\delta g^{cd}) - \nabla^c(\phi\delta g^a{}_a)$. Using Stokes theorem to integrate the last term of eq. (B.6) yields boundary terms which are cancelled by the variation of the Gibbons-Hawking-York term for the Brans-Dicke action $S_{GHY} = \int_{\partial\mathcal{M}} \mathrm{d}^d x\,\sqrt{-\gamma}\phi K$, with K being the trace of the extrinsic curvature and *gamma* the determinant of the induced boundary metric.

Moreover, the calculation of the equations of motion of the action used in Chapter 5 to study momentum relaxation, eq. (5.16), follows in the same way except for another extra term due to the dependence of the coupling $Z(TrX)$ on the metric. Namely, eq. (B.2) is replaced by

$$\delta\sqrt{-g}ZR = Z\sqrt{-g}\delta g^{ab}G_{ab} + Zg^{ab}\delta R_{ab} + \sqrt{-g}R\delta Z\,, \tag{B.7}$$

$$\delta Z = \frac{1}{2}(\partial_{TrX}Z)\sum_I \nabla_a X^I \nabla_b X^I\,. \tag{B.8}$$

Repeating the integration by parts outlined above, the EOMs for this case, eq. (5.21), follow easily. Regarding the GHY term in this model, it is similar to that used in BD

gravity but replacing ϕ by Z; in fact in more general $f(R)$ theories of gravity the GHY term is [357] $S_{GHY} = \int_{\partial\mathcal{M}} \mathrm{d}^d x \sqrt{-\gamma} f'(R) K$.

B.2 Gravitational background with $Z \neq 1$, $Y = 1$ and $V \neq 1$ in four bulk dimensions

In this appendix we study the number of independent parameters of the model defined in eq. (5.16) with couplings given in eq. (5.29). In Fig. B.1 we show the metric functions used in the BD backgrounds, eq. (5.17), at nonzero temperature.

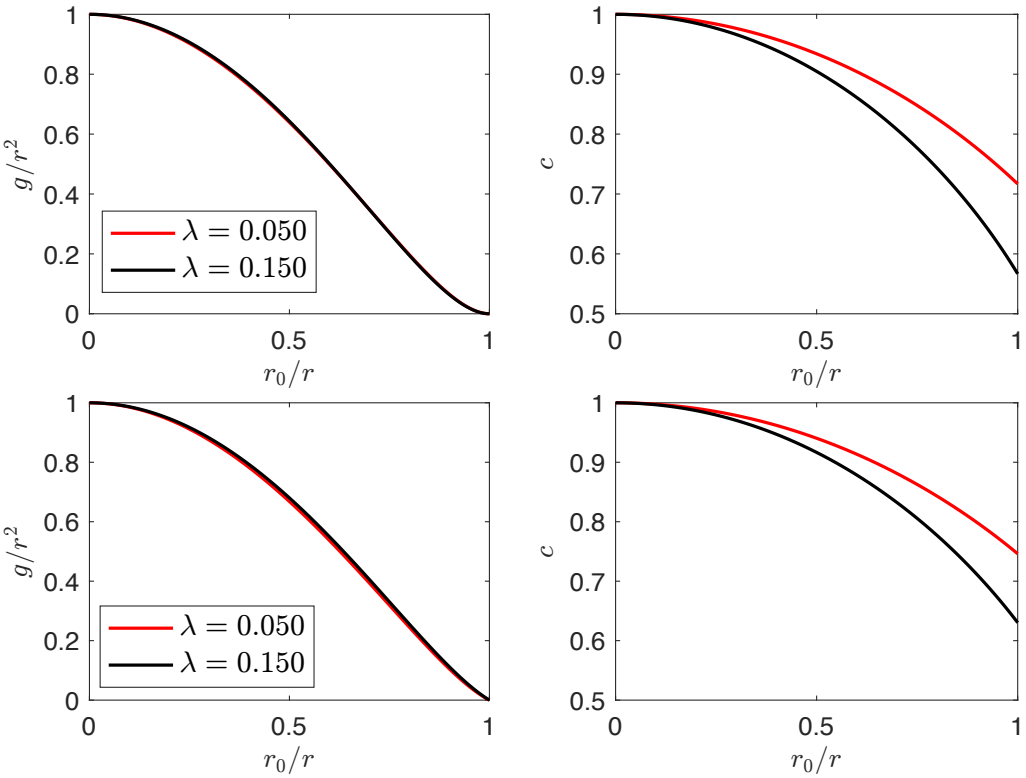

Fig. B.1 Metric functions g (blackening factor) and c, eq. (5.17) for two different temperatures; top row: $T = 10^{-4}$ and bottom row: $T = 0.08$. We fix the charge density $\rho = 1$, $\kappa = 1$ and $\lambda_{eff} = \lambda\alpha^2 = 0.15$. Each line corresponds to $\alpha^2 = \lambda_{eff}/\lambda$ for the corresponding λ, which is given in the legends. The legends also refer to the right-hand side figures. Moreover, for a fixed temperature and λ_{eff}, the dc conductivity is different for the two choices of λ and α. We conclude that, in the presence of V in the action, λ and α are two independent parameters associated with the translational symmetry breaking.

The lines correspond to a fixed $\lambda_{eff} \equiv \lambda\alpha^2$ but different λ and α, defined in eq. (5.29). Most notably, the function c at the horizon shows a difference of about 20%, while the blackening factor is very similar throughout the bulk. Fig. B.1 shows that the model defined in eqs. (5.16) and (5.29) contains three independent parameters, κ, α and λ.

C

Size effects in superconducting thin films coupled to a substrate[†]

C.1 Introduction

Research on superconducting thin films has a long tradition in condensed matter physics. In the early 1960s, theoretical mean-field models [359] predicted oscillations of the superconducting gap and the critical temperature for nanosize film thickness with peaks that greatly exceeded the bulk limit. This nonmonotonic size dependence, usually referred to as shape resonances, has a simple origin. As thickness increases from the two-dimensional limit, new states become eventually available with the quantum numbers of an infinite well of size the thickness of the film. This additional subband enhances superconductivity as the spectral density is proportional to the dimensionless electron-phonon coupling constant. After the first peak, for larger thicknesses, the spectral density decreases until a new subband becomes available and a new peak occurs in the critical temperature.

Initial experimental results in granular thin films of Al [360] and other materials [361] also reported a substantial enhancement of the critical temperature with respect to the bulk limit. However, granular materials are intrinsically disordered and impurities suppress shape resonances so a direct relation between theoretical and experimental results was hard to establish.

It was later realized [362, 363] that no enhancement is observed in more realistic theoretical models that impose charge neutrality at the interfaces. More refined experiments with smoother films and a better experimental control [364] observed no enhancement of

[†]A version of this chapter may be found in [358], which has been published at *Physical Review B* and is authored by Antonio M. García-García and A. R. B.

superconductivity but rather a transition at a temperature lower than the bulk mean-field theory prediction.

Recent progresses in nanotechnology and surface science, in particular epitaxial deposition and scanning tunneling microscopy/spectroscopy (STM), have dramatically improved the experimental control in low dimensions, which has led to many exciting results [365–368]. For instance, experiments on ultrathin Pb films with thicknesses ranging from a single to a few atomic monolayers [369, 365, 366] found that superconductivity is still present although weaker than in the bulk limit. Oscillations of the superconducting gap and the critical temperature, below the bulk value, for intermediate thickness, were also reported. Theoretical models proposed to described these results [370, 371] had free parameters and did not include important features such as the role of the substrate, the finite lifetime of quasiparticles, or an adequate description of the interface. As the thickness decreases, we expect that these features become increasingly important. More detailed first-principles calculations [372] of the interface in the ultrathin limit do not address superconductivity explicitly. Strikingly, experimental results in oxide interfaces [373], and even single- layered iron-based superconductors [374], exhibit, in some cases, an enhancement of the critical temperature with respect to the bulk limit. The theoretical reasons of this behavior are not yet well understood.

Motivated by these challenges, we put forward a minimal model for ultrathin superconducting films coupled to the substrate which is analytically tractable but that we expect to capture most of the relevant physics without free parameters, except the quasiparticle lifetime. However, we have found that its role is relatively minor at least in STM experiments. A refined model of the film/substrate interface, based on experimental data, would probably account for this parameter, however, this is beyond the scope of the paper.

In order to avoid the intricacies of the Kosterlitz-Thouless transition, we restrict ourselves to the low-temperature limit of weakly coupled one-band superconductor where a mean- field approach is still accurate. The film and the substrate are described by an asymmetric potential well plus a finite quasiparticle lifetime. Charge neutrality is included, although in some cases, such as in complex oxide heterostructures [375], it is unclear whether it applies. We note that in these materials, charge spreading across the interface alters boundary conditions at the interfaces leading to an electrostatic binding between the layers that can prevent the charge neutrality condition to hold. Disorder is not considered as the experiments can be carried out in the limit where the effect of impurities is negligible.

We report results for the superconducting gap (Δ) at zero temperature as a function of the film thickness for a broad range of the parameters that define the substrate and also for different electron-phonon coupling constants. The dependence of the results on the validity of the charge neutrality condition [363] is also investigated in detail. On average, the superconducting gap decreases with thickness. However, remnants of the shape resonances

are still observed in some range of parameters. For a weak coupling to the substrate, and a weak electron-phonon coupling, a modest enhancement of superconductivity is observed for certain thicknesses even if the charge neutrality condition holds. Much larger enhancement is expected for material in which the charge neutrality condition does not hold. Finally, we show that this theoretical model provides a fair qualitative description of the Pb ultrathin-film experiments mentioned above.

The paper is organized as follows. In the next section, we introduce the microscopic model that describes superconductivity and the asymmetric potential well that, together with the finite lifetime, models the substrate. The model is then solved in Sec. C by a combination of mean-field and semiclassical techniques. Then, we present results of the superconducting gap as a function of the thickness for different values of the parameters. Based on this information, we discuss the range of realistic experimental settings for which it is feasible to observe shape resonance and/or an enhancement of superconductivity and discuss the relevance of these results for recent Pb ultrathin-film experiments.

C.2 Model

We put forward a model for a superconducting thin film coupled to the substrate. Superconductivity is described by a mean-field approach. The substrate is modeled by an asymmet- ric finite well that depends on the difference between the bulk chemical potential of the materials in the film and the substrate. This confinement leads to the quantization of the momentum component perpendicular to the film plane. We also introduce a finite quasiparticle finite lifetime to describe tunneling into the substrate and any other source of decoherence. Charge neutrality is also taken into account to model the interface, but we also present present results without it as we believe that in some materials it might not fully apply. We start with a description of the theoretical model employed to describe superconductivity.

C.2.1 Mean field approach to superconductivity in thin films

In a finite-size system, the BCS Hamiltonian in terms of a set of good quantum numbers is given by

$$H = \sum_{n,\sigma} \xi_n c^\dagger_{n\sigma} c_{n\sigma} - \rho \mathcal{V} \tilde{\delta} \sum_{n,n'} c^\dagger_{n\uparrow} c^\dagger_{n\downarrow} \tilde{V}_{n,n'} c_{n'\downarrow} c_{n'\uparrow}, \tag{C.1}$$

where ρ is the dimensionless coupling constant, $\mathcal{V}$ is the system volume, $\tilde{\delta}$ is the mean level spacing [inverse of the spectral density of states at the Fermi energy (E_F)], σ is the spin index, $\xi_n = \epsilon_n - \mu$, $c_{n\sigma}$ and $c^\dagger_{n\sigma}$ are the usual quasiparticle annihilation and creation operators. The interaction matrix elements are $\tilde{V}_{n,n'} = \int_{\mathcal{V}} |\Psi_n(\vec{r})|^2 |\Psi_{n'}(\vec{r})|^2 d^3\vec{r}$ where $\Psi_n(\vec{r}) \propto e^{i(k_y y + k_z z)} \psi_n(x)$ are the three-dimensional quasiparticle eigenfunctions with

$\psi_n(x)$ the eigenstates of the one-dimensional problem in the direction perpendicular to the film.

A mean field approach to the Hamiltonian above leads to the following Bardeen-Cooper-Schrieber (BCS) gap equation at zero temperature,

$$\Delta_n = \rho\mathcal{V}\tilde{\delta}\sum_{n'}\frac{\Delta_{n'}\tilde{V}_{n,n'}}{2\sqrt{(E_{n'}-\mu)^2+\Delta_{n'}^2}}. \tag{C.2}$$

The sum is restricted to those states such that $E_{n'}$ is inside the Debye window: $|E_{n'}-\mu| < \hbar\omega_D$ where ω_D is the Debye frequency.

We consider a thin film of lateral size much larger than its thickness. Therefore, the sum in eq. (C.2) can be substituted by an integral in the in-plane momentum components, where we imposed periodic boundary conditions, and a finite sum in the perpendicular dimension.

With the previous considerations eq. (C.2) leads to the following system of equations for Δ_{k_n}, $n \in \mathbb{N}$:

$$\Delta_{k_n} = \rho\mathcal{V}\tilde{\delta}\frac{g_{2D}}{L^2}\sum_{n'=1}^{\nu}\Delta_{k_{n'}}V_{k_n,k_{n'}}\text{asinh}\left(\frac{\hbar\omega_D}{\Delta_{k_{n'}}}\right), \tag{C.3}$$

where $L^2 \to \infty$ is the thin-film area, and $V_{k_n,k_{n'}} = \int_0^a dx|\psi_{k_n}(x)|^2|\psi_{k_{n'}}(x)|^2$ (a is the film thickness) is obtained after having performed the y and z integrals in $\tilde{V}_{k_n,k_{n'}}$. $g_{2D} = m_{yz}L^2/(\pi\hbar^2)$ is the two-dimensional density of states and m_{yz} the in-plane effective mass. The factor $\text{asinh}(\hbar\omega_D/\Delta_{k_{n'}})$ comes from the integration in the in-plane momentum components.

Since $V_{k_n,k_{n'}}$ depends on k_n, eq. (C.3) is a system of non-linear equations which leads to a momentum-dependent order parameter, Δ_{k_n}. Assuming that the mean level spacing is much smaller than the bulk gap, we define the superconducting gap as [376] the minimum energy needed to excite quasiparticles, namely $\min_n \Delta_{k_n}$. This observable, which is measured by STM and other spectroscopic techniques, is the one that we use to characterize superconductivity in the system. In order to eliminate the momentum dependence of the gap, and further simplify the calculation, we replace k_n by k_ν, the highest occupied state. In this way, an approximate solution of eq. (C.3) is simply,

$$\Delta = \frac{\hbar\omega_D}{\sinh\left[K/\sum_{n=1}^{\nu}V_{k_\nu,k_n}\right]}, \quad K = \frac{\pi\hbar^2}{m_{yz}\rho\mathcal{V}\tilde{\delta}}. \tag{C.4}$$

In figs. C.3 and C.4, we show explicitly that, especially for larger values of the electron-phonon coupling constant, this is a good approximation, namely, $\Delta \approx \min_n \Delta_{k_n}$. Another reason to use this additional approximation is that the corrections of the superconducting

gap induced by a finite quasiparticle lifetime, studied in Sec. C, can easily be computed from eq. (C.4), while a calculation from eq. (C.3) is technically very demanding.

C.2.2 Model of the thin-film coupling to the substrate

The model of the coupling between the thin film and the substrate/vacuum has three ingredients: the effective potential felt by the quasiparticles due to the substrate, the finite quasiparticle lifetime, and the charge neutrality condition.

Effective potential: An asymmetric finite well

The model of an asymmetric finite well has been previously implemented [377] to study the energy spectrum and size effects in nonsuperconducting thin films. We employ the same effective potential felt by the quasiparticles in the thin film as a consequence of the substrate. As is sketched in Fig. C.1, the potential has three parameters: the height V_s of the film/substrate interface, the height V_0 of the film/vacuum interface, and the film thickness a.

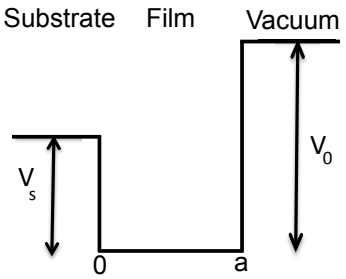

Fig. C.1 Asymmetric finite well. The values of V_s and V_0 are discussed in Sec. C.

For V_0 we take the sum of the ionization level plus the (bulk) Fermi energy of the film material. For V_s we choose the mismatch between E_F and the Fermi energy of the substrate, or conduction band edge (CBE), plus an extra contribution due to the height of a Schottky barrier at the interface. In principle a more complicated potential above the CBE might give better quantitative results. However we stick to a simpler more general approach as a truly realistic potential could result in a time-dependent problem [378]. Moreover the exact details of the potential are expected to be sensitive to the substrate material.

Before turning our attention to the solution of the Schrödinger equation in this potential we briefly comment on the dispersion relation and the boundary condition that we have employed.

Dispersion relation. Following previous works [359] we use a quadratic dispersion relation but with three parameters,

$$E(k) = a_0 + \frac{\hbar^2}{2m_x}(k + k_L)^2 \tag{C.5}$$

where a_0 and k_L determine the position of the band and the effective mass m_x controls the curvature. The motivation for introducing k_L is that it allows to describe a back-folded conduction band (see Fig. C.2) in *sp* metals such as Pb and Al commonly employed in thin-film experiments [369, 365, 379, 366, 380].

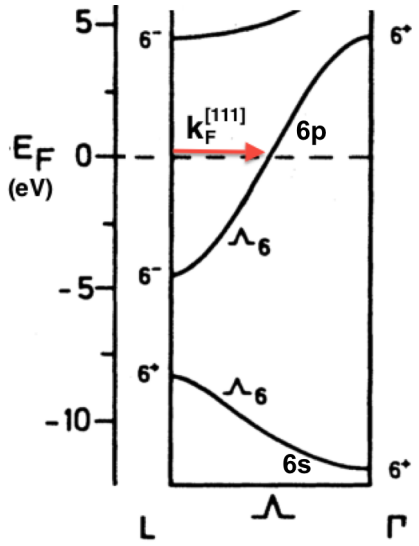

Fig. C.2 (Color online) Pb band diagram in the [111] direction [381].

For comparison with experimental results we take that quantization in the momentum-space direction ΓL, where Γ and L are the crystallographic points corresponding to zero momentum and $k \propto (1,1,1)$. This fixes $k_L = \pi/d$ where d is the distance between atomic planes in the [111] direction. For a face-centered cubic cell $d = \frac{\sqrt{3}}{3}\times$(lattice constant). We do not consider the decrease in the lattice constant at low temperatures. On the other hand $k_F^{[111]}$ (the maximum value of k in eq. (C.5)) corresponds to the momentum at which the band reaches the Fermi energy. It is such that the Fermi momentum obtained from de Haas-van Alphen experiments equals $k_F^{[111]} + k_L$.

BenDaniel-Duke boundary conditions. As usual, we impose continuity of the wavefunction in both interfaces. For the continuity of the first derivative we consider the effective masses in the film and substrate. These are known as the BenDaniel-Duke boundary conditions, commonly used in heterostructures [382],

$$\frac{1}{m_x}\frac{\partial\psi}{\partial x}\bigg|_{x=0} = \frac{1}{m_s}\frac{\partial\psi}{\partial x}\bigg|_{x=0}, \quad \frac{1}{m_x}\frac{\partial\psi}{\partial x}\bigg|_{x=a} = \frac{1}{m_e}\frac{\partial\psi}{\partial x}\bigg|_{x=a}. \tag{C.6}$$

We have placed the film/substrate interface at $x = 0$ and the film/vacuum interface at $x = a$. We have defined m_x and m_s as the effective masses in the film and substrate, respectively. In the vacuum region, we have taken the free electron mass, m_e.

With the previous considerations, the quantization condition for k (the component perpendicular to the film) is

$$(k_n + k_L)a = n\pi + \text{atan}\left(\frac{\tilde{\kappa}_0}{k_n + k_L}\right) + \text{atan}\left(\frac{\tilde{\kappa}_s}{k_n + k_L}\right) \tag{C.7}$$

with $n \in \mathbb{N}$, $\kappa_0 = \sqrt{\frac{2m_e}{\hbar^2}[V_0 - E(k_n)]}$, $\kappa_s = \sqrt{\frac{2m_e}{\hbar^2}[V_s - E(k_n)]}$, $\tilde{\kappa}_s = \frac{m_x}{m_s}\kappa_s$, and $\tilde{\kappa}_0 = \frac{m_x}{m_e}\kappa_0$. The total thin-film eigenstates are then given by

$$\begin{aligned}
\Psi_{\vec{k}}(\vec{r}) &\propto \frac{e^{i(k_y y + k_z z)}}{L^2}\psi_{k_n}(x), \\
\psi_{k_n}(x) &= A(k_n)\sin\left(k_n x + \theta\right), \ \theta = \text{atan}\frac{k_n + k_L}{\tilde{\kappa}_s} \\
A(k_n) &= \left[\frac{2k_n a + \sin(2\theta) - \sin(2k_n a + 2\theta)}{4k_n} + \right. \\
&\left. + \frac{\sin^2\theta}{2\kappa_s} + \frac{\sin^2(k_n a + \theta)}{2\kappa_0}\right]^{-\frac{1}{2}},
\end{aligned} \tag{C.8}$$

where $L^2 \to \infty$ and k_z and k_y, the in-plane momentum components, are subject to periodic boundary conditions.

Charge neutrality

As was mentioned earlier, Dirichlet/rigid boundary conditions at the interfaces, a key ingredient for the observation of large shape resonances, are not consistent [362] with the principle of charge neutrality in film surfaces. Despite the fact that our boundary conditions allow the eigenstates to extend beyond the interface, with a typical size controlled by the step heights V_0 and V_s, charge neutrality is not yet satisfied.

In order to comply with this condition, it was proposed [383] to extend the potential a distance b which is chosen so that surface charge neutrality holds. This shift b induces a phase shift, kb, which together with $\theta(k)$, the phase shift induced by the potential, must satisfy,

$$\int_0^{k_F} \left[\theta(k) + kb\right]\, k\, \mathrm{d}k = \frac{\pi k_F^2}{8}. \tag{C.9}$$

The length b is obtained by using eq. (C.8) and taking into account that the quantized component of the momentum is $k_L + k_n$,

$$\frac{\pi(k_L + k_F)^3}{8} = \int_0^{k_F} dk(k + k_L)\left[(k + k_L)b + \text{atan}\left(\frac{k + k_L}{\tilde{\kappa}_s}\right)\right]. \tag{C.10}$$

As was shown elsewhere [363], the larger b the stronger the average suppression of superconductivity. Once b is known, the quantized energy levels and eigenstates are computed for a well of thickness $\tilde{a} = a + 2b$ where a is the geometrical film thickness. We shall

see that the charge neutrality condition also modifies the chemical potential, the matrix elements $V_{k_n,k_{n'}}$, and therefore the superconducting energy gap.

Effectively, a finite b caused by charge neutrality, amounts to a modification of the boundary conditions. Therefore, it should not change the electron density or the phonon-mediated interaction. We also stress that this approximate method to satisfy charge neutrality is only valid as long as $k_F^{-1} \ll a$ [384]. Such condition might not be satisfied for films of only a few monolayers (ML) thick. Furthermore, in the film/substrate interface, there is a transition layer (*wetting layer*) [385] in which the film atoms are bonded to both the substrate and other atoms of the film. Thus, it is not clear to what extent charge neutrality is applicable in this interface. Moreover, as was mentioned previously, in complex oxide heterostructures [375] and other materials, net electric fields in the surface could severely suppress charge neutrality.

Finite lifetime

In this section, we introduce the last ingredient of our model for the coupling of the thin film to the substrate: a finite quasiparticle lifetime. The introduction of a finite quasiparticle lifetime is motivated by the existence of a non-zero probability of tunneling into the substrate. It is also an effective way to account for the realistic potential at the interface and other sources of quasiparticle decoherence, such as inelastic scattering. We shall see that it also plays an important role in the calculation of the superconducting gap and the chemical potential. We start with a theoretical description of the level broadening caused by a finite quasiparticle lifetime τ.

Smoothing of the spectral density. From the quantization condition (C.7), n can be expressed as a function of the energy, $n = n(E)$. After using the Poisson summation formula, the density of states of one-dimensional quantum well is expressed as [386]

$$g(E) = \frac{dn(E)}{dE}\left[1 + 2\sum_{l=1}^{\infty}\kappa(l)\cos\left(2l\pi n(E)\right)\right] + \frac{1}{2}\delta(E - E_1)\,, \tag{C.11}$$

where E_1 is the lowest energy state. For no level broadening ($\tau \to \infty$) $\kappa(l) = 1$ which results in a set of Dirac delta functions. However, as mentioned above, tunneling into the substrate or any decoherence mechanism induces a broadening of the energy levels which effectively is described by introducing the cutoff function $\kappa(l)$. The precise form of $\kappa(l)$ depends to some extent of the physical mechanism that induces the broadening but, in most cases, $\lim_{l\to\infty}\kappa(l) = 0$ at least exponentially fast. Here, following the results of Sec. 5.5 in Ref. [386] for the case of tunneling, we employ a Gaussian cutoff,

$$\kappa(l) \approx e^{-(lt/\tau)^2}, \tag{C.12}$$

where $t = \frac{2m_x a}{\hbar(k+k_L)}$, m_x is the effective mass in the direction perpendicular to the film, and τ is the lifetime. Once the energy spectrum is smoothed by a finite lifetime, it is straightforward to calculate the chemical potential and the superconducting order parameter. However, before doing so, we have to evaluate the modification of the matrix elements which also enter in the gap equation.

Matrix elements for states with a finite lifetime. In order to calculate how the matrix elements are modified for a finite quasiparticle lifetime we use the approach put forward by Dijk and Nogami [378] based on the calculation of the probability of an initial state to stay inside the well.

The study of unstable or unbound eigenstates in a quantum system is an intrinsically time-dependent problem. Even though we are not interested in a time-evolution analysis, this framework allows to obtain the superposition between the initial wavefunction and the bound states. This superposition is given by the probability to stay in the film,

$$P(t) = \int_0^L |\psi(x,t)|^2 dx, \tag{C.13}$$

where $\psi(x,t)$ is the initial wavefunction expressed as a linear combination of the bound and quasi-bound eigenstates. The latter can be casted as Moshinsky functions [378] which eventually escape from the potential. Therefore, for large times, $P(t)$ is given by the product of the amplitude of the bound states inside the potential, $\int_0^L dx|\psi_b(x)|^2$, multiplied by the superposition of the initial state and the bound eigenstate, namely $|c_b|^2$, where $c_b = \int_{-\infty}^{\infty} \psi_b(x)\psi(x,0)dx$, i.e.,

$$P(t \to \infty) \to |c_b|^2 \int_0^L dx|\psi_b(x)|^2, \tag{C.14}$$

where $\psi_b(x)$ is a bound state of the potential well. For large times it is expected that $\psi(x,0) \to c_b\psi_b(x)$. Therefore the probability of finding the particle confined in the well will be very small provided that c_b is small. It is then natural to express the matrix elements that enter in the gap equation as,

$$V_{k_n,k_{n'}} = \int_0^a dx|c_b(k_n)\psi_{k_n}(x)|^2|c_b(k_{n'})\psi_{k_{n'}}(x)|^2. \tag{C.15}$$

We now rewrite the eigenstates in eq. (C.8) as

$$\psi^b_{k_n}(x) = \begin{cases} C_4 e^{\kappa_s x}, & x < 0 \\ C_2 e^{i(k_n+k_L)x} + C_3 e^{-i(k_n+k_L)x}, & 0 < x < a \\ C_1 e^{-\kappa_0(x-a)}, & x > a \end{cases} \tag{C.16}$$

where, κ_0, κ_s were defined previously and $C_2 = \frac{C_4}{2}\left[1 + \frac{\tilde{\kappa}_s}{i(k_n+k_L)}\right]$, $C_3 = \frac{C_4}{2}\left[1 - \frac{\tilde{\kappa}_s}{i(k_n+k_L)}\right]$, $C_1 = C_2 e^{i(k_n+k_L)a} + C_3 e^{-i(k_n+k_L)a}$ and, from the normalization condition,

$$|C_4|^{-2} = \frac{1}{2\kappa_s} + \frac{|C_1|^2}{2\kappa_0|C_4|^2} + \frac{1}{|C_4|^2}\int_0^a dx|\psi_n^b(x)|^2.$$

We also assume that the 'initial" unstable state has an energy: $E = E_n + i\Gamma/2 = E_n + i\hbar/(2\tau)$, where E_n is the quantized energy given by eqs. (C.5) and (C.7). The initial state is given by the same type of wavefunction as eq. (C.16) but with the following modifications:

- We replace κ_0 and κ_s (see Sec. C) by $\kappa_0 = \text{Re}\left[\sqrt{\frac{2m_e}{\hbar^2}(V_0 - E_n - i\frac{\hbar}{2\tau})}\right]$ and $\kappa_s = \text{Re}\left[\sqrt{\frac{2m_e}{\hbar^2}(V_s - E_n - i\frac{\hbar}{2\tau})}\right]$. A complex part in κ_s or κ_0 leads to divergent terms in the matrix elements.

- For $0 < x < a$ we substitute the quantized momentum $k_n \in \mathbb{R}$ by a complex-valued λ_n. We let $\lambda_r = \text{Re}(\lambda_n)$ and $\lambda_i = \text{Im}(\lambda_n)$ and substitute $\lambda_n = \lambda_r + i\lambda_i$ in the dispersion relation of eq. (C.5), with $A = \frac{2m_x}{\hbar^2}(E_n - a_0)$ and $B = \frac{2m_x}{\hbar^2}\frac{\hbar}{2\tau}$. Moreover C_2, C_3 and C_1 above are replaced by, $D_2 = \frac{C_4}{2}\left[1 + \frac{\tilde{\kappa}_s}{i(\lambda_n+k_L)}\right]$, $D_3 = \frac{C_4}{2}\left[1 - \frac{\tilde{\kappa}_s}{i(\lambda_n+k_L)}\right]$ and $D_1 = D_2 e^{i(\lambda_n+k_L)a} + D_3 e^{-i(\lambda_n+k_L)a}$. That results in the following expression for the energy levels,

$$\begin{aligned} E_n + i\frac{\hbar}{2\tau} &= a_0 + \frac{\hbar^2}{2m_x}(\lambda_r + i\lambda_i + k_L)^2\,, \text{where} \\ &\begin{cases} \lambda_r = -k_L + \frac{1}{\sqrt{2}}\sqrt{A + \sqrt{A^2+B^2}} \\ \lambda_i = \sqrt{2}\frac{A}{\sqrt{B}}\sqrt{A + \sqrt{A^2+B^2}} + \\ \quad - \frac{1}{\sqrt{2}B}\left(\sqrt{A + \sqrt{A^2+B^2}}\right)^3 \end{cases} \end{aligned} \tag{C.17}$$

We have now all the necessary information to compute the initial state $\psi_{\lambda_n}(x,0)$ and then the weighting factor $c_b(k_n) = \int_{-\infty}^{\infty}\psi_{k_n}^b(x)\psi_{\lambda_n}(x,0)dx$. We find it more convenient to express $c_b(k_n)$ as a function of energy E since the BCS gap equation will be expressed also in terms of this variable. To that end, we substitute $k_{n'}$ in eq. (C.15) by $k(E) = -k_L + \sqrt{(E-a_0)2m_x/\hbar^2}$. The resulting final expression for the matrix elements is therefore,

$$\begin{aligned} V(\tilde{E}, E) &= \int_0^a dx|c_{b(\tilde{E})}\psi_{k(\tilde{E})}^b(x)|^2|c_{b(E)}\psi_{k(E)}^b(x)|^2, \\ c_{b(E)} &= \int_{-\infty}^{\infty}\psi_{k(E)}^b(x)\psi_{\lambda(E)}(x,0)dx. \end{aligned} \tag{C.18}$$

Superconductivity in thin films in the presence of a substrate and a finite quasiparticle lifetime

Having obtained explicit expressions for the matrix elements (C.18) and the spectral density (C.11), it is straightforward to find the chemical potential μ and the superconducting gap Δ. For instance, for μ,

$$\begin{aligned} N &= \int_0^{\mu} dE_x \sum_{n'=1}^{\nu} \delta(E_x - E_n) \int_0^{\mu - E_x} dE_{yz} g_{2D} \rightarrow \\ \frac{N}{V}\frac{\pi\hbar^2 a}{m_{yz}} &= \sum_{n'=1}^{\nu} (\mu - E_n) = \nu\mu - \sum_{n'=1}^{\nu} E_n, \end{aligned} \tag{C.19}$$

where N/V is the electron density, E_x and E_{yz} are the energies corresponding to the out-of-plane and in-plane momentum components, respectively. The former is quantized, $E_x = E_n$, and ν is the number of occupied states. The smoothed spectrum is taken into account by replacing the sum in n' by an integral in energy,

$$\sum_{n=1}^{\nu} (\mu - E_n) \rightarrow \int_{E_1}^{\mu} dE(\mu - E) g(E) = \frac{N}{V}\frac{\pi\hbar^2 a}{m_{yz}} \tag{C.20}$$

valid for $E_1 < \mu < V_s$. Similarly, for the energy-dependent order parameter [Eq. (C.3)],

$$\Delta(\tilde{E}) = \frac{1}{K}\int_{E_1}^{\mu} dE g(E)\Delta(E) \operatorname{asinh}\left(\frac{\hbar\omega_D}{\Delta(E)}\right) V(\tilde{E}, E) \tag{C.21}$$

where $V(\tilde{E}, E)$ is given in eq. (C.18) and $K = \frac{\pi\hbar^2}{m_{yz}\rho\mathcal{V}\tilde{\delta}}$. This is a non-linear Fredholm integral equation of the second kind with a non-degenerate kernel. A more tractable expression is obtained by substituting $\tilde{E}$ by E_ν in the previous equation. In other words the gap is approximated by the order parameter evaluated at the energy of the highest occupied state $\Delta(E_\nu)$ and, for consistency, the interaction $V(\tilde{E}, E)$ is replaced with $V(E_\nu, E)$. These approximations, that neglect the energy dependence of the order parameter, result in the following algebraic expression for the energy gap,

$$\Delta = \frac{\hbar\omega_D}{\sinh\left[K/\int_{E_1}^{\mu} dE\ V(E_\nu, E) g(E)\right]}, \quad K = \frac{\pi\hbar^2}{m_{yz}\rho\mathcal{V}\tilde{\delta}}. \tag{C.22}$$

Numerical results, depicted in figs. C.3 and C.4, show that the substitution $\tilde{E}$ by E_ν or equivalently k_n by k_ν in eq. (C.3) is in general a good approximation for the spectroscopic gap $\min_n \Delta(k_n)$, namely, $\Delta \approx \min_n \Delta(k_n)$. In the rest of the paper, unless it is explicitly stated otherwise, we use eq.(C.22) to compute the superconducting gap.

C.3 Results

In this section we study the superconducting order parameter Δ [eq.(C.22)] for a one-band thin film coupled to a substrate as a function of film thickness and the parameters that define the substrate and the superconducting material. Our calculation includes the charge neutrality condition which should hold in Pb and other metallic superconductors except maybe in the limit of a few ML thickness. We also present results without imposing the charge neutrality condition as it is believed that in some materials, such as complex oxide heterostructures [375] might not hold. We have two main motivations for this study: to provide a qualitative description of recent experiments involving Pb ultra-thin [369, 366] films and also to clarify whether, in some range of parameters, size effects in thin films can enhance the critical temperature with respect to the bulk limit.

As was mentioned previously, the coupling to the substrate is modeled by the asymmetric finite well depicted in Fig. C.1. The height in the film/vacuum interface V_s is taken to be the bulk Fermi energy of the film plus the work function of the corresponding material. The height V_0 in the film/substrate interface is chosen to be the mismatch of the Fermi energies of the thin film and substrate materials plus the height of the Schottky barrier. We assign a finite quasiparticle lifetime τ to all states, including those under the barrier. This is necessary as the exact details of the potential at the interface are not well understood. Moreover, inelastic scattering and other processes will induce level broadening even when tunneling is not relevant. Based on recent experiments in Pb films [379], we assume a linear dependence of $\tau = \beta + \gamma a$. The first term on the right-hand side, with a the film thickness, describes tunneling into the substrate. The constant β accounts for other size-independent mechanisms of level broadening.

C.3.1 Parameters: Pb films grown over a Si substrate

In this section, we introduce the range of parameters that we use in the calculation of the superconducting gap. First, we focus in one of the best studied settings [369]: Pb thin films grown over a Si substrate.

As discussed in Sec. C, the dispersion relation is described in terms of three parameters k_L, a_0, and m_x, the effective mass in the direction perpendicular to the film. The first is fixed by the inter-atomic plane distance $k_L = \pi/d$ while the other two are set in order to describe the bulk Pb Fermi level and the minimum of the Pb band in the crystallographic L point. Other relevant parameters in the calculation of the chemical potential and the energy gap are the in-plane effective mass and the electron density $\frac{N}{V}$. The exact value of the in-plane effective mass m_{yz} and its dependence with the film thickness are still a subject of discussion [387, 388]. We are not interested to study this effect at the moment and fix it to a constant value. We also impose that for a very large thickness, eq.(C.19) leads to a chemical potential equal to the Fermi energy. With these considerations in mind

we now state the values of the parameters we employ,

$$\begin{aligned} m_x = 1.180 m_e, \quad a_0 = 1.57 \text{ eV}, \\ k_L = \frac{\pi}{d} = 10.99 \text{ nm}^{-1}, \quad k_F^{[111]} = 0.450 \frac{\pi}{d} = 4.95 \text{ nm}^{-1}, \\ m_{yz} = 1.380 m_e, \quad \frac{N}{V} = 20.69 \text{ nm}^{-3}, \ E_F = 9.77 \text{ eV}. \end{aligned} \tag{C.23}$$

m_x is close to the value reported in the literature $m_x = 1.14 m_e$ [389], while $k_F^{[111]}$ is taken from Refs. [365, 390]. $d = \frac{\sqrt{3}}{3} 0.4951 = 0.2858$ nm is the distance between (111) planes. With these parameters, the energy of the band that we study (see Fig. C.2) ranges from 5.47 eV at the L point to the Fermi energy, 9.77 eV [381]. Finally, for the substrate effective mass in the direction perpendicular to the interface we take $m_s = 0.28 m_e$ [391].

The next step to model the thin film is to the impose the charge neutrality condition. From eq.C.10) and by using the parameters above, we have found that, in order to comply with this condition, the thin-film thickness a must be effectively extended to $a \to a + 2b$ with,

$$b = 0.0686 \text{ nm}. \tag{C.24}$$

This is less than half the distance between (111) atomic planes approximately. This correction is smaller than for a free-standing film [363] since the potential from Fig. C.1, in contrast to an infinite potential well, allows already leaking of probability out of the film.

The parameters of the asymmetric potential that characterize the substrate are chosen as follows: for the height in the film/vacuum interface, we take the work function above the Fermi energy, $W_F = 4.25$ eV. The height of potential at the substrate–thin-film interface is the mismatch between the CBE of the substrate and the bulk Fermi energy of the film plus the height of the Schottky barrier. For Pb/Si films, the Si CBE is 0.8 eV above the Pb Fermi energy [379] while we use 0.9 eV for the height of the Schottky barrier corresponding to the $(\sqrt{3} \times \sqrt{3})R30°$ orientation [392]. The asymmetric well potential is therefore characterized by,

$$V_s = E_F + 0.80\text{eV} + 0.90\text{eV} = 11.47 \text{ eV}, \ V_0 = 14.02 \text{ eV}. \tag{C.25}$$

Pb is not a weakly coupled superconductor so in principle the Eliashberg theory of superconductivity is more suitable to describe its properties. However the BCS prediction for the temperature dependence of the superconducting order parameter describes the experimental data reasonably well [393, 365], even for a single Pb atomic monolayer [366]. For that reason, and taking into account that our main interest is the superconducting gap, we have decided to use the simpler BCS introduced previously to describe size effect in this material. We employ the following values of the Debye energy and the dimensionless

coupling constant [394]

$$\hbar\omega_D = 9.048 \text{ meV}, \;\; \rho = 0.385 \rightarrow \Delta_0 = 1.35 \text{ meV}, \tag{C.26}$$

The last element in our model is the quasipartcle lifetime τ. For sufficiently small $\tau = \tau_0$, we expect suppression of all size effects. This scale corresponds to a level broadening comparable to the one-dimensional mean level spacing, $\frac{\Gamma_0}{2} \sim \delta_{1\text{D}} = \frac{1}{g_{1\text{D}}(E_F)} = \frac{2}{a}\frac{E_F - a_0}{k_F}$, where a_0 is defined in eq. (C.5). The lifetime related to this energy is,

$$\tau_0 = \frac{2\hbar}{\Gamma_0} \sim \frac{\hbar k_F}{2(E_F - a_0)} a, \tag{C.27}$$

which for Pb is $\tau_0 = 0.18(N-1)$ fs, where N is the number of monolayers. Therefore, for $\tau \gg \tau_0$, decoherence effects are small but for $\tau \sim \tau_0$ size effects related to quantum coherence will be strongly suppressed.

We employ a simple linear model for the lifetime,

$$\tau = \beta + \gamma a. \tag{C.28}$$

with $\beta, \gamma > 0$ and a the thickness. As was explained above, if tunneling into the substrate is relevant, τ is expected to be proportional to the thickness a. This a good approximation provided the tunneling probability is constant for every thickness considered. In other words, we assume the interface potential does not change as the film thickness changes. Additionally, we include a constant term β which accounts for other decoherence effects. In principle, it is tempting to relate β to level broadening by electron-electron scattering. The scattering rate can be estimated from Fermi liquid theory: $\Gamma_{e-e} = \alpha(E - E_F)^2$ by substituting $E - E_F$ by $\delta_{1\text{D}}$, the one-dimensional mean level spacing. This yields a scattering rate $\Gamma_{e-e} \simeq \frac{0.02}{a^2}$ eV, with a in nm, which is more than two orders of magnitude smaller than the critical broadening $\Gamma_0 \propto 1/\tau_0$. Therefore, it seems that it does not play a significant role in our system. We take $\beta \sim \tau_0$ so that, by tuning γ, we can study the full range of corrections induced by a finite lifetime. In that way we can determine, for a given set of parameters, the range of τ's for which corrections due to a fine lifetime are relevant. Finally we also assume that the smoothing of the spectral density is well described by eq. (C.11).

C.3.2 Size effects in the superconducting energy gap

In this section, we first investigate the superconducting order parameter for Pb thin films coupled to a Si substrate in the absence of tunneling. We study the role of the coupling to the substrate in the shape resonances as well the effect of charge neutrality in suppressing superconductivity. We then discuss the smoothing of size effects by a finite lifetime τ. Finally, we move from Pb in order to investigate size effects in a weakly

coupled superconducting thin film by simply modifying the Debye energy and dimensionless coupling constant while leaving the rest of the parameters unchanged.

Infinite lifetime

In this section, we consider the limit of no level broadening ($\tau \to \infty$) with the substrate described by the asymmetric well (Fig. C.1). The momentum-dependent order parameter is obtained from eq. (C.3) where, as was mentioned in Sec. C, the superconducting gap is the minimum of the order parameter. We also approximate the solution of eq. (C.3) by assuming a $k-$independent order parameter eq. (C.4). In figs. C.3 and C.4, we analyze the differences between the two predictions for different values of the asymmetric potential.

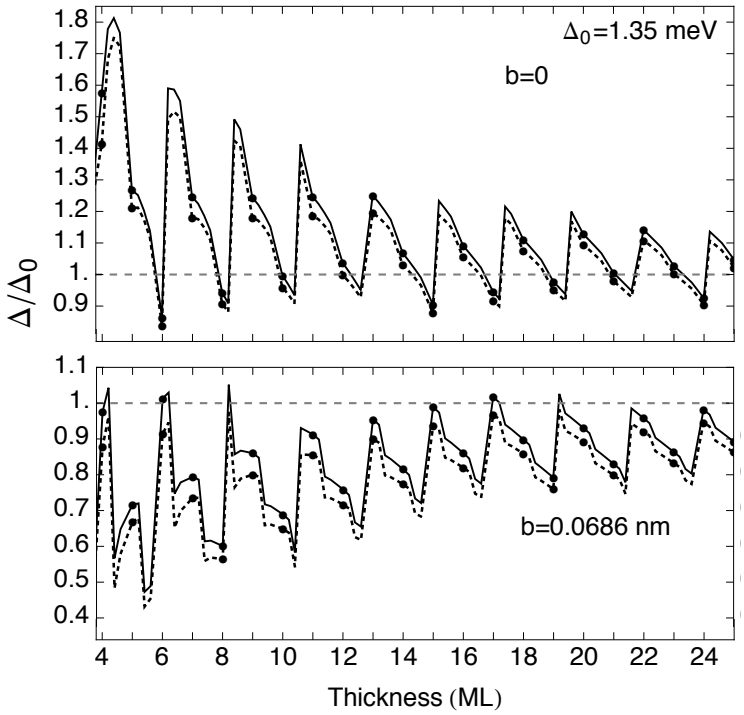

Fig. C.3 Superconducting order parameter Δ for a Pb thin-film coupled to a Si substrate. Δ_0 is the bulk Pb gap. The film/interface coupling is modeled by an asymmetric well potential with $V_s = E_F + 1.70$ eV, $V_0 = E_F + 4.25$ eV. Level broadening is assumed to be negligible. The dimensionless coupling constant is $\rho = 0.385$ and the Debye energy $\hbar\omega_D = 9.048$ meV. The band structure parameters are given in eq. (C.23). The upper plot does not satisfy the charge neutrality condition while the lower plot does it with b obtained from eq.(C.10). Lines show the evolution of the order parameter as a function of the thickness. Dots correspond to the estimate positions of Pb monolayers. The continuous and dashed lines show the difference between the $k-$dependent gap with $\Delta = \min_n \Delta(k_n)$ from eq. (C.3) and the $k-$independent Δ from eq. (C.4) respectively. We note the pattern of shape resonances is more intricate than in Ref. [359] as a consequence of the interplay between the finite number of states in the asymmetric well potential and the more realistic dispersion relation.

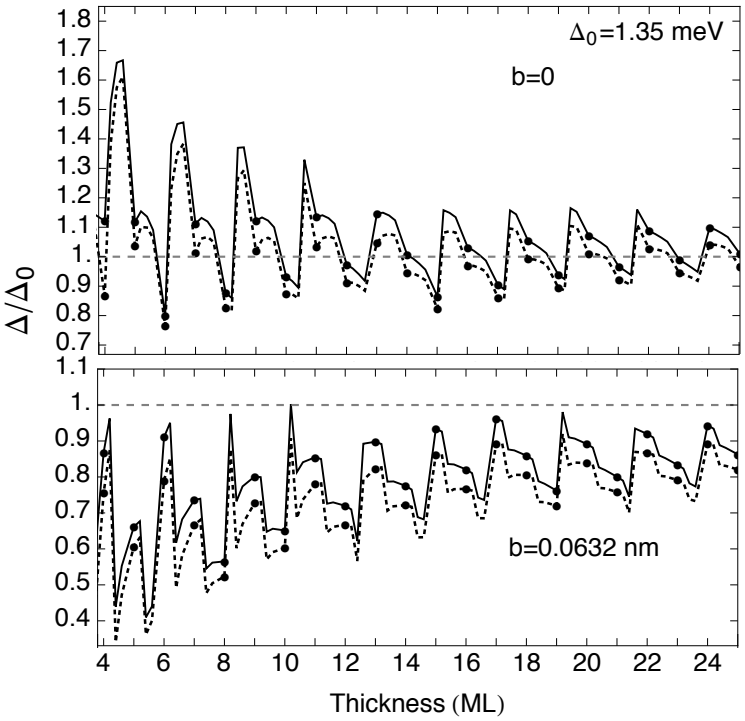

Fig. C.4 Superconducting order parameter Δ for a Pb film coupled to a Si substrate with no level broadening. $V_s = E_F + 0.9$ eV, $V_0 = E_F + 4.25$ eV. Δ_0 is the bulk Pb gap. The parameters correspond to those of Fig. C.3 except for the smaller step V_s and b obtained from eq. (C.10). The continuous line corresponds to the $k-$dependent gap with $\Delta = \min_n \Delta(k_n)$ from eq. (C.3) and the dashed line corresponds to the $k-$independent Δ from eq. (C.4). The $k-$independent approximation becomes less accurate as the step height decreases. As was expected, reducing the height of the film/substrate interface increases the leaking of probability out of the film which, reduces both the superconducting gap Δ and the effect of the charge neutrality condition measured by b. Moreover, the pattern of shape resonances is richer as the number of bound states is smaller in this case.

The pattern of shape resonances is qualitatively similar in both cases. It is clear however that the approximate solution (C.4) is always below the actual gap (C.3). This difference is more evident in Fig. C.4 where the potential is shallower and the coupling to the substrate is therefore stronger. Given that the system of equations (C.3), can easily be solved without any approximation, in principle there is no substantial advantage in using the approximate solution. However, once a finite lifetime is considered, the approximate solution to the order parameter is still easily obtained from eq. (C.22), while the momentum-dependent order parameter ought to be calculated from the integral equation (C.21), is much more difficult to solve. For that reason, and because the results are qualitatively similar, we stick to eq. (C.22) to compute the superconducting gap in the rest of the paper.

We are now ready to study the role of the substrate in our results. In Fig. C.3, we compute the superconducting gap with the parameters defined in eq. (C.23). For the

film/substrate height we take $V_s = E_F + 1.7$ eV which accounts for the Fermi level mismatch with the substrate plus the height of the Schottky barrier. In Fig. C.4 we remove the Schottky barrier contribution leaving $V_s = E_F + 0.8$ eV where 0.8 eV corresponds to the Fermi level mismatch with the substrate. As was expected from the model used to couple the film to the substrate, introduced in Sec. C, and the expressions of the BCS interaction matrix elements, introduced in Sec. C, we observe that a decrease of the potential height is accompanied by an average suppression of superconductivity. This is a simple consequence of two facts, the states are more extended into the substrate and the potential has less bound states.

Moreover, as a consequence of the coupling to the substrate, the pattern of shape resonances differs from that of an infinite well [359] where Δ decreases monotonically with the thickness until another state is occupied. Our results, depicted in figs. C.3 and C.4, show as the potential height decreases, the momentum dependence of the order parameter becomes more relevant yielding an additional non monotonic behavior with additional features. These extra features are originated by the combined effect of the momentum-dependent interaction, the finite number of states in the asymmetric well, and the off-centered dispersion relation (C.5). The maxima and minima do not necessarily correspond to a different number of occupied states in the considered band ($6p$ band in Fig. C.2).

As the thickness increases, the occupied states are lowered in the potential well (more bounded) which yields the moderate, smooth increase observed in the above plots between two prominent peaks. For some thickness the lower state in the upper band reaches the minimum at the L point and thereupon this electron occupies a state in the lower $6s$ band. At the same time another available state in the $6p$ band is occupied and thus, even though the number of occupied states in the $6p$ band is the same, these are higher in energy (less bounded) yielding a sudden decrease. Finally, for a larger thickness the number of occupied states in the $6p$ band increases and a large increase is observed.

The previous figures show the effect of charge neutrality is qualitatively similar to that in an infinite potential well [363], the average Δ decreases the thinner the film is. Furthermore, as V_s decreases, the charge neutrality correction, measured by b, is smaller. In other words, both charge neutrality and a reduction of the potential height have a similar effect: to suppress superconductivity so that for all thicknesses the gap is below the bulk limit.

As was mentioned in Sec. C, the method used to impose charge neutrality is only valid in the limit $k_F^{-1} \ll a$. For Pb films in the range of thickness studied $k_F^{-1} \leq 15\times$thickness, however, the validity of the method is less clear as the thickness decreases. Furthermore, it is still under discussion as to whether, or to what extent, this condition realizes in realistic nano-structures [395].

Finite lifetime

We now study the role of a finite lifetime τ that describes tunneling out of the film and other sources of decoherence. Following results of previous sections we use the smoother density of states (C.11) to compute first the chemical potential (C.20) and finally the superconducting energy gap (C.22).

We assume a linear dependence of τ with the thickness. Shape resonances in the superconducting gap at zero temperature, depicted in Fig. C.5, are suppressed for τ comparable to τ_0 [Eq. (C.27)], the time scale related to the mean level spacing in the asymmetric well potential. More precisely, for Pb/Si films of less than 10 ML the suppression is considerable when $\tau \leq 10\tau_0$ (see the blue data). This suppression is clearer if one considers the experimentally accessible thicknesses (integer numbers of monolayers): the red and blue dots in the previous figure show that it is indeed expected to measure small oscillations in Δ of a Pb thin film.
For smaller τ, the effect of level broadening completely smears size effects however in this range of lifetime the leading effect is to suppress superconductivity, $\Delta \to 0$, due to the modification introduced in the interaction matrix elements [Eq.(C.18)].

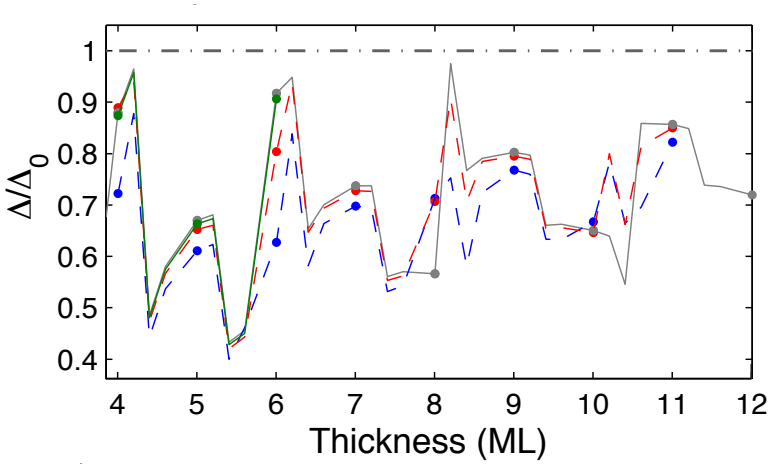

Fig. C.5 (Color online) Superconducting order parameter Δ at $T = 0$ for Pb films on a Si substrate for different quasiparticle lifetimes. Δ_0 is the bulk Pb gap, $\rho = 0.385$, and $\hbar\omega_D = 9.048$ meV. Results include the charge neutrality condition. The gray line corresponds to the limit of no level broadening ($\tau \to \infty$) [Eq. (C.4)] (green) $\tau(\text{fs}) = \tau_0 + 3N$,(red) $\tau(\text{fs}) = \tau_0 + 1.5N$, and (blue) $\tau(\text{fs}) = \tau_0 + 0.7N$ where N is the number of ML. These values are chosen in order to estimate the range in which finite-τ corrections are relevant. For less than 10ML this occurs for $\tau \leq 10\tau_0$, with τ_0 given by eq. (C.27). Dots correspond to the exact position of the Pb monolayers.

It is also clear that, especially for small thicknesses, charge neutrality is the dominant mechanism for suppression of superconductivity. It reduces substantially the value of the gap Δ so that it is under the bulk value in the full range of parameters investigated.

Comparison with experiments

Recent STM experiments on a single monolayer of Pb deposited on Si [366] indicate sharp peaks in the tunneling data which correspond, approximately, to τ, two orders of magnitude larger than the one used here. This suggests that in this setting, tunneling into the substrate is negligible even for one atomic monolayer.

In this limit (see results depicted in figs. C.3 and C.4), we have observed that, in agreement with the experimental results, size effects in the presence of the substrate, and including the charge neutrality condition, lead to a superconducting gap which is below the bulk limit. As the film thickness approaches the 1-ML limit, the exponential tails of the thin-film eigenstates into the substrate become longer and therefore we expect a strong suppression of the gap. Strictly speaking, this limit can not be studied quantitatively within our model since we neglect other effects that might become relevant in this situation, such as surface phonons or the enhancement of Coulomb interactions. However, our model still predicts a strong suppression superconductivity.

The results presented in Fig. C.5, which include a finite lifetime, provide a good description of the superconducting gap in thin Pb/Si films obtained by transport measurements [369]. Our model reproduces correctly the small oscillations of the critical temperature observed experimentally in the region $\sim$ 20ML, the gradual suppression of the average gap as thickness is reduced and the smoothing of shape resonance for $\leq$ 15ML.

We note that the main difference between the two experiments is the presence of a capped layer in Ref. [369] needed to carry out transport measurements. Even if tunneling into the substrate is negligible, as the STM results of Ref. [366] suggest, the film coupling to the overlayer still causes important decoherence effects which in our model correspond to a much smaller choice of τ than in the description of the STM experiment.

In summary, by tuning τ we are able to describe qualitatively the experimental results of Refs. [369, 366]. We note in the particular case of Pb/Si films the Si band gap in the crystallographic direction perpendicular to the interface yields a strong state confinement in the Pb film and thus tunneling into the substrate is suppressed. However, for other cases, such as Al films, the confinement is not caused [396] by a band gap and thus tunneling can be a relevant source of decoherence that can be included with the model presented in Sec. C. Nonetheless, in this case it is likely that more sophisticated theoretical models of the interface are necessary for a quantitative description of the experimental results.

Weakly coupled superconductors

From the results of the previous section it seems rather unrealistic, at least in Pb, to enhance superconductivity by size effects. Lead is a strong coupled superconductor so it would be interesting to explore whether size effects are stronger in materials characterized by a weaker coupling constant ρ. Indeed, from eq. (C.4) it is straightforward to show that the first-order correction to Δ is inversely proportional to the coupling constant ρ.

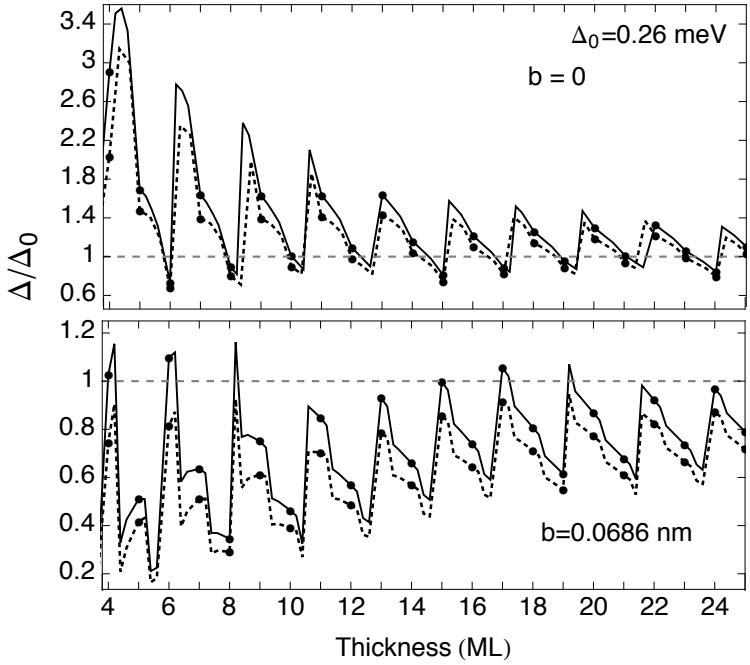

Fig. C.6 Superconducting gap Δ in units of the bulk gap Δ_0 for $\tau \to \infty$. All parameters are equal to those of Fig. C.3 except the dimensionless coupling constant $\rho = 0.180$ and the Debye energy $\hbar\omega = 33.882$ meV. Results in the upper plot do not satisfy the charge neutrality condition while the lower plot does include it with b obtained from eq.(C.10). The gap $\Delta = \min_n \Delta(k_n)$ (continuous line) shows a moderate enhancement of superconductivity, even when charge neutrality is imposed. By contrast no enhancement is observed (dashed line) in the approximate solution eq. (C.4).

Therefore, the smaller ρ, the larger the finite size correction. Even if charge neutrality applies, the oscillations of the superconducting gap are expected to show higher maxima, with respect to the bulk limit, for smaller ρ which might lead to an enhancement of superconductivity. In this section, the dimensionless coupling constant is decreased to $\rho = 0.180$ and the Debye energy is set to $\hbar\omega = 33.882$ meV. We analyze the case of $\tau \to \infty$ and maintain the same parameters for the band structure and the asymmetric potential [Eqs. (C.23)-(C.25)], as here our goal is to explore the dependence on the coupling constant ρ rather than to model a specific material.

The results, depicted in Fig. C.6, show a considerable enhancement of superconductivity when charge neutrality is not imposed. If it is included a moderate enhancement is still observed for a few values of the thickness. As for Pb, see figs. C.3 and C.4, the exact solution $\Delta = \min_n \Delta(k_n)$ (continuous line), eq. (C.3), predicts a larger gap than the approximation, eq. (C.4) (dashed line). Indeed we observe a net enhancement only in the case $\Delta = \min_n \Delta(k_n)$. This is a strong suggestion that an enhancement of superconductivity might occur for a finite lifetime provided that the gap is computed directly from eq. (C.21). We note that the approximate solution (blue) shows no enhancement of Δ with respect to the bulk limit even for $\tau \to \infty$ so finite τ corrections, eq. (C.22), would induce a further suppression of the energy gap.

In summary, weakly coupled superconducting materials are more promising candidates to observe an enhancement of superconductivity in thin films and nanostructures provided the quasiparticle lifetime is much larger than τ_0, eq. (C.27).

C.4 Conclusions

We have investigated analytically the effect of the substrate on superconducting thin films. We aim to provide a description of recent Pb thin-film experiments and also to identify a region of parameters in which size effects could enhance superconductivity. Superconductivity is modeled by a mean-field formalism. The model of the coupling of the thin film to the substrate has three ingredients: an asymmetric quantum well, a finite quasiparticle lifetime (that describes tunnelling into the substrate and other decoherence mechanisms), and the charge neutrality condition on the interfaces. For Pb on a Si substrate, we observe small oscillations, remnants of shape resonances, of the energy gap as thickness is decreased but always below the bulk limit for realistic values of the quasiparticle lifetime and the interface potential. This is fully consistent with the transport measurements of Ref. [369] in which a capped layer induces additional level broadening, for sufficiently thin films. In the limit of negligible broadening our results are also consistent with the *in situ* STM experiments of Ref. [366] in which a capped layer is not present. For materials with a smaller electron-phonon coupling constant, size effects are stronger. We identify a range of parameters, $\tau > 20$fs, thicknesses ≤ 10ML, for which a modest enhancement of superconductivity is feasible even if charge neutrality holds. A stronger enhancement is expected provided that charge neutrality does not apply. This seems to be the case in complex oxide heterostructures.

D

Shape resonances and shell effects in thin film multi-band superconductors[†]

D.1 Introduction

Advances in sample growth and a better experimental control have substantially reinvigorated research in low-dimensional superconductivity [398–400, 368, 401, 402]. Refined scanning tunneling microscope techniques have been recently employed [368, 403] to study superconductivity in single isolated nanograins and also measure its size. It has also become possible [401, 402] to measure with unprecedented precision the size dependence of the capacitance in nanoscale superconducting islands. Epitaxial growth of superconducting thin films by adding single atomic layers [398–400], together with scanning tunneling microscope techniques, have permitted one to track the evolution of superconductivity as the film approaches the two-dimensional limit. For Pb, it was found that, on average, the critical temperature (T_c) is a decreasing function of the thickness. Oscillations, below the bulk critical temperature, were observed for intermediate thicknesses [398].

These oscillations in T_c have been predicted theoretically [359] in the limit of no coupling to the substrate. However, the maxima of the oscillating pattern, usually referred to as shape resonances, were expected to correspond to T_c substantially higher than in the bulk limit. These shape resonances occur as a consequence of an enhancement of the spectral density at the Fermi energy for thicknesses for which a new quantum state becomes available in the well potential that describes the confinement in the dimension perpendicular to the thin film. It was later realized [362, 363, 404, 370] that more realistic

[†]A version of this chapter may be found in [397], which has been published at *Physical Review B* and is authored by Antonio M. García-García and A. R. B.

boundary conditions, including the charge neutrality condition, suppress this enhancement. In contrast, recent studies of heterostructures and interfaces based on cuprates [405], iron pnictides [406] and $LaAlO_3/SrTiO_3$ [407] heterostructures have clearly shown that superconductivity can occur on a single atomic layer and that the critical temperature can be enhanced with respect to the bulk limit.

From these results it is not yet clear whether it is possible to enhance superconductivity in thin films by simply tuning the thickness. The enhancement observed in interfaces and heterostructures based on cuprates or iron-based superconductors, which is of special interest due to its high critical temperature, is difficult to model theoretically as there is not yet a good understanding of these materials. In contrast, magnesium diboride (MgB_2), a two-band superconductor, is a more attractive choice as it has a relatively high critical temperature ($\sim$ 39 K) but still is a conventional superconductor [408] for which many theoretical tools are available. In recent experiments, it has been possible to grow good quality MgB_2 films of thicknesses less than 10nm [409, 366, 410]. Despite these advances the experimental control and growth techniques in MgB_2 films are still not comparable to Pb and other metallic superconductors, but the gap is rapidly closing.

It is, therefore, timely to develop a theoretical description of quantum size effects in multiband thin-film superconductors that can clarify whether superconductivity is enhanced in some region of parameters. Indeed, several papers [411–416] have already studied size effects in thin-film multiband superconductors, but a definitive answer is still missing: Bianconi and co-workers [412–415] were the first to suggest, by combining qualitative arguments with numerical simulations, that shape resonances could enhance superconductivity in MgB_2 and others multiband superconductors. Shell effects in multi-band superconductors [416], though suppressed with respect to the one-band case, are still capable of increasing the critical temperature with respect to the bulk limit. By contrast, a numerical analysis of MgB_2 thin films [411] that included the charge neutrality condition at the surface, but did not address directly the role of the substrate or shell effects, showed no enhancement of superconductivity.

Here we generalize the one-band model of Thompson and Blatt [359] for infinite thin film to the multiband case, including finite lateral size effects and the coupling to the substrate. Explicit analytical results are obtained by combining mean-field and semi-classical techniques. Therefore, our model is capable of accounting for the interplay of shape resonances and shell effects that can enhance superconductivity and the multi-band structure and the substrate that tend to suppress these coherence effects. All of these ingredients are important in the description of realistic thin films with negligible disorder.

The main results of the paper are summarized as follows: for an infinite, free-standing, multiband thin film, we observe that the critical temperature is a non monotonous function of the thickness with maxima well above the bulk limit but smaller than in the one-band case. Once the substrate is included, the oscillations in the T_c are significantly reduced.

For MgB_2 , we do not observe a substantial enhancement of the critical temperature. For materials, such as metallic superconductors, with a longer coherence length, or weaker electron-phonon coupling, size effects are stronger and an enhancement of T_c by tuning the thickness is feasible. A finite lateral size does also affect the average value of the shape resonances and induces shell effects with the potential to further increase T_c with respect to the bulk limit.

The paper is organized as follows. First we review the one-band thin-film model of Thompson and Blatt. [359] Then, within a mean-field approach, we generalize it to the case of two-band superconductors including, by semiclassical techniques, the effect of a finite lateral size and the leakage of probability due to the coupling with the substrate. In the second part of the paper we explore the evolution of T_c with thickness as a function of the lateral size, band structure parameters, electron-phonon interaction strength and the coupling to the substrate. We discuss the optimal settings to enhance superconductivity in realistic multiband thin films. Explicit results are presented for MgB_2 as well as for other band structure parameters and electron-phonon coupling constants.

D.2 Background: One-band superconducting thin film

We start with a brief summary of the Thompson and Blatt [359] mean-field description of shape resonances in free-standing–Dirichlet boundary conditions–one-band thin films. For a thin film of infinite lateral size, the one-particle electron eigenstates are simply

$$\psi_{\vec{k}}(\vec{r}) \sim u_n(x)\frac{1}{L}e^{i(k_y y+k_z z)}, \tag{D.1}$$

where periodic boundary conditions have been imposed in the lateral dimensions, y and z, and $\psi_{\vec{k}}(x=0)=\psi_{\vec{k}}(x=a)=0$ in the perpendicular dimension x where a is the thin-film thickness. The latter results in

$$u_n(x)=\sqrt{\frac{2}{a}}\sin\left(\frac{n\pi x}{a}\right),\ n\in\mathbb{N}. \tag{D.2}$$

For a finite-size system, where the spectrum is discrete, the BCS Hamiltonian in terms of a set of good quantum numbers, for instance n in eq. (D.2), is,

$$\begin{aligned} H &= \sum_{n,\sigma\alpha}\xi_{n\alpha}c^{\alpha\dagger}_{n\sigma}c^{\alpha}_{n\sigma}+\sum_{n,n',\alpha,\beta}c^{\alpha\dagger}_{n\uparrow}c^{\alpha\dagger}_{n\downarrow}V_{\alpha n,\beta n'}c^{\beta}_{n'\downarrow}c^{\beta}_{n'\uparrow\beta} \\ V_{\alpha n,\beta n'} &= -\lambda_{\alpha\beta}\tilde{\delta}_\alpha\mathcal{V}\int_{\mathcal{V}}\psi^2_{n\alpha}(\vec{r})\psi^2_{n'\beta}(\vec{r})d^3\vec{r} \end{aligned} \tag{D.3}$$

where $V_{\alpha n,\beta n'}$ are the interaction matrix elements, $\lambda_{\alpha\beta}$ are the dimensionless inter- and intraband coupling constants, $\mathcal{V}$ is the volume, $\tilde{\delta}_\alpha$ is the mean level spacing (the inverse of the density of states at the Fermi level), σ is the spin index, α and β are the band indices,

and $\xi_{n\alpha} = \epsilon_{n\alpha} - \mu$ and $c_{n\sigma}$, $c^{\dagger}_{n\sigma}$ are the usual quasiparticle annihilation and creation operators.

The maximum quantum number allowed, $n \equiv \nu$ in eq. (D.2) must occur for a film thickness in the interval $[a_\nu, a_{\nu+1}]$, where[359]

$$a_\nu^3 = \frac{\pi}{2N/V}\left(\frac{2}{3}\nu^3 - \frac{\nu^2}{2} - \frac{\nu}{6}\right). \tag{D.4}$$

For a thickness $a \in [a_\nu, a_{\nu+1}]$, the superconducting order parameter Δ, obtained from the Hamiltonian given by eq. (D.3) in the mean-field approximation, and chemical potential μ are given by [359]

$$\begin{aligned} \mu &= \frac{\pi\hbar^2 a}{\nu m}\left[\frac{N}{V} + \frac{\pi}{6a^3}\nu(\nu+\frac{1}{2})(\nu+1)\right] \\ \Delta &= \frac{\hbar\omega_D}{\sinh[Ka/(\nu+1/2)]},\ K = \frac{1}{\lambda}\left(\frac{3N}{\pi V}\right)^{1/3} \end{aligned} \tag{D.5}$$

where λ is the dimensionless coupling constant, N/V is the number of electrons per unit volume and $\hbar\omega_D$ is the Debye energy.

For sufficiently small thicknesses a, $\nu = 0$ and the system is purely two dimensional. However, as the thickness is increased, eventually $\nu = 1$, which corresponds to a subband of allowed states in the perpendicular dimension. This increases the spectral density around the Fermi energy. The dimensionless electron-phonon coupling constant is proportional to the spectral density, so an enhancement of the latter increases the former. As a consequence, the order parameter and the critical temperature increase as well. This is what is usually called a shape resonance. As the thickness further increases, there exists a region in which still $\nu = 1$. The spectral density gradually becomes smaller and the critical temperature decreases. For the smallest thickness for which $\nu = 2$ a new sub-band is available which induces a new enhancement of superconductivity. As is depicted in fig. D.1, that results in a saw-like dependence of the superconducting gap and the critical temperature as a function of the film thickness.

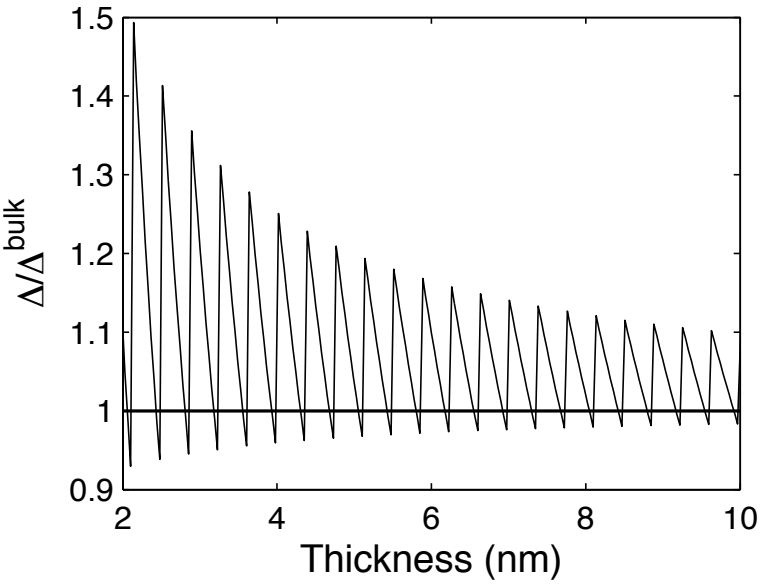

Fig. D.1 The superconducting order parameter Δ at $T = 0$ K in units of the bulk value Δ^{bulk} as a function of the film thickness for a free standing one-band superconducting thin film. [359] Shape resonances are clearly observed as the thickness is increased each time a new state becomes available in the direction perpendicular to the film.

D.3 Two-band superconducting thin film

D.3.1 Free-standing film model

In this section, we extend the Blatt and Thompson formalism to the case of a two-band superconductor. Assuming again periodic boundary conditions in the lateral dimensions and Dirichlet boundary conditions in the perpendicular dimension, we have the equivalent of eq. (D.1) in each band, but now with two quantum numbers: n_σ, n_π, analogous to n in eq. (D.2). The dispersion relation is still quadratic,

$$\begin{aligned}
\epsilon_{\vec{k}}^{(\sigma)} &= \frac{\hbar^2}{2}\left(\frac{(k_y^{(\sigma)})^2}{m_{2\sigma}} + \frac{(k_z^{(\sigma)})^2}{m_{3\sigma}}\right) + \frac{\hbar^2}{2m_{1\sigma}}\left(\frac{n_\sigma \pi}{a}\right)^2 \\
\epsilon_{\vec{k}}^{(\pi)} &= \frac{\hbar^2}{2}\left(\frac{(k_y^{(\pi)})^2}{m_{2\pi}} + \frac{(k_z^{(\pi)})^2}{m_{3\pi}}\right) + \frac{\hbar^2}{2m_{1\pi}}\left(\frac{n_\pi \pi}{a}\right)^2 + e_{0\pi}
\end{aligned} \tag{D.6}$$

but with an offset $e_{0\pi}$ between the two bands. A mean-field treatment of the microscopic Hamiltonian given by eq. (D.3) for the two-band system [414–416, 411] results in the following two coupled gap equations at zero temperature:

$$\begin{aligned}\Delta_\sigma &= -\frac{1}{2}\sum_{k'}\left[\frac{\Delta_\sigma V_{\sigma k\sigma k'}}{\sqrt{(\epsilon_\sigma-\mu)^2+\Delta_\sigma^2}}+\frac{\Delta_\pi V_{\sigma k\pi k'}}{\sqrt{(\epsilon_\pi-\mu)^2+\Delta_\pi^2}}\right]\\ \Delta_\pi &= -\frac{1}{2}\sum_{k'}\left[\frac{\Delta_\sigma V_{\pi k\sigma k'}}{\sqrt{(\epsilon_\sigma-\mu)^2+\Delta_\sigma^2}}+\frac{\Delta_\pi V_{\pi k\pi k'}}{\sqrt{(\epsilon_\pi-\mu)^2+\Delta_\pi^2}}\right]\end{aligned} \tag{D.7}$$

while at finite temperature a factor $\tanh[\sqrt{(\epsilon_\alpha-\mu)^2+\Delta_\alpha^2}/2k_BT]$ multiplies each term on the right-hand side of the equations; the index α takes the value of the index of the order parameter in the corresponding term.

$V_{\alpha k\beta k'}$ are the interaction matrix elements corresponding to two intraband coupling constants and two interband coupling constants,

$$V_{\alpha k\beta k'} = -J_{\alpha\beta}\int_{\mathcal{V}} d^3\vec{r}\,|\psi_{\mathbf{k}}^{(\alpha)}(\vec{r})|^2|\psi_{\mathbf{k}'}^{(\beta)}(\vec{r})|^2 = -\frac{J_{\alpha\beta}}{aL^2}\left(1+\frac{1}{2}\delta_{n_\alpha n'_\beta}\right), \tag{D.8}$$

where α and β take the value of the band labels σ and π. $J_{\alpha\beta}=\lambda_{\alpha\beta}\mathcal{V}\tilde{\delta}_\alpha$ and $\psi_{\mathbf{k}}^{(\alpha)}(\vec{r})$ are of the form given by eq. (D.1).

We then substitute eq. (D.8) into (D.7) and perform the sums in $k_y^{(\sigma)}$, $k_z^{(\sigma)}$, $k_y^{(\pi)}$, $k_z^{(\pi)}$ by introducing the two-dimensional density of states in each band.[1] After carrying out the resulting integrations, we obtain the following system of two coupled equations at $T=0$:

$$\begin{aligned}\Delta_\sigma &= \frac{1}{2aL^2}\left[\Delta_\sigma J_{\sigma\sigma}g_{2D}^{(\sigma)}f(\sigma)+J_{\sigma\pi}\Delta_\pi g_{2D}^{(\pi)}f(\pi)\right]\\ \Delta_\pi &= \frac{1}{2aL^2}\left[\Delta_\pi J_{\pi\pi}g_{2D}^{(\pi)}f(\pi)+J_{\pi\sigma}\Delta_\sigma g_{2D}^{(\sigma)}f(\sigma)\right],\end{aligned} \tag{D.9}$$

with $f(\alpha)=\left(\nu_\alpha+\frac{1}{2}\right)\operatorname{asinh}\left(\frac{\hbar\omega_D}{\Delta_\alpha}\right)$.

For the calculation of the critical temperature a simple algebraic manipulation of eq. (D.7) leads to the following relation between the two gaps,

$$\frac{1+\frac{1}{2}\sum_{k'}\frac{V_{\sigma k\sigma k'}}{\sqrt{(\epsilon_\sigma-\mu)^2+\Delta_\sigma^2}}\tanh\frac{\sqrt{(\epsilon_\sigma-\mu)^2+\Delta_\sigma^2}}{2k_BT}}{\frac{1}{2}\sum_{k'}\frac{V_{\pi k\sigma k'}}{\sqrt{(\epsilon_\sigma-\mu)^2+\Delta_\sigma^2}}\tanh\frac{\sqrt{(\epsilon_\sigma-\mu)^2+\Delta_\sigma^2}}{2k_BT}} = \frac{\frac{1}{2}\sum_{k'}\frac{V_{\sigma k\pi k'}}{\sqrt{(\epsilon_\pi-\mu)^2+\Delta_\pi^2}}\tanh\frac{\sqrt{(\epsilon_\pi-\mu)^2+\Delta_\pi^2}}{2k_BT}}{1+\frac{1}{2}\sum_{k'}\frac{V_{\pi k\pi k'}}{\sqrt{(\epsilon_\pi-\mu)^2+\Delta_\pi^2}}\tanh\frac{\sqrt{(\epsilon_\pi-\mu)^2+\Delta_\pi^2}}{2k_BT}}. \tag{D.10}$$

[1] For the dispersion relations given by eq. (D.6), the two-dimensional density of states is $g_{2D}^{(\alpha)}=\frac{L^2\sqrt{m_{1\alpha}m_{2\alpha}}}{\pi\hbar^2}$.

Repeating the steps described previously to obtain eq. (D.9) and taking the limits $\Delta_\sigma, \Delta_\pi \to 0$ and $T \to T_c$ gives,

$$\frac{1-\frac{J_{\sigma,\sigma}g^{\sigma}_{2D}}{2aL^2}(\nu_\sigma+\frac{1}{2})F(T_c)}{-\frac{J_{\pi,\sigma}g^{\sigma}_{2D}}{2aL^2}(\nu_\sigma+\frac{1}{2})F(T_c)}=\frac{-\frac{J_{\sigma,\pi}g^{\pi}_{2D}}{2aL^2}(\nu_\pi+\frac{1}{2})F(T_c)}{1-\frac{J_{\pi,\pi}g^{\pi}_{2D}}{2aL^2}(\nu_\pi+\frac{1}{2})F(T_c)}. \tag{D.11}$$

We have used that for $b \gg 1$, $\int_0^b \mathrm{d}x \tanh(x)/x \simeq \log\left(\frac{4e^\gamma}{\pi}b\right) = F(T)$, with γ the Euler-Mascheroni constant and $b = \frac{\hbar\omega_D}{2k_BT_c}$. We note that ν_π and ν_σ, i.e., the generalization of ν in Thompson and Blatt's one-band model given by eqs. (D.4) and (D.5), are the maximum integers for which the condition $|\epsilon^{(\alpha)}_{\vec{k}} - \mu| \leq \hbar\omega_D$ holds. The superconducting gaps $\Delta_\alpha(T=0)$ and the critical temperature T_c are therefore obtained by solving eqs. (D.9) and (D.11), respectively. Similarly, the chemical potential μ is obtained analytically from

$$\begin{aligned} N &= \int_0^\mu [g^\sigma_{3D}(E) + g^\pi_{3D}(E)]\mathrm{d}E = \sum_{j=1}^{\nu_\sigma}\int_0^{\mu-\eta^\sigma_j} g^\sigma_{2D}\mathrm{d}\xi^\sigma_{xy} + \sum_{j=1}^{\nu_\pi}\int_0^{\mu-\eta^\pi_j} g^\pi_{2D}\mathrm{d}\xi^\pi_{xy} = \\ &= \sum_{j=1}^{\nu_\sigma} g^\sigma_{2D}(\mu-\eta^\sigma_j) + \sum_{j=1}^{\nu_\pi} g^\pi_{2D}(\mu-\eta^\pi_j) \end{aligned} \tag{D.12}$$

where $\eta^\pi_j(a) = e_{0\pi} + \frac{\hbar^2\pi^2j^2}{2m_{1\pi}a^2}$ and $\eta^\sigma_j(a) = \frac{\hbar^2\pi^2j^2}{2m_{1\sigma}a^2}$.

Using Faulhaber's formula for the second power sum of the first n positive integers, it is also straightforward to obtain and explicit expression for the chemical potential,

$$\mu = \frac{a\pi\hbar^2}{\nu_\sigma m^{*\sigma} + \nu_\pi m^{*\pi}}\left[\frac{N}{V} + \frac{\pi}{2a^3}\left(\frac{m^{*\sigma}h(\nu_\sigma)}{m_{1\sigma}} + \frac{m^{*\pi}h(\nu_\pi)}{m_{1\pi}}\right)\right] + \frac{e_{0\pi}\nu_\pi m^{*\pi}}{\nu_\sigma m^{*\sigma} + \nu_\pi m^{*\pi}}, \tag{D.13}$$

with $m^{*\alpha} = \sqrt{m_{2\alpha}m_{3\alpha}}$ and $h(\nu_\alpha) = \frac{\nu^3_\alpha}{3} + \frac{\nu^2_\alpha}{2} + \frac{\nu_\alpha}{6}$.

In order to find $a = a(\nu_\sigma, \nu_\pi)$ we first assume a value of ν_σ, ν_π such that $\mu \simeq \eta^\pi_{\nu_\pi}(a) \simeq \eta^\sigma_{\nu_\sigma}(a)$, i.e.,

$$\nu_\sigma \simeq \sqrt{\frac{m_{1\sigma}}{m_{1\pi}}\nu^2_\pi + \frac{2m_{1\sigma}a^2}{\pi^2\hbar^2}e_{0\pi}}. \tag{D.14}$$

Substituting, for every $\nu_\pi = 1, 2, 3...$, both μ and ν_σ in eq. (D.13), we solve for a and then calculate all of the possible states that are occupied as the thickness increases. In order to proceed, we start with arbitrary values of ν_σ, ν_π and assume that either $\eta^\sigma_{\nu_\sigma} > \eta^\pi_{\nu_\pi}$ or $\eta^\sigma_{\nu_\sigma} < \eta^\pi_{\nu_\pi}$, which results either in $\mu \simeq \eta^\sigma_{\nu_\sigma}$ or in $\mu \simeq \eta^\pi_{\nu_\pi}$ where, in order to simplify the notation, we have dropped the dependence in the thickness a. By substituting these expressions into eq. (D.12) we obtain two equations for a which are solved numerically. Once a is obtained, we check which assumption ($\eta^\sigma_{\nu_\sigma} > \eta^\pi_{\nu_\pi}$ or $\eta^\sigma_{\nu_\sigma} < \eta^\pi_{\nu_\pi}$) holds and obtain the chemical potential from eq. (D.13).

From these solutions we get the chemical potential given by eq. (D.13), the gap given

by eq. (D.9), and the critical temperature given by eq. (D.11) for a fixed ν_σ, ν_π and $a \in [a_{\nu_\sigma\nu_\pi}, a_{\tilde{\nu}_\sigma\tilde{\nu}_\pi}]$, where $\nu_\sigma\nu_\pi$, $\tilde{\nu}_\sigma\tilde{\nu}_\pi$ are consecutive states of the spectrum.

D.3.2 Role of the substrate

In realistic circumstances, a thin film is never isolated. It is usually placed on a substrate so there is some probability for the electrons to hop from the film into the substrate or at least penetrate a finite distance in it. Generally, this can be taken into account by assigning a finite lifetime to the quantized states and also by modeling the substrate thin-film interface by a potential more realistic than an infinite well.
The details of the coupling between the substrate and the thin film are very sensitive to the substrate material and the nature of the interface which depends on the growth techniques. A detailed microscopic description of the tunneling process is beyond the scope of this paper.
Here we use recent experimental results [410] for MgB_2 and assume a linear dependence for the level broadening with the film thickness. We note that both the energy spectrum and the wavefunctions inside the film are modified by tunneling into the substrate. The latter has a direct impact on the interaction matrix elements given by eq. (D.8), while the former smoothes out the one dimensional density of states from a set of isolated Dirac's delta functions to a distribution with broader peaks.
In order to proceed, we write the density of states [386] as,

$$g^\alpha(E) = \frac{dn^\alpha(E)}{dE}\left[1 + 2\sum_{l=1}^{\infty}\kappa(l)\cos\left(2l\pi n^\alpha(E)\right)\right], \tag{D.15}$$

where $n^\alpha(E) = \sqrt{(E - e_{0\alpha})/E_0^\alpha}$ and $n \in \mathbb{N}$ in the case of an infinite well potential, $E_0^\alpha = \hbar^2\pi^2/(2m_{1\alpha}a^2)$, $e_{0\sigma} = 0$ and $e_{0\pi} \neq 0$. For no tunneling into the substrate, $\kappa(l) = 1$ and we recover the usual expression in terms of Dirac delta functions. Tunneling or any other decoherence mechanism makes the system open which effectively induces level broadening, namely, the eigenvalues become complex. A natural way to mimic this effect is to introduce a cutoff,

$$\kappa(l) \approx e^{-(lt/\tau)^2}, \tag{D.16}$$

where $t = 2m_{1\alpha}a/\hbar k_n^\alpha$ and τ is the typical lifetime of a quasiparticle at that energy. Physically, it is the typical time that an electron stays in the thin film. The specific functional form of $\kappa(l)$ depends to some extent on the mechanism that causes decoherence. The above result is obtained (see sec. 5.5 in Ref. [386] for more details) by replacing the original Dirac delta functions with Gaussians of width $\Gamma \sim \hbar/\tau$.

Regarding the energy quantization, we model the thin film plus the substrate as a semi-infinite potential well, infinite in the film/vacuum interface and finite in the film/substrate interface. The height of the step corresponds to the mismatch between the bulk Fermi levels of the film and substrate materials. Furthermore it will also be assumed that the

lifetime of all of the states is described by a single parameter since the total energy of the states is always very close to the Fermi level.

D.3.3 Chemical potential of a two-band film on a substrate

In order to compute the chemical potential in the presence of the substrate, we apply the Poisson summation formula, [417] given in eq. (D.6.29), to eq. (D.12) (see Appendix). This results in the following transcendental equation for μ:

$$N = \sum_{j=1}^{\nu_\sigma} g_{2D}^{\sigma}(\mu - \eta_j^{\sigma}) + \sum_{j=1}^{\nu_\pi} g_{2D}^{\pi}(\mu - \eta_j^{\pi}) =$$
$$= \sum_{\alpha} g_{2D}^{\alpha} \left\{ \frac{2}{3\sqrt{E_0^{\alpha}}}(\mu - e_{0\alpha})^{3/2} - \frac{\mu - e_{0\alpha}}{2} + \sum_{l=1}^{\infty} \left[-\frac{\sqrt{(\mu - e_{0\alpha})E_0^{\alpha}}}{\pi^2 l^2} \cos\left(2\pi l \sqrt{\frac{\mu - e_{0\alpha}}{E_0^{\alpha}}}\right) \right.\right.$$
$$\left.\left. + \frac{E_0^{\alpha}}{2\pi^3 l^3} \sin\left(2\pi l \sqrt{\frac{\mu - e_{0\alpha}}{E_0^{\alpha}}}\right) \right] e^{-(lt/\tau_\alpha)^2} \right\}, \tag{D.17}$$

where the sum over α refers to both bands, $E_0^{\alpha} = \hbar^2\pi^2/(2m_{1\alpha}a^2)$, $e_{0\sigma} = 0$ and $e_{0\pi} \neq 0$.

D.3.4 Matrix elements and critical temperature of a two-band film on a substrate

Before we proceed to the computation of the critical temperature we study the modification of the interaction matrix elements by the coupling to the substrate. We expect smaller matrix elements than those given by the infinite potential well model[359] since the amplitude of probability for all of the states inside the well is smaller. Moreover, since the energy states have a finite lifetime, the interaction is weighted by a smooth density of states, resulting in smooth shape resonances. The eigenstates inside a semi-infinite potential well are

$$u_n^{(in)}(x) = A_n \sin(k_n x), \tag{D.18}$$

where k_n is the solution of the quantization condition: $k_n a = n\pi - 2\arctan(-k/\tilde{\kappa}_n)$, $\tilde{\kappa}_n = \frac{m_{in}}{m_{out}}\kappa_n = \frac{m_{in}}{m_{out}}\sqrt{\frac{2m_{out}}{\hbar^2}(V_0 - E_n)}$ obtained after imposing the BenDanield-Duke boundary conditions:[382]

$$\frac{1}{m_{out}} \frac{\partial u_n^{(out)}}{\partial x}\bigg|_{x=b} = \frac{1}{m_{in}} \frac{\partial u_n^{(in)}}{\partial x}\bigg|_{x=b} \tag{D.19}$$

where b is the position of the interface and m_{out} (m_{in}) is the effective mass outside (inside) of the well. We have taken the free electron mass for m_{out} and $m_{1\alpha}$ for m_{in}.
The matrix elements resulting from the above expression for u_n lead to a system of equations for two momentum-dependent superconducting order parameters, which are difficult to solve. In order to have a more tractable expression, we approximate the interaction of all of the states by the interaction of the states whose energies are equidistant between those

corresponding to the highest and lowest occupied levels. If the highest (lowest) occupied states were used to estimate the interaction, the eigenstates' leakage out of the film would be overestimated (underestimated). In our notation, this means the replacement of A_n by A_{m_α} and k_n by k_{m_α}, where m_α refers, from now on, to the state whose energy is the closest to being equidistant from the highest- and the lowest-energy states. Moreover, we approximate k_n in the argument of the sine of eq. (D.18) by $n\pi/a$, while leaving the amplitude A_n unchanged.

With these further simplifications, the matrix elements are,

$$V_{\alpha k\beta k'} = -\frac{aJ_{\alpha\beta}}{4L^2}K_{\alpha\beta}\left(1+\frac{1}{2}\delta_{n_\alpha n'_\beta}\right), \tag{D.20}$$

with $K_{\alpha\beta} = |A_{m_\alpha}|^2|A_{m_\beta}|^2$, given explicitly in eq. (D.6.31). We now take into account the smoothed spectrum given by eq. (D.15) due to the substrate. The sums of the matrix elements in eq. (D.10) are simplified to

$$\begin{aligned}\sum_{n'_\beta=1}^{\nu_\beta}\left(1+\frac{1}{2}\delta_{n_\alpha n'_\beta}\right) &= \frac{1}{2}+\int_{e_{0\beta}}^{\mu} g^\beta(E)dE = f(\beta),\\ f(\beta) &\equiv \frac{1}{2}+\sqrt{\frac{\mu-e_{0\beta}}{E_0^\beta}}+\sum_{l=1}^{\infty}\frac{e^{-\frac{tl}{\tau_\beta}}}{\pi l}\sin\left(2\pi l\sqrt{\frac{\mu-e_{0\beta}}{E_0^\beta}}\right),\end{aligned} \tag{D.21}$$

where $e_{0\sigma}=0$ and $e_{0\pi}\neq 0$. Finally we substitute eqs. (D.20) and (D.21) into eq. (D.10) to obtain

$$\frac{1-\frac{aJ_{\sigma,\sigma}g_{2D}^\sigma}{8L^2}K_{\sigma\sigma}f(\sigma)F(T_c)}{-\frac{aJ_{\pi,\sigma}g_{2D}^\sigma}{8L^2}K_{\pi\sigma}f(\sigma)F(T_c)} = \frac{-\frac{aJ_{\sigma,\pi}g_{2D}^\pi}{8L^2}K_{\sigma\pi}f(\pi)F(T_c)}{1-\frac{aJ_{\pi,\pi}g_{2D}^\pi}{8L^2}K_{\pi\pi}f(\pi)F(T_c)}, \tag{D.22}$$

where $F(T_c)=\log\left(\frac{4e^\gamma}{\pi}\frac{\hbar\omega_D}{2k_BT_c}\right)$, $K_{\alpha\beta}$ is given in eq. (D.6.31), and $f(\alpha)$ is given in eq. (D.21). The final step to compute the critical temperature is to solve eq. (D.22) for T_c and different thicknesses.

D.3.5 Lateral size effects in a two-band superconducting thin film

We now study the case in which the thin-film lateral size dimensions ($y=L_1$ and $z=L_2$) become comparable to the film thickness a. We will not go through the details of the calculations regarding the modification of the two-dimensional density of states. A detailed derivation can be found in Ref. [418]. The underlying idea is to use the semiclassical approximation, valid in the limit $(k_FL)^{-1}\ll 1$ with L in this case the lateral film size, to write down the density of states as a sum over the classical periodic orbits of the two-dimensional system. The density of states is an oscillatory function of the energy around the Fermi level so, in principle, it should enter explicitly in the sums over k_y and k_z which are needed to solve the gap equation (D.7). However, it was demonstrated in Ref.

[418] that the density of states can be taken out of the integral, provided it is smoothed out, as follows:

$$\tilde{g}_{2D}^{(\alpha)} \simeq g_{2D}^{(\alpha)}[1 + \overline{g}^{(\alpha)} + g_l^{(\alpha)}], \tag{D.23}$$

where the correction $\overline{g}^{(\alpha)}$ is an average term, while $g_l^{(\alpha)}$ is an oscillatory term that depends on the length l of the periodic orbits in the yz plane. These corrections are,

$$\begin{aligned} \overline{g}^{(\alpha)} &= -\frac{L_1 + L_2}{k_{yz}^{(\alpha)} L_1 L_2}, \\ g_l^{(\alpha)} &= g_{12}^{(2\alpha)} - \frac{1}{2} g_1^{(1\alpha)} - \frac{1}{2} g_2^{(1\alpha)}, \end{aligned} \tag{D.24}$$

and

$$\begin{aligned} g_{12}^{(2\alpha)} &= \sum_{\vec{n}\neq\vec{0}}^{\infty} J_0(k_{yz}^{(\alpha)} L_{\vec{n}}^{1,2}) \times K_0(L_{\vec{n}}^{1,2}/\xi^{(\alpha)}), \\ g_1^{(1\alpha)} &= \frac{4}{k_{yz}^{(\alpha)} L_2} \sum_{n=1}^{\infty} \cos\left(k_{yz}^{(\alpha)} L_n^{(1)}\right) \times K_0(L_n^{(1)}/\xi^{(\alpha)}), \\ g_2^{(1\alpha)} &= \frac{4}{k_{yz}^{(\alpha)} L_1} \sum_{n=1}^{\infty} \cos\left(k_{yz}^{(\alpha)} L_n^{(2)}\right) \times K_0(L_n^{(2)}/\xi^{(\alpha)}), \end{aligned} \tag{D.25}$$

with α the band index and $k_{yz}^{(\alpha)}$ the in-plane Fermi momentum. $L_{\vec{n}}^{1,2} = 2\sqrt{L_1^2 n_1^2 + L_2^2 n_2^2}$, $L_n^{(1)} = 2nL_1$, $L_n^{(2)} = 2nL_2$, $n,\ n_1,\ n_2 \in \mathbb{N}$ are the lengths of the periodic orbits. $J_0(x)$ is the Bessel function of the first kind and $K_0(x)$ is the modified Bessel function of the first kind which suppresses the contribution of orbits longer than the superconducting coherence length in the yz-plane, $\xi^{(\alpha)}$. Therefore, replacing $g_{2D}^{(\alpha)}$ by $\tilde{g}_{2D}^{(\alpha)}$ in the equations obtained for an infinite thin film, we simulate a finite lateral size, comparable but still larger than the thickness.

D.3.6 Quantum and thermal fluctuations

The mean-field formalism that we use is only applicable for sufficiently large systems for which quantum and thermal fluctuations are negligible. In the case of a thin film with infinite lateral size, quantum fluctuations due to size effects are negligible. At finite temperature, experimental results [366, 393, 400] seem to be well described by a mean-field theory even in the limit of few monolayers. This is, at first glance, surprising because, at least in the strictly two-dimensional limit, it is expected that at finite temperature there is a Kosterlitz-Thouless transition due to vortex anti-vortex unbinding. A reason for this unexpected behavior might be that the coupling to the substrate increases the effective system dimensionality. However, this must still be considered an open problem. Here we take a conservative approach and present results for thin films of at least several monolayers where it is expected, especially taking into account the coupling of the substrate, that a

mean-field approach is applicable.
As the finite lateral size enters the nanoscale region, the thin film becomes effectively a zero-dimensional grain. At very low temperatures ($T \ll T_c$), the deviations from mean-field predictions caused by quantum fluctuations can be neglected when the mean level spacing δ is smaller than the BCS bulk energy gap $\delta/\Delta_{bulk} \ll 1$ [419, 420]. At finite temperature, thermal fluctuations smear out the superconducting phase transition in a region of temperatures γT_c, with $\gamma = \sqrt{\delta/k_B T_c}$, around the bulk T_c [421]. We restrict the range of lateral sizes so that these deviations from the mean-field predictions are negligible.

D.4 Results

In this section, we employ the theoretical formalism developed previously in order to study the interplay between shape resonances and shell effects that, in some cases, enhance superconductivity. We also investigate the influence of the coupling to the substrate and the multi-band structure that tend to suppress these size effects.
We present explicit results for the evolution of superconductivity in a two-band thin film as a function of the thickness, including also the coupling to the substrate. First we report results on the differences between one and two bands, the dependence of T_c on the coupling constant, and the band structure parameters. We then investigate the role of shell effects that occurs when the lateral size becomes comparable to the thickness. Most results correspond to MgB_2 , but we also explore a broader range of parameters (see below) in order to clarify whether in realistic situations it is feasible to observe an enhancement of superconductivity due to shape resonances.
The coupling to the substrate is modeled by a finite step potential of height (V_0), which corresponds to the difference between the substrate and the thin-film chemical potential. Moreover we assign a phenomenological finite lifetime to all of the states $\tau = \gamma + \beta a$, where a is the thickness and the parameters β and γ are estimated from recent experimental results in MgB_2 thin films [410].
As was mentioned previously, V_0 and τ modify the density of states in the superconductor and therefore are important to understand its role to suppress size effects.

The effective masses that enter in quadratic dispersion relation for each band, calculated from $m_{i\alpha} = |\partial^2 E^{(\alpha)}/\partial k_i^2|$ where $E^{(\alpha)}$ is the full energy band for MgB_2,[422] are, in units of the electron mass,

$$\begin{aligned} m_{1\sigma} &= 3.27, \quad m_{2\sigma} = m_{3\sigma} = 0.28 \\ m_{1\pi} &= 0.33, \quad m_{2\pi} = m_{3\pi} = 1.00. \end{aligned} \tag{D.26}$$

The constant $e_{0\pi}$ is set to different values as a way to study the influence of the band structure on superconductivity. The Debye temperature in MgB_2 is $\theta_D = 1050$ K, which corresponds to a Debye energy $E_D = \hbar\omega_D = 90.48$ meV. The factors $J_{\alpha,\beta} g_{2D}^{\beta}/2aL^2$ in eq. (D.11) and $aJ_{\alpha,\beta} g_{2D}^{\beta} K_{\alpha\beta}/8L^2$ in eq. (D.22) were fixed such that the solution in the bulk

limit is the MgB_2 critical temperature $T_c \approx 38.01$ K. Finally, we use the following set of coupling constants [411]:

$$\begin{aligned} g_\sigma = 0.149 \text{ eV}^{-1} \quad g_\pi = 0.29 \text{ eV}^{-1} \\ \tilde{V}_{\sigma,\sigma} = 0.694 \text{ eV} \quad \tilde{V}_{\pi,\pi} = 0.056 \text{ eV} \quad \tilde{V}_{\sigma,\pi} = \tilde{V}_{\pi,\sigma} = 0.353 \text{ eV} \\ \lambda_{\sigma\sigma} = 0.206 \quad \lambda_{\pi\pi} = 0.033 \quad \lambda_{\sigma\pi} = 0.205 \quad \lambda_{\pi\sigma} = 0.105. \end{aligned} \tag{D.27}$$

In sec. D, we employ another set of $\lambda_{\alpha\beta}$ in order to study the dependence of size effects on the electron-phonon coupling.

D.4.1 Influence of the band structure on the shape resonances of a two-band thin film

In this section, we analyze in detail the influence of the band structure parameters on the shape resonances observed in a two-band thin film of infinite lateral size. As it has been explained previously [359], the superconducting properties of thin films show a non monotonous dependence with the thickness. A sawlike dependence is observed for one-band thin films where the peaks are located at values of the thickness for which a new energy subband of allowed states is occupied. Once such state is occupied, the spectral density decreases and the critical temperature drops as the thickness increases, until the following empty state can be filled. If two conduction bands are present, the same mechanism applies to each one separately. Therefore, the shape resonances pattern in the two-band case is presumably more complex or intricate than that of a one-band film depicted in fig. D.1.

According to eq. (D.6), the parameters that control the dispersion relation are the offset between the bands $e_{0\pi}$ and the effective masses $m_{1\alpha}$. As $e_{0\pi}$ is slowly increased, the number of smaller peaks, corresponding to subbands in the π band not present in the one-band case, is expected to increase. This behavior is straightforward to explain by simple inspection of the two dispersion relations; see fig. D.2.

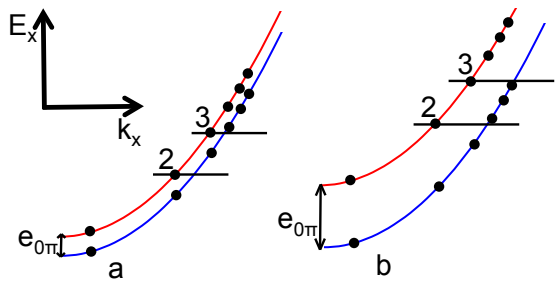

Fig. D.2 Sketch of the dispersion relation for the σ band (blue) and π band (red). The number of available states in the σ band between two consecutive states of the π band increases as $e_{0\pi}$ increases.

We observe that, as the energy increases, states in the two bands become closer in energy. At the same time, for larger $e_{0\pi}$ [see fig. D.2(b)], the number of states in the σ band (blue) between two consecutive states of the π band (red), labeled "2" and "3" in the figure, is larger than for smaller $e_{0\pi}$; see fig. D.2(a). Therefore, as $e_{0\pi}$ increases, there are more occupied states in the σ band before the next state in the π band is filled.

Furthermore, as $m_{1\sigma}$ and $m_{1\pi}$ decrease, the discrete energy states are less closely packed. Therefore when a new state is occupied the change in the chemical potential is larger. This produces larger shape resonances in T_c.

Results for the critical temperature, depicted in fig. D.3, are fully consistent with this picture. Shown in black and blue are the oscillations in T_c for different effective masses and the same $e_{0\pi} = 1.3$ eV. As was expected, the shape resonances (blue) for $m_{1\sigma} = 1.089m_e$, $m_{1\pi} = 0.330m_e$ are slightly larger than those (black) for $m_{1\sigma} = 1.500m_e$, $m_{1\pi} = 1.336m_e$. Moreover, in agreement with the theoretical prediction, we observe that as $e_{0\pi}$ increases (red line) more peaks around the one corresponding to the one-band case start to be observed.

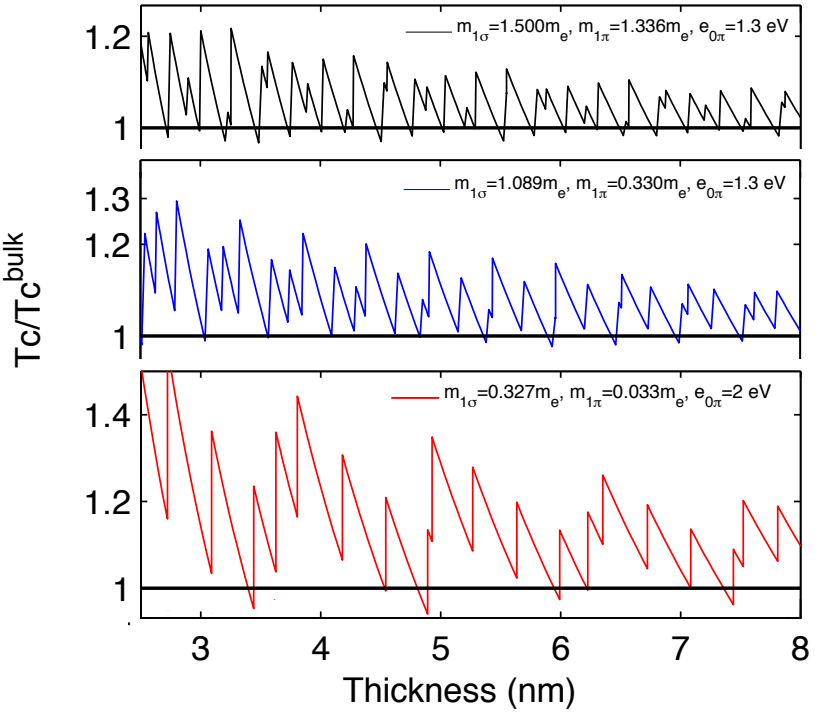

Fig. D.3 T_c in units of $T_c^{bulk} = 38.0$ K as a function of the film thickness for two-band free-standing films [eq. (D.11)] and different effective masses. The rest of the parameters are those of MgB_2 [eq.(D.27)]. In order to observe more clearly the shape resonances, we show the region between 2.5 and 8 nm. The in-plane effective masses are set to $m_{3\alpha}$, $m_{2\alpha}$ in eq. (D.26), while $e_{0\pi}$ and $m_{1\alpha}$ are indicated in each figure. Band parameters not only change the position of the shape resonances' pattern but also their amplitude.

To summarize, the band structure of the film plays an important role not only in the pattern of the shape resonances, but also in their amplitude.

D.4.2 Differences between one and two band

In the previous section, we have studied the intricate pattern of shape resonances observed in two-band superconducting films. In this section we compare it to the one observed in a one-band thin film with similar parameters.

The one-band case can be recovered in two ways: the first, in which we are not interested, corresponds to the limit $e_{0\pi} \to \infty$, i.e., there is only one band available. Here we focus instead in the situation in which there are occupied states with similar energies in both bands. Provided that $e_{0\pi} = 0$, we obtain states with identical quantized energies simply by setting $m_{1\sigma} = m_{1\pi} = 3.27 m_e$.

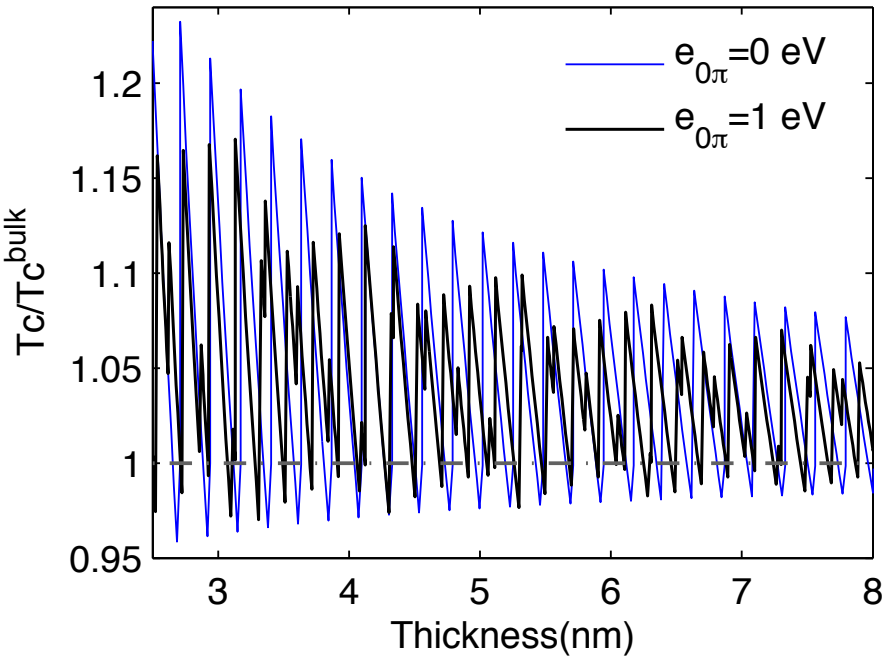

Fig. D.4 T_c in units of $T_c^{bulk} = 38.0$ K as a function of the film thickness for a one-band (blue) and a two-band (black) free-standing thin film. The parameters are those of MgB_2 eq. (D.27) with $m_{1\sigma} = m_{1\pi} = 3.27 m_e$ and in-plane masses $m_{2\alpha}$, $m_{3\alpha}$ from eq. (D.26). The offset value $e_{0\pi} = 0$ corresponds to the one-band limit. The pattern of the shape resonances becomes more regular as the offset decreases and the the masses become more similar. In the one-band limit, the shape resonances have larger amplitude than in the two-band case (black). Therefore, multiband structure suppresses size effects.

Using the free-standing model introduced in sec. D, we obtain more regular shape resonances, depicted in fig. D.4, than those for $m_{1\sigma} \neq m_{1\pi}$, depicted in fig. D.3. In fig. D.4, we compare the case of $e_{0\pi} = 1$ eV (black line) with $e_{0\pi} = 0$ (blue line). In the latter case the quantized components of the momentum are identical in both bands, which results in the same sawlike pattern as in the one-band superconducting film shown in fig. D.1. By contrast, for the reasons given in the previous section, the oscillating pattern in the two-band case has a more complex distribution of maxima and minima. Furthermore, the amplitude of the shape resonances is also smaller than in the one-band limit. This

indicates that finite-size effects in two-band superconducting films are smaller than in the one-band case.

D.4.3 Role of the substrate in an infinite two-band thin film

Once the shape resonances in the critical temperature of a two-band superconducting free-standing film have been studied, we address the problem of the substrate influence by using the model introduced in sec. D–D. We compute the critical temperature T_c and chemical potential μ as a function of the thickness and compare them to those corresponding to a free-standing film. We restrict to infinite lateral size and thicknesses in the window [2,12] nm, a region for which recent experimental results suggest that the mean field approximation holds reasonably well.

The substrate is modeled by two parameters: the height of the step function V_0, namely, the mismatch between the bulk Fermi levels of the film and substrate, and the phenomenological quasiparticle lifetime τ. The first determines the eigenstate extension out of the film. The smaller the V_0, the larger the leaking of probability outside the film. The second parameter controls the broadening of the energy levels. We have chosen V_0 between 0.9 and 1.9 eV above the bulk film Fermi energy. This is the typical mismatch found for example in Pb films grown over a Si substrate [379].
The quasiparticle lifetime τ smoothes the shape resonances and decreases their amplitude. Since quasiparticles reach the film/substrate interface more frequently the thinner the film is, it is expected tunneling to be stronger as the thickness decreases. More specifically we expect a linear dependence with the thickness. Based on this fact and on the recent (see fig. 3 of Ref. [410]) experimental scattering rate Γ ($\tau = 2\hbar/\Gamma$) results in MgB_2 thin films we propose a phenomenological expression for $\tau \approx (c_1 + c_2 a)$ where a is the film thickness and $c_1 = 44.76$ fs, $c_2 = 0.83$ fs nm^{-1} are obtained from the experimental results of Ref. [410] between 6 and 14 nm. Even though the scattering rates in Ref. [410] are attributed to the film granularity, tunneling into the substrate is expected to also contribute to the level broadening. In any case, decoherence of any form is effectively modelled by a finite τ so our results are, at least qualitatively, applicable to more general situations.

As is explained in secs. D and D, in order to obtain momentum-independent matrix elements, we approximate the interaction between all of the states by that between eigenstate whose energy is closer to being equidistant from the highest and the lowest occupied energy level.

We are now ready to analyze size effects in a two-band infinite thin film for three different couplings to the substrate. In fig. D.5 we depict the dependence of T_c on the thickness for various values of V_0. It is clearly observed that shape resonances are smaller in amplitude as both the quasiparticle lifetime τ and V_0 decrease. Shape resonances are not substantially smoothed by the finite τ estimated from experimental results [410]. The reason for that is that the energy associated to a finite lifetime, $\Gamma \sim \hbar/\tau$, is still much smaller than the mean spacing of energy levels in the one-dimensional potential that

describes confinement in the direction perpendicular to the film. Typical lifetimes of a few femtoseconds are needed to substantially smooth out the peaks and fully suppress size effects for thicknesses ~ 5 nm.

In summary, as V_0 or τ decreases, the substrate becomes more important and any enhancement of superconductivity due to size effects is severely suppressed. We note that even the small enhancement observed in certain cases is likely not to be observable for materials for which the surface charge neutrality condition fully applies.

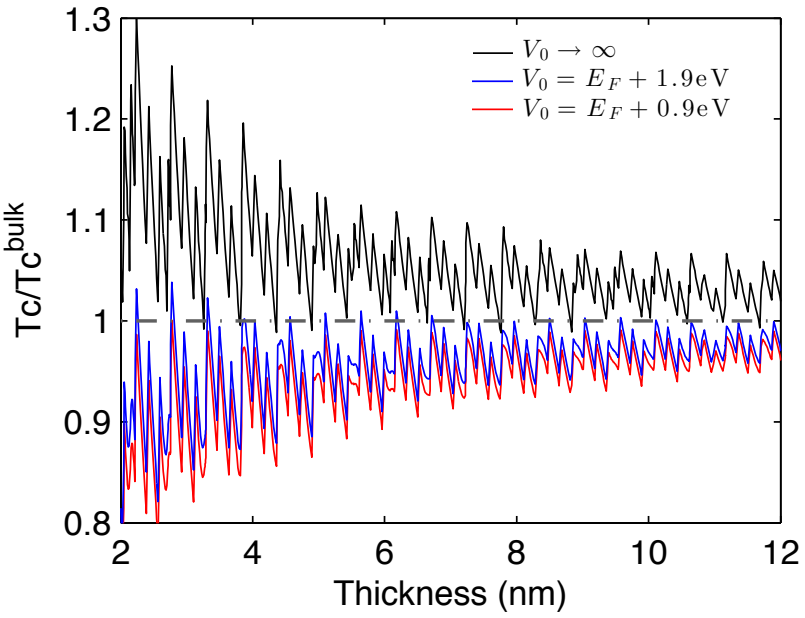

Fig. D.5 T_c in units of $T_c^{bulk} = 38.0$ K as a function of the film thickness for different couplings to the substrate, given by eq. (D.22) in sec. D. $e_{0\pi} = 0.05$ eV, the effective masses are given in eq. (D.26) and the coupling constants are given in eq. (D.27). The lifetime is $\tau \to \infty$ (black) for the free standing film while (red and blue) $\tau(\text{fs}) = c_1 + c_2 a$, $c_1 = 44.76$ fs, $c_2 = 0.83$ fs nm^{-1} and a in nm. These parameters were obtained by fitting the data from 6 to 15 nm in fig. 3 of Ref. [410]. In the region of strong coupling to the substrate (blue and red lines), shape resonances are only slightly smoothed, but a significant suppression relative to the free-standing limit (black) is observed. Much smaller values of the lifetime are needed for a substantial smoothing of the shape resonances.

Shown in fig. D.6 are the shape resonances in the chemical potential for a thickness in the same region as in fig. D.5. The overall magnitude of μ shows no significant difference compared to the free-standing limit. However (see inset of fig. D.6), the pattern is slightly smoothed. As in the case of T_c, a smaller τ results in a smoother behavior which becomes monotonically decreasing for sufficiently small lifetime.

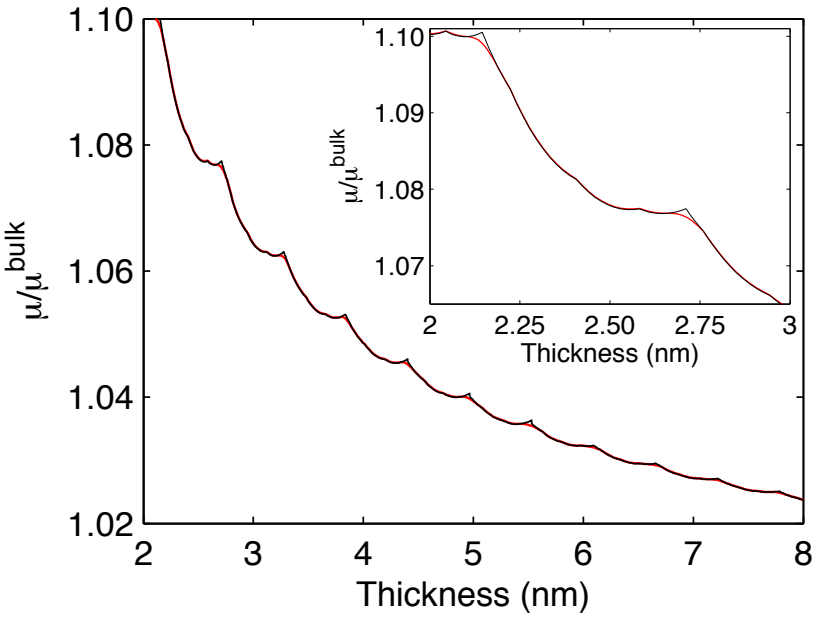

Fig. D.6 μ in units of $\mu^{bulk} = 3.6$ eV as a function of the film thickness. Free-standing (black) and substrate (red) of height $V_0 = E_F + 0.9$ eV (red). The lifetime is $\tau \to \infty$ (black) for the free-standing, film while (red and blue) $\tau(\text{fs}) = c_1 + c_2 a$, $c_1 = 44.76$ fs, $c_2 = 0.83$ fs nm^{-1}, and a in nm. Masses are given by eq. (D.26) and $e_{0\pi} = 0.05$ eV. For the free-standing film [eq. (D.13)], sharp shape resonances are clearly observed. Once the film is coupled to the substrate [eq. (D.17)], shape resonances become smoother. In the inset, smaller peaks, corresponding to the occupation of states in one band, are observed between two larger ones corresponding to the filling of states in the other band.

D.4.4 Influence of the electron-phonon coupling constants

In this section, we study size effects for different electron-phonon coupling constants and fixed band structure parameters. We take the effective masses given in eq. (D.26), $e_{0\pi} = 0.05$ eV, $V_0 = E_F + 0.9$ eV, and $\tau(\text{fs}) = c_1 + c_2 a$, $c_1 = 44.76$ fs, $c_2 = 0.83$ fs nm^{-1}, and a in nm.

Black lines in fig. D.7 correspond to the coupling constant employed in previous sections [eq. (D.27)] and are also shown in fig. D.5. Shown in blue are the results corresponding to the coupling constants from Ref. [423] and a Debye energy $\hbar\omega_D = 7.4$ meV [424] that gives $T_c^{bulk} = 38.3$ K. Red lines correspond to a set of coupling constants and a Debye energy, not related to MgB_2, but with the same bulk critical temperature $T_c^{bulk} = 38.2$ K. It is clearly observed (see fig. D.7) that larger coupling constants lead to weaker finite-size effects and less suppression of T_c with respect to the bulk limit. This follows straightforwardly from eqs. (D.4) and (D.5) by calculating the first order correction to Δ which is inversely proportional to the dimensionless coupling constant. Therefore, a larger coupling constant leads to smaller finite size effects.

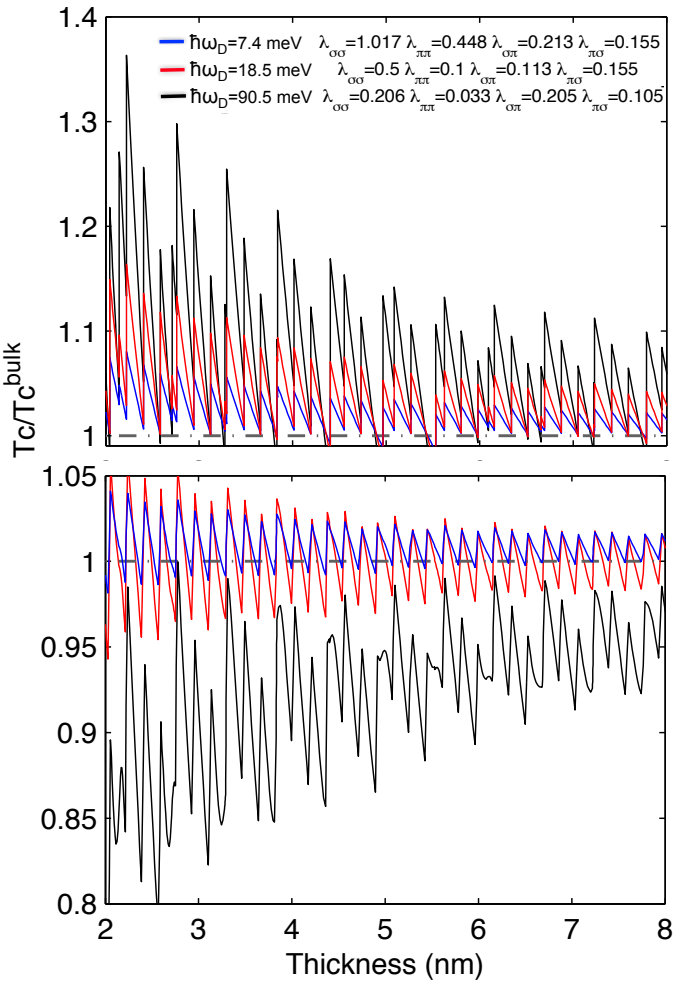

Fig. D.7 T_c in units of $T_c^{bulk} \approx 38.0$ K as a function of the film thickness for different values of the electron-phonon coupling constant. Upper: free standing film, eq. (D.11). Lower: substrate, from eq. (D.22), included. Masses in all cases are given by eq. (D.26) and $e_{0\pi} = 0.05$ eV. The Debye energy is tuned so that in all cases, $T_c^{bulk} \approx 38.0$ K. As the coupling constant decreases, finite-size effects are clearly stronger, though the suppression due to the substrate is also stronger. The optimal setting results from a delicate balance between these two factors.

D.4.5 Finite lateral size and shell effects

In this section we study the role of a finite lateral size in the two-band thin films studied previously. In order to neglect thermal fluctuations, which are beyond the mean-field approximation, we restrict to lateral sizes of the order of, but larger than the film thickness $\sim$ 10nm. Technically, the first consequence of a finite lateral size is that the integrals over k_y and k_z in the gap equations have to replaced by discrete sums. Moreover, due to the isotropic in-plane effective masses and assuming a square shape, we expect level degeneracy, namely, several states occupy the same energy level, usually referred to as a shell. This bunching of levels induces larger fluctuations in the spectral density, i.e., the so-called shell effects, that are also expected to have an important impact on the superconducting properties of the material [425, 426, 404].

In sec. D, we discussed that shell effects can be analytically included by simply replacing the bulk two-dimensional density of states in each band, $g_{2D}^{(\alpha)} = m_{2D}^{(\alpha)} L^2/\pi\hbar^2$ by $\tilde{g}_{2D}^{(\alpha)} \simeq g_{2D}^{(\alpha)}[1 + \overline{g}^{(\alpha)} + g_l^{(\alpha)}]$. The latter only depends on the lateral size, in-plane coherence lengths $\xi^{(\alpha)} = \xi_{yz}^{(\alpha)}$, and the in-plane Fermi momentum $k_{yz}^{(\alpha)}$. Therefore, $\tilde{g}_{2D}$ is constant in energy for all films with the same lateral size. As a consequence we can replace $g_{2D}^{(\alpha)}$ by $\tilde{g}_{2D}^{(\alpha)}$ in eq. (D.22).

In order to get explicit results we use MgB_2 parameters. For the in-plane coherence lengths, we take $\xi_{yz}^{(\sigma)} = 13$ nm, $\xi_{yz}^{(\pi)} = 51$nm (at $T = 0$),[427] while a simple calculation of the in-plane Fermi momenta yields $k_{yz}^{(\alpha)} = \sqrt{m_{2\alpha} m_{3\alpha}} v_{yz}^{(\alpha)}/\hbar$. These are the components corresponding to the crystallographic ab-plane of the MgB_2 cell, which is the yz-plane in our coordinate system. The effective masses are given in eq. (D.26) and the in-plane components of the Fermi velocities $v_{yz}^{(\alpha)}$ are taken from Ref. [428], $v_{yz}^{(\sigma)} = 4.40 \times 10^5$ m/s and $v_{yz}^{(\pi)} = 5.35 \times 10^5$ m/s,

$$k_{yz}^{(\sigma)} = 1.0710 \text{ nm}^{-1}, \quad k_{yz}^{(\pi)} = 4.6311 \text{ nm}^{-1}. \tag{D.28}$$

As was mentioned in sec. D, a mean-field approach is only valid for sizes in which fluctuations are not important which, for thermal fluctuations, depends on the ratio between the mean level spacing and T_c. For conventional superconductors, a lateral size and thickness of at least ~ 10 and ~ 5 nm, respectively, are typical requirements for a mean-field formalism to be applicable. For MgB_2 first-principles calculations [422] suggest that the density of states at E_F in each band is $N_\sigma(E_F) = 0.150$ states/(eV-spin-cell) and $N_\pi(E_F) = 0.205$ states/(eV spin cell). Using the unit cell parameters [408] $a = 3.086$ Å (not to be confused with the film thickness) and $c = 3.524$ Å the mean level spacing for each band is, $\delta_\sigma = \frac{0.097}{\mathcal{V}}$ eV, $\delta_\pi = \frac{0.070}{\mathcal{V}}$ eV, where $\mathcal{V}$ is the film volume in nm^3. For an isolated film of thickness $a = 6$ nm and lateral size $L = 12 \times 12$ nm^2 at $T_c = 38$ K the magnitude of thermal fluctuations is controlled by the parameter,

$$\sqrt{\frac{\delta_\sigma}{k_B T_c}} \simeq 0.19, \quad \sqrt{\frac{\delta_\pi}{k_B T_c}} \simeq 0.16.$$

For free-standing films, this is the typical minimum size for which thermal fluctuations are negligible and a mean-field approach is applicable. We expect that the presence of the substrate reduces fluctuations induced by size effects. However, we take a conservative stance and restrict our study to volumes $\geq 6 \times 12 \times 12$ nm^3.

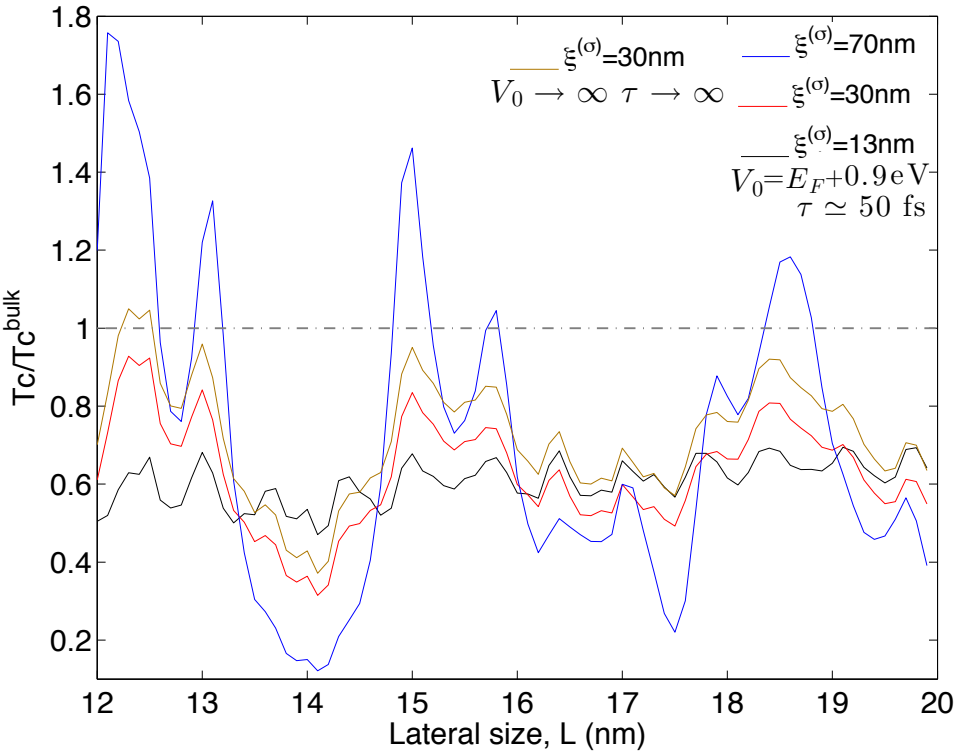

Fig. D.8 T_c in units of $T_c^{bulk} = 38.0$ K as a function of the lateral size for a thickness equal to 6.16 nm. As in the previous figures the band parameters are those of MgB_2. We employ eq. (D.22) but replace $g_{2D}^{(\alpha)}$ by $\tilde{g}_{2D}^{(\alpha)}$, given by eqs. (D.23)–(D.25), to study shell effects for different in-plane coherence lengths in the σ band. In the other band, $\xi_\pi = 51$ nm and masses can be found in eq. (D.26). For the range of thicknesses in which thermal fluctuations are not important, and including the coupling to the substrate, shell effects enhance superconductivity only for coherence lengths considerably larger (by a factor of two) than the film lateral size. In the free-standing film limit (yellow line) a moderate enhancement is observed for $L \sim 12$ nm. For a substantial enhancement of superconductivity, the coherence length of the material must be much larger than that of MgB_2.

Results depicted in fig. D.8 show that for a finite lateral size $\sim$ 12nm, shell effects induce corrections in T_c which are much stronger than those of a thin film with a finite thickness of the same order and infinite lateral size as seen in fig. D.5. For MgB_2 (in black), no enhancement of superconductivity with respect to the bulk limit is observed. This is due to the small coherence length in the σ band of MgB_2, compared to the lateral size. In this situation, the oscillating terms $g_l^{(\alpha)}$ are suppressed by the modified Bessel functions K_0, given by eq. (D.25). As a result the leading correction is $\overline{g}_{2D}^{(\alpha)}$, given by eq. (D.24), which is negative. Therefore, $g_{2D}^{\sigma} \approx g_{2D}^{\sigma}[1 + \overline{g}_{2D}^{(\alpha)}] < g_{2D}^{\sigma}$, given by eq. (D.23) and superconductivity is suppressed by a finite lateral size. In the limit $L \to \infty$, we recover the infinite lateral size result $T_c(L \to \infty)$.

In the case of a superconducting coherence length (blue line) much larger than the lateral size, we observe a substantial enhancement of the critical temperature. This is a

consequence of shell effects in the two dimensional spectral density that are not smoothed out by a small coherence length.

D.4.6 Limitations and limits of applicability of the model

We briefly review the limits of applicability of the results and the different approximations that we employ across the paper.

The mean-field approach that we employ neglects quantum and thermal fluctuations. As was mentioned previously, this is a good approximation for sufficiently large lateral sizes, though we note that even for an infinite lateral size we expect that the mean-field approach breaks down in the strictly two dimensional limit where a Kosterlitz-Thouless transition occurs at a lower temperature. However results from recent experiments [398–400] in Pb ultra-thin films that explore the two dimensional limit were, at least qualitatively, well described by a mean-field formalism. A reason for that behavior is that the substrate increases the effective dimensionality of the system and consequently suppresses the Kosterlitz-Thouless transition. Since this issue is not yet settled here we have opted to present results only for thicknesses of at least 2nm where a mean field formalism should still be applicable.

The coupling to the substrate is modeled by a phenomenological quasiparticle lifetime to describe tunneling into the substrate and a step potential to describe the substrate thin-film interface. A more realistic model of the tunneling mechanism, beyond the scope of this paper, requires a much more detailed knowledge of the interface which depends on the growth techniques and the material substrate.

We have used the zero temperature coherence length of MgB_2. However estimations [429] of the coherence length in Pb film show substantial changes in the coherence length for different system sizes. This coherence length is an input in our model so that once the coherence length in nanoscale samples is known the calculation of T_c could easily be updated accordingly.

We do not consider the full band dispersion relation but rather we have expanded it up to second order around the Fermi level. This approximation might neglect some non-trivial influence of the bands specially in observables, such as the conductivity, which involve energies substantially larger than the gap. However, we expect this approximation to be fair in the calculation of quantities such as T_c and the superconducting gap that involves energies close to the Fermi energy.

We have considered crystalline films in the absence of impurities or strain due to lattice mismatch with the substrate. Current state of the art experimental techniques are capable of manufacturing samples with these properties.

D.5 Conclusions

We have investigated analytically the evolution of superconductivity, including the coupling to the substrate, in multi-band thin-films as the thickness and lateral size enter the nanoscale region.
Shape-resonances in two-band thin films, neglecting the substrate, are more irregular and lead to a more modest enhancement of superconductivity than in one-band films. Size effects are stronger as the effective electron-phonon coupling is decreased. Qualitatively similar results are obtained for different effective masses describing the band structure though smaller masses tend to induce stronger size effects. We have observed that a finite lateral size $\sim$ 10nm induces additional size effects, i.e., the so-called shell effects, which can enhance superconductivity in materials in which the coherence length is much longer than the lateral size. For smaller lateral sizes, thermal fluctuations, not included in our model, become important and our results are not reliable.
Once the substrate is considered the average enhancement is strongly suppressed. As thickness is decreased, tunneling is expected to be more important, smoothing the pattern of shape resonances. However, in the range of parameters used, this smoothing is rather weak. The critical temperature and the amplitude of shape resonances decrease as well. The case of MgB_2, a two-band superconductor, is discussed in detail. In the relatively broad range of parameters that we explore we did not observe a substantial enhancement of superconductivity once the multi-band structure and the substrate are considered simultaneously. It is likely that even this modest enhancement of T_c is not observable for materials in which the charge neutrality condition applies.

D.6 Appendix

D.6.1 Poisson summation formula

Given f as non-negative, decreasing, and continuous on $[0,\infty)$ and that $\lim_{b\to\infty}\int_0^b f(x)dx$ exists, then

$$\sqrt{\sigma}\left[\frac{1}{2}f(0)+\sum_{n=1}^{\infty}f(n\sigma)\right]=\sqrt{\lambda}\left[\frac{1}{2}h(0)+\sum_{l=1}^{\infty}h(l\lambda)\right], \tag{D.6.29}$$

where $\sigma\lambda=2\pi$ and $h(y)=\sqrt{2/\pi}\int_0^\infty f(m)\cos(my)dm$ [417]. Setting $\sigma=1$, $\lambda=2\pi$ and defining $f(n)=\mu-\eta^\alpha(n)$, where $\eta^\alpha(n)=e_{0\alpha}+E_0^\alpha n^2$ we substitute Eq. (D.6.29) into Eq. (D.12). To simplify notation, we omit the band index α.

$f(n)$ satisfies the necessary conditions to use Eq. (D.6.29) when $\eta\in[e_0,\mu]$. Thus, integrating in energy between e_0 and μ and restricting the sum on the left-hand side from

$n = 1$ to ν, the Poisson summation formula leads to

$$\begin{aligned}\frac{\mu - e_0}{2} + \sum_{n=1}^{\nu} (\mu - \eta_n) &= \frac{2}{3\sqrt{E_0}}(\mu - e_0)^{3/2} \\ + \sum_{l=1}^{\infty} \left[-\frac{\sqrt{E_0(\mu - e_0)}}{\pi^2 l^2} \cos\left(2\pi l \sqrt{\frac{\mu - e_0}{E_0}}\right) + \frac{E_0}{2\pi^3 l^3} \sin\left(2\pi l \sqrt{\frac{\mu - e_0}{E_0}}\right) \right] &.\end{aligned} \tag{D.6.30}$$

D.6.2 Factors $K_{\alpha\beta}$

Here we present factors from the interaction matrix elements. k_{m_α} and κ_{m_α} are defined in sec. D.

$$K_{\alpha\beta} = \frac{1}{\frac{a}{2} - \frac{\sin(2k_{m_\alpha}a)}{4\kappa_{m_\alpha}} + \frac{\sin^2(2k_{m_\alpha}a)}{2\kappa_{m_\alpha}}} \frac{1}{\frac{a}{2} - \frac{\sin\left(2k_{m_\beta}a\right)}{4\kappa_{m_\beta}} + \frac{\sin^2(2k_{m_\beta}a)}{2\kappa_{m_\beta}}} \ . \tag{D.6.31}$$

References

[1] L. D. Landau, *The theory of a Fermi Liquid*, *Sov. Phys. JETP* **3** (1957) 920. (See p. 1.)

[2] L. D. Landau, *Oscillations in a Fermi Liquid*, *Sov. Phys. JETP* **5** (1957) 101. (See p. 2.)

[3] L. D. Landau, *On the theory of the Fermi Liquid*, *Sov. Phys. JETP* **8** (1959) 70. (See page of previous reference.)

[4] E. M. Lifshitz and L. P. Pitaevskii, *Statistical Physics Part 2*. Butterworth-Heinemann, Oxford, 1995. (See p. 1.)

[5] G. D. Mahan, *Many-Particle Physics*. Kluwer Academic/Plenum Publishers, New York, 2000. (See pp. 1, 2, 13 and 27.)

[6] G. Baym and C. Pethick, *Landau Fermi-Liquid Theory*. Wiley-VCH, Weinheim, 2004. (See pp. 2 and 3.)

[7] D. Pines and P. Nozières, *Theory of Quantum Liquids*. Addison-Wesley, New York, 1966. (See pp. 1, 2 and 3.)

[8] P. W. Anderson, *The Theory of Superconductivity in the High Tc Cuprates*. Princeton University Press, Princeton, New Jersey, 1995. (See pp. 1, 2, 3 and 4.)

[9] N. W. Ashcroft and N. Mermin, *Solid State Physics*. Harcourt College Publishers, New York, 1976. (See p. 1.)

[10] S. Sachdev, *Quantum Criticality: competing ground states in low dimensions*, *Science* **288** (2000) 475, [cond-mat/0009456]. (See p. 1.)

[11] C. M. Varma, Z. Nussinov, and W. Van Saarloos, *Singular or non-Fermi liquids*, *Phys. Rep.* **361** (2002) 267, [cond-mat/0103393]. (See p. 2.)

[12] T. Giamarchi, *Quantum Physics in One Dimension*. Oxford University Press, Oxford, 2003. (See pp. 1, 2 and 4.)

[13] P. Fulde, *Correlated Electrons in Quantum Matter*. World Scientific Publishing Co., New Jersey, 2012. (See p. 2.)

[14] T. Giamarchi, A. Iucci, and C. Berthod, *Many Body Physics*. Lecture notess: http://dqmp.unige.ch/giamarchi/local/people/thierry.giamarchi/pdf/many-body.pdf, . (See pp. 2 and 3.)

[15] P. Coleman, *Introduction to Many-Body Physics*. Cambridge University Press, Cambridge, 2015. (See pp. 2 and 3.)

[16] T. Giamarchi, *Umklapp process and resistivity in one-dimensional fermion systems*, *Phys. Rev. B* **44** (1991) 2905. (See p. 3.)

[17] A. B. Migdal, *Theory of finite Fermi systems and applications to atomic nuclei.* Interscience Publishers, Wiley and Sons, New York, 1967. (See p. 3.)

[18] H. V. Löhneysen, A. Rosch, M. Vojta, and P. Wölfle, *Fermi-liquid instabilities at magnetic quantum phase transitions*, *Rev. Mod. Phys.* **79** (2007) 1015, [cond-mat/0606317]. (See p. 3.)

[19] H. Padamsee, J. E. Neighbor, and C. A. Shiffman, *Quasiparticle phenomenology for thermodynamics of strong-coupling superconductors*, *J. Low Temp. Phys.* **12** (1973) 387. (See page of previous reference.)

[20] L. Taillefer, R. Newbury, G. Lonzarich, Z. Fisk, and J. Smith, *Direct observation of heavy quasiparticles in UPt3 via the dHvA effect*, *J. Magn. Magn. Mater.* **63-64** (1987) 372. (See page of previous reference.)

[21] W. Stephan, K. J. von Szczepanski, M. Ziegler, and P. Horsch, *Quasi-Particles in the Strong-Coupling Limit of the 2D Hubbard Model*, *Europhys. Lett.* **11** (1990) 675. (See page of previous reference.)

[22] S. A. Kivelson and D. S. Rokhsar, *Bogoliubov quasiparticles, spinons, and spin-charge decoupling in superconductors*, *Phys. Rev. B* **41** (1990) 11693. (See page of previous reference.)

[23] D. Coffey, *Strong-coupling features due to quasiparticle interactions in two-dimensional superconductors*, *Phys. C* **305** (1998) 139, [cond-mat/9712088]. (See page of previous reference.)

[24] E. V. Shuryak and I. Zahed, *Rethinking the properties of the quark-gluon plasma at $T_c < T < 4T_c$*, *Phys. Rev. C* **70** (2004) 021901, [hep-ph/0307267]. (See p. 3.)

[25] M. Gurvitch and A. T. Fiory, *Resistivity of $La_{1.825}Sr_{0.175}CuO_4$ and $YBa_2Cu_3O_7$*, *Phys. Rev. Lett.* **59** (1987) 1337. (See p. 3.)

[26] G. A. Thomas, J. Orenstein, D. H. Rapkine, M. Capizzi, A. J. Millis, R. N. Bhatt, L. F. Schneemeyer, and J. V. Waszczak, *$Ba_2YCu_3O_{7-\delta}$ Electrodynamics of Crystals with High Reflectivity*, *Phys. Rev. Lett.* **61** (1988) 1313. (See p. 3.)

[27] T. Chien, Z. Wang, and N. Ong, *Effect of Zn impurities on the normal-state Hall angle in single-crystal $YBa_2Cu_{3-x}Zn_xO_{7-\delta}$*, *Phys. Rev. Lett.* **67** (1991) 2088. (See p. 3.)

[28] P. W. Anderson, *Hall effect in the two-dimensional Luttinger liquid*, *Phys. Rev. Lett.* **67** (1991) 2092. (See p. 3.)

[29] Y. Zhang, N. P. Ong, Z. a. Xu, K. Krishana, R. Gagnon, and L. Taillefer, *Determining the Wiedemann-Franz ratio from the thermal hall conductivity: application to Cu and YBa2Cu3O6.95.*, *Phys. Rev. Lett.* **84** (2000) 2219, [cond-mat/0001037]. (See p. 3.)

[30] D. van der Marel, H. J. A. Molegraaf, J. Zaanen, Z. Nussinov, F. Carbone, A. Damascelli, H. Eisaki, M. Greven, P. H. Kes, and M. Li, *Quantum critical behaviour in a high-Tc superconductor*, *Nature* **425** (2003) 271. (See p. 3.)

[31] E. H. Lieb and F. Y. Wu, *Absence of mott transition in an exact solution of the short-range, one-band model in one dimension*, *Phys. Rev. Lett.* **20** (1968) 1445. (See p. 3.)

[32] P. W. Anderson, *The Resonating Valence Bond State in La_2CuO_4 and Superconductivity*, *Science* **235** (1987) 1196. (See page of previous reference.)

[33] P. W. Anderson, *"Luttinger-liquid" behavior of the normal metallic state of the 2D Hubbard model*, *Phys. Rev. Lett.* **64** (1990) 1839. (See p. 3.)

[34] H. J. Schulz, *Fermi liquids and non–Fermi liquids*, [cond-mat/9503150]. (See p. 4.)

[35] N. E. Hussey, *Universality of the Mott-Ioffe-Regel limit in metals*, *Phil. Mag.* **84** (2004) 2847, [cond-mat/0404263]. (See p. 4.)

[36] C. M. Varma, P. B. Littlewood, S. Schmitt-Rink, E. Abrahams, and A. E. Ruckenstein, *Phenomenology of the normal state of Cu-O high-temperature superconductors*, *Phys. Rev. Lett.* **63** (1989) 1996. (See p. 4.)

[37] H. D. Politzer, *Reliable perturbative results for strong interactions?*, *Phys. Rev. Lett.* **30** (1973) 1346. (See p. 4.)

[38] D. J. Gross and F. Wilczek, *Ultraviolet behavior of non-abelian gauge theories*, *Phys. Rev. Lett.* **30** (1973) 1343. (See p. 4.)

[39] D. J. Gross and F. Wilczek, *Asymptotically Free Gauge Theories*, *Phys. Rev. D* **8** (1973) 3633. (See p. 4.)

[40] E. Shuryak, *Why does the quark–gluon plasma at RHIC behave as a nearly ideal fluid?*, *Prog. Part. Nucl. Phys.* **53** (2004) 273, [hep-ph/0312227]. (See p. 4.)

[41] P. Arnold, G. D. Moore, and L. G. Yaffe, *Transport coefficients in high temperature gauge theories (I): leading-log results*, *JHEP* **11** (2000) 001, [hep-ph/0010177]. (See p. 4.)

[42] S. Jeon, *Hydrodynamic transport coefficients in relativistic scalar field theory*, *Phys. Rev. D* **52** (1995) 3591, [hep-ph/9409250]. (See p. 5.)

[43] M. Luzum and P. Romatschke, *Conformal Relativistic Viscous Hydrodynamics: Applications to RHIC results at $\sqrt{s_{NN}} = 200$ GeV*, *Phys. Rev. C* **78** (2008) 034915, [arXiv:0804.4015]. (See pp. 5 and 8.)

[44] J. Maldacena, *The large-N limit of superconformal field theories and supergravity*, *Int. J. Theor. Phys.* **38** (1999) 1113. (See pp. 5, 6, 13, 19 and 69.)

[45] S. Gubser, I. Klebanov, and A. Polyakov, *Gauge theory correlators from non-critical string theory*, *Phys. Lett. B* **428** (1998) 105, [hep-th/9802109]. (See pp. 5, 8, 13, 21 and 22.)

[46] E. Witten, *Anti De Sitter Space And Holography*, *Adv. Theor. Math. Phys.* **2** (1998) 253, [hep-th/9802150]. (See pp. 5, 8, 13, 19, 21 and 22.)

[47] H. Kramers and G. Wannier, *Statistics of the Two-Dimensional Ferromagnet. Part I*, *Phys. Rev.* **60** (1941) 252. (See p. 5.)

[48] R. Savit, *Duality in field theory and statistical systems*, *Rev. Mod. Phys.* **52** (1980) 453. (See p. 5.)

[49] A. Font, L. E. Ibáñez, D. Lüsst, and F. Quevedo, *Strong-weak coupling duality and non-perturbative effects in string theory*, *Phys. Lett. B* **249** (1990) 35. (See p. 5.)

[50] E. Kiritsis, *String theory in a nutshell*. Princeton University Press, Princeton, New Jersey, 2011. (See pp. 5, 6, 8, 13, 14, 15, 16, 17, 19 and 35.)

[51] O. Aharony, S. S. Gubser, J. Maldacena, H. Ooguri, and Y. Oz, *Large N Field Theories, String Theory and Gravity*, *Phys. Rep.* **323** (1999) 183, [hep-ph/9905111]. (See pp. 5, 6, 13, 15, 16, 17, 19, 22 and 23.)

[52] G. 't Hooft, *Dimensional Reduction in Quantum Gravity*, [gr-qc/9310026]. (See pp. 6 and 20.)

[53] S. Weinberg and E. Witten, *Limits on massless particles*, *Phys. Lett. B* **96** (1980) 59. (See p. 6.)

[54] H. E. Stanley, *Spherical model as the limit of infinite spin dimensionality*, *Phys. Rev.* **176** (1968) 718. (See p. 6.)

[55] E. Brézin and D. J. Wallace, *Critical behavior of a classical Heisenberg ferromagnet with many degrees of freedom*, *Phys. Rev. B* **7** (1973) 1967. (See page of previous reference.)

[56] S. Sachdev and J. Ye, *Universal quantum-critical dynamics of two-dimensional antiferromagnets*, *Phys. Rev. Lett.* **69** (1992) 2411. (See page of previous reference.)

[57] I. Affleck, *Large- n Limit of SU(n) Quantum "Spin" Chains*, *Phys. Rev. Lett.* **54** (1985) 966. (See page of previous reference.)

[58] A. V. Chubukov, S. Sachdev, and J. Ye, *Theory of two-dimensional quantum Heisenberg antiferromagnets with a nearly critical ground state*, *Phys. Rev. B* **49** (1994) 11919, [cond-mat/9304046]. (See p. 6.)

[59] G. 't Hooft, *A planar diagram theory for strong interactions*, *Nucl. Phys. B* **72** (1974) 461. (See pp. 6, 7 and 19.)

[60] A. D'Adda, M. Lüscher, and P. Di Vecchia, *A expandable series of non-linear σ models with instantons*, *Nucl. Phys. B* **146** (1978) 63. (See p. 6.)

[61] G. 't Hooft, *A two-dimensional model for mesons*, *Nucl. Phys. B* **75** (1974) 461. (See p. 6.)

[62] A. V. Manohar, *Large N QCD*, [hep-th/9802419]. (See page of previous reference.)

[63] R. Gopakumar and D. J. Gross, *Mastering the master field*, *Nucl. Phys. B* **451** (1995) 379, [hep-th/9411021v1]. (See p. 6.)

[64] A. Migdal, *Multicolor QCD as a dual-resonance theory*, *Ann. Phys. (N. Y).* **109** (1977) 365. (See p. 6.)

[65] I. Bars and M. B. Green, *Poincaré- and gauge-invariant two-dimensional quantum chromodynamics*, *Phys. Rev. D* **17** (1978) 537. (See p. 6.)

[66] E. Witten, *Baryons in the expansion*, *Nucl. Phys. B* **160** (1979) 57. (See page of previous reference.)

[67] S. Dalley and I. R. Klebanov, *String spectrum of $(1+1)$-dimensional large-N QCD with adjoint matter*, *Phys. Rev. D* **47** (1993) 2517. (See page of previous reference.)

[68] G. Bhanot, K. Demeterfi, and I. R. Klebanov, *(1 + 1)-dimensional large-N QCD coupled to adjoint fermions*, *Phys. Rev. D* **48** (1993) 4980. (See page of previous reference.)

[69] I. Bigi, M. Shifman, N. Uraltsev, and A. Vainshtein, *Heavy flavor decays, OPE, and duality in the two-dimensional 't Hooft model*, *Phys. Rev. D* **59** (1999) 054011, [hep-ph/9805241]. (See p. 6.)

[70] J. Polchinski, *Dirichlet Branes and Ramond-Ramond Charges*, *Phys. Rev. Lett.* **75** (1995) 4724. (See pp. 7, 16 and 17.)

[71] J. Casalderrey-Solana, H. Liu, D. Mateos, K. Rajagopal, and U. Wiedemann, *Gauge/string duality, hot QCD and heavy ion collisions*. Cambridge University Press, Cambridge, 2014. (See pp. 7, 13, 15, 20 and 23.)

[72] A. Karch and E. Katz, *Adding flavor to AdS/CFT*, *JHEP* **06** (2002) 043, [hep-th/0205236]. (See p. 7.)

[73] M. Kruczenski, D. Mateos, R. C. Myers, and D. J. Winters, *Meson spectroscopy in AdS/CFT with flavour*, *JHEP* **07** (2003) 049, [hep-th/0304032]. (See p. 7.)

[74] U. Gürsoy and E. Kiritsis, *Exploring improved holographic theories for QCD: part I*, *JHEP* **02** (2008) 032, [arXiv:0707.1324]. (See pp. 7 and 8.)

[75] G. Policastro, D. T. Son, and A. O. Starinets, *Shear Viscosity of Strongly Coupled $N = 4$ Supersymmetric Yang-Mills Plasma*, *Phys. Rev. Lett.* **87** (2001) 081601, [hep-th/0104066v2]. (See pp. 7 and 108.)

[76] R. A. Janik and R. Peschanski, *Asymptotic perfect fluid dynamics as a consequence of AdS/CFT correspondence*, *Phys. Rev. D* **73** (2006) 045013, [hep-th/0512162]. (See p. 8.)

[77] R. A. Janik and R. Peschanski, *Gauge-gravity duality and thermalization of a boost-invariant perfect fluid*, *Phys. Rev. D* **74** (2006) 046007, [hep-th/0606149]. (See page of previous reference.)

[78] M. P. Heller, R. a. Janik, and R. Peschanski, *Hydrodynamic Flow of the Quark-Gluon Plasma and Gauge/Gravity Correspondence*, *Acta Phys. Pol. B* **39** (2008) 3183, [arXiv:0811.3113]. (See page of previous reference.)

[79] P. Figueras, V. E. Hubeny, M. Rangamani, and S. F. Ross, *Dynamical black holes and expanding plasmas*, *JHEP* **04** (2009) 137, [arXiv:0902.4696]. (See p. 8.)

[80] E. Witten, *Anti-de Sitter space, thermal phase transition, and confinement in gauge theories*, *Adv. Theor. Math. Phys.* **2** (1998) 505, [hep-th/9803131]. (See p. 8.)

[81] J. Polchinski and M. J. Strassler, *Hard Scattering and Gauge/String Duality*, *Phys. Rev. Lett.* **88** (2002) 031601, [hep-th/0109174]. (See p. 8.)

[82] U. Gürsoy, E. Kiritsis, and F. Nitti, *Exploring improved holographic theories for QCD: part II*, *JHEP* **02** (2008) 019. (See p. 8.)

[83] U. Gürsoy, E. Kiritsis, L. Mazzanti, and F. Nitti, *Deconfinement and Gluon Plasma Dynamics in Improved Holographic QCD*, *Phys. Rev. Lett.* **101** (2008) 181601, [arXiv:0804.0899]. (See page of previous reference.)

[84] M. Järvinen and E. Kiritsis, *Holographic models for QCD in the Veneziano limit*, *JHEP* **3** (2012) 002, [arXiv:1112.1261v]. (See page of previous reference.)

[85] D. Marolf, M. Rangamani, and T. Wiseman, *Holographic thermal field theory on curved spacetimes*, *Class. Quant. Gravity* **31** (2014) 063001, [arXiv:1312.0612]. (See p. 8.)

[86] S.-S. Lee, *Non-Fermi liquid from a charged black hole: A critical Fermi ball*, *Phys. Rev. D* **79** (2009) 086006, [arXiv:0809.3402]. (See p. 8.)

[87] H. Liu, J. McGreevy, and D. Vegh, *Non-Fermi liquids from holography*, *Phys. Rev. D* **83** (2011) 065029, [arXiv:0903.2477]. (See p. 9.)

[88] T. Faulkner, N. Iqbal, H. Liu, J. McGreevy, and D. Vegh, *Strange Metal Transport Realized by Gauge/Gravity Duality*, *Science (80-.).* **329** (2010) 1043. (See p. 8.)

[89] T. Faulkner, H. Liu, J. McGreevy, and D. Vegh, *Emergent quantum criticality, Fermi surfaces, and AdS_2*, *Phys. Rev. D* **83** (2011) 125002, [arXiv:0907.2694]. (See pp. 8 and 9.)

[90] M. Cubrovic, J. Zaanen, and K. Schalm, *String Theory, Quantum Phase Transitions, and the Emergent Fermi Liquid*, *Science* **325** (2009) 439, [arXiv:0904.1993]. (See pp. 8 and 9.)

[91] B. S. Kim, E. Kiritsis, and C. Panagopoulos, *Holographic quantum criticality and strange metal transport*, *New J. Phys.* **14** (2012) 043045, [1012.3464]. (See p. 8.)

[92] A. Donos and S. A. Hartnoll, *Universal linear in temperature resistivity from black hole superradiance*, *Phys. Rev. D* **86** (2012) 124046. (See page of previous reference.)

[93] C. Hoyos, B. S. Kim, and Y. Oz, *Lifshitz hydrodynamics*, *JHEP* **11** (2013) 145, [arXiv:1304.7481]. (See p. 8.)

[94] C. Charmousis, B. Goutéraux, B. Soo Kim, E. Kiritsis, and R. Meyer, *Effective holographic theories for low-temperature condensed matter systems*, *JHEP* **11** (2010) 151, [arXiv:1005.4690]. (See pp. 8, 9, 11, 30, 33, 49, 69, 73, 95, 108 and 115.)

[95] R. A. Davison, K. Schalm, and J. Zaanen, *Holographic duality and the resistivity of strange metals*, *Phys. Rev. B* **89** (2014) 245116, [arXiv:1311.2451]. (See pp. 8 and 139.)

[96] G. T. Horowitz, J. E. Santos, and D. Tong, *Optical conductivity with holographic lattices*, *JHEP* **07** (2012) 168, [arXiv:1204.0519]. (See p. 8.)

[97] G. T. Horowitz, J. E. Santos, and D. Tong, *Further evidence for lattice-induced scaling*, *JHEP* **11** (2012) 102, [arXiv:1209.1098]. (See p. 8.)

[98] A. Donos and J. P. Gauntlett, *The thermoelectric properties of inhomogeneous holographic lattices*, *JHEP* **1** (2015) 35, [arXiv:1409.6875]. (See p. 8.)

[99] E. Kiritsis and F. Peña-Benitez, *Scaling of the holographic AC conductivity for non-Fermi liquids at criticality*, *JHEP* **11** (2015) 177, [arXiv:1507.05633]. (See pp. 8, 9 and 131.)

[100] I. R. Klebanov and E. Witten, *AdS/CFT correspondence and symmetry breaking*, *Nucl. Phys. B* **556** (1999) 89, [hep-th/9905104]. (See pp. 8, 13, 21 and 23.)

[101] P. Kovtun, D. T. Son, and A. O. Starinets, *Holography and hydrodynamics: diffusion on stretched horizons*, *JHEP* **10** (2003) 064, [hep-th/0309213]. (See p. 9.)

[102] D. T. Son and A. O. Starinets, *Hydrodynamics of R-charged black holes*, *JHEP* **03** (2006) 052, [hep-th/0601157]. (See pp. 69, 70, 79 and 87.)

[103] A. Karch and A. O'Bannon, *Metallic AdS/CFT*, *JHEP* **09** (2007) 024, [arXiv:0705.3870]. (See p. 9.)

[104] J. P. Gauntlett, J. Sonner, and T. Wiseman, *Holographic Superconductivity in M Theory*, *Phys. Rev. Lett.* **103** (2009) 151601, [arXiv:0907.3796]. (See page of previous reference.)

[105] S. S. Gubser, C. P. Herzog, S. S. Pufu, and T. Tesileanu, *Superconductors from Superstrings*, *Phys. Rev. Lett.* **103** (2009) 141601, [arXiv:0907.3510]. (See page of previous reference.)

[106] O. DeWolfe, S. S. Gubser, and C. Rosen, *Fermi Surfaces in Maximal Gauged Supergravity*, *Phys. Rev. Lett.* **108** (2012) 251601, [arXiv:1112.3036v]. (See page of previous reference.)

[107] O. Dewolfe, S. S. Gubser, and C. Rosen, *Fermi surfaces in $\mathcal{N} = 4$ super-Yang-Mills theory*, *Phys. Rev. D* **86** (2012) 1–29, [arXiv:1207.3352]. (See pp. 9, 69 and 70.)

[108] S. A. Hartnoll and P. K. Kovtun, *Hall conductivity from dyonic black holes*, *Phys. Rev. D* **76** (2007) 066001, [arXiv:0704.1160]. (See p. 9.)

[109] S. A. Hartnoll and C. P. Herzog, *Ohm's Law at strong coupling: S duality and the cyclotron resonance*, *Phys. Rev. D* **76** (2007) 106012, [arXiv:0706.3228]. (See pp. 33, 69 and 70.)

[110] S. A. Hartnoll, P. K. Kovtun, M. Müller, and S. Sachdev, *Theory of the Nernst effect near quantum phase transitions in condensed matter and in dyonic black holes*, *Phys. Rev. B* **76** (2007) 144502, [arXiv:0706.3215]. (See pp. 33, 69, 70 and 86.)

[111] S. A. Hartnoll and D. M. Hofman, *Locally critical resistivities from umklapp scattering*, *Phys. Rev. Lett.* **108** (2012) 241601, [arXiv:1201.3917]. (See pp. 9 and 139.)

[112] S. S. Gubser, *Breaking an Abelian gauge symmetry near a black hole horizon*, *Phys. Rev. D* **78** (2008) 065034. (See pp. 9, 39 and 41.)

[113] S. A. Hartnoll, C. P. Herzog, and G. T. Horowitz, *Building a Holographic Superconductor*, *Phys. Rev. Lett.* **101** (2008) 031601, [arXiv:0803.3295]. (See pp. 9 and 138.)

[114] S. A. Hartnoll, C. P. Herzog, and G. T. Horowitz, *Holographic superconductors*, *JHEP* **12** (2008) 015, [arXiv:0810.1563]. (See pp. 9, 39, 41, 48, 69, 85, 88, 97 and 138.)

[115] S. Gubser and F. Rocha, *Gravity Dual to a Quantum Critical Point with Spontaneous Symmetry Breaking*, *Phys. Rev. Lett.* **102** (2009) 061601. (See pp. 39, 40, 49 and 138.)

[116] G. T. Horowitz and M. M. Roberts, *Zero temperature limit of holographic superconductors*, *JHEP* **11** (2009) 015, [arXiv:0908.3677v]. (See pp. 46 and 49.)

[117] T. Faulkner, G. T. Horowitz, J. McGreevy, M. M. Roberts, and D. Vegh, *Photoemission "experiments" on holographic superconductors*, *JHEP* **2010** (2010) 121. (See pp. 9 and 41.)

[118] R. Emparan, R. Suzuki, and K. Tanabe, *The large D limit of General Relativity*, *JHEP* **6** (2013) 9. (See pp. 9, 38, 43, 61 and 65.)

[119] A. Altland and B. D. Simons, *Condensed Matter Field Theory*. Cambridge University Press, Cambridge, 2010. (See p. 9.)

[120] S. Sachdev, *Quantum Phase Transitions*. Cambridge University Press, Cambridge, 2011. (See p. 9.)

[121] M. Edalati, J. Jottar, and R. Leigh, *Transport coefficients at zero temperature from extremal black holes*, *JHEP* **01** (2010) 18, [arXiv:0910.0645]. (See pp. 9, 69 and 70.)

[122] S. Jain, *Universal thermal and electrical conductivity from holography*, *JHEP* **11** (2010) 92, [arXiv:1008.2944]. (See pp. 33, 69, 70, 73, 74, 75, 76, 78, 96, 108, 111, 112, 113, 114, 115 and 134.)

[123] B. Goutéraux and E. Kiritsis, *Generalized holographic quantum criticality at finite density*, *JHEP* **12** (2011) 36. (See p. 95.)

[124] B. Goutéraux and E. Kiritsis, *Quantum critical lines in holographic phases with (un)broken symmetry*, *JHEP* **4** (2013) 53, [arXiv:1212.2625]. (See page of previous reference.)

[125] B. Goutéraux, *Charge transport in holography with momentum dissipation*, *JHEP* **4** (2014) 181, [arXiv:1401.5436]. (See pp. 10, 35, 102 and 125.)

[126] A. Donos, B. Goutéraux, and E. Kiritsis, *Holographic metals and insulators with helical symmetry*, *JHEP* **9** (2014) 38, [arXiv:1406.6351]. (See p. 33.)

[127] E. Kiritsis and J. Ren, *On Holographic Insulators and Supersolids*, *JHEP* **09** (2015) 168, [arXiv:1503.03481]. (See pp. 10, 11, 35, 69, 70, 75, 95, 96, 102, 108, 109, 115, 122, 125 and 139.)

[128] R. A. Davison, B. Goutéraux, and S. A. Hartnoll, *Incoherent transport in clean quantum critical metals*, *JHEP* **10** (2015) 112, [arXiv:1507.07137]. (See pp. 33, 69, 70, 73, 74, 75, 86, 105, 108, 111, 112, 113, 114 and 115.)

[129] E. Kiritsis and L. Li, *Holographic competition of phases and superconductivity*, *JHEP* **01** (2016) 147, [arXiv:1510.00020]. (See p. 9.)

[130] A. Adams and S. Yaida, *Disordered holographic systems: Functional renormalization*, *Phys. Rev. D* **92** (2015) 126008, [arXiv:1102.2892]. (See pp. 10, 33, 108 and 141.)

[131] D. Areán, A. Farahi, L. A. Pando Zayas, I. S. Landea, and A. Scardicchio, *Holographic superconductor with disorder*, *Phys. Rev. D* **89** (2014) 106003, [arXiv:1308.1920v]. (See p. 33.)

[132] S. A. Hartnoll and J. E. Santos, *Disordered Horizons: Holography of Randomly Disordered Fixed Points*, *Phys. Rev. Lett.* **112** (2014) 231601. (See page of previous reference.)

[133] D. K. O'Keeffe and A. W. Peet, *Perturbatively charged holographic disorder*, *Phys. Rev. D* **92** (2015) 46004. (See page of previous reference.)

[134] A. M. García-García and B. Loureiro, *Marginal and irrelevant disorder in Einstein-Maxwell backgrounds*, *Phys. Rev. D* **93** (2016) 65025. (See p. 141.)

[135] M. Araujo, D. Arean, and J. M. Lizana, *Noisy Branes*, . (See pp. 10, 33 and 108.)

[136] D. Vegh, *Holography without translational symmetry*, [arXiv:1301.0537]. (See pp. 10, 13, 33 and 34.)

[137] R. A. Davison, *Momentum relaxation in holographic massive gravity*, *Phys. Rev. D* **88** (2013) 086003, [arXiv:1306.5792]. (See pp. 35, 100, 128 and 139.)

[138] M. Blake and D. Tong, *Universal resistivity from holographic massive gravity*, *Phys. Rev. D* **88** (2013) 106004, [arXiv:1308.4970]. (See pp. 10, 102 and 139.)

[139] T. Andrade and B. Withers, *A simple holographic model of momentum relaxation*, *JHEP* **05** (2014) 101, [arXiv:1311.5157]. (See pp. 10, 13, 33, 34, 35, 99, 100, 102, 108, 119, 120, 121, 128, 135 and 139.)

[140] A. Donos and J. P. Gauntlett, *Holographic Q-lattices*, *JHEP* **04** (2014) 40, [arXiv:1311.3292]. (See page of previous reference.)

[141] A. Donos and J. P. Gauntlett, *Thermoelectric DC conductivities from black hole horizons*, *JHEP* **11** (2014) 081, [arXiv:1406.4742]. (See pp. 10, 33, 35, 116 and 134.)

[142] S. Grozdanov, A. Lucas, S. Sachdev, and K. Schalm, *Absence of disorder-driven metal-insulator transitions in simple holographic models*, *Phys. Rev. Lett.* **115** (2015) 221601. (See pp. 10, 109, 123, 124 and 135.)

[143] M. Baggioli and O. Pujolas, *On holographic disorder-driven metal-insulator transitions*, [arXiv:1601.07897]. (See pp. 10, 109, 119, 122, 124, 130, 135 and 140.)

[144] B. Goutéraux, E. Kiritsis, and W.-J. Li, *Effective holographic theories of momentum relaxation and violation of conductivity bound*, [arXiv:1602.01067]. (See pp. 10, 35, 109, 119, 122, 135 and 140.)

[145] P. Figueras and T. Wiseman, *Stationary Holographic Plasma Quenches and Numerical Methods for Non-Killing Horizons*, *Phys. Rev. Lett.* **110** (2013) 171602, [arXiv:1212.4498]. (See p. 10.)

[146] P. Figueras and S. Tunyasuvunakool, *Localized plasma balls*, *JHEP* **06** (2014) 0–23, [arXiv:1404.0018]. (See page of previous reference.)

[147] P. Figueras and S. Tunyasuvunakool, *Black rings in global anti-de Sitter space*, *JHEP* **3** (2015) 149, [arXiv:1412.5680]. (See page of previous reference.)

[148] Ó. J. C. Dias, J. E. Santos, and B. Way, *Lumpy* $\mathrm{AdS}_5 \times S^5$ *black holes and black belts*, *JHEP* **4** (2015) 60, [arXiv:1501.06574]. (See page of previous reference.)

[149] O. J. C. Dias, J. E. Santos, and B. Way, *Localised* $\mathrm{AdS}_5 \times S^5$ *Black Holes*, [arXiv:1605.04911]. (See page of previous reference.)

[150] C. A. R. Herdeiro and E. Radu, *Static black holes with no spatial isometries in AdS-electrovacuum*, [arXiv:1606.02302]. (See p. 10.)

[151] S. Ryu and T. Takayanagi, *Holographic Derivation of Entanglement Entropy from the anti–de Sitter Space/Conformal Field Theory Correspondence*, *Phys. Rev. Lett.* **96** (2006) 181602. (See pp. 11, 51 and 63.)

[152] J. Tarrío and S. Vandoren, *Black holes and black branes in Lifshitz spacetimes*, *JHEP* **9** (2011) 17. (See pp. 11, 89 and 90.)

[153] Y. Korovin, K. Skenderis, and M. Taylor, *Lifshitz as a deformation of Anti-de sitter*, *JHEP* **08** (2013) 26, [arXiv:1304.7776]. (See pp. 11, 93 and 94.)

[154] D. Forster, *Hydrodynamic Fluctuations, Broken Symmetry, and Correlation Functions*. W. A. Benjamin, Inc., Reading, MA, 1975. (See pp. 13, 26, 82 and 83.)

[155] G. F. Mazenko, *Nonequilibrium Statistical Mechanics*. Wiley-VCH, Weinheim, 2006. (See pp. 13, 26, 82 and 83.)

[156] J. Schwinger, *The Special Canonical Group*, *Proc. Natl. Acad. Sci.* **46** (1960) 1401. (See pp. 13 and 27.)

[157] O. Konstantinov and V. Perel, *A Diagram Technique for Evaluating Transport Quantities*, *Sov. Phys. JETP* **12** (1961) 142. (See page of previous reference.)

[158] J. Schwinger, *Brownian Motion of a Quantum Oscillator*, *J. Math. Phys.* **2** (1961) 407. (See page of previous reference.)

[159] L. P. Kadanoff and G. Baym, *Quantum Statistical Mechanics*. Benjamin, New York, 1962. (See page of previous reference.)

[160] L. V. Keldysh, *Diagram Technique for Nonequilibrium Processes*, *JETP* **20** (1965) 1018. (See p. 27.)

[161] A. Kamenev, *Field Theory of Non-Equilibrium Systems*. Cambridge University Press, Cambridge, 2011. (See p. 27.)

[162] G. Stefanucci and R. van Leeuwen, *Nonequilibrium many-body theory of quantum systems: a modern introduction*. Cambridge University Press, Cambridge, 2013. (See pp. 13 and 27.)

[163] D. T. Son and A. O. Starinets, *Minkowski-space correlators in AdS/CFT correspondence: recipe and applications*, *JHEP* **09** (2002) 042. (See pp. 13, 28, 29 and 42.)

[164] C. P. Herzog and D. T. Son, *Schwinger-Keldysh propagators from AdS/CFT correspondence*, *JHEP* **0303** (2003) 046, [hep-th/0212072]. (See pp. 13, 28 and 29.)

[165] S. A. Hartnoll, *Lectures on holographic methods for condensed matter physics*, *Class. Quant. Gravity* **26** (2009) 224002, [arXiv:0903.3246]. (See pp. 13, 23, 25, 29, 30, 32 and 69.)

[166] J. Zaanen, Y. Liu, Y.-W. Sun, and K. Schalm, *Holographic duality in condensed matter physics*. Cambridge University Press, Cambridge, 2015. (See pp. 13, 15, 24 and 29.)

[167] I. R. Klebanov, *TASI Lectures: Introduction to the AdS/CFT Correspondence*, [hep-th/0009139]. (See p. 24.)

[168] M. Ammon and J. Erdmenger, *Gauge/gravity duality: foundations and applications*. Cambridge University Press, Cambridge, 2015. (See pp. 15, 16, 17, 18, 19, 20, 22, 23 and 24.)

[169] S. Weinberg, *The Quantum Theory of Fields*. Cambridge University Press, Cambridge, 1996. (See p. 34.)

[170] T. Matsubara, *A New Approach to Quantum-Statistical Mechanics*, *Prog. Theor. Phys.* **14** (1955) 351. (See p. 27.)

[171] A. Zaffaroni, *Introduction to the AdS-CFT correspondence*, sep, 2000. (See page of previous reference.)

[172] C. P. Herzog, *Lectures on holographic superfluidity and superconductivity*, *J. Phys. A Math. Theor.* **42** (2009) 343001. (See pp. 23, 41, 42, 85 and 88.)

[173] J. McGreevy, *Holographic Duality with a View Toward Many-Body Physics*, *Adv. High Energy Phys.* **2010** (2010) 723105, [arXiv:0909.0518v]. (See p. 22.)

[174] J. McGreevy, *TASI lectures on quantum matter (with a view toward holographic duality)*, [arXiv:1606.08953]. (See p. 13.)

[175] R. Blumenhagen and E. Plauschinn, *Introduction to Conformal Field Theory - With Applications to String Theory*. Springer, Berlin, Heidelberg, 2009. (See p. 14.)

[176] G. F. R. Ellis and S. W. Hawking, *The large scale structure of space-time*. Cambridge University Press, Cambridge, 1973. (See pp. 15 and 24.)

[177] D. Tong, *String Theory lecture notes*, [arXiv:0908.0333]. (See pp. 15 and 16.)

[178] G. T. Horowitz and A. Strominger, *Black strings and p-branes*, *Nucl. Phys. B* **360** (1991) 197. (See pp. 16 and 17.)

[179] R. LEIGH, *DIRAC-BORN-INFELD ACTION FROM DIRICHLET σ-MODEL*, *Mod. Phys. Lett. A* **04** (1989) 2767. (See p. 17.)

[180] E. D'Hoker and D. Z. Freedman, *Supersymmetric Gauge Theories and the AdS/CFT Correspondence*, [hep-th/0201253]. (See p. 17.)

[181] O. Aharony, O. Bergman, D. L. Jafferis, and J. Maldacena, $\mathcal{N} = 6$ *superconformal Chern-Simons-matter theories, M2-branes and their gravity duals*, *JHEP* **10** (2008) 091, [arXiv:0806.1218]. (See p. 19.)

[182] J. H. Schwarz, *Spontaneous compactification of extended supergravity in ten dimensions*, *Physica* **124A** (1984) 543. (See p. 20.)

[183] M. Günaydin and N. Marcus, *The spectrum of the S^5 compactification of the chiral $N = 2$, $D = 10$ supergravity and the unitary supermultiplets of U(2,2/4)*, *Class. Quant. Gravity* **2** (1985) L11. (See page of previous reference.)

[184] H. J. Kim, L. J. Romans, and P. Van Nieuwenhuizen, *Mass spectrum of chiral ten-dimensional $\mathcal{N} = 2$ supergravity on S^5*, *Phys. Rev. D* **32** (1985) 389. (See page of previous reference.)

[185] M. J. Duff, *TASI Lectures on Branes, Black Holes and Anti-de Sitter Space*, [hep-th/9912164]. (See p. 20.)

[186] L. Susskind, *The world as a hologram*, *J. Math. Phys.* **36** (1995) 6377, [hep-th/9409089]. (See p. 20.)

[187] K. Skenderis, *Lecture notes on holographic renormalization*, *Class. Quant. Gravity* **19** (2002) 5849, [hep-th/0209067]. (See pp. 22, 25 and 30.)

[188] P. K. Townsend, *Black Holes*, [gr-qc/9707012]. (See p. 24.)

[189] G. W. Gibbons and S. W. Hawking, *Action integrals and partition functions in quantum gravity*, *Phys. Rev. D* **15** (1977) 2752. (See p. 24.)

[190] S. S. Gubser, I. R. Klebanov, and A. W. Peet, *Entropy and temperature of black 3-branes*, *Phys. Rev. D* , [hep-th/9602135]. (See p. 24.)

[191] V. Balasubramanian and P. Kraus, *A Stress Tensor for Anti-de Sitter Gravity*, *Commun. Math. Phys.* **208** (1999) 413, [hep-th/9902121]. (See p. 25.)

[192] J. Rammer, *Quantum Field Theory of Non-equilibrium States*. Cambridge University Press, Cambridge, 2007. (See pp. 27 and 28.)

[193] L. Fidkowski, V. Hubeny, M. Kleban, and S. Shenker, *The Black Hole Singularity in AdS/CFT*, *JHEP* **0402** (2004) 014, [hep-th/0306170]. (See p. 29.)

[194] A. Chamblin, R. Emparan, C. V. Johnson, and R. C. Myers, *Charged AdS Black Holes and Catastrophic Holography*, *Phys. Rev. D* **60** (1999) 064018, [hep-th/9902170]. (See p. 30.)

[195] K. Balasubramanian and J. McGreevy, *An analytic Lifshitz black hole*, *Phys. Rev. D* **80** (2009) 104039. (See pp. 30 and 89.)

[196] C. De Rham, G. Gabadadze, and A. J. Tolley, *Resummation of massive gravity*, *Phys. Rev. Lett.* **106** (2011) 231101, [arXiv:1011.1232]. (See p. 33.)

[197] S. F. Hassan and R. A. Rosen, *Resolving the Ghost Problem in Nonlinear Massive Gravity*, *Phys. Rev. Lett.* **108** (2012) 041101, [arXiv:1106.3344]. (See p. 33.)

[198] Y. Akrami, S. Hassan, F. Könnig, A. Schmidt-May, and A. R. Solomon, *Bimetric gravity is cosmologically viable*, *Phys. Lett. B* **748** (2015) 37, [arXiv:1503.07521]. (See p. 33.)

[199] K. Hinterbichler, *Theoretical aspects of massive gravity*, *Rev. Mod. Phys.* **84** (2012) 671, [arXiv:1105.3735]. (See p. 34.)

[200] Y. Bardoux, M. M. Caldarelli, and C. Charmousis, *Shaping black holes with free fields*, *JHEP* **05** (2012) 054, [arXiv:1202.4458]. (See pp. 34 and 99.)

[201] R. D. Peccei and H. R. Quinn, *CP conservation in the presence of pseudoparticles*, *Phys. Rev. Lett.* **38** (1977) 1440. (See p. 34.)

[202] T. Azeyanagi, W. Li, and T. Takayanagi, *On string theory duals of Lifshitz-like fixed points*, *JHEP* **06** (2009) 084, [arXiv:0905.0688]. (See pp. 34 and 35.)

[203] D. Mateos and D. Trancanelli, *Anisotropic $\mathcal{N} = 4$ super-Yang-Mills plasma and its instabilities*, *Phys. Rev. Lett.* **107** (2011) 101601, [arXiv:1105.3472]. (See pp. 34 and 35.)

[204] L. E. Ibáñez and A. M. Uranga, *String theory and particle physics: An introduction to string phenomenology*. Cambridge University Press, Cambridge, United Kingdom, 2012. (See p. 35.)

[205] A. M. García-García and A. Romero-Bermúdez, *Conductivity and entanglement entropy of high dimensional holographic superconductors*, *JHEP* **09** (2015) 33, [arXiv:1502.03616]. (See pp. 37, 65 and 125.)

[206] W. Metzner and D. Vollhardt, *Correlated Lattice Fermions in $d = \infty$ Dimensions*, *Phys. Rev. Lett.* **62** (1989) 324. (See p. 38.)

[207] A. Georges and G. Kotliar, *Hubbard model in infinite dimensions*, *Phys. Rev. B* **45** (1992) 6479. (See p. 38.)

[208] M. Jarrell, *Hubbard model in infinite dimensions: A quantum Monte Carlo study*, *Phys. Rev. Lett.* **69** (1992) 168. (See p. 38.)

[209] J. K. Freericks and D. J. Scalapino, *Weak-coupling expansions for the attractive Holstein and Hubbard models*, *Phys. Rev. B* **49** (1994) 6368. (See page of previous reference.)

[210] S. Ciuchi, F. de Pasquale, C. Masciovecchio, and D. Feinberg, *Superconductivity and Density Waves in High Dimensions*, *Europhys. Lett.* **24** (1993) 575. (See page of previous reference.)

[211] M. E. Fisher and D. S. Gaunt, *Ising Model and Self-Avoiding Walks on Hypercubical Lattices and "High-Density" Expansions*, *Phys. Rev.* **133** (1964) A224. (See p. 38.)

[212] A. Schiller and K. Ingersent, *Systematic $1/d$ Corrections to the Infinite-Dimensional Limit of Correlated Lattice Electron Models*, *Phys. Rev. Lett.* **75** (1995) 113. (See p. 38.)

[213] A. Georges, G. Kotliar, W. Krauth, and M. J. Rozenberg, *Dynamical mean-field theory of strongly correlated fermion systems and the limit of infinite dimensions*, *Rev. Mod. Phys.* **68** (1996) 13. (See p. 38.)

[214] D. S. Gaunt, M. F. Sykes, and H. Ruskin, *Percolation processes in d-dimensions*, *J. Phys. A* **9** (1976) 1899. (See p. 38.)

[215] R. Abou-Chacra, D. J. Thouless, and P. W. Anderson, *A selfconsistent theory of localization*, *J. Phys. C* **6** (1973) 1734. (See p. 38.)

[216] A. M. García-García and E. Cuevas, *Dimensional dependence of the metal-insulator transition*, *Phys. Rev. B* **75** (2007) 174203. (See p. 38.)

[217] A. Strominger, *Inverse-dimensional expansion in quantum gravity*, *Phys. Rev. D* **24** (1981) 3082. (See p. 38.)

[218] N. E. J. Bjerrum-Bohr, *Quantum gravity at a large number of dimensions*, *Nucl. Phys.* **B 684** (2004) 209. (See p. 38.)

[219] R. Gregory and R. Laflamme, *Black strings and p-branes are unstable*, *Phys. Rev. Lett.* **70** (1993) 2837. (See p. 38.)

[220] R. Emparan and K. Tanabe, *Holographic superconductivity in the large D expansion*, *JHEP* **2014** (2014) 145. (See pp. 38, 43, 65 and 145.)

[221] R. Emparan and K. Tanabe, *Universal quasinormal modes of black holes in the limit of large number of dimensions*, *Phys. Rev. D* **89** (2014) 64028, [arXiv:1401.1957]. (See p. 65.)

[222] R. Emparan, R. Suzuki, and K. Tanabe, *Quasinormal modes of (Anti-)de Sitter black holes in the 1/D expansion*, *JHEP* **04** (2015) 85, [arXiv:1502.02820]. (See pp. 38 and 65.)

[223] D. Z. Freedman, S. D. Mathur, A. Matusis, and L. Rastelli, *Correlation functions in the CFT_d/AdS_{d+1} correspondence*, *Adv. Theor. Math. Phys.* **3** (1999) 363, [hep-th/9804058v2]. (See p. 40.)

[224] S. S. Gubser and A. Nellore, *Ground states of holographic superconductors*, *Phys. Rev. D* **80** (2009) 105007. (See p. 41.)

[225] G. Horowitz and M. Roberts, *Holographic superconductors with various condensates*, *Phys. Rev. D* **78** (2008) 126008, [arXiv:0810.1077v]. (See pp. 43, 44 and 51.)

[226] P. Basu, *Low temperature properties of holographic condensates*, *JHEP* **3** (2011) 142, [arXiv:1101.0215]. (See p. 46.)

[227] Z. Ding-Fang and Z. Kai, *(n + 1)-Dimensional Gravity Duals to Quantum Criticalities with Spontaneous Symmetry Breaking*, *Commun. Theor. Phys.* **60** (2013) 458, [arXiv:1309.7594]. (See pp. 48 and 49.)

[228] K.-Y. Kim, J. P. Shock, and J. Tarrío, *The open string membrane paradigm with external electromagnetic fields*, *JHEP* **2011** (2011) 17. (See p. 48.)

[229] S. S. Gubser, S. S. Pufu, and F. D. Rocha, *Quantum critical superconductors in string theory and M-theory*, *Phys. Lett. B* **683** (2010) 201, [arXiv:0908.0011]. (See pp. 48 and 49.)

[230] B. Goutéraux, *Universal scaling properties of extremal cohesive holographic phases*, *JHEP* **01** (2014) 80, [arXiv:1308.2084]. (See pp. 49 and 96.)

[231] R.-G. Cai, S. He, L. Li, and Y.-L. Zhang, *Holographic entanglement entropy in insulator/superconductor transition*, *JHEP* **07** (2012) 88, [arXiv:1203.6620]. (See p. 51.)

[232] T. Albash and C. V. Johnson, *Holographic studies of entanglement entropy in superconductors*, *JHEP* **05** (2012) 79, [arXiv:1202.2605]. (See pp. 51, 58, 63 and 138.)

[233] Y. Peng and Q. Pan, *Holographic entanglement entropy in general holographic superconductor models*, *JHEP* **6** (2014) 11, [arXiv:1404.1659]. (See p. 51.)

[234] Y. Peng and Y. Liu, *A general holographic metal/superconductor phase transition model*, *JHEP* **02** (2015) 82, [arXiv:1410.7234]. (See p. 51.)

[235] X.-M. Kuang, E. Papantonopoulos, and B. Wang, *Entanglement entropy as a probe of the proximity effect in holographic superconductors*, *JHEP* **05** (2014) 130, [arXiv:1401.5720]. (See p. 51.)

[236] T. Albash and C. V. Johnson, *Holographic entanglement entropy and renormalization group flow*, *JHEP* **2012** (2012) 95. (See p. 52.)

[237] S. Ryu and T. Takayanagi, *Aspects of holographic entanglement entropy*, *JHEP* **08** (2006) 045. (See pp. 54 and 63.)

[238] T. Nishioka, S. Ryu, and T. Takayanagi, *Holographic entanglement entropy: an overview*, *J. Phys. A Math. Theor.* **42** (2009) 504008. (See pp. 55 and 56.)

[239] R. Emparan, D. Grumiller, and K. Tanabe, *Large-D Gravity and Low-D Strings*, *Phys. Rev. Lett.* **110** (2013) 251102. (See pp. 65 and 125.)

[240] S. Bhattacharyya, M. Mandlik, S. Minwalla, and S. Thakur, *A charged membrane paradigm at large D*, *JHEP* **04** (2016) 128, [arXiv:1504.06613]. (See p. 65.)

[241] K. Tanabe, *Black rings at large D*, *JHEP* **02** (2016) 151, [arXiv:1510.02200]. (See page of previous reference.)

[242] B. Chen, Z.-Y. Fan, P. Li, and W. Ye, *Quasinormal modes of Gauss-Bonnet black holes at large D*, *JHEP* **1** (2016) 85, [arXiv:1511.08706]. (See page of previous reference.)

[243] E.-D. Guo, M. Li, and J.-R. Sun, *CFT dual of charged AdS black hole in the large dimension limit*, *Int. J. Mod. Phys. D* **25** (2016) 1650085, [arXiv:1512.08349]. (See page of previous reference.)

[244] T. Andrade, S. A. Gentle, and B. Withers, *Drude in D major*, [arXiv:1512.06263]. (See page of previous reference.)

[245] R. Emparan, K. Izumi, R. Luna, R. Suzuki, and K. Tanabe, *Hydro-elastic Complementarity in Black Branes at large D*, [arXiv:1602.05752]. (See page of previous reference.)

[246] A. Sadhu and V. Suneeta, *Non-spherically symmetric black string perturbations in the large D limit*, [arXiv:1604.0595]. (See page of previous reference.)

[247] K. Tanabe, *Charged rotating black holes at large D*, [arXiv:1605.08854]. (See page of previous reference.)

[248] C. P. Herzog, M. Spillane, and A. Yarom, *The holographic dual of a Riemann problem in a large number of dimensions*, [arXiv:1605.01404]. (See page of previous reference.)

[249] M. Rozali and A. Vincart-Emard, *On Brane Instabilities in the Large D Limit*, [arXiv:1607.01747]. (See p. 65.)

[250] A. M. García-García and A. Romero-Bermúdez, *Drude weight and Mazur-Suzuki bounds in holography*, *Phys. Rev. D* **93** (2016) 66015, [arXiv:1512.04401]. (See pp. 67, 108 and 125.)

[251] X. Zotos, F. Naef, and P. Prelovsek, *Transport and conservation laws*, *Phys. Rev. B* **55** (1997) 11029. (See pp. 68, 80, 82 and 86.)

[252] S. Fujimoto and N. Kawakami, *Exact Drude weight for the one-dimensional Hubbard model at finite temperatures*, *J. Phys. A* **31** (1998) 465. (See p. 68.)

[253] S. Fujimoto and N. Kawakami, *Drude Weight at Finite Temperatures for Some Nonintegrable Quantum Systems in One Dimension*, *Phys. Rev. Lett.* **90** (2003) 197202. (See p. 68.)

[254] C. Karrasch, J. H. Bardarson, and J. E. Moore, *Finite-Temperature Dynamical Density Matrix Renormalization Group and the Drude Weight of Spin-1/2 Chains*, *Phys. Rev. Lett.* **108** (2012) 227206. (See p. 68.)

[255] J. Sirker, R. G. Pereira, and I. Affleck, *Conservation laws, integrability, and transport in one-dimensional quantum systems*, *Phys. Rev. B* **83** (2011) 35115, [arXiv:1011.1354]. (See p. 68.)

[256] X. Zotos, *Finite Temperature Drude Weight of the One-Dimensional Spin- 1/2 Heisenberg Model*, *Phys. Rev. Lett.* **82** (1999) 1764. (See pp. 68 and 82.)

[257] W. Kohn, *Theory of the Insulating State*, *Phys. Rev.* **133** (1964) A171. (See pp. 68 and 80.)

[258] P. Mazur, *Non-ergodicity of phase functions in certain systems*, *Physica* **43** (1969) 533. (See pp. 68 and 80.)

[259] M. Suzuki, *Ergodicity, constants of motion, and bounds for susceptibilities*, *Physica* **51** (1971) 277. (See pp. 68, 80 and 82.)

[260] T. b. ž. Prosen, *Open XXZ Spin Chain: Nonequilibrium Steady State and a Strict Bound on Ballistic Transport*, *Phys. Rev. Lett.* **106** (2011) 217206, [arXiv:1103.1350]. (See p. 68.)

[261] E. Ilievski and T. Prosen, *Thermodyamic bounds on Drude weights in terms of almost-conserved quantities*, *Commun. Math. Phys.* **318** (2013) 809, [arXiv:1111.3830]. (See p. 68.)

[262] E. H. Lieb and D. W. Robinson, *The finite group velocity of quantum spin systems*, *Commun. Math. Phys.* **28** (1972) 251. (See p. 68.)

[263] H. Castella, X. Zotos, and P. Prelovšek, *Integrability and Ideal Conductance at Finite Temperatures*, *Phys. Rev. Lett.* **74** (1995) 972. (See pp. 68 and 86.)

[264] M. Mierzejewski, P. Prelovšek, and T. Prosen, *Breakdown of the Generalized Gibbs Ensemble for Current-Generating Quenches*, *Phys. Rev. Lett.* **113** (2014) 20602, [arXiv:1405.2557]. (See pp. 68 and 86.)

[265] S. Sachdev, *What can gauge-gravity duality teach us about condensed matter physics?*, *Annu. Rev. Condens. Matter Phys.* **3** (2011) 9, [arXiv:1108.1197]. (See p. 69.)

[266] S. Chakrabarti, S. Chakrabortty, and S. Jain, *Proof of universality of electrical conductivity at finite chemical potential*, *JHEP* **02** (2011) 73, [arXiv:1011.3499]. (See pp. 69, 70, 73, 74, 96, 108, 111, 112, 113, 114 and 115.)

[267] S. S. Gubser and F. D. Rocha, *Peculiar properties of a charged dilatonic black hole in* AdS_5, *Phys. Rev. D* **81** (2010) 46001, [arXiv:0911.2898]. (See pp. 69 and 70.)

[268] C. Hoyos, A. O'Bannon, and J. Wu, *Zero sound in strange metallic holography*, *JHEP* **09** (2010) 86, [arXiv:1007.0590]. (See pp. 69 and 70.)

[269] O. DeWolfe, S. S. Gubser, and C. Rosen, *Dynamic critical phenomena at a holographic critical point*, *Phys. Rev. D* **84** (2011) 126014, [arXiv:1108.2029]. (See pp. 69, 70, 86 and 87.)

[270] D. Giataganas and K. Sfetsos, *Non-integrability in non-relativistic theories*, *JHEP* **06** (2014) 18, [arXiv:1403.2703]. (See pp. 69 and 86.)

[271] D. Klemm, M. Nozawa, and M. Rabbiosi, *On the integrability of Einstein–Maxwell–(A) dS gravity in the presence of Killing vectors*, *Class. Quant. Gravity* **32** (2015) 205008, [arXiv:1506.09017]. (See pp. 69 and 86.)

[272] S. Jain, S. Mukherji, and S. Mukhopadhyay, *Notes on R-charged black holes near criticality and gauge theory*, *JHEP* **11** (2009) 51, [arXiv:0906.5134]. (See pp. 69, 75, 76, 86 and 105.)

[273] B. Bradlyn, M. Goldstein, and N. Read, *Kubo formulas for viscosity: Hall viscosity, Ward identities, and the relation with conductivity*, *Phys. Rev. B* **86** (2012) 245309, [arXiv:1207.7021]. (See pp. 70, 71, 72 and 132.)

[274] L. P. Kadanoff and P. C. Martin, *Hydrodynamic equations and correlation functions*, *Ann. Phys. (N. Y).* **24** (1963) 419. (See p. 71.)

[275] E. Taylor and M. Randeria, *Viscosity of strongly interacting quantum fluids: Spectral functions and sum rules*, *Phys. Rev. A* **81** (2010) 053610, [arXiv:1002.0869]. (See pp. 72 and 132.)

[276] P. Kovtun, *Lectures on hydrodynamic fluctuations in relativistic theories*, *J. Phys. A Math. Theor.* **45** (2012) 473001, [arXiv:1205.5040]. (See pp. 72 and 85.)

[277] R. A. Davison and B. Goutéraux, *Momentum dissipation and effective theories of coherent and incoherent transport*, *JHEP* **1** (2015) 39, [arXiv:1411.1062v]. (See pp. 72 and 139.)

[278] S. Jain, *Holographic electrical and thermal conductivity in strongly coupled gauge theory with multiple chemical potentials*, *JHEP* **03** (2010) 101, [arXiv:0912.2228]. (See pp. 75, 78 and 79.)

[279] K. Behrndt, R. Kallosh, J. Rahmfeld, M. Shmakova, and W. K. Wong, *STU black holes and string triality*, *Phys. Rev. D* **54** (1996) 6293. (See pp. 77 and 78.)

[280] K. Behrndt, M. Cvetič, and W. A. Sabra, *Non-extreme black holes of five-dimensional $\mathcal{N} = 2$ AdS supergravity*, *Nucl. Phys. B* **553** (1999) 317. (See p. 77.)

[281] M. Cvetič, M. J. Duff, P. Hoxha, J. T. Liu, H. Lü, J. X. Lu, R. Martinez-Acosta, C. N. Pope, H. Sati, and T. A. Tran, *Embedding AdS black holes in ten and eleven dimensions*, *Nucl. Phys. B* **558** (1999) 96, [arXiv:0910.3722]. (See p. 77.)

[282] Y. Matsuo, S. J. Sin, S. Takeuchi, T. Tsukioka, and C. M. Yoo, *Sound modes in holographic hydrodynamics for charged AdS black hole*, *Nucl. Phys. B* **820** (2009) 593, [arXiv:0910.3722]. (See p. 85.)

[283] C. Hoyos, B. S. Kim, and Y. Oz, *Ward identities for transport in 2+1 dimensions*, *JHEP* **03** (2015) 164, [arXiv:1501.05756]. (See p. 85.)

[284] K. Maeda, M. Natsuume, and T. Okamura, *Dynamic critical phenomena in the AdS/CFT duality*, *Phys. Rev. D* **78** (2008) 1–11, [arXiv:0809.4074]. (See p. 86.)

[285] S. Kachru, X. Liu, and M. Mulligan, *Gravity duals of Lifshitz-like fixed points*, *Phys. Rev. D* **78** (2008) 106005, [arXiv:0808.1725]. (See p. 89.)

[286] M. Taylor, *Non-relativistic holography*, [arXiv:0812.0530]. (See pp. 89 and 92.)

[287] E. Kiritsis and Y. Matsuo, *Charge-hyperscaling violating Lifshitz hydrodynamics from black-holes*, *JHEP* **12** (2015) 76, [arXiv:1508.02494]. (See p. 90.)

[288] J. Hartong, E. Kiritsis, and N. A. Obers, *Lifshitz space–times for Schrödinger holography*, *Phys. Lett. B* **746** (2015) 318, [arXiv:1409.1519]. (See p. 92.)

[289] J. Hartong, E. Kiritsis, and N. A. Obers, *Field theory on Newton-Cartan backgrounds and symmetries of the Lifshitz vacuum*, *JHEP* **8** (2015) 6, [arXiv:1502.0228]. (See page of previous reference.)

[290] J. Hartong, E. Kiritsis, and N. A. Obers, *Schrödinger invariance from Lifshitz isometries in holography and field theory*, *Phys. Rev. D* **92** (2015) 066003, [1409.1522]. (See pp. 90 and 92.)

[291] M. H. Dehghani, A. Sheykhi, and S. E. Sadati, *Thermodynamics of nonlinear charged Lifshitz black branes with hyperscaling violation*, [arXiv:1505.01134]. (See p. 91.)

[292] M. Alishahiha, E. Ó. Colgáin, and H. Yavartanoo, *Charged black branes with hyperscaling violating factor*, *JHEP* **11** (2012) 137, [arXiv:1209.3946]. (See p. 91.)

[293] J.-R. Sun, S.-Y. Wu, and H.-Q. Zhang, *Mimic the optical conductivity in disordered solids via gauge/gravity duality*, *Phys. Lett. B* **729** (2014) 177, [arXiv:1306.1517]. (See page of previous reference.)

[294] X.-M. Kuang and J.-P. Wu, *Transport coefficients from hyperscaling violating black brane: shear viscosity and conductivity*, [arXiv:1511.03008]. (See p. 91.)

[295] S. F. Ross and O. Saremi, *Holographic stress tensor for non-relativistic theories*, *JHEP* **2009** (2009) 009–009. (See p. 92.)

[296] S. F. Ross, *Holography for asymptotically locally Lifshitz spacetimes*, *Class. Quant. Gravity* **28** (2011) 215019. (See page of previous reference.)

[297] R. B. Mann and R. McNees, *Holographic renormalization for asymptotically Lifshitz spacetimes*, *JHEP* **2011** (2011) 129. (See page of previous reference.)

[298] M. Baggio, J. Boer, and K. Holsheimer, *Anomalous breaking of anisotropic scaling symmetry in the quantum lifshitz model*, *JHEP* **2012** (2012) 99, [arXiv:1112.6416]. (See p. 92.)

[299] T. Griffin, P. Hořava, and C. M. Melby-Thompson, *Conformal Lifshitz gravity from holography*, *JHEP* **2012** (2012) 10, [arXiv:1112.5660]. (See p. 92.)

[300] M. Baggio, J. de Boer, and K. Holsheimer, *Hamilton-Jacobi renormalization for Lifshitz spacetime*, *JHEP* **2012** (2012) 58. (See p. 92.)

[301] W. Chemissany and I. Papadimitriou, *Lifshitz holography: The whole shebang*, *JHEP* **01** (2015) 52, [arXiv:1408.0795]. (See p. 92.)

[302] Y. Korovin, K. Skenderis, and M. Taylor, *Lifshitz from AdS at finite temperature and top down models*, *JHEP* **11** (2013) 127, [arXiv:1306.3344]. (See pp. 93 and 94.)

[303] R. A. Davison and B. Goutéraux, *Disecting holographic conductivities*, *JHEP* **09** (2015) 90, [arXiv:1505.05092]. (See pp. 96, 99, 100 and 139.)

[304] S. A. Hartnoll, *Horizons, holography and condensed matter*, [arXiv:1106.4324]. (See p. 96.)

[305] S. A. Hartnoll, D. M. Hofman, and D. Vegh, *Stellar spectroscopy: Fermions and holographic Lifshitz criticality*, *JHEP* **2011** (2011) 96, [arXiv:1105.3197]. (See p. 96.)

[306] S. Sachdev, *Holographic metals and the fractionalized fermi liquid*, *Phys. Rev. Lett.* **105** (2010) 1–4, [arXiv:1006.3794]. (See p. 96.)

[307] L. Huijse and S. Sachdev, *Fermi surfaces and gauge-gravity duality*, *Phys. Rev. D* **84** (2011) 1–18, [arXiv:1104.5022]. (See p. 96.)

[308] M. Kaminski, K. Landsteiner, J. Mas, J. P. Shock, and J. Tarrío, *Holographic operator mixing and quasinormal modes on the brane*, *JHEP* **2010** (2010) 21. (See pp. 99, 100 and 101.)

[309] I. Amado, M. Kaminski, and K. Landsteiner, *Hydrodynamics of holographic superconductors*, *JHEP* **05** (2009) 021, [arXiv:0903.2209]. (See page of previous reference.)

[310] K.-Y. Kim, K. K. Kim, Y. Seo, and S.-J. Sin, *Gauge invariance and holographic renormalization*, *Phys. Lett. B* **749** (2015) 108, [arXiv:1502.02100]. (See p. 100.)

[311] R. A. Davison and B. Goutéraux, *Momentum dissipation and effective theories of coherent and incoherent transport*, *JHEP* **01** (2015) 39, [arXiv:1411.1062]. (See p. 101.)

[312] A. M. García-García, B. Loureiro, and A. Romero-Bermúdez, *Transport in a gravity dual with a varying gravitational coupling constant*, [arXiv:1606.01142]. (See pp. 107, 112, 113 and 115.)

[313] H. Goenner, *Some remarks on the genesis of scalar-tensor theories*, *Gen. Relativ. Gravit.* **44** (2012) 2077, [arXiv:1204.3455]. (See p. 108.)

[314] C. Brans and R. H. Dicke, *Mach's Principle and a Relativistic Theory of Gravitation*, *Phys. Rev.* **124** (1961) 925. (See pp. 108 and 149.)

[315] G. Kang, *Black hole area in Brans-Dicke theory*, *Phys. Rev. D* **54** (1996) 7483, [gr-qc/9606020]. (See pp. 108, 110 and 112.)

[316] A. Sheykhi and M. M. Yazdanpanah, *Thermodynamics of charged Brans-Dicke AdS black holes*, *Phys. Lett. Sect. B Nucl. Elem. Part. High-Energy Phys.* **679** (2009) 311, [arXiv:0904.1777v]. (See p. 108.)

[317] A. Sheykhi, M. H. Dehghani, and S. H. Hendi, *Thermodynamic instability of charged dilaton black holes in AdS spaces*, *Phys. Rev. D* **81** (2010) 84040. (See pp. 108, 114 and 115.)

[318] S. Gopalakrishnan, M. Müller, V. Khemani, M. Knap, E. Demler, and D. A. Huse, *Low-frequency conductivity in many-body localized systems*, *Phys. Rev. B* **92** (2015) 104202. (See p. 109.)

[319] G. T. Horowitz and J. E. Santos, *General relativity and the cuprates*, *JHEP* **06** (2013) 087. (See pp. 109 and 130.)

[320] C. H. Brans, *The roots of scalar-tensor theory: an approximate history*, [gr-qc/0506063]. (See p. 114.)

[321] C. J. Gao and S. N. Zhang, *Higher-dimensional dilaton black holes with cosmological constant*, *Phys. Lett. B* **605** (2005) 185. (See p. 115.)

[322] I. L. Shapiro and H. Takata, *Conformal transformation in gravity*, *Phys. Lett. B* **361** (1995) 31, [hep-th/9504162]. (See p. 115.)

[323] I. L. Shapiro, *On the conformal transformation and duality in gravity*, *Class. Quant. Gravity* **14** (1997) 391, [hep-th/9610129]. (See page of previous reference.)

[324] T. P. Sotiriou and V. Faraoni, *$f(R)$ theories of gravity*, *Rev. Mod. Phys.* **82** (2010) 451, [arXiv:0805.1726]. (See pp. 115, 116 and 149.)

[325] T. P. Sotiriou, S. Liberati, and V. Faraoni, *Theory of Gravitation Theories: A No-Progress Report*, *Int. J. Mod. Phys. D* **17** (2008) 399, [arXiv:0707.2748]. (See p. 115.)

[326] R. Brustein and A. J. M. Medved, *Ratio of shear viscosity to entropy density in generalized theories of gravity*, *Phys. Rev. D* **79** (2009) 21901, [arXiv:0808.3498]. (See p. 116.)

[327] R. Brustein, D. Gorbonos, and M. Hadad, *Wald's entropy is equal to a quarter of the horizon area in units of the effective gravitational coupling*, *Phys. Rev. D* **79** (2009) 44025, [arXiv:0712.3206]. (See p. 116.)

[328] S. Nojiri and S. D. Odintsov, *Non-Singular Modified Gravity Unifying Inflation with Late-Time Acceleration and Universality of Viscous Ratio Bound in $f(R)$ Theory*, *Prog. Theor. Phys. Suppl.* **190** (2011) 155. (See p. 116.)

[329] S. Chatterjee, M. Parikh, and S. Sarkar, *The black hole membrane paradigm in $f(R)$ gravity*, *Class. Quant. Gravity* **29** (2012) 35014, [arXiv:1012.6040]. (See page of previous reference.)

[330] R. Pourhasan, *Spacetime entanglement with $f(R)$ gravity*, *JHEP* **2014** (2014) 4, [arXiv:1403.0951]. (See p. 116.)

[331] J. Santos, J. S. Alcaniz, M. J. Reboucas, and F. C. Carvalho, *Energy conditions in f(R)-gravity*, *Phys. Rev. D* **76** (2007) 083513, [arXiv:0708.0411]. (See p. 122.)

[332] P. Burikham and N. Poovuttikul, *Shear viscosity in holography and effective theory of transport without translational symmetry*, [arXiv:1601.04624]. (See pp. 132 and 133.)

[333] S. A. Hartnoll, D. M. Ramirez, and J. E. Santos, *Entropy production, viscosity bounds and bumpy black holes*, [arXiv:1601.02757]. (See pp. 132 and 133.)

[334] X. H. Ge, Y. Ling, C. Niu, and S. J. Sin, *Thermoelectric conductivities, shear viscosity, and stability in an anisotropic linear axion model*, *Phys. Rev. D* **92** (2015) 1–31, [arXiv:1412.8346v]. (See p. 133.)

[335] M. Sadeghi and S. Parvizi, *Hydrodynamics of a Black Brane in Gauss-Bonnet Massive Gravity Gravity Setup and the Black Brane Solution*, *Class. Quant. Gravity* **33** (2015) 35005, [arXiv:1507.07183]. (See p. 133.)

[336] Y. Ling, Z.-Y. Xian, and Z. Zhou, *Holographic Shear Viscosity in Hyperscaling Violating Theories without Translational Invariance*, [arXiv:1605.03879]. (See p. 133.)

[337] A. Rebhan and D. Steineder, *Violation of the holographic viscosity bound in a strongly coupled anisotropic plasma*, *Phys. Rev. Lett.* **108** (2012) 2–5, [arXiv:1110.6825]. (See p. 133.)

[338] K. A. Mamo, *Holographic RG ow of the shear viscosity to entropy density ratio in strongly coupled anisotropic plasma*, *JHEP* **10** (2012) 070, [arXiv:1205.1797]. (See page of previous reference.)

[339] S. I. Finazzo, R. Critelli, R. Rougemont, and J. Noronha, *Momentum transport in strongly coupled anisotropic plasmas in the presence of strong magnetic fields*, [arXiv:1605.06061]. (See p. 133.)

[340] L. Alberte, M. Baggioli, and O. Pujolas, *Viscosity bound violation in holographic solids and the viscoelastic response*, [arXiv:1601.03384]. (See p. 133.)

[341] I. Giannakis, D. Hou, J.-r. Li, and H.-c. Ren, *Low shear viscosity due to Anderson localization*, *Phys. Rev. D* **77** (2008) 27701. (See p. 133.)

[342] T. Faulkner, A. Lewkowycz, and J. Maldacena, *Quantum corrections to holographic entanglement entropy*, *JHEP* **11** (2013) 74, [arXiv:1307.2892]. (See p. 135.)

[343] H. B. Zeng, *Possible Anderson localization in a holographic superconductor*, *Phys. Rev. D* **88** (2013) 126004, [arXiv:1310.5753]. (See p. 141.)

[344] A. Lucas, S. Sachdev, and K. Schalm, *Scale-invariant hyperscaling-violating holographic theories and the resistivity of strange metals with random-field disorder*, *Phys. Rev. D* **89** (2014) 066018, [arXiv:1401.7993]. (See page of previous reference.)

[345] A. Lucas and S. Sachdev, *Conductivity of weakly disordered strange metals: From conformal to hyperscaling-violating regimes*, *Nucl. Phys. B* **892** (2015) 239, [arXiv:1411.3331]. (See page of previous reference.)

[346] S. A. Hartnoll, D. M. Ramirez, and J. E. Santos, *Emergent scale invariance of disordered horizons*, *JHEP* **9** (2015) 160, [1504.0332]. (See page of previous reference.)

[347] S. A. Hartnoll, D. M. Ramirez, and J. E. Santos, *Thermal conductivity at a disordered quantum critical point*, *JHEP* **4** (2016) 22, [arXiv:1508.04435]. (See page of previous reference.)

[348] A. Donos and J. P. Gauntlett, *The thermoelectric properties of inhomogeneous holographic lattices*, *JHEP* **1** (2015) 35, [arXiv:1409.6875]. (See p. 141.)

[349] A. Kitaev, *A simple model of quantum holography*, in *KITP strings Semin. Entanglement 2015 Progr.*, 2015. (See p. 141.)

[350] S. Sachdev and J. Ye, *Gapless spin-fluid ground state in a random quantum Heisenberg magnet*, *Phys. Rev. Lett.* **70** (1993) 3339. (See p. 141.)

[351] J. Polchinski and V. Rosenhaus, *The Spectrum in the Sachdev-Ye-Kitaev Model*, [arXiv:1601.06768]. (See p. 141.)

[352] J. Maldacena and D. Stanford, *Comments on the Sachdev-Ye-Kitaev model*, [arXiv:1604.07818]. (See p. 141.)

[353] C. P. Herzog, *Analytic holographic superconductor*, *Phys. Rev. D* **81** (2010) 126009. (See p. 143.)

[354] J. Alsup, G. Siopsis, and J. Therrien, *Hair on near-extremal Reissner-Nordström AdS black holes*, *Phys. Rev. D* **86** (2012) 025002. (See p. 143.)

[355] G. Siopsis and J. Therrien, *Analytic calculation of properties of holographic superconductors*, *JHEP* **2010** (2010) 13. (See p. 144.)

[356] Q. Pan, J. Jing, B. Wang, and S. Chen, *Analytical study on holographic superconductors with backreactions*, *JHEP* **6** (2012) 87, [arXiv:1205.3543v]. (See p. 144.)

[357] A. Guarnizo, L. Castañeda, and J. M. Tejeiro, *Boundary term in metric f (R) gravity: field equations in the metric formalism*, *Gen. Relativ. Gravit.* **42** (2010) 2713, [arXiv:1002.0617]. (See p. 151.)

[358] A. Romero-Bermúdez and A. M. García-García, *Size effects in superconducting thin films coupled to a substrate*, *Phys. Rev. B* **89** (2014) 064508, [arXiv:1311.4193]. (See p. 153.)

[359] C. J. Thompson and J. M. Blatt, *Shape resonances in superconductors - II simplified theory*, *Phys. Lett.* **5** (1963) 6. (See pp. 153, 157, 167, 169, 175, 176, 177, 178, 179, 183 and 187.)

[360] R. W. Cohen and B. Abeles, *Superconductivity in Granular Aluminum Films*, *Phys. Rev.* **168** (1968) 444. (See p. 153.)

[361] V. Kresin and B. Tavger, *Superconducting transition temperature of a thin film*, *Zh. Eksp. Teor. Fiz.* **50** (1966) 1689. (See p. 153.)

[362] R. E. Allen, *Superconducting transition temperature and other properties of thin metallic films*, *Phys. Rev. B* **12** (1975) 3650. (See pp. 153, 159 and 175.)

[363] M. Yu, M. Strongin, and A. Paskin, *Consistent calculation of boundary effects in thin superconducting films*, *Phys. Rev. B* **14** (1976) 996. (See pp. 153, 154, 159, 165, 169 and 175.)

[364] H. M. Jaeger, D. B. Haviland, B. G. Orr, and A. M. Goldman, *Onset of superconductivity in ultrathin granular metal films*, *Phys. Rev. B* **40** (1989) 182. (See p. 153.)

[365] S. Qin, J. Kim, Q. Niu, and C.-K. Shih, *Superconductivity at the two-dimensional limit.*, *Science* **324** (2009) 1314. (See pp. 154, 158 and 165.)

[366] Y. Zhang, Z. Lin, Q. Dai, D. Li, Y. Wang, Y. Zhang, Y. Wang, and Q. Feng, *Ultrathin MgB_2 films fabricated on Al2O3 substrate by hybrid physical–chemical vapor deposition with high Tc and Jc*, *Supercond. Sci. Technol.* **24** (2010) 15013, [arXiv:1102.5625]. (See pp. 154, 158, 164, 165, 171, 173, 176 and 185.)

[367] C. Brun, I.-P. Hong, F. Patthey, I. Sklyadneva, R. Heid, P. Echenique, K. Bohnen, E. Chulkov, and W.-D. Schneider, *Reduction of the Superconducting Gap of Ultrathin Pb Islands Grown on Si(111)*, *Phys. Rev. Lett.* **102** (2009) 207002. (See page of previous reference.)

[368] S. Bose, A. M. García-García, M. M. Ugeda, J. D. Urbina, C. H. Michaelis, I. Brihuega, and K. Kern, *Observation of shell effects in superconducting nanoparticles of Sn*, *Nat. Mat.* **9** (2010) 550. (See pp. 154 and 175.)

[369] Y. Guo, Y.-F. Zhang, X.-Y. Bao, T.-Z. Han, Z. Tang, L.-X. Zhang, W.-G. Zhu, E. G. Wang, Q. Niu, Z. Q. Qiu, J.-F. Jia, Z.-X. Zhao, and Q.-K. Xue, *Superconductivity modulated by quantum size effects.*, *Science* **306** (2004) 1915. (See pp. 154, 158, 164, 171 and 173.)

[370] B. Chen, Z. Zhu, and X. C. Xie, *Quantum size effects in thermodynamic superconducting properties of ultrathin films*, *Phys. Rev. B* **74** (2006) 132504. (See pp. 154 and 175.)

[371] A. A. Shanenko, M. D. Croitoru, and F. M. Peeters, *Oscillations of the superconducting temperature induced by quantum well states in thin metallic films: Numerical solution of the Bogoliubov–de Gennes equations*, *Phys. Rev. B* **75** (2007) 14519. (See p. 154.)

[372] Y. Jia, B. Wu, H. H. Weitering, and Z. Zhang, *Quantum size effects in Pb films from first principles: The role of the substrate*, *Phys. Rev. B* **74** (2006) 35433. (See p. 154.)

[373] N. Reyren, S. Thiel, A. D. Caviglia, L. F. Kourkoutis, G. Hammerl, C. Richter, C. W. Schneider, T. Kopp, A.-S. Rüetschi, D. Jaccard, and Others, *Superconducting interfaces between insulating oxides*, *Science* **317** (2007) 1196. (See p. 154.)

[374] D. Liu, W. Zhang, D. Mou, J. He, Y.-B. Ou, Q.-Y. Wang, Z. Li, L. Wang, L. Zhao, S. He, Y. Peng, X. Liu, C. Chen, L. Yu, G. Liu, X. Dong, J. Zhang, C. Chen, Z. Xu, J. Hu, X. Chen, X. Ma, Q. Xue, and X. J. Zhou, *Electronic Origin of High Temperature Superconductivity in Single-Layer FeSe Superconductor*, *Nat. Commun.* **3** (2012) 931, [arXiv:1202.5849]. (See p. 154.)

[375] P. Zubko, S. Gariglio, M. Gabay, P. Ghosez, and J.-M. Triscone, *Interface physics in complex oxide heterostructures*, *Annu. Rev. Condens. Matter Phys.* **2** (2011) 141. (See pp. 154, 160 and 164.)

[376] P. G. de Gennes, *Boundary Effects in Superconductors*, *Rev. Mod. Phys.* **36** (1964) 225. (See p. 156.)

[377] P. Czoschke, H. Hong, L. Basile, and T. C. Chiang, *Quantum size effects in the surface energy of Pb/Si(111) film nanostructures studied by surface x-ray diffraction and model calculations*, *Phys. Rev. B* **72** (2005) 75402. (See p. 157.)

[378] W. van Dijk and Y. Nogami, *Analytical approach to the wave function of a decaying quantum system*, *Phys. Rev. C* **65** (2002) 24608. (See pp. 157 and 161.)

[379] P. S. Kirchmann, L. Rettig, X. Zubizarreta, V. M. Silkin, E. V. Chulkov, and U. Bovensiepen, *Quasiparticle lifetimes in metallic quantum-well nanostructures*, *Nat. Phys.* **6** (2010) 782. (See pp. 158, 164, 165 and 190.)

[380] L. Aballe, C. Rogero, P. Kratzer, S. Gokhale, and K. Horn, *Probing Interface Electronic Structure with Overlayer Quantum-Well Resonances: Al/Si(111)*, *Phys. Rev. Lett.* **87** (2001) 156801. (See p. 158.)

[381] K. Horn, B. Reihl, A. Zartner, D. E. Eastman, K. Hermann, and J. Noffke, *Electronic energy bands of lead: Angle-resolved photoemission and band-structure calculations*, *Phys. Rev. B* **30** (1984) 1711. (See pp. 158 and 165.)

[382] D. J. BenDaniel and C. B. Duke, *Space-Charge Effects on Electron Tunneling*, *Phys. Rev.* **152** (1966) 683. (See pp. 158 and 183.)

[383] A. Sugiyama, *Theory of Formation Energy of the External and the Internal Surface for Free Electron Metals*, *J. Phys. Soc. Jp.* **15** (1960) 965. (See p. 159.)

[384] F. Garcia-Moliner and F. Flores, *Introduction to the Theory of Solid Surfaces*. Cambridge University Press, 1979. (See p. 160.)

[385] T.-L. Chan, C. Z. Wang, M. C. Hupalo, M. Tringides, Z.-Y. Lu, and K. M. Ho, *First-principles studies of structures and stabilities of Pb/Si(111)*, *Phys. Rev. B* **68** (2003) 45410. (See p. 160.)

[386] M. Brack and R. Bhaduri, *Semicalssical Physics*. Addison-Wesley, 1997. (See pp. 160 and 182.)

[387] M. H. Upton, C. M. Wei, M. Y. Chou, T. Miller, and T. C. Chiang, *Thermal Stability and Electronic Structure of Atomically Uniform Pb Films on Si(111)*, *Phys. Rev. Lett.* **93** (2004) 26802. (See p. 164.)

[388] J. H. Dil, J. W. Kim, T. Kampen, K. Horn, and A. Ettema, *Electron localization in metallic quantum wells: Pb versus In on Si(111)*, *Phys. Rev. B* **73** (2006) 161308. (See p. 164.)

[389] J. R. Anderson and A. V. Gold, *Fermi Surface, Pseudopotential Coefficients, and Spin-Orbit Coupling in Lead*, *Phys. Rev.* **139** (1965) A1459. (See p. 165.)

[390] S. Pan, Q. Liu, F. Ming, K. Wang, and X. Xiao, *Interface effects on the quantum well states of Pb thin films.*, *J. Phys. Condens. Matter* **23** (2011) 485001. (See p. 165.)

[391] G. Dresselhaus, A. F. Kip, and C. Kittel, *Cyclotron Resonance of Electrons and Holes in Silicon and Germanium Crystals*, *Phys. Rev.* **98** (1955) 368. (See p. 165.)

[392] D. R. Heslinga, H. H. Weitering, D. P. VanderWerf, T. M. Klapwijk, and T. Hibma, *Atomic Structure Dependent Schottky Barrier at Epitaxial Pb/Si(111) interfaces*, *Phys. Rev. Lett.* **64** (1990) 1589. (See p. 165.)

[393] D. Eom, S. Qin, M. Chou, and C. K. Shih, *Persistent Superconductivity in Ultrathin Pb Films : A Scanning Tunneling Spectroscopy Study*, *Phys. Rev. Lett.* **96** (2006) 27005. (See pp. 165 and 185.)

[394] C. P. J. Poole, H. P. Farach, and R. J. Creswick, *Superconductivity*. Academic Press, Amsterdam, second ed., 2007. (See p. 166.)

[395] H. Chaib, L. M. Eng, and T. Otto, *Dielectric polarization and refractive indices of ultrathin barium titanate films on strontium titanate single crystals*, *J. Phys Cond. Mat.* **17** (2005) 161. (See p. 169.)

[396] L. Aballe, C. Rogero, S. Gokhale, S. Kulkarni, and K. Horn, *Quantum-well states in ultrathin aluminium films on Si(111)*, *Surf. Sci.* **485** (2001) 488. (See p. 171.)

[397] A. Romero-Bermúdez and A. M. García-García, *Shape resonances and shell ef- fects in thin-film multiband superconductors*, *Phys. Rev. B* **89** (2014) 024510, [arXiv:1311.0698]. (See p. 175.)

[398] Y. Guo, Y.-F. Zhang, X.-Y. Bao, T.-Z. Han, Z. Tang, L.-X. Zhang, W.-G. Zhu, E. G. Wang, Q. Niu, Z. Q. Qiu, and Others, *Superconductivity modulated by quantum size effects*, *Science* **306** (2004) 1915. (See pp. 175 and 196.)

[399] T. Zhang, P. Cheng, W.-J. Li, Y.-J. Sun, G. Wang, X.-G. Zhu, K. He, L. Wang, X. Ma, X. Chen, and Others, *Superconductivity in one-atomic-layer metal films grown on Si (111)*, *Nat. Phys.* **6** (2010) 104. (See page of previous reference.)

[400] S. Qin, J. Kim, Q. Niu, and C.-K. Shih, *Superconductivity at the two-dimensional limit*, *Science* **324** (2009) 1314. (See pp. 175, 185 and 196.)

[401] C. Brun, I.-P. Hong, F. Patthey, I. Y. Sklyadneva, R. Heid, P. M. Echenique, K. P. Bohnen, E. V. Chulkov, and W.-D. Schneider, *Reduction of the Superconducting Gap of Ultrathin Pb Islands Grown on Si(111)*, *Phys. Rev. Lett.* **102** (2009) 207002. (See p. 175.)

[402] C. Brun, K. H. Müller, I.-P. Hong, F. Patthey, C. Flindt, and W.-D. Schneider, *Dynamical Coulomb Blockade Observed in Nanosized Electrical Contacts*, *Phys. Rev. Lett.* **108** (2012) 126802, [arXiv:1006.0333]. (See p. 175.)

[403] I. Brihuega, A. M. García-García, P. Ribeiro, M. M. Ugeda, C. H. Michaelis, S. Bose, and K. Kern, *Experimental observation of thermal fluctuations in single superconducting Pb nanoparticles through tunneling measurements*, *Phys. Rev. B* **84** (2011) 104525, [arXiv:0904.0354]. (See p. 175.)

[404] A. A. Shanenko, M. D. Croitoru, and F. M. Peeters, *Oscillations of the superconducting temperature induced by quantum well states in thin metallic films: Numerical solution of the Bogoliubov–de Gennes equations*, *Phys. Rev. B* **75** (2007) 14519. (See pp. 175 and 193.)

[405] A. Gozar, G. Logvenov, L. F. Kourkoutis, A. T. Bollinger, L. A. Giannuzzi, D. A. Muller, and I. Bozovic, *High-temperature interface superconductivity between metallic and insulating copper oxides*, *Nature* **455** (2008) 782, [arXiv:0810.1890]. (See p. 176.)

[406] D. Liu, W. Zhang, D. Mou, J. He, Y.-B. Ou, Q.-Y. Wang, Z. Li, L. Wang, L. Zhao, S. He, and Others, *Electronic origin of high-temperature superconductivity in single-layer FeSe superconductor*, *Nat. Commun.* **3** (2012) 931, [arXiv:1202.5849]. (See p. 176.)

[407] N. Reyren, S. Thiel, A. D. Caviglia, L. F. Kourkoutis, G. Hammerl, C. Richter, C. W. Schneider, T. Kopp, A.-S. Ruetschi, D. Jaccard, M. Gabay, D. A. Muller, J.-M. Triscone, and J. Mannhart, *Superconducting Interfaces Between Insulating Oxides*, *Science* **317** (2007) 1196. (See p. 176.)

[408] J. Nagamatsu, N. Nakagawa, T. Muranaka, Y. Zenitani, and J. Akimitsu, *Superconductivity at 39 K in magnesium diboride.*, *Nature* **410** (2001) 63. (See pp. 176 and 194.)

[409] H. Shimakage, M. Tatsumi, and Z. Wang, *Ultrathin MgB_2 films fabricated by the co-evaporation method at high Mg evaporation rates*, *Supercond. Sci. Technol.* **21** (2008) 95009. (See p. 176.)

[410] C. Zhang, Y. Wang, D. Wang, Y. Zhang, Z.-H. Liu, Q.-R. Feng, and Z.-Z. Gan, *Suppression of superconductivity in epitaxial MgB_2 ultrathin films*, *J. App. Phys.* **114** (2013) 23903. (See pp. 176, 182, 186, 190 and 191.)

[411] K. Szałowski, *Critical temperature of MgB_2 ultrathin superconducting films: BCS model calculations in the tight-binding approximation*, *Phys. Rev. B* **74** (2006) 94501, [arXiv:1407.3717]. (See pp. 176, 179 and 187.)

[412] A. Bussmann-Holder and A. Bianconi, *Raising the diboride superconductor transition temperature using quantum interference effects*, *Phys. Rev. B* **67** (2003) 132509. (See p. 176.)

[413] A. Bianconi, S. Agrestini, and A. Bussmann-Holder, *The Tc Amplification by "Shape Resonance" in Doped MgB_2*, *J. Supercond.* **17** (2004) 205. (See page of previous reference.)

[414] D. Innocenti, N. Poccia, A. Ricci, A. Valletta, S. Caprara, A. Perali, and A. Bianconi, *Resonant and crossover phenomena in a multiband superconductor: Tuning the chemical potential near a band edge*, *Phys. Rev. B* **82** (2010) 184528, [arXiv:1007.0510]. (See p. 179.)

[415] D. Innocenti, S. Caprara, N. Poccia, A. Ricci, A. Valletta, and A. Bianconi, *Shape resonance for the anisotropic superconducting gaps near a Lifshitz transition: the effect of electron hopping between layers*, *Supercond. Sci. Technol.* **24** (2010) 15012, [arXiv:1011.4548]. (See p. 176.)

[416] M. A. N. Araújo, A. M. García-García, and P. D. Sacramento, *Enhancement of the critical temperature in iron pnictide superconductors by finite-size effects*, *Phys. Rev. B* **84** (2011) 172502, [arXiv:1103.3290]. (See pp. 176 and 179.)

[417] T. M. Apostol, *Mathematical Analysis*. Addison-Wesley, 1973. (See pp. 183 and 197.)

[418] A. M. García-García, J. D. Urbina, E. A. Yuzbashyan, K. Richter, and B. L. Altshuler, *BCS superconductivity in metallic nanograins: Finite-size corrections, low-energy excitations, and robustness of shell effects*, *Phys. Rev. B* **83** (2011) 14510, [arXiv:0911.1559]. (See pp. 184 and 185.)

[419] K. Matveev and A. Larkin, *Parity Effect in Ground State Energies of Ultrasmall Superconducting Grains*, *Phys. Rev. Lett.* **78** (1997) 3749. (See p. 186.)

[420] E. A. Yuzbashyan, A. A. Baytin, and B. L. Altshuler, *Finite-size corrections for the pairing Hamiltonian*, *Phys. Rev. B* **71** (2005) 94505. (See p. 186.)

[421] B. Mühlschlegel, D. J. Scalapino, and R. Denton, *Thermodynamic properties of small superconducting particles*, *Phys. Rev. B* **6** (1972) 1767. (See p. 186.)

[422] Y. Kong, O. Dolgov, O. Jepsen, and O. Andersen, *Electron-phonon interaction in the normal and superconducting states of MgB_2*, *Phys. Rev. B* **64** (2001) 1–4. (See pp. 186 and 194.)

[423] A. A. Golubov, J. Kortus, O. Dolgov, O. Jepsen, and ..., *Specific heat of MgB 2 in a one- and a two-band model from first-principles calculations*, *J. Phys. Condens. Matter* **14** (2002) 1353. (See p. 192.)

[424] A. Liu, I. Mazin, and J. Kortus, *Beyond Eliashberg Superconductivity in MgB_2: Anharmonicity, Two-Phonon Scattering, and Multiple Gaps*, *Phys. Rev. Lett.* **87** (2001) 087005. (See p. 192.)

[425] R. H. Parmenter, *Size Effect in a Granular Superconductor*, *Phys. Rev.* **166** (1968) 392. (See p. 193.)

[426] A. M. García-García, J. D. Urbina, E. A. Yuzbashyan, K. Richter, and B. L. Altshuler, *Bardeen-Cooper-Schrieffer Theory of Finite-Size Superconducting Metallic Grains*, *Phys. Rev. Lett.* **100** (2008) 187001. (See p. 193.)

[427] V. Moshchalkov, M. Menghini, T. Nishio, Q. H. Chen, A. V. Silhanek, V. H. Dao, L. F. Chibotaru, N. D. Zhigadlo, and J. Karpinski, *Type-1.5 Superconductivity*, *Phys. Rev. Lett.* **102** (2009) 117001, [arXiv:0902.0997]. (See p. 194.)

[428] A. Brinkman, A. A. Gloubov, H. Rogalla, O. Dolgov, J. Kortus, Y. Kong, O. Jepsen, and O. Andersen, *Multiband model for tunneling in MgB_2 junctions*, *Phys. Rev. B* **65** (2002) 180517. (See p. 194.)

[429] M. M. Ozer, J. R. Thompson, and H. H. Weitering, *Hard superconductivity of a soft metal in the quantum regime*, *Nat. Phys.* **2** (2006) 173. (See p. 196.)